International Journal of Dentistry

Digital Dentistry: New Materials and Techniques

Guest Editors: Francesco Mangano, Jamil A. Shibli, and Thomas Fortin

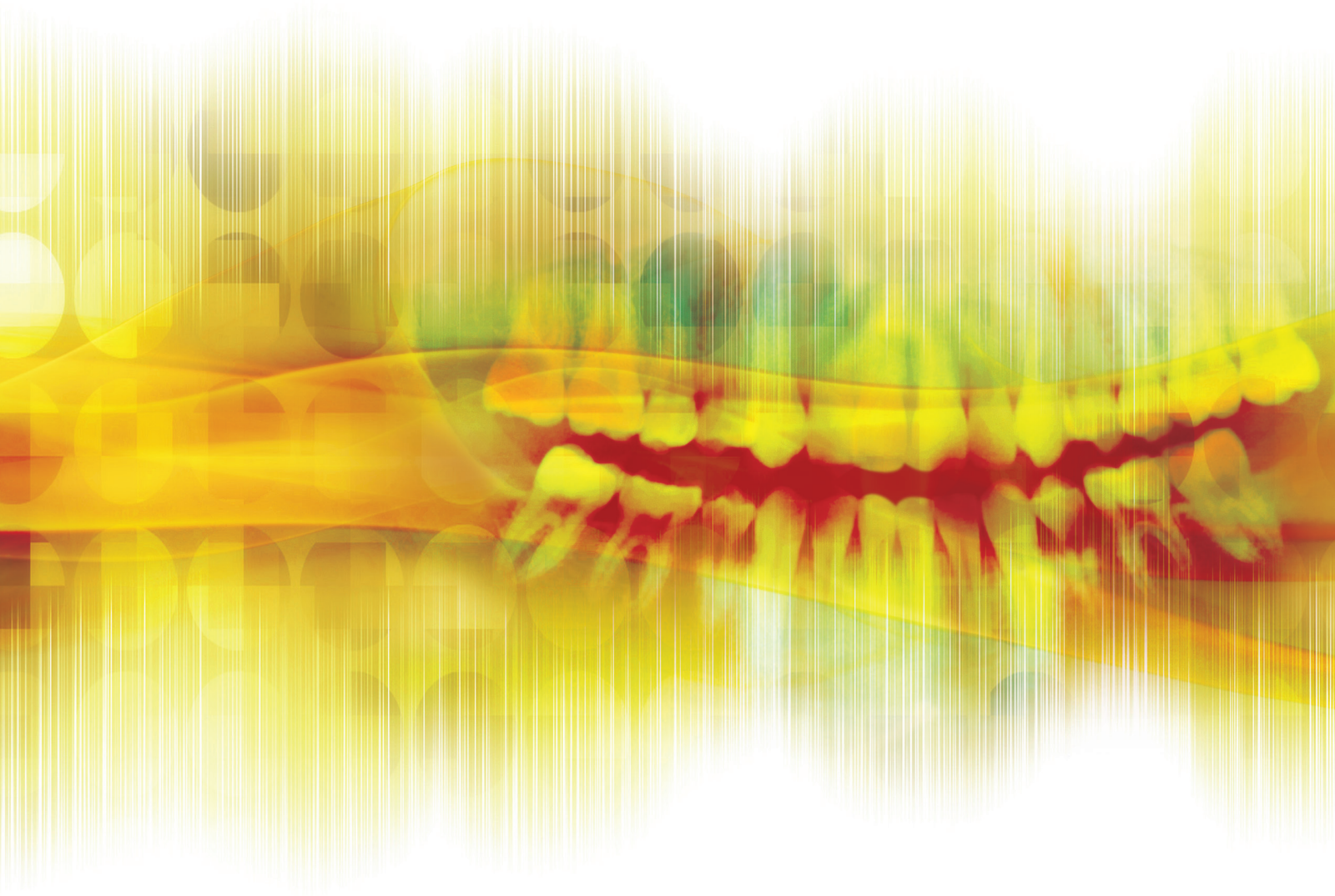

Digital Dentistry: New Materials and Techniques

International Journal of Dentistry

Digital Dentistry: New Materials and Techniques

Guest Editors: Francesco Mangano, Jamil A. Shibli, and Thomas Fortin

Editorial Board

Contents

Hindawi Publishing Corporation
International Journal of Dentistry
Volume 2016, Article ID 5261247, 2 pages
http://dx.doi.org/10.1155/2016/5261247

Editorial

Digital Dentistry: New Materials and Techniques

Francesco Mangano,[1,2] Jamil A. Shibli,[3] and Thomas Fortin[4]

[1]*Department of Surgical and Morphological Science, Dental School, University of Varese, Varese, Italy*
[2]*Academic Unit of Digital Dentistry, IRCCS San Raffaele Hospital, Milan, Italy*
[3]*Guarulhos University, Guarulhos, SP, Brazil*
[4]*University of Lyon, Lyon, France*

Correspondence should be addressed to Francesco Mangano; francescomangano1@mclink.net

Received 27 September 2016; Accepted 28 September 2016

The digital revolution is changing the world, and dentistry is no exception.

The introduction of a whole range of digital devices (intraoral, extraoral, face scanners and cone beam computed tomography (CBCT) with low dose radiation) and processing software (computer-assisted-design/computer-assisted-manufacturing (CAD/CAM) prosthetic software, software for planning implant surgery), together with new aesthetic materials and powerful manufacturing and prototyping tools (milling machines and 3D printers), is radically transforming the dental profession.

Classically, case history and physical examination, together with X-ray data from two-dimensional radiology (periapical, panoramic, and cephalometric radiographs), represented the necessary preparatory stages for formulating a treatment plan and for carrying out the therapy. With only two-dimensional X-ray data available, making a correct diagnosis and an appropriate treatment plan could be difficult; therapies essentially depended on the manual skills and experience of the operator.

Today, the digital revolution is changing the workflow and consequently changing operating procedures. In modern digital dentistry, the four basic phases of work are image acquisition, data preparation/processing, the production, and the clinical application on patients.

Image acquisition is the first operational phase of digital dentistry and this employs powerful tools such as digital cameras, intraoral scanners, and CBCT.

Digital photography, combined with the use of appropriate software for image processing, allows us to design a patient's smile virtually: this is digital smile design, a valuable tool for previsualization and communication in modern aesthetic and cosmetic dentistry.

Intraoral scanners allow us to take accurate optical impression of the dental arches, using only a beam of light. The optical impression is now supplanting the classic method with tray and impression materials: this last procedure, never liked by patients and often technically difficult, is likely to disappear over the next few years. The information on dentogingival tissues acquired from an optical impression can be used not only to make a diagnosis and for communication, but also to design prosthetic restorations. Indeed, optical impression data (e.g., the scanning of prosthetic preparations) is easily imported into processing software for designing/planning prosthetic restorations; the models created in this way are then physically produced with materials of high aesthetic value, with powerful milling machines. These restorations are then delivered to patients. In simple cases (e.g., in the case of inlays/onlays, temporary restorations in resin or single crowns), all these procedures can be performed directly in the dental office, without the help of a dental technician, through a "full in-office" or "chairside" procedure. In the case of more complex restorations (such as crowns and monolithic bridges or copings and frameworks which need to be veneered with ceramic), collaboration with a dental technician is fundamental. Optical impressions can find application in orthodontics and surgery, too. In orthodontics, they are useful in diagnosis and in the design of a whole series of custom devices, such as invisible aligners. In surgery, optical impressions allow useful data to be obtained for

the planning of implant operations. Indeed, information on dentogingival tissues can be combined and overlaid with that relating to the patient's bone structure obtained from CBCT, by using specific planning software packages. Within these processing software packages, the surgeon can design templates for guided implant placement, which are physically manufactured by milling or 3D printing and used clinically. Implants positioned through a guided surgical procedure can be loaded immediately, using prosthetic restorations in resin, printed in 3D before the fixtures are positioned. This is known as the "full-digital" technique.

The data obtained by CBCT can also be used for designing personalized implants ("custom-made"), or personalized bone grafts, to be used in implant and regenerative surgery, respectively. In fact, by importing data from CBCT into specific modelling software, it is currently possible for the surgeon to design a whole series of customized implants (root analogue implants, blade implants, and maxillofacial implants); such implants can be physically produced by means of additive manufacturing and 3D printing procedures, such as direct metal laser forming (printing of metals). The use of customized implants offers the patient several advantages. With 3D printing techniques (the real "third industrial revolution") becoming established in the biomedical field, the cost of equipment will fall and the printers will also increasingly become accessible to dental professionals: hence, it is likely that such modelling procedures and the fabrication of "customized" implants will spread. The production of personalized bone grafts for regenerative surgery also comes under this heading. The possibility of using custom-made bone grafts, offering macro- and microtopography with controlled characteristics, represents an undoubted advantage for the practitioner and for the patient. In fact, the availability of customized grafts which fit the individual patient's bone defect perfectly will greatly simplify and speed up otherwise complex regenerative operations; reducing the surgical time will allow the risk of infection to be lowered and improve healing. Thus, the outcome of regenerative therapy will also be improved with significant benefit for the patient.

In this special issue, the first in the world dedicated entirely to the topic of digital dentistry, you will find that we have gathered together a number of scientific and clinical papers which deal with various "digital" themes: we hope that you will find them interesting and that they will attract your attention.

Francesco Mangano
Jamil A. Shibli
Thomas Fortin

Hindawi Publishing Corporation
International Journal of Dentistry
Volume 2016, Article ID 9823025, 7 pages
http://dx.doi.org/10.1155/2016/9823025

Clinical Study

The Prosthetic Workflow in the Digital Era

Lidia Tordiglione,[1] Michele De Franco,[2] and Giovanni Bosetti[3]

[1]*Department of Surgical and Morphological Science, University of Insubria, 21100 Varese, Italy*
[2]*Private Practice, Abbiategrasso, Milan, Italy*
[3]*Private Practice, 21100 Varese, Italy*

Correspondence should be addressed to Lidia Tordiglione; lidia.tordiglione@gmail.com

Received 24 February 2016; Revised 28 June 2016; Accepted 26 September 2016

Academic Editor: Thomas Fortin

The purpose of this retrospective study was to clinically evaluate the benefits of adopting a full digital workflow for the implementation of fixed prosthetic restorations on natural teeth. To evaluate the effectiveness of these protocols, treatment plans were drawn up for 15 patients requiring rehabilitation of one or more natural teeth. All the dental impressions were taken using a Planmeca PlanScan® (Planmeca OY, Helsinki, Finland) intraoral scanner, which provided digital casts on which the restorations were digitally designed using Exocad® (Exocad GmbH, Germany, 2010) software and fabricated by CAM processing on 5-axis milling machines. A total of 28 single crowns were made from monolithic zirconia, 12 vestibular veneers from lithium disilicate, and 4 three-quarter vestibular veneers with palatal extension. While the restorations were applied, the authors could clinically appreciate the excellent match between the digitally produced prosthetic design and the cemented prostheses, which never required any occlusal or proximal adjustment. Out of all the restorations applied, only one exhibited premature failure and was replaced with no other complications or need for further scanning. From the clinical experience gained using a full digital workflow, the authors can confirm that these work processes enable the fabrication of clinically reliable restorations, with all the benefits that digital methods bring to the dentist, the dental laboratory, and the patient.

1. Introduction

It is very frustrating for dentists to complete a prosthetic rehabilitation, whether complex and simple, only to discover that the oral situation does not correspond to the dental technician's casts.

A wide variety of materials and techniques are available for taking impressions of the oral cavity.

The complexity consists in acquiring critical knowledge of the various impression materials (polyethers, polyvinyl siloxanes, polysulfides, hydrocolloids and others) in terms of both their chemical-physical characteristics and their different clinical use and handling [1].

In the age of digital dentistry, we can now replace these various impression materials with an intraoral scanner [2].

Intraoral scanners represent the first step in a totally digital process of design and fabrication of dental prostheses.

The possibility of implementing prosthetic restorations, on both natural teeth and implants, using fully digital workflows is now a reality, and any clinic can avail of the modern digital methods to improve its daily clinical practice.

The advantages of the digital method not only are in terms of the new range of materials that can be used but also can be seen along the entire workflow, from impression and design, for completion of the prosthesis [3–6].

The methods for scanning dental arches using intraoral systems provide comparable impressions to traditional materials in terms of clinical accuracy [7], eliminating operator-dependent variability, reducing the time and treatment costs for rehabilitation, and improving patient compliance [8–11]. There are also several benefits for patients: scan requires less time than taking conventional impressions, the images can be immediately analysed by the operator, and it can be easily repeated, if necessary, either entirely or partially. In addition, the dimensions of the scanner tip make it much more comfortable in terms of encumbrance than the use of

traditional materials, particularly for patients with a sensitive gag reflex or fear of choking [12–14].

The purpose of this paper is to present a fully digital workflow based on the latest techniques, now widely validated, from digital scan of intraoral impressions and processing with CAD dental design software to fabrication through the prototyping of diagnostic crown and subtraction milling of the finished prosthetic tooth in order to standardise the workflow and minimise possible errors.

2. Materials and Methods

2.1. Patient Selection. This is a clinical follow-up examination of 14 patients who had been given single-unit or multiple-unit zirconia and lithium disilicate crowns and veneers by seeking to make the best use of the new working methods and implement fully digital workflows. The clinical phases were conducted in the period from January 2014 to December 2014.

The clinical cases were selected based on the following parameters: eight patients requiring fixed prosthetic rehabilitation on individual natural teeth were initially selected to perfect the technique and reduce the author's learning curve, three more patients were then selected needing prosthetic rehabilitation on two adjacent teeth, followed by two patients requiring work on up to four teeth distributed between both dental arches and, finally, a complicated prosthetic rehabilitation on natural abutments was completed on a patient with multiple abrasions, loss of vertical dimension, and reduction in clinical crown height.

Patient's inclusion criteria were age of at least 18 years, without any systemic pathologies, sufficient oral hygiene, low caries activity with less than five new restorations during the preceding five-year period, with no signs of active bone resorption, furcation involvement, periapical pathology, or mobility. Only natural teeth or fixed prosthesis without treatment needs was accepted as antagonists. Root canal therapy had been conducted, where necessary, on the selected teeth at least six months before the prosthetic rehabilitation, and they had to be symptom-free with no X-rays signs of periapical lesion. Teeth that had still been vital, with no need for root canal therapy, had remained vital. Periodontal health was required: probing depth <4 mm, maximum grade 1 mobility, and no vertical bone pocket.

2.2. Intraoral Scan. All the impressions required for the implementation of the arranged treatment plans were taken using a Planmeca PlanScan intraoral scanner (Planmeca OY, Helsinki, Finland). This is a device that relies on short wavelength laser light projection (450 nm). The scanner does not require the application of powder on the intraoral surface and it has several interchangeable autoclavable tips, in various sizes, to suit the clinical situation. It can be used simply by connecting it to a computer or prepared dental unit, allowing it to be operated easily in various workstations. In addition, the scanning software allows digital casts to be exported in the open STL format, giving the clinician complete freedom in the management of the subsequent stages of the prosthetic rehabilitation using Exocad software (Exocad GmbH, Germany, 2010).

Figure 1: Intraoral preoperative conditions. Notice widespread cervical abrasions and abfractions.

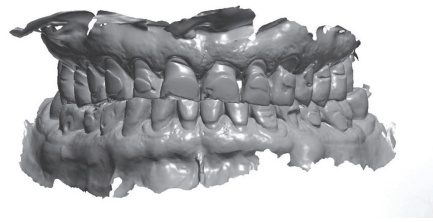

Figure 2: 3D image of the preoperative situation originated from the intraoral scan.

To validate the procedure, two steps were taken during the first cases: prototype casts were created in order to test the accuracy of the prosthetic restoration, and resin diagnostic crowns were made to be tested and modified, if necessary, directly in the patient's mouth. After verifying the reliability of the technique, we decided to eliminate these two steps.

2.3. The Full Digital Workflow. A total of four clinical appointments were initially required:

(i) Scanning of the arches performed with the intraoral scanner (IS) to allow the design of the temporary crown based on the digital casts (Figures 1 and 2). All the scanning was performed using a Planmeca PlanScan (Planmeca Oy, Helsinki, Finland), which does not require the use of opacifying powder. We first produced a scan of the entire arch involved as far as the second molar, followed by a scan of the opposite arch with a similar extension, and then a scan of both arches in the maximum intercuspation position (MIP), which allowed the imaging software to immediately relate the two scans.

(ii) Dental preparation and adjustment of the resin temporary crown milled from PMMA are carried out (Figure 3); scanning of the final intraoral impression is performed if the marginal periodontium was not affected by the fitting of the temporary crown; otherwise scanning was scheduled for the following session. The final scanning was similar to that described for the temporary crown (Figure 4). The only difference was that two gingival retraction cords were positioned in the gingival sulcus of the prepared teeth, with the more coronal one removed a few moments before taking the impression.

Figure 3: Clinical evaluation of the aesthetic and functional outcome of the provisional.

Figure 4: Intraoral digital scan of the preparations of both dental arches.

Figure 5: Clinical test and evaluation of the definitive crowns design through the 3D printed crowns: analysis of the finishing lines, interproximal areas, occlusal contacts, and aesthetic result.

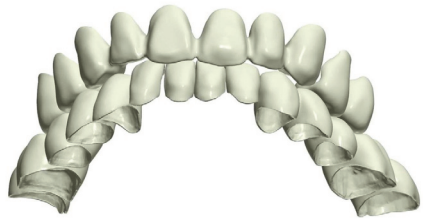

Figure 6: Development of the 3D design project of the definitive crowns.

Temporary PMMA restorations were cemented with eugenol-free cement (Temp Bond NE, Kerr GmbH, Rastatt, Germany, or Freegenol, GC, Bad Homburg, Germany).

(iii) Try-in procedure is as follows: fitting the resin (Figure 5) and making any necessary occlusal and/or proximal adjustments on the diagnostic crowns.

The diagnostic crowns were obtained using the 020D DigitalWax® rapid prototyping machine (DWS, Vicenza 2007), featuring a BluEdge® laser source, which combines high speed with precision and surface quality. It also has a vertical positioning device that allows the base of the modelling platform to emerge to an extent corresponding to the thickness of the solidified layer, thanks to its synchronised laser. The photosensitive resin for DigitalWax RD096 stereolithography systems (DWS, Vicenza 2007) was used, which provides high definition, high resolution, and durability.

A third scan was then performed and imported into the CAD software Exocad (Exocad GmbH, Germany, 2010) in order to transfer on the digital project any clinical adjustment achieved on the diagnostic crown. This third scan was performed with an intraoral scan of the diagnostic crowns in the right position and an extraoral scan of the crowns themselves focusing on the cervical design.

(iv) Delivery and cementing of the final prosthesis are carried out (Figures 6 and 7).

The materials selected for the construction of the prostheses were lithium silicate and monolithic zirconia due to their biocompatibility, biomechanical behaviour, aesthetic qualities, and diamagnetic characteristics.

All the final prostheses, both monolithic zirconia single crowns and vestibular lithium disilicate and three-quarter lithium disilicate vestibular veneers with palatal extension, were fabricated using a Granite 5-axis numerically controlled milling machine by Dental Machine (Dental machine, Piacenza, Italy). All 5 axes are interpolated continuously and managed by electronically controlled brushless digital motors, with automatic current and position management, and are able to work with all materials (wax, PMMA, various resins, composite material, presintered zirconia or aluminum oxide, lithium disilicate titanium (grades 2 and 5), and Cr-Co alloy).

All the zirconia monolithic crowns were milled out of Zirite® discs (Kéramo, Tavernerio, Como, Italy): isostatic pressed partly sintered zirconium oxide stabilized with yttrium and colored by Colorodent NANO-ZC® (Orodent, Castelnuovo del Garda, Verona, Italia) colorant immersion for 3–8 seconds depending on the thickness of the restoration and sintered according to the manufacturer's instructions in a Nabertherm sintering furnace (Nabertherm GmbH, Lilienthal, Germany).

Lithium disilicate veneers were milled from IPS® e.max pressed ceramics blocks (Ivoclar Vivadent,

Table 1: Number of single zirconia crowns (Zn); multiple unit prosthetic rehabilitation with zirconia crown (Zn) and lithium disilicate vestibular veneer (DSL vest. veneer); complex rehabilitation with single zirconia crown (Zn), lithium disilicate vestibular veneer and lithium disilicate vestibular veneer with palatal extension (DSL 3/4 veneer) and their distribution in posterior (P: premolars, molars) and anterior (A: incisors and canines) areas.

Single crown	Multiple unit		Complex rehabilitation			
Zn	Zn	DSL vest. veneer	Single Zn crown		DSL vest. veneer	DSL 3/4 veneer
P	P	A	P	A	A	P
8	10	2	8	2	10	4

Figure 7: Clinical intraoral result after cementation.

Schaan, Liechtenstein), colored with IPS e.max CAD Crystall Shades (Ivoclar-Vivadent, Schaan, Liechtenstein), and crystallized in ceramic furnaces following the manufacturer's instructions.

The marginal fit of the abutments was assessed with a silicone pressure indicator paste (Fit Checker, GC, Bad Homburg, Germany).

The lithium disilicate restoration surfaces were etched with 5% hydrofluoric acid (IPS Ceramic Etching Gel, Ivoclar Vivadent, Schaan, Liechtenstein) for 60 seconds and then rinsed and air-dried. Then silane Monobond Plus (Ivoclar Vivadent) was applied and allowed to react for 20 seconds. The inner restoration surfaces of Zirconium crowns were sandblasted and cleaned in an ultrasonic unit for about 1 minute and then rinsed and air-dried. Abutment surfaces were conditioned with Multilink Primer A/B mixed in a 1 : 1 ratio and applied and scrubbed for at least 30 seconds. All restorations were luted adhesively with a self-curing luting composite Multilink Automix (Ivoclar Vivadent, Schaan, Liechtenstein).

Finally, static and dynamic occlusions were checked with a 40 μ microthin Articulating Papers (Bausch, Köln, Germany).

Initially, a total of four clinical appointments were required: preparation and adjustment of the temporary crown, scanning for the intraoral impression, testing of the diagnostic crown, and delivery and cementing of the final prosthesis. Later on, when the operators had gained more experience, we were able to avoid the clinical test on the diagnostic crown and reduce the appointments to three by applying occlusal and proximal adjustments directly to the final prosthesis.

2.4. The Follow-Up. The clinical examination and radiographic checkups were scheduled for one month after the final cementing, six months, and one year.

The recall examination was accomplished by the two operators that conducted the treatments. Both biological and technical parameters were recorded during each recall.

Biological parameters included probing depths of the abutment teeth, its papilla bleeding index (PBI), secondary caries, endodontic complications, and fractures of the abutment teeth. Technical evaluation included fracture or chipping of the crown or veneer, loss of retention wear or surface roughness, and aesthetic characteristics.

The parameters recorded for vestibular veneers, three-quarter vestibular veneer with palatal extension, and crowns were the same.

3. Results

A total of 44 prostheses were installed in 14 patients (8 women and 6 men). Of these, 8 patients were selected for single crown rehabilitation on posterior teeth with milled monolithic zirconia (5 women and 3 men); 5 patients needed multiple unit prosthetic rehabilitation: of these 2 required monolithic zirconia crown on two adjacent posterior teeth (2 men), 1 woman required two lithium disilicate vestibular veneer on anterior teeth, and two women needed zirconia monolithic crown on three teeth distributed between both dental arches. Finally, complete prosthetic rehabilitation was accomplished: it consisted of 10 monolithic zirconia single crowns (8 on posterior teeth and 2 on anterior teeth), 10 lithium disilicate vestibular veneers, and 4 lithium disilicate vestibular veneer with palatal extension (Table 1).

None of the final prostheses made using the digital method needed adjustment of the occlusal and interproximal surfaces, while the occlusal adjustments to the diagnostic crowns were entirely comparable to those performed on prosthetic devices made in the traditional manner.

No failure of the prosthetic component occurred on any of the crowned teeth. In one single case, there was a fracture of a three-quarter vestibular veneer with palatal coverage on one premolar, attributed to an occlusal overload. There was no need to reprocess the digital cast, as the CAD STL processing file was used for remilling, so that the veneer could be directly replaced. After balancing the tooth contact as well as possible

and instructing the patient to use a protective night guard, the problem no longer occurred.

4. Discussion

CAD/CAM digital processing, just like traditional processing, requires a digital cast from which the restoration can be designed. The digital cast can be obtained by digitising a physical cast, generated from traditional impressions, or based on a cast created digitally using an intraoral scanner.

Both the laboratory scanner and the intraoral scanner provide clinically acceptable accuracy for the creation of prosthetic structures [15, 16]. The former, however, is affected by intrinsic errors and variability due to the use of conventional impression materials and their development in plaster. Intraoral scans can greatly facilitate and standardise dental impression taking also in more difficult cases such as full-arch scans [17] and even in the case of edentulous arches [18], although further clinical studies would need to be conducted for these types of clinical cases. It should be noted, however, that there is some variability with regard to the precision and accuracy of various intraoral scanning systems [19].

The advantages of using the digital method also include considerable saving of time and steps, both for the dentist in the clinic and for the dental technician in the laboratory. Compared with traditional impressions, digitalised impressions dispense with the need to select an impression tray, the consumption of material, the disinfection of the material and the impression tray, and the need for packaging and delivery of the impression. Thanks to this technique, the laboratory can now dispense with the steps of casting the impression and refining the cast and the use of articulators.

A study by Lee and Gallucci has also shown that the digital method is noticeably more appreciated by operators than the traditional method and that its application enables considerable savings in time [20].

Acquisition and mastery of the technique by the operators was much simpler and more efficient, given the possibility of modifying and rescanning during the course of the work [21].

CAD/CAM processing methods were among the first digital innovations to be introduced to dentistry in around 1980 [22]. They allow processing of traditional materials, such as cobalt-chromium alloys, composite and acrylic resins, feldspathic ceramics, some reinforced glass ceramics, and wax through subtraction processes, using CNC milling machines [23]. These machining processes are faster and less expensive compared to traditional processing, while maintaining an excellent level of quality [24]. One of the main benefits of using CAD/CAM methods, however, is the possibility of working with materials that otherwise could not be used in dentistry. These materials include titanium, titanium alloys, and polycrystalline ceramics such as zirconium oxide.

Thanks to its characteristics, zirconium oxide has now become one of the most widely used materials for the fabrication of fixed prostheses with CAD/CAM [25] processing. It has high resistance to bending and fracture, a low specific weight compared to other prosthetic materials, and diamagnetic behaviour in the event that an MRI scan is required. However, its aesthetic superiority to metal structures, the possibility of being more conservative with hard dental tissues, as thicknesses can be reduced compared to those of metal-ceramic crowns, its excellent biocompatibility, and the possibility of achieving metal-free restorations are the reasons for the increase in its use. The biocompatibility of zirconia has been demonstrated in numerous in vitro [26] and in vivo [27, 28] studies, which have shown the absence of cellular genome mutations and other adverse reactions in biological tissues exposed to the samples of zirconium oxide. These same studies show that its high biocompatibility is mainly due to its intrinsic ionic stability, which minimises the inflammatory response. Zirconia is now used for the production of prosthetic substructures, implant abutments, monolithic restorations including inlays, crowns, bridges and full arches, and orthodontic brackets [29].

Contrary to what is often believed, the milling of zirconium oxide requires a very reliable and structurally stabile removal system. In fact, when milling a disk of the material in the green state, the speed, force, and movements of the machine have to be controlled and supervised in order to prevent fractures (visible or invisible and very insidious) and the oversizing of undercuts.

For this reason, we used a 5-axis industrial milling machine with tools capable of ensuring excellent milling precision on thicknesses of 1.5 tenths, thanks to their structural stability and shrink-fit mounting system.

This result, after sintering in the kiln and first coloring to bring out its potential translucency, proves visibly and palpably to be a surprisingly thin artefact, capable of adapting perfectly to the anatomical structure of the patient's tooth.

This study is concordant with the literature already available in affirming that the possibility of digitally designing a prosthetic artefact directly from the scanned model, thus avoiding the traditional steps of taking an impression and casting the model, reduces the possibility of error and improves the marginal precision of the prosthesis and the proximal contacts [30].

5. Conclusion

The authors agree with the literature in affirming that the entire digital workflow, from the scanning of the impression to the fabrication of the prosthetic product, has been proven to be reliable and reproducible in clinical practice.

Although further comparative studies on the precision and accuracy of intraoral scanners may be necessary, the clinical outcome, improved patient compliance, and saving of time and materials achieved with this method represent a significant advance in prosthetic dentistry, and the choice of innovative materials that it allows is undoubtedly an important step in scientific and biological progress.

Competing Interests

The authors report no competing interests related to this study.

Acknowledgments

The authors would like to thank Francodental, Pavia, for making the intraoral scanner PlanScan available to the clinical procedures and engineer Massimo Bosetti for his assistance regarding the digital technology.

References

[1] G. Kugel, "Impression-taking: conventional methods remain steadfast as digital technology progresses," *Compendium of Continuing Education in Dentistry*, vol. 35, no. 3, pp. 202–203, 2014.

[2] M. Zimmermann, A. Mehl, W. H. Mörmann, and S. Reich, "Intraoral scanning systems—a current overview," *International Journal of Computerized Dentistry*, vol. 18, no. 2, pp. 101–129, 2015.

[3] K. Ueda, F. Beuer, M. Stimmelmayr, K. Erdelt, C. Keul, and J.-F. Güth, "Fit of 4-unit FDPs from CoCr and zirconia after conventional and digital impressions," *Clinical Oral Investigations*, vol. 20, no. 2, pp. 283–289, 2016.

[4] T. Abdel-Azim, K. Rogers, E. Elathamna, A. Zandinejad, M. Metz, and D. Morton, "Comparison of the marginal fit of lithium disilicate crowns fabricated with CAD/CAM technology by using conventional impressions and two intraoral digital scanners," *Journal of Prosthetic Dentistry*, vol. 114, no. 4, pp. 554–559, 2015.

[5] G. Pradíes, C. Zarauz, A. Valverde, A. Ferreiroa, and F. Martínez-Rus, "Clinical evaluation comparing the fit of all-ceramic crowns obtained from silicone and digital intraoral impressions based on wavefront sampling technology," *Journal of Dentistry*, vol. 43, no. 2, pp. 201–208, 2015.

[6] J. Ng, D. Ruse, and C. Wyatt, "A comparison of the marginal fit of crowns fabricated with digital and conventional methods," *Journal of Prosthetic Dentistry*, vol. 112, no. 3, pp. 555–560, 2014.

[7] D. Ahrberg, H. C. Lauer, M. Ahrberg, and P. Weigl, "Evaluation of fit and efficiency of CAD/CAM fabricated all-ceramic restorations based on direct and indirect digitalization: a double-blinded, randomized clinical trial," *Clinical Oral Investigations*, vol. 20, no. 2, pp. 291–300, 2016.

[8] S. B. M. Patzelt, C. Lamprinos, S. Stampf, and W. Att, "The time efficiency of intraoral scanners: an in vitro comparative study," *Journal of the American Dental Association*, vol. 145, no. 6, pp. 542–551, 2014.

[9] T. Joda and U. Brägger, "Time-efficiency analysis comparing digital and conventional workflows for implant crowns: a prospective clinical crossover trial," *The International Journal of Oral & Maxillofacial Implants*, vol. 30, no. 5, pp. 1047–1053, 2015.

[10] H. Tamim, H. Skjerven, A. Ekfeldt, and H. J. Rønold, "Clinical evaluation of CAD/CAM metal-ceramic posterior crowns fabricated from intraoral digital impressions," *The International Journal of Prosthodontics*, vol. 27, no. 4, pp. 331–337, 2014.

[11] S. Ting-shu and S. Jian, "Intraoral digital impression technique: a review," *Journal of Prosthodontics*, vol. 24, no. 4, pp. 313–321, 2015.

[12] E. Yuzbasioglu, H. Kurt, R. Turunc, and H. Bilir, "Comparison of digital and conventional impression techniques: evaluation of patients' perception, treatment comfort, effectiveness and clinical outcomes," *BMC Oral Health*, vol. 14, no. 1, article 10, 2014.

[13] T. Joda and U. Brägger, "Patient-centered outcomes comparing digital and conventional implant impression procedures: a randomized crossover trial," *Clinical Oral Implants Research*, 2015.

[14] E. Yuzbasioglu, H. Kurt, R. Turunc, and H. Bilir, "Comparison of digital and conventional impression techniques: evaluation of patients' perception, treatment comfort, effectiveness and clinical outcomes," *BMC Oral Health*, vol. 14, article 10, 7 pages, 2014.

[15] J. S. Almeida e Silva, K. Erdelt, D. Edelhoff et al., "Marginal and internal fit of four-unit zirconia fixed dental prostheses based on digital and conventional impression techniques," *Clinical Oral Investigations*, vol. 18, no. 2, pp. 515–523, 2014.

[16] R. Scotti, P. Cardelli, P. Baldissara, and C. Monaco, "Clinical fitting of CAD/CAM zirconia single crowns generated from digital intraoral impressions based on active wavefront sampling," *Journal of Dentistry*, 2011.

[17] A. Ender and A. Mehl, "In-vitro evaluation of the accuracy of conventional and digital methods of obtaining full-arch dental impressions," *Quintessence International*, vol. 46, no. 1, pp. 9–17, 2015.

[18] P. Papaspyridakos, G. O. Gallucci, C.-J. Chen, S. Hanssen, I. Naert, and B. Vandenberghe, "Digital versus conventional implant impressions for edentulous patients: accuracy outcomes," *Clinical Oral Implants Research*, vol. 27, no. 4, pp. 465–472, 2016.

[19] P. Seelbach, C. Brueckel, and B. Wöstmann, "Accuracy of digital and conventional impression techniques and workflow," *Clinical Oral Investigations*, vol. 17, no. 7, pp. 1759–1764, 2013.

[20] S. J. Lee and G. O. Gallucci, "Digital vs. conventional implant impressions: efficiency outcomes," *Clinical Oral Implants Research*, vol. 24, no. 1, pp. 111–115, 2013.

[21] A. S. K. Persson, A. Odén, M. Andersson, and G. Sandborgh-Englund, "Digitization of simulated clinical dental impressions: virtual three-dimensional analysis of exactness," *Dental Materials*, vol. 25, no. 7, pp. 929–936, 2009.

[22] T. Miyazaki, Y. Hotta, J. Kunii, S. Kuriyama, and Y. Tamaki, "A review of dental CAD/CAM: current status and future perspectives from 20 years of experience," *Dental Materials Journal*, vol. 28, no. 1, pp. 44–56, 2009.

[23] F. Zarone, S. Russo, and R. Sorrentino, "From porcelain-fused-to-metal to zirconia: clinical and experimental considerations," *Dental Materials*, vol. 27, no. 1, pp. 83–96, 2011.

[24] L. M. Kane, D. Chronaios, M. Sierraalta, and F. M. George, "Marginal and internal adaptation of milled cobalt-chromium copings," *The Journal of Prosthetic Dentistry*, vol. 114, no. 5, pp. 680–685, 2015.

[25] R. Sorrentino, G. De Simone, S. Tetè, S. Russo, and F. Zarone, "Five-year prospective clinical study of posterior three-unit zirconia-based fixed dental prostheses," *Clinical Oral Investigations*, vol. 16, no. 3, pp. 977–985, 2012.

[26] V. V. Silva, F. S. Lameiras, and Z. I. P. Lobato, "Biological reactivity of zirconia-hydroxyapatite composites," *Journal of Biomedical Materials Research*, vol. 63, no. 5, pp. 583–590, 2002.

[27] P. Christel, A. Meunier, M. Heller, J. P. Torre, and C. N. Peille, "Mechanical properties and short-term in-vivo evaluation of yttrium-oxide-partially-stabilized zirconia," *Journal of Biomedical Materials Research*, vol. 23, no. 1, pp. 45–61, 1989.

[28] P. F. Manicone, P. Rossi Iommetti, and L. Raffaelli, "An overview of zirconia ceramics: basic properties and clinical applications," *Journal of Dentistry*, vol. 35, no. 11, pp. 819–826, 2007.

[29] M. Ferrari, A. Vichi, and F. Zarone, "Zirconia abutments and restorations: from laboratory to clinical investigations," *Dental Materials*, vol. 31, no. 3, pp. e63–e76, 2015.

[30] S. Quaas, H. Rudolph, and R. G. Luthardt, "Direct mechanical data acquisition of dental impressions for the manufacturing of CAD/CAM restorations," *Journal of Dentistry*, vol. 35, no. 12, pp. 903–908, 2007.

Hindawi Publishing Corporation
International Journal of Dentistry
Volume 2016, Article ID 9840594, 10 pages
http://dx.doi.org/10.1155/2016/9840594

Review Article

"Digitally Oriented Materials": Focus on Lithium Disilicate Ceramics

Fernando Zarone,[1] Marco Ferrari,[2] Francesco Guido Mangano,[3] Renato Leone,[1] and Roberto Sorrentino[2]

[1]*Department of Neurosciences, Reproductive and Odontostomatological Sciences, Division of Fixed Prosthodontics, "Federico II" University of Naples, 80100 Naples, Italy*
[2]*Department of Medical Biotechnologies, Division of Fixed Prosthodontics, University of Siena, 53100 Siena, Italy*
[3]*Department of Surgical and Morphological Sciences, Dental School, University of Varese, 21100 Varese, Italy*

Correspondence should be addressed to Fernando Zarone; zarone@unina.it

Received 26 February 2016; Accepted 25 July 2016

Academic Editor: Patricia Pereira

The present paper was aimed at reporting the state of the art about lithium disilicate ceramics. The physical, mechanical, and optical properties of this material were reviewed as well as the manufacturing processes, the results of in vitro and in vivo investigations related to survival and success rates over time, and hints for the clinical indications in the light of the latest literature data. Due to excellent optical properties, high mechanical resistance, restorative versatility, and different manufacturing techniques, lithium disilicate can be considered to date one of the most promising dental materials in Digital Dentistry.

1. Introduction

In the last decade, the development of new technologies has moved in parallel with a rapid evolution of restorative materials on the rails of Digital Dentistry, opening new horizons in the field of Prosthodontics. The implementation in the daily practice of the most advanced technologies, like CAD/CAM, laser-sintering/melting, and 3D-printing, has got a synergic impulse from the enhanced mechanical and manufacturing properties of the new generation of dental materials: high strength ceramics, hybrid composites and technopolymers, high precision alloys, and so forth. Among these, metal-free ceramics offer unchallenged advantages like high esthetic potential, astounding optical characteristics, reliable mechanical properties, excellent consistency in terms of precision and accuracy due to the manufacturing technologies, lower costs, and more convenient production timing. In particular, lithium disilicate in the last years has gained maximum popularity in the dental scientific community, offering undeniable advantages.

2. Physical-Mechanical Properties and Fabrication Techniques

Lithium disilicate (SiO_2-Li_2O) was introduced in the field of glass ceramics in 1998 as a core material, obtained by heat-pressing ingots (Empress 2, Ivoclar Vivadent, Lichtenstein), with a procedure similar to the lost-wax technique used for dental alloys (lithium disilicate heat extrusion at 920°), showing an optimal distribution of the elongated, small, needle-shaped crystals in a glassy matrix with a low number and small dimensions of pores [1]; the core is eventually veneered with fluorapatite-based ceramics, showing noticeable translucency and, at the same time, higher flexural strength (350 MPa) compared to older glass ceramics like the leucite-based ones [2, 3]. Such a material has been discontinued since 2009, replaced in the market by an upgraded typology of lithium disilicate, IPS e.max Press (Ivoclar Vivadent, Schaan, Liechtenstein), in which both the optical and mechanical properties have been enhanced by introducing technical improvements in the production

processes [4]. The crystals are smaller and more uniformly distributed; at the same time, this new, more versatile material has introduced the possibility of producing anatomically shaped, monolithic restorations, with no veneering ceramic, just colored on the surface; this innovative indication has become more and more popular in the last years, highly reducing technical complications like chippings and fractures, mainly used for restorations in the posterior areas, where such failures have been shown to be more frequent [5–11]. In order to accommodate the material to the needs of chairside CAD/CAM production processes, another technique has been introduced, based on the use of partially, precrystallized blocks (IPS e.max CAD, Ivoclar Vivadent), containing both 40% lithium metasilicate (Li_2SiO_3) crystals and lithium disilicate ($Li_2Si_2O_5$) crystal nuclei; it is available in different shades and degrees of translucency, depending on the size and density of crystals. In the initial condition, such machineable, bluish blocks show moderate hardness and strength (around 130 MPa); consequently, they are easier to mill, reducing wear of the machining devices at the same time, with evident advantages during chairside procedures [12]. After milling, heat treatment (840–850° for 10 min) determines full crystallization of the material: lithium metasilicates tend to evolve to form lithium disilicates (70%) [13], increasing the flexure strength up to 262 ± 88 MPa [14] with a fracture toughness of 2.5 $MPa{\cdot}m^{1/2}$ [15]. Compared to the e.max CAD, hot-pressed lithium disilicate exhibits better mechanical properties, like higher flexure strength (440 MPa) and fracture toughness (2.75 $MPa{\cdot}m^{1/2}$ - IPS e.max Press, Ivoclar Vivadent) [16].

The fabrication processes and machinability affect the restorative quality of monolithic lithium disilicate glass ceramics. A recent investigation analyzed the diamond tool wear, chip control, machining forces, and surface integrity of lithium disilicate after occlusal adjustments. Minimum bur wear but significant chip accumulation was evidenced; furthermore, machining forces were significantly higher than with other glass ceramics. Although the final surface roughness of lithium disilicate was comparable to other glass ceramics, occlusal adjustment caused intergranular and transgranular microcracks, resulting in shear-induced plastic deformations and penetration-induced brittle fractures; such behavior is distinctive of lithium disilicate and very uncommon in other glass ceramics. Consequently, lithium disilicate should be considered the most difficult to machine among glass ceramics for intraoral adjustments [17]. Moreover, thermal processing can influence crystallization kinetics, crystalline microstructure and strength of lithium disilicate restorations. Particularly, extended temperature range (820–840°C versus 750–840°C) and protracted holding time (14 min versus 7 min) produced significantly higher elastic-modulus and hardness properties but showed flexural strength and fracture toughness properties similar to controls (i.e., 750–840°C for 7 min). Rapid growth of lithium disilicates happened when the maximum formation of lithium metasilicates had ended [13].

Recently, innovative fabrication techniques have been proposed to improve the microstructure of lithium disilicate ceramics. Particularly, spark plasma sintering (SPS) was developed specifically for CAD-CAM dental materials. This fabrication process allowed refining the microstructure of lithium disilicate; its densification resulted in textured and fine nanocrystalline microstructures with major lithium disilicate/lithium metasilicate phases and minor lithium orthophosphate and cristobalite/quartz phases [18].

3. Mechanical Testing and Fracture Resistance

Due to its intrinsic brittle behavior, lithium disilicate suffers from fatigue failure during clinical service. Microcracks usually initiate in load bearing and/or stress concentration areas, eventually fusing under dynamic loads and creating major flaws that could weaken the lithium disilicate structure; when the ultimate mechanical strength is overcome, catastrophic failures occur [19–22].

Several laboratory studies investigated the fatigue resistance of lithium disilicate single crowns (SCs) and fixed dental prostheses (FDPs) to evaluate experimental designs and testing parameters [20–24]. Different laboratory variables were proved to influence the fatigue resistance of lithium disilicate restorations, such as magnitude of load, number of cycles, abutment and antagonist material, wet environment, and thermocycling; conversely, chewing frequency, lateral movements, and aging technique were considered not influential factors [23]. Single load to fracture after fatigue tests (i.e., combination of dynamic and static loading until fracture) reported highly variable ultimate strength values for this material: from 980.8 N to 4173 N for monolithic SCs and from 390 N to 1713 N for posterior FDPs [23, 24]. Significant comparisons between data were not possible because of the heterogeneity of research designs and testing modalities [24].

Fairly consistent agreement between in vitro and in vivo results was reported. As to SCs, after 2 years of simulated or real service, 100% survival rates were noticed in both laboratory [25] and clinical investigations [26]; in in vitro studies 100% survival rate was reported after 5 years of simulated function as well [20, 27] while the percentage changed to 97.8% in in vivo clinical investigations [26]. Differently, as regards FDPs, the cumulative survival rates at 5 years ranged from 75% to 100% in vitro [28, 29] while the equivalent clinical rate was 78.1% [26]; long-term laboratory investigations simulating more than 10 years of service showed 70% survival rate [30], comparable to the in vivo cumulative survival rate of 70.9% after 10 years of function [26]. The sound level of agreement between in vitro and in vivo data confirmed that laboratory investigations could represent a good simulation of the clinical scenario; nonetheless, this conclusion has to be considered only indicative, since the amount of data is not large enough to indicate consolidated clinical guidelines [24].

A recent systematic review showed significant heterogeneity leading to data inconsistency, because of different study setups and testing parameters. The lack of testing standardization made it almost impossible to perform consistent comparisons between laboratory studies. Consequently, to date, indicative and comparable data about dynamic mechanical testing of lithium disilicate restorations remain

still controversial; further investigations with specific standardization criteria are needed [24].

According to in vitro results of dynamic loading, CAD-CAM lithium disilicate SCs should have a thickness of at least 1.5 mm to withstand occlusal loads in posterior areas [22]. Being a filled glass-ceramic, lithium disilicate's final performance as a dental material is strongly related to the type of adhesive cement and accuracy of procedure [31]. To achieve the highest microtensile bond strength (μ-TBS) values and best clinical performances, the restorations have to be adhesively luted to the substrates [32, 33]. CAD-CAM monolithic posterior SCs made of lithium disilicate and luted with self-adhesive resin cements showed significantly higher fatigue resistance than feldspathic ceramic restorations. Particularly, lithium disilicate SCs effectively bore the physiological range of masticatory loads, mainly showing repairable fractures. Catastrophic failures were noticed only after load-to-failure tests up to 4500 N [33, 34].

As to implant-supported restorations, although this material showed the highest ultimate strength when compared to feldspathic ceramic and resin nanoceramic onto implant titanium abutments in vitro, no accordance was found between the initial and maximum fracture resistance values of lithium disilicate after chewing simulation with thermocycling simulating 5 years of clinical service [35].

Furthermore, CAD-CAM monolithic lithium disilicate SCs showed an optimum in vitro stiffness and strength values when cemented onto both prefabricated titanium abutments and customized zirconia abutments [36].

4. Machinability, Wear Mechanism, and Behavior

Friction and wear effects of lithium disilicate on the opposing natural tooth enamel have been also investigated, with and without fluorapatite coating, showing that they were less severe in unveneered specimens [37]. The initial surface roughness did not influence the final wear but the topography of the wear pattern affected the corresponding wear loss, since a smoother final wear aspect was associated with lower wear. Moreover, superficial wear of lithium disilicate was reported to be sensitive to environmental pH, showing higher friction and wear behavior in basic pH conditions; this was due to the fact that wettability, surface charge, and dissolution trend of lithium disilicate are pH-dependent. The presence of fluorapatite veneering resulted in increased wear of both lithium disilicate crowns and opposing natural teeth; therefore, veneering of the occlusal surface should be avoided.

These results are in agreement with another recent in vitro investigation reporting that zirconia showed less wear than lithium disilicate; in any case, the latter showed occlusal wear equivalent to sound enamel. Enamel wear was reduced after ceramic surface polishing and this supports that this procedure is advisable after performing occlusal adjustments of both lithium disilicate and zirconia restorations. Veneering porcelain significantly increased enamel abrasion; consequently, the use of monolithic zirconia and lithium disilicate should be preferred in areas of strong occlusal contact, in order to limit enamel damage of the opposing teeth over time [38].

After friction against dental enamel, lithium disilicate and monolithic zirconia specimens did not become as rough as feldspathic ceramics. Particularly, when comparing wear effects onto rough, smooth, and glazed surface finishing, eventually rough lithium disilicate became significantly smoother than fine feldspathic porcelain [39].

However, when compared to type III gold, lithium disilicate was more abrasive against human enamel. Enamel opposing lithium disilicate in vitro showed cracks, plow furrows, and surface loss typical of abrasive wear mechanism, resulting in worse wear resistance and friction coefficient than in the presence of antagonist gold [40].

Opposing steatite in chewing simulations, monolithic lithium disilicate yielded higher antagonistic wear and worse wear behavior than monolithic translucent and shaded zirconia, but about half as high as the enamel reference (274.14 μm); particularly, more severe wear patterns on both ceramics and opponents were observed after grinding and glazing [41].

Initial surface finishing and occlusal loads significantly affected the surface roughness, friction, and wear mechanisms of lithium disilicate: as the load increased, surface roughness became more severe and friction coefficient and wear volumes increased in turn. The abrasive wear process can be divided into 2 typologies: 2-body and 3-body abrasive wear. Particularly, in 2-body abrasion wear is caused by hard protuberances on one surface sliding over another while in 3-body abrasion particles are trapped between 2 surfaces but are free to roll and slide. In the presence of smooth lithium disilicate surfaces, 2-body abrasion was dominant while, in case of rough surfaces, 3-body abrasive wear was more significative. Worn lithium disilicate surfaces demonstrated higher sensitivity to delaminations, plastic deformations, and brittle fractures [42].

Two-body wear of lithium disilicate ceramic was found to be comparable to that of human enamel. Furthermore, abrasive toothbrushing significantly reduced gloss and increased roughness of all materials except zirconia [43]. When evaluating mechanical and optical properties, CAD-CAM lithium disilicate glass-ceramic (IPS e.max CAD) demonstrated the most favourable discoloration rate and the lowest 2-body wear on the material side when compared to CAD-CAM composites, hybrid materials, and leucite ceramic; in this study, the wear rate was analyzed in a chewing simulator using human teeth as antagonists [44].

Similarly to other glass ceramics, lithium disilicate can be intraorally repaired in case of chipping. In vitro results using resin composites as restorative materials demonstrated that lithium disilicate can be effectively repaired with hydrofluoric acid etching followed by silanization and adhesive bonding [7, 8, 45].

5. Impression Techniques and Accuracy of Fit

Both conventional and digital impression techniques allow for the fabrication of lithium disilicate restorations but the

results in terms of marginal accuracy are still controversial [46–51].

An in vitro study reported similar marginal accuracy between conventional and digital impression techniques ($112.3 \pm 35.3\ \mu$m and $89.8 \pm 25.4\ \mu$m, resp.) and no statistically significant differences were noticed among the different approaches [51]. Differently, the results of a recent in vitro study suggested that pressed and milled lithium disilicate SCs from digital impressions had a better internal fit to the abutment tooth than pressed SCs from polyvinylsiloxane impressions in terms of total volume of internal space, average thickness of internal space, and percentage of internal space at or below $120\ \mu$m [50]. Similarly, another in vitro investigation proved that the fully digital workflow provided better margin fit than the conventional fabrication [48]. These results were not in agreement with other investigations demonstrating that the combination of polyvinylsiloxane impressions and Press fabrication techniques for lithium disilicate SCs produced the most accurate 2D and 3D marginal fits [46] and that the combination of digital impressions and pressed lithium disilicate SCs produced the least accurate internal fit [49].

To date, in general, marginal and internal fit of lithium disilicate restorations is significantly influenced by the employed digital impression technique. Although almost all actual digital impression systems show accuracy values within the thresholds of clinical acceptability, significant fit discrepancies are still evident among different digital systems [52].

In vitro microscopical analyses demonstrated that CAD-CAM lithium disilicate SCs had significantly smaller marginal gaps than CAD-CAM anatomic contour zirconia restorations. As to the absolute marginal discrepancy, lithium disilicate SCs showed some overextended margins. Both finish line geometry and fabrication systems significantly influenced the absolute marginal discrepancy [53].

In vivo results by means of the replica technique showed that CAD-CAM lithium disilicate SCs had significantly larger internal axial and occlusal gaps than porcelain-fused-to-metal (PFM) SCs; conversely, marginal gaps were not significantly different. Nevertheless, both PFM and lithium disilicate SCs showed clinically acceptable marginal fit [54]. As regards the restoration adaptation (i.e., marginal and internal fit) of the different manufacturing techniques, evidence is growing that these parameters are more favourable with the hot-pressing technique than with the precrystallized, CAD/CAM milled blocks [46, 55, 56].

6. Biocompatibility

Biologic safety of dental ceramics is another main topic on which dental research has been focusing in the last years; such a property can be different even within the same class of materials. Lithium disilicate exhibited more severe in vitro cytotoxicity than dental alloys and composites and became more cytotoxic after polishing [57].

In vitro, human gingival fibroblasts cellular response may reflect variability in soft tissue reaction to different surface materials for prosthetic restorations. In a study by Tetè et al., polished zirconia showed a better integration in respect to the other materials [58]. Analysis on human epithelial tissue cultures, on the other side, demonstrated that lithium disilicate showed the best biocompatibility when compared to zirconia and cobalt-chromium alloys. Consequently, lithium disilicate can be considered a suitable material even for subgingival restorations directly contacting the sulcular epithelial tissues [59]. As to in vivo evidences, the presence of all-ceramic restorations did not induce inflammatory reactions in periodontally healthy patients; no differences between gingival reactions to lithium disilicate and zirconia restorations could be shown [60, 61].

7. Clinical Indications and Outcomes

For its outstanding optical properties, mechanical characteristics, ease of processing, and possibility of etching/adhesive bonding, ensuring a minimally invasive approach, lithium disilicate glass ceramics have rapidly become some of the most popular restorative materials in almost all the indications of fixed Prosthodontics [8].

Their primary use was addressed for single crowns (SCs). The first clinical studies were conducted on the early typology of lithium disilicate (IPS Empress, Ivoclar Vivadent) and reported quite promising short-term results for the veneered crowns [62, 63]; in particular, Marquardt and Strub, in their prospective clinical trial on both crowns and anterior FDPs, showed for the SCs a survival rate of 100% after 5 years of clinical service [63]. Gehrt et al. [6] analyzed the medium-long term clinical performance of 74 lithium disilicate full-coverage, anterior and posterior crowns after a service time of at least 5 years; all the frameworks, made with the hot-pressing technique from ceramic ingots (IPS e.max Press), were at least 0.8 mm thick and were eventually veneered with a fluorapatite ceramic. The survival rate was 97.4% after 5 years and 94.8% after 8 years of clinical service; among the technical complications, 3 crowns resulted affected by minor chipping. The study revealed that the survival rate was not influenced by cementation type (conventional versus adhesive) or by crown location (anterior versus posterior); on the other hand, in vitro researches have clearly demonstrated that lithium disilicate can bear high stress conditions, like in posterior crowns [64, 65]. Esquivel-Upshaw et al. [66] conducted a 3-year clinical study comparing the performance of veneered lithium disilicate (Empress 2), monolithic lithium disilicate (e-Max Press, glazed), and metal-ceramic crowns (IPS d.SIGN veneer); they observed similar, highly positive results, although a higher degree of surface roughening was detected in the veneered lithium disilicate-based crowns, compared to metal-ceramics, between years 2 and 3. This problem was probably due to degradation/water corrosion of glaze ceramic. Another retrospective, multicentric study on 860 lithium disilicate restorations, both tooth- and implant-supported, including full crowns, laminate veneers, and onlays, reported cumulative survival and success rates beyond 95% for an observational period ranging from 12 to 72 months [8]. The analyzed restorations were both bilayered and monolithic type. More recently, other retrospective studies, with longer observational times, have confirmed low

failure rates and very favourable cumulative survival rates with lithium disilicate crowns [65, 67, 68]. Positive clinical outcomes of lithium disilicate reinforced glass ceramics have been confirmed by a recent systematic review [11], showing that 5-year survival rates of all-ceramic SCs made out of lithium disilicate or oxide ceramics (i.e., alumina and zirconia) were similar to the gold standard, metal-ceramic crowns. The widespread diffusion in the daily practice of full-anatomic, monolithic lithium disilicate restorations, characterized by favourable mechanical properties, together with the possibility of manufacturing low thickness restorations adhesively bonded to the dental substrate, has introduced the use of inlays, onlays, and "tabletops" made of this material in the posterior sites, taking advantage of a minimally invasive approach and of a resistant, biocompatible ceramic (Figures 1–4). In that research, low fracture rates were reported: 0.91% for monolithic and 1.83% for bilayered single crowns (twice the rate of the monolithic); 4.55% for monolithic FDPs; 1.3% for monolithic; and 1.53% for bilayered veneers (Figures 5–9). Guess et al. [69] conducted a 7-year prospective "split-mouth" study on both pressed lithium disilicate (IPS e.max Press, Ivoclar Vivadent) and CAD/CAM leucite-reinforced glass-ceramic (ProCAD, Ivoclar Vivadent) partial-coverage restorations. The preparation was performed reducing the entire occlusal surface for a 2 mm thickness, creating a butt joint design at level of the nonsupporting cusps and a rounded shoulder for the supporting cusps. The authors reported high survival rates with both types of restorations, recommending them for a minimally aggressive treatment of extended lesions in posterior teeth. In a recent in vitro research, Sasse et al. [70] advised the need of a lithium disilicate minimum thickness of 0.7–1.0 mm when nonretentive, full-coverage adhesively retained occlusal veneers are used. As regards 3-unit FDPs, according to the manufacturer's recommendations, the use of lithium disilicate should be limited to the replacement of anterior teeth or premolars. Clinical data on this topic is quite controversial. The early, short/medium-term studies, mainly conducted on Empress 2 bilayered lithium disilicate bridges, suggested a certain cautiousness for such an indication: Taskonak and Sertgöz [71] reported a 50% survival rate at 2 years; a prospective clinical trial by Marquardt and Strub showed a fracture rate of 30% after 5 years of clinical service [63]. Makarouna et al. [72], in a randomized controlled trial, after 6 years observed a survival rate of 63% for lithium disilicate FDPs, compared to a much more favourable 95% in the control group (metal-ceramic FDPs).

In a 10-year prospective study conducted by Solá-Ruiz et al. on Empress 2 FDPs, a survival rate of 71.4% was detected, the most frequent complications being postoperative sensitivity, recessions, and marginal discolorations [73]. The introduction of the monolithic, anatomically shaped lithium disilicate FDPs has recently made achieving more favourable outcomes possible.

Some in vitro studies [29, 74, 75] have pointed out that lithium disilicate monolithic crowns and FDPs, both CAD/CAM and hot-pressed, are more resistant to fatigue fracture compared to bilayered, hand veneered ones, showing higher fracture loads (1900 N), that are comparable to the

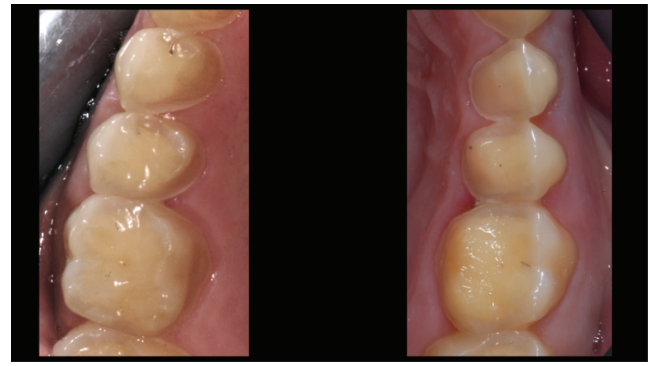

Figure 1: *Case 1* (Monolithic Lithium Disilicate Onlays). Maxillary posterior teeth in a 25-year-old female patient affected by severe food behavior disorder (bulimia). One year before the dental treatment, she was considered healed by a psychotherapist and declared recovered. The teeth were not prepared; only minimal smoothing of some sharp edges was performed.

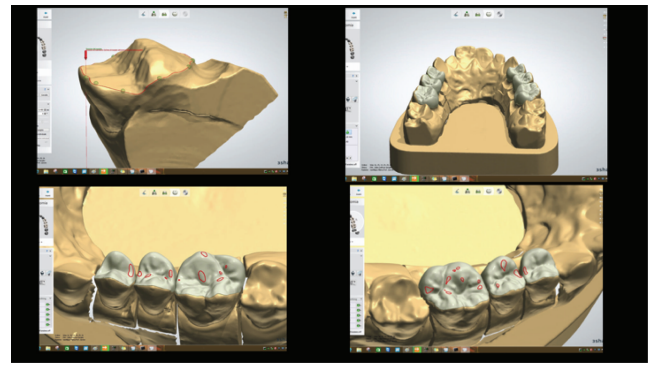

Figure 2: *Case 1* (Monolithic Lithium Disilicate Onlays). After conventional impressions, the casts were scanned by a 3-Shape D700 (3 Shape, Copenhagen, Denmark) digital scanner and analyzed by means of a Dental System 15.5.0 software (3 Shape) and the restorative finish lines were detected. Then, occlusal shape design and contacts were defined.

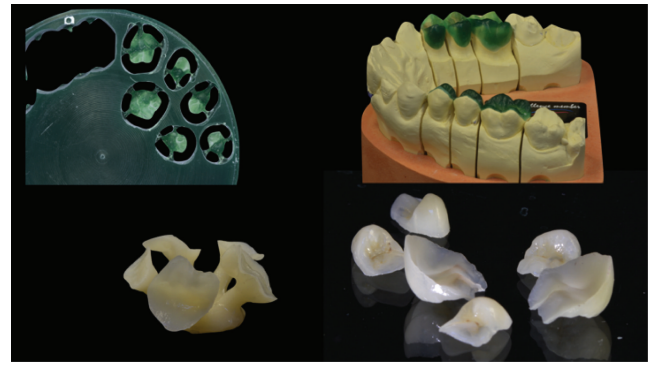

Figure 3: *Case 1* (Monolithic Lithium Disilicate Onlays). The wax patterns of the posterior onlays were milled out of a wax disk (Cera SDD98A18RWC, Sintesi Sud, Avellino, Italy) using a Roland DWX-50 Dental Milling Machine (Whip Mix GmbH, Louisville, KY, USA) and then repositioned on the cast. After careful checking, the lithium disilicate heat pressed onlays (IPS e.max Press MT, Ivoclar Vivadent) were made and eventually polished.

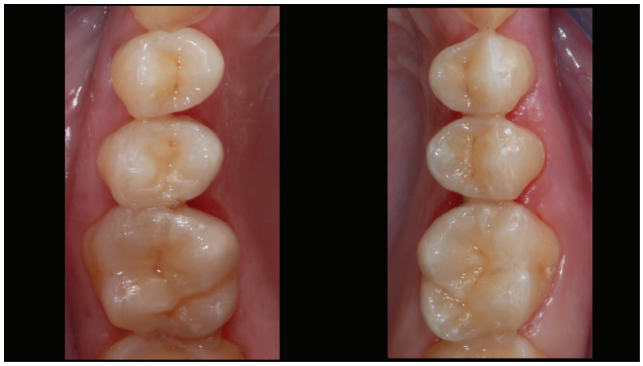

Figure 4: *Case 1* (Monolithic Lithium Disilicate Onlays). The onlays after adhesive cementation.

Figure 5: *Case 2* (Bilayered Lithium Disilicate Veneer Replacement). A female patient asked for the replacement of 6 porcelain laminate veneers with discolored and fractured margins. After the study of the case, done with the aid of digital software programs, a crown lengthening procedure was performed.

Figure 6: *Case 2* (Bilayered Lithium Disilicate Veneer Replacement). The old veneers were carefully removed under stereomicroscopic control; after the new supragingival preparations, an intraoral scanning device (3-Shape D700) was used to take digital impressions of both dental arches.

Figure 7: *Case 2* (Bilayered Lithium Disilicate Veneer Replacement). The new smile design was cut away and inserted in the patient's physiognomic image. After designing the new veneers, they were pressed with lithium disilicate (IPS e.max Press MT) and veneered.

metal-ceramic standard. The lack of the esthetic, weaker veneering material allows a thicker bulk of high strength disilicate; in any case, as regards FDPs, it has to be pointed out that their mechanical performance is multifactorial, being strongly related to many factors, like shape of the structure and size and radius of the connectors among others.

In a long-term prospective study, Kern et al. [5] evaluated the clinical performance of 3-unit, monolithic lithium disilicate FDPs (IPS e.max Press, Ivoclar Vivadent). In this research, the bridges were used not only for the replacement of anterior teeth or premolars (as suggested) but also for missing molars. After 5 years, the survival and success rates were 100% and 91.1%, respectively; after 10 years, they were reduced to 87.9% and 69.8%. Considering that 10-year survival rates of 87.0 to 89.2% have been reported for the "reference" metal-ceramic FDPs by some systematic reviews [11, 76] and that the major, catastrophic failures occurred lately in FDPs replacing missed molars (beyond the manufacturer's recommendations), these evidences advise that the monolithic lithium disilicate can be regarded as a promising candidate to replace metal-ceramics for short-span freestanding bridges.

In the last years, in the light of the concepts of minimal invasivity, economy, and long-term durability, alternative treatment strategies for the anterior single tooth replacement have become more and more popular, taking advantage of the materials' high strength and of the possibility of a reliable adhesive bonding to dental substrates. In particular, cantilevered, all-ceramic, resin-bonded, fixed partial dentures (RBFPD) have been increasingly gaining approval from the dental community, offering a feasible alternative to implant therapy in many cases, particularly when indications for implant therapy are not present, due to general, anatomic, economic, or patient's compliance factors. In such cases, instead of a complete crown, a single veneer adhesively bonded to the lingual side of the support tooth can be used; a careful occlusal check is mandatory, in order to get a proper distribution of stress and a stress limitation on the cantilevered tooth, avoiding lateral and protrusive contacts on the pontic. Also, for this kind of restoration, clinical outcomes are highly encouraging, although data is quite limited to medium-term studies and case series [77–80].

Figure 8: *Case 2* (Bilayered Lithium Disilicate Veneer Replacement). The new veneers at the end of the treatment.

Figure 9: *Case 2* (Bilayered Lithium Disilicate Veneer Replacement). The patient's smile.

In the last years, the chairside production workflow is gaining more and more interest in the prosthodontic realm, for the speed of delivery and cost reduction of SCs and inlays. The first clinical trials report encouraging results. In the study by Reich and Schierz, besides a survival rate of 96.3% after 4 years, a few biological complications (secondary caries below the crown margin, changing of sensibility perception) and technical complications (need of cervical composite filling) were observed [81].

Recently, Sulaiman et al. [82] have analyzed the clinical outcomes of different IPS e.max lithium disilicate prostheses (SCs, FDPs, veneers, inlays, and onlays), both in the bilayered and monolithic forms, in a 4-year retrospective study on a total of 21.340 restorations. In that research, low fracture rates were reported: 0.91% for monolithic and 1.83% for bilayered single crowns (twice the rate of the monolithic); 4.55% for monolithic FDPs; 1.3% for monolithic and 1.53% for bilayered veneers; and 1.01% for monolithic inlays/onlays. Finally, in the last years, the use of lithium disilicate single crowns bonded onto CAD/CAM zirconia abutments has become increasingly widespread, taking advantage of the high strength and biocompatibility of zirconia, in contact with the peri-implant soft tissues, together with the prosthetic versatility and optical characteristics of lithium disilicate. In vitro studies have demonstrated that these prosthetic solutions exhibit high fracture loads [27, 83] and, at the same time, short-term clinical studies have shown fairly positive outcomes [84], also onto one-piece zirconia implants (Spies). Another clinical approach, also supported by favourable short-term outcomes, makes use of zirconia implant-supported full-arch frameworks ("implant bridges") on which monolithic lithium disilicate crowns are adhesively bonded [7, 85].

8. Conclusions

It is a far from indisputable fact that all of the innovative solutions offered by lithium disilicate are widening the restorative scenario more and more; thanks to the excellent optical properties, the high mechanical resistance, the unique restorative versatility, and the different manufacturing techniques, it is no doubt one of the most promising dental materials in the realm of Digital Dentistry, although more light is still to be shed on some clinical and technical aspects.

Competing Interests

The authors declare that they have no competing interests.

Acknowledgments

The authors would like to thank the Master Dental Technician Mr. Luigi De Stefano (Naples, Italy) for the technical support, the digital expertise, and the kind commitment in the prosthetic manufacturing.

References

[1] M. Albakry, M. Guazzato, and M. V. Swain, "Influence of hot pressing on the microstructure and fracture toughness of two pressable dental glass-ceramics," *Journal of Biomedical Materials Research B: Applied Biomaterials*, vol. 71, no. 1, pp. 99–107, 2004.

[2] N. V. Raptis, K. X. Michalakis, and H. Hirayama, "Optical behavior of current ceramic systems," *International Journal of Periodontics and Restorative Dentistry*, vol. 26, no. 1, pp. 31–41, 2006.

[3] Y.-M. Chen, R. J. Smales, K. H.-K. Yip, and W.-J. Sung, "Translucency and biaxial flexural strength of four ceramic core materials," *Dental Materials*, vol. 24, no. 11, pp. 1506–1511, 2008.

[4] C. F. J. Stappert, W. Att, T. Gerds, and J. R. Strub, "Fracture resistance of different partial-coverage ceramic molar restorations: an in vitro investigation," *Journal of the American Dental Association*, vol. 137, no. 4, pp. 514–522, 2006.

[5] M. Kern, M. Sasse, and S. Wolfart, "Ten-year outcome of three-unit fixed dental prostheses made from monolithic lithium disilicate ceramic," *Journal of the American Dental Association*, vol. 143, no. 3, pp. 234–240, 2012.

[6] M. Gehrt, S. Wolfart, N. Rafai, S. Reich, and D. Edelhoff, "Clinical results of lithium-disilicate crowns after up to 9 years of service," *Clinical Oral Investigations*, vol. 17, no. 1, pp. 275–284, 2013.

[7] G. Fabbri, R. Sorrentino, M. Brennan, and A. Cerutti, "A novel approach to implant screw-retained restorations: adhesive combination between zirconia frameworks and monolithic lithium disilicate," *The International Journal of Esthetic Dentistry*, vol. 9, no. 4, pp. 490–505, 2014.

[8] G. Fabbri, F. Zarone, G. Dellificorelli et al., "Clinical evaluation of 860 anterior and posterior lithium disilicate restorations: retrospective study with a mean follow-up of 3 years and a maximum observational period of 6 years," *The International Journal of Periodontics & Restorative Dentistry*, vol. 34, no. 2, pp. 165–177, 2014.

[9] D. Guichet, "Digitally enhanced dentistry: the power of digital design," *Journal of the California Dental Association*, vol. 43, no. 3, pp. 135–141, 2015.

[10] S. Reich, "Tooth-colored CAD/CAM monolithic restorations," *International Journal of Computerized Dentistry*, vol. 18, no. 2, pp. 131–146, 2015.

[11] I. Sailer, N. A. Makarov, D. S. Thoma, M. Zwahlen, and B. E. Pjetursson, "All-ceramic or metal-ceramic tooth-supported fixed dental prostheses (FDPs)? A systematic review of the survival and complication rates. Part I: single crowns (SCs)," *Dental Materials*, vol. 31, no. 6, pp. 603–623, 2015.

[12] I. Denry and J. A. Holloway, "Ceramics for dental applications: a review," *Materials*, vol. 3, no. 1, pp. 351–368, 2010.

[13] W. Lien, H. W. Roberts, J. A. Platt, K. S. Vandewalle, T. J. Hill, and T.-M. G. Chu, "Microstructural evolution and physical behavior of a lithium disilicate glass-ceramic," *Dental Materials*, vol. 31, no. 8, pp. 928–940, 2015.

[14] M. Lupu and R. A. Giordano, "Flexural strength of CAD/CAM ceramic framework materials," *Journal of Dental Research*, vol. 88, p. 224, 2007.

[15] K. Fischer, P. Bühler-Zemp, and T. Völkel, "IPS e.max CAD," Scientific Documentation, Ivoclar Vivadent, Schaan, Liechtenstein, 2005.

[16] P. Bühler-Zemp, T. Völkel, and K. Fischer, *Scientific Documentation IPS e.Max Press*, Ivoclar Vivadent, Schaan, Liechtenstein, 2011.

[17] X.-F. Song, H.-T. Ren, and L. Yin, "Machinability of lithium disilicate glass ceramic in in vitro dental diamond bur adjusting process," *Journal of the Mechanical Behavior of Biomedical Materials*, vol. 53, pp. 78–92, 2016.

[18] F. Al Mansour, N. Karpukhina, S. Grasso, R. M. Wilson, M. J. Reece, and M. J. Cattell, "The effect of spark plasma sintering on lithium disilicate glass-ceramics," *Dental Materials*, vol. 31, no. 10, pp. e226–e235, 2015.

[19] H. W. A. Wiskott, J. I. Nicholls, and U. C. Belser, "Stress fatigue: basic principles and prosthodontic implications," *The International Journal of Prosthodontics*, vol. 8, pp. 105–116, 1995.

[20] K. Zhao, Y.-R. Wei, Y. Pan, X.-P. Zhang, M. V. Swain, and P. C. Guess, "Influence of veneer and cyclic loading on failure behavior of lithium disilicate glass-ceramic molar crowns," *Dental Materials*, vol. 30, no. 2, pp. 164–171, 2014.

[21] B. Seydler, S. Rues, D. Müller, and M. Schmitter, "In vitro fracture load of monolithic lithium disilicate ceramic molar crowns with different wall thicknesses," *Clinical Oral Investigations*, vol. 18, no. 4, pp. 1165–1171, 2014.

[22] M. Dhima, A. B. Carr, T. J. Salinas, C. Lohse, L. Berglund, and K.-A. Nan, "Evaluation of fracture resistance in aqueous environment under dynamic loading of lithium disilicate restorative systems for posterior applications. Part 2," *Journal of Prosthodontics*, vol. 23, no. 5, pp. 353–357, 2014.

[23] M. Rosentritt, M. Behr, R. Gebhard, and G. Handel, "Influence of stress simulation parameters on the fracture strength of all-ceramic fixed-partial dentures," *Dental Materials*, vol. 22, no. 2, pp. 176–182, 2006.

[24] N. Nawafleh, M. Hatamleh, S. Elshiyab, and F. Mack, "Lithium disilicate restorations fatigue testing parameters: a systematic review," *Journal of Prosthodontics*, vol. 25, no. 2, pp. 116–126, 2016.

[25] J.-O. Clausen, M. Abou Tara, and M. Kern, "Dynamic fatigue and fracture resistance of non-retentive all-ceramic full-coverage molar restorations. Influence of ceramic material and preparation design," *Dental Materials*, vol. 26, no. 6, pp. 533–538, 2010.

[26] S. Pieger, A. Salman, and A. S. Bidra, "Clinical outcomes of lithium disilicate single crowns and partial fixed dental prostheses: a systematic review," *Journal of Prosthetic Dentistry*, vol. 112, no. 1, pp. 22–30, 2014.

[27] M. Mitsias, S.-O. Koutayas, S. Wolfart, and M. Kern, "Influence of zirconia abutment preparation on the fracture strength of single implant lithium disilicate crowns after chewing simulation," *Clinical Oral Implants Research*, vol. 25, no. 6, pp. 675–682, 2014.

[28] S. Chitmongkolsuk, G. Heydecke, C. Stappert, and J. R. Strub, "Fracture strength of all-ceramic lithium disilicate and porcelain-fused-to-metal bridges for molar replacement after dynamic loading," *The European Journal of Prosthodontics and Restorative Dentistry*, vol. 10, no. 1, pp. 15–22, 2002.

[29] S. Schultheis, J. R. Strub, T. A. Gerds, and P. C. Guess, "Monolithic and bi-layer CAD/CAM lithium-disilicate versus metal-ceramic fixed dental prostheses: comparison of fracture loads and failure modes after fatigue," *Clinical Oral Investigations*, vol. 17, no. 5, pp. 1407–1413, 2013.

[30] M. Rosentritt, G. Siavikis, M. Behr, C. Kolbeck, and G. Handel, "Approach for valuating the significance of laboratory simulation," *Journal of Dentistry*, vol. 36, no. 12, pp. 1048–1053, 2008.

[31] E. Yassini, M. Mirzaei, A. Alimi, and M. Rahaeifard, "Investigation of the fatigue behavior of adhesive bonding of the lithium disilicate glass ceramic with three resin cements using rotating fatigue method," *Journal of the Mechanical Behavior of Biomedical Materials*, vol. 61, pp. 62–69, 2016.

[32] R. Frankenberger, V. E. Hartmann, M. Krech et al., "Adhesive luting of new CAD/CAM materials," *International Journal of Computing*, vol. 18, pp. 9–20, 2015.

[33] A. O. Carvalho, G. Bruzi, R. E. Anderson, H. P. Maia, M. Giannini, and P. Magne, "Influence of adhesive core buildup designs on the resistance of endodontically treated molars restored with lithium disilicate CAD/CAM crowns," *Operative Dentistry*, vol. 41, pp. 76–82, 2016.

[34] A. O. Carvalho, G. Bruzi, M. Giannini, and P. Magne, "Fatigue resistance of CAD/CAM complete crowns with a simplified cementation process," *The Journal of Prosthetic Dentistry*, vol. 111, no. 4, pp. 310–317, 2014.

[35] D. O. Dogan, O. Gorler, B. Mutaf, M. Ozcan, G. B. Eyuboglu, and M. Ulgey, "Fracture resistance of molar crowns fabricated with monolithic all-ceramic CAD/CAM materials cemented on titanium abutments: an in vitro study," *Journal of Prosthodontics*, 2015.

[36] T. Joda, A. Bürki, S. Bethge, U. Brägger, and P. Zysset, "Stiffness, strength, and failure modes of implant-supported monolithic lithium disilicate crowns: influence of titanium and zirconia abutments," *The International Journal of Oral & Maxillofacial Implants*, vol. 30, no. 6, pp. 1272–1279, 2015.

[37] C. G. Figueiredo-Pina, N. Patas, J. Canhoto et al., "Tribological behaviour of unveneered and veneered lithium disilicate dental material," *Journal of the Mechanical Behavior of Biomedical Materials*, vol. 53, pp. 226–238, 2016.

[38] N. C. Lawson, S. Janyavula, S. Syklawer, E. A. McLaren, and J. O. Burgess, "Wear of enamel opposing zirconia and lithium disilicate after adjustment, polishing and glazing," *Journal of Dentistry*, vol. 42, no. 12, pp. 1586–1591, 2014.

[39] R. Amer, D. Kürklü, and W. Johnston, "Effect of simulated mastication on the surface roughness of three ceramic systems," *Journal of Prosthetic Dentistry*, vol. 114, no. 2, pp. 260–265, 2015.

[40] A. Lee, M. Swain, L. He, and K. Lyons, "Wear behavior of human enamel against lithium disilicate glass ceramic and type III gold," *Journal of Prosthetic Dentistry*, vol. 112, no. 6, pp. 1399–1405, 2014.

[41] V. Preis, F. Weiser, G. Handel, and M. Rosentritt, "Wear performance of monolithic dental ceramics with different surface treatments," *Quintessence International*, vol. 44, no. 5, pp. 393–405, 2013.

[42] Z. Peng, M. Izzat Abdul Rahman, Y. Zhang, and L. Yin, "Wear behavior of pressable lithium disilicate glass ceramic," *Journal of Biomedical Materials Research Part B: Applied Biomaterials*, vol. 104, no. 5, pp. 968–978, 2016.

[43] W. H. Mörmann, B. Stawarczyk, A. Ender, B. Sener, T. Attin, and A. Mehl, "Wear characteristics of current aesthetic dental restorative CAD/CAM materials: two-body wear, gloss retention, roughness and Martens hardness," *Journal of the Mechanical Behavior of Biomedical Materials*, vol. 20, pp. 113–125, 2013.

[44] B. Stawarczyk, A. Liebermann, M. Eichberger, and J.-F. Güth, "Evaluation of mechanical and optical behavior of current esthetic dental restorative CAD/CAM composites," *Journal of the Mechanical Behavior of Biomedical Materials*, vol. 55, pp. 1–11, 2015.

[45] C. A. Neis, N. L. G. Albuquerque, I. de Souza Albuquerque et al., "Surface treatments for repair of feldspathic, leucite- and lithium disilicate-reinforced glass ceramics using composite resin," *Brazilian Dental Journal*, vol. 26, no. 2, pp. 152–155, 2015.

[46] E. Anadioti, S. A. Aquilino, D. G. Gratton et al., "3D and 2D marginal fit of pressed and CAD/CAM lithium disilicate crowns made from digital and conventional impressions," *Journal of Prosthodontics*, vol. 23, no. 8, pp. 610–617, 2014.

[47] F. D. Neves, C. J. Prado, M. S. Prudente et al., "Micro-computed tomography evaluation of marginal fit of lithium disilicate crowns fabricated by using chairside CAD/CAM systems or the heat-pressing technique," *Journal of Prosthetic Dentistry*, vol. 112, no. 5, pp. 1134–1140, 2014.

[48] J. Ng, D. Ruse, and C. Wyatt, "A comparison of the marginal fit of crowns fabricated with digital and conventional methods," *Journal of Prosthetic Dentistry*, vol. 112, no. 3, pp. 555–560, 2014.

[49] E. Anadioti, S. A. Aquilino, D. G. Gratton et al., "Internal fit of pressed and computer-aided design/computer-aided manufacturing ceramic crowns made from digital and conventional impressions," *Journal of Prosthetic Dentistry*, vol. 113, no. 4, pp. 304–309, 2015.

[50] D. P. Alfaro, N. D. Ruse, R. M. Carvalho, and C. C. Wyatt, "Assessment of the internal fit of lithium disilicate crowns using micro-CT," *Journal of Prosthodontics*, vol. 24, no. 5, pp. 381–386, 2015.

[51] T. Abdel-Azim, K. Rogers, E. Elathamna, A. Zandinejad, M. Metz, and D. Morton, "Comparison of the marginal fit of lithium disilicate crowns fabricated with CAD/CAM technology by using conventional impressions and two intraoral digital scanners," *Journal of Prosthetic Dentistry*, vol. 114, no. 4, pp. 554–559, 2015.

[52] O. Schaefer, M. Decker, F. Wittstock, H. Kuepper, and A. Guentsch, "Impact of digital impression techniques on the adaption of ceramic partial crowns in vitro," *Journal of Dentistry*, vol. 42, no. 6, pp. 677–683, 2014.

[53] M.-K. Ji, J.-H. Park, S.-W. Park, K.-D. Yun, G.-J. Oh, and H.-P. Lim, "Evaluation of marginal fit of 2 CAD-CAM anatomic contour zirconia crown systems and lithium disilicate glass-ceramic crown," *Journal of Advanced Prosthodontics*, vol. 7, no. 4, pp. 271–277, 2015.

[54] S.-J. Nam, M.-J. Yoon, W.-H. Kim, G.-J. Ryu, M.-K. Bang, and J.-B. Huh, "Marginal and internal fit of conventional metal-ceramic and lithium disilicate CAD/CAM crowns," *The International Journal of Prosthodontics*, vol. 28, no. 5, pp. 519–521, 2015.

[55] P. C. Guess, T. Vagkopoulou, Y. Zhang, M. Wolkewitz, and J. R. Strub, "Marginal and internal fit of heat pressed versus CAD/CAM fabricated all-ceramic onlays after exposure to thermo-mechanical fatigue," *Journal of Dentistry*, vol. 42, no. 2, pp. 199–209, 2014.

[56] H. A. Mously, M. Finkelman, R. Zandparsa, and H. Hirayama, "Marginal and internal adaptation of ceramic crown restorations fabricated with CAD/CAM technology and the heat-press technique," *Journal of Prosthetic Dentistry*, vol. 112, no. 2, pp. 249–256, 2014.

[57] R. L. W. Messer, P. E. Lockwood, J. C. Wataha, J. B. Lewis, S. Norris, and S. Bouillaguet, "In vitro cytotoxicity of traditional versus contemporary dental ceramics," *Journal of Prosthetic Dentistry*, vol. 90, no. 5, pp. 452–458, 2003.

[58] S. Tetè, V. L. Zizzari, B. Borelli et al., "Proliferation and adhesion capability of human gingival fibroblasts onto Zirconia, lithium disilicate and feldspathic veneering ceramic in vitro," *Dental Materials Journal*, vol. 33, no. 1, pp. 7–15, 2014.

[59] A. Forster, K. Ungvári, Á. Györgyey, Á. Kukovecz, K. Turzó, and K. Nagy, "Human epithelial tissue culture study on restorative materials," *Journal of Dentistry*, vol. 42, no. 1, pp. 7–14, 2014.

[60] R. W. K. Li, T. W. Chow, and J. P. Matinlinna, "Ceramic dental biomaterials and CAD/CAM technology: state of the art," *Journal of Prosthodontic Research*, vol. 58, no. 4, pp. 208–216, 2014.

[61] K. Ariaans, N. Heussen, H. Schiffer et al., "Use of molecular indicators of inflammation to assess the biocompatibility of all-ceramic restorations," *Journal of Clinical Periodontology*, vol. 43, no. 2, pp. 173–179, 2016.

[62] S. Toksavul and M. Toman, "A short-term clinical evaluation of IPS empress 2 crowns," *International Journal of Prosthodontics*, vol. 20, no. 2, pp. 168–172, 2007.

[63] P. Marquardt and J. R. Strub, "Survival rates of IPS Empress 2 all-ceramic crowns and fixed partial dentures: results of a 5-year prospective clinical study," *Quintessence International*, vol. 37, no. 4, pp. 253–259, 2006.

[64] J. H. Kim, S.-J. Lee, J. S. Park, and J. J. Ryu, "Fracture load of monolithic CAD/CAM lithium disilicate ceramic crowns and veneered zirconia crowns as a posterior implant restoration," *Implant Dentistry*, vol. 22, no. 1, pp. 66–70, 2013.

[65] N. R. F. A. Silva, V. P. Thompson, G. B. Valverde et al., "Comparative reliability analyses of zirconium oxide and lithium disilicate restorations in vitro and in vivo," *Journal of the American Dental Association (1939)*, vol. 142, supplement 2, pp. 4S–9S, 2011.

[66] J. F. Esquivel-Upshaw, K. J. Anusavice, H. Young, J. Jones, and C. Gibbs, "Clinical performance of a lithia disilicate-based core

ceramic for three-unit posterior FPDs," *International Journal of Prosthodontics*, vol. 17, no. 4, pp. 469–475, 2004.

[67] P. Simeone and S. Gracis, "Eleven-year retrospective survival study of 275 veneered lithium disilicate single crowns," *The International Journal of Periodontics and Restorative Dentistry*, vol. 35, no. 5, pp. 685–694, 2015.

[68] M. Valenti and A. Valenti, "Retrospective survival analysis of 110 lithium disilicate crowns with feather-edge marginal preparation," *The International Journal of Esthetic Dentistry*, vol. 10, no. 2, pp. 246–257, 2015.

[69] P. C. Guess, C. F. Selz, Y.-N. Steinhart, S. Stampf, and J. R. Strub, "Prospective clinical split-mouth study of pressed and CAD/CAM all-ceramic partial-coverage restorations: 7-year results," *The International Journal of Prosthodontics*, vol. 26, no. 1, pp. 21–25, 2013.

[70] M. Sasse, A. Krummel, K. Klosa, and M. Kern, "Influence of restoration thickness and dental bonding surface on the fracture resistance of full-coverage occlusal veneers made from lithium disilicate ceramic," *Dental Materials*, vol. 31, no. 8, pp. 907–915, 2015.

[71] B. Taskonak and A. Sertgöz, "Two-year clinical evaluation of lithia-disilicate-based all-ceramic crowns and fixed partial dentures," *Dental Materials*, vol. 22, no. 11, pp. 1008–1013, 2006.

[72] M. Makarouna, K. Ullmann, K. Lazarek, and K. W. Boening, "Six-year clinical performance of lithium disilicate fixed partial dentures," *The International Journal of Prosthodontics*, vol. 24, no. 3, pp. 204–206, 2011.

[73] M. F. Solá-Ruiz, E. Lagos-Flores, J. L. Román-Rodriguez, J. D. R. Highsmith, A. Fons-Font, and M. Granell-Ruiz, "Survival rates of a lithium disilicate-based core ceramic for three-unit esthetic fixed partial dentures: a 10-year prospective study," *The International Journal of Prosthodontics*, vol. 26, no. 2, pp. 175–180, 2013.

[74] P. C. Guess, R. A. Zavanelli, N. R. Silva, E. A. Bonfante, P. Coehlo, and V. P. Thompson, "Monolithic CAD/CAM lithium dislocate versus veneered Y-TZP crowns: comparison of failure modes and reliability after fatigue," *The International Journal of Prosthodontics*, vol. 23, pp. 434–442, 2010.

[75] K. Zhao, Y. Pan, P. C. Guess, X.-P. Zhang, and M. V. Swain, "Influence of veneer application on fracture behavior of lithium-disilicate-based ceramic crowns," *Dental Materials*, vol. 28, no. 6, pp. 653–660, 2012.

[76] B. E. Pjetursson, U. Brägger, N. P. Lang, and M. Zwahlen, "Comparison of survival and complication rates of tooth-supported fixed dental prostheses (FDPs) and implant-supported FDPs and single crowns (SCs)," *Clinical Oral Implants Research*, vol. 18, no. 3, pp. 97–113, 2007.

[77] C. A. Barwacz, M. Hernandez, and R. H. Husemann, "Minimally invasive preparation and design of a cantilevered, all-ceramic, resin-bonded, fixed partial denture in the esthetic zone: a case report and descriptive review," *Journal of Esthetic and Restorative Dentistry*, vol. 26, no. 5, pp. 314–323, 2014.

[78] M. Sasse, S. Eschbach, and M. Kern, "Randomized clinical trial on single retainer all-ceramic resin-bonded fixed partial dentures: influence of the bonding system after up to 55 months," *Journal of Dentistry*, vol. 40, no. 9, pp. 783–786, 2012.

[79] Q. Sun, L. Chen, L. Tian, and B. Xu, "Single-tooth replacement in the anterior arch by means of a cantilevered IPS e.max Press veneer-retained fixed partial denture: case series of 35 patients," *The International Journal of Prosthodontics*, vol. 26, no. 2, pp. 181–187, 2013.

[80] M. Foitzik, A. M. Lennon, and T. Attin, "Successful use of a single-retainer all-ceramic resin-bonded fixed partial denture for replacement of a maxillary canine: a clinical report," *Quintessence International*, vol. 38, no. 3, pp. 241–246, 2007.

[81] S. Reich and O. Schierz, "Chair-side generated posterior lithium disilicate crowns after 4 years," *Clinical Oral Investigations*, vol. 17, no. 7, pp. 1765–1772, 2013.

[82] T. A. Sulaiman, A. J. Delgado, and T. E. Donovan, "Survival rate of lithium disilicate restorations at 4 years: a retrospective study," *Journal of Prosthetic Dentistry*, vol. 114, no. 3, pp. 364–366, 2015.

[83] T. Albrecht, A. Kirsten, H. F. Kappert, and H. Fischer, "Fracture load of different crown systems on zirconia implant abutments," *Dental Materials*, vol. 27, no. 3, pp. 298–303, 2011.

[84] L. F. Cooper, C. Stanford, J. Feine, and M. McGuire, "Prospective assessment of CAD/CAM zirconia abutment and lithium disilicate crown restorations: 2.4 year results," *The Journal of Prosthetic Dentistry*, vol. 116, no. 1, pp. 33–39, 2016.

[85] A. Pozzi, M. Tallarico, and A. Barlattani, "Monolithic lithium disilicate full-contour crowns bonded on CAD/CAM zirconia complete-arch implant bridges with 3 to 5 years of follow-up," *Journal of Oral Implantology*, vol. 41, no. 4, pp. 450–458, 2015.

Hindawi Publishing Corporation
International Journal of Dentistry
Volume 2016, Article ID 7358423, 7 pages
http://dx.doi.org/10.1155/2016/7358423

Clinical Study

From Guided Surgery to Final Prosthesis with a Fully Digital Procedure: A Prospective Clinical Study on 15 Partially Edentulous Patients

Giorgio Andrea Dolcini,[1] Marco Colombo,[2] and Carlo Mangano[3]

[1]*Private Practice, 21100 Como, Italy*
[2]*Private Practice, 21052 Busto Arsizio, Italy*
[3]*Department of Dental Sciences, University Vita Salute San Raffaele, 20132 Milan, Italy*

Correspondence should be addressed to Giorgio Andrea Dolcini; giorgio.dolcini@hotmail.it

Received 20 March 2016; Accepted 19 June 2016

Academic Editor: Thomas Fortin

Scope. To demonstrate guided implant placement and the application of fixed, implant-supported prosthetic restorations with a fully digital workflow. *Methods.* Over a 2-year period, all patients with partial edentulism of the posterior maxilla, in need of fixed implant-supported prostheses, were considered for inclusion in this study. The protocol required intraoral scanning and cone beam computed tomography (CBCT), the superimposition of dental-gingival information on bone anatomy, surgical planning, 3D-printed teeth-supported surgical templates, and modelling and milling of polymethylmethacrylate (PMMA) temporaries for immediate loading. After 3 months, final optical impression was taken and milled zirconia frameworks and 3D-printed models were fabricated. The frameworks were veneered with ceramic and delivered to the patients. *Results.* Fifteen patients were selected for this study. The surgical templates were stable. Thirty implants were placed (BTK Safe®, BTK, Vicenza, Italy) and immediately loaded with PMMA temporaries. After 3 months, the temporaries were replaced by the final restorations in zirconia-ceramic, fabricated with a fully digital process. At 6 months, none of the patients reported any biological or functional problems with the implant-supported prostheses. *Conclusions.* The present procedure for fully digital planning of implants and short-span fixed implant-supported restorations has been shown to be reliable. Further studies are needed to validate these results.

1. Introduction

Digital workflow has an increasingly important role to play in contemporary dentistry [1, 2].

The advantage of guided implant surgery is that the implant is placed in a safer, more predictable manner, using a surgical template designed and produced using computer-aided-design/computer-aided-manufacturing (CAD/CAM) technology; this prosthetically guided placement is achieved using software for virtual implant planning [2, 3]. Guided implant surgery can also help the dentist to perform flapless implant surgery with less discomfort for the patient and faster working and healing times [2, 3].

Digital scanning and Cone Beam Computer Tomography (CBCT) are the procedures now used for digital workflow for planning guided implant surgery [4, 5]. Taking optical impressions with powerful intraoral scanners for fabricating permanent prostheses on natural teeth and dental implants is becoming widespread and has many advantages over the conventional way of taking impressions, involving less discomfort for the patient, as well as greater speed, accuracy, precision, and reproducibility [6–9]. Optical impression-taking enables collection of all the three-dimensional (3D) information of dentogingival tissues [7, 8]. CBCT on the other hand allows collection all 3D information on the anatomy of the residual crest bone, including height, thickness, and angle [4, 10].

The composition and superimposition of dental and gingival information acquired by intraoral scanning, as well as bone information acquired by CBCT, now allow virtual planning for placing the implants, fabricating the templates

for guided surgery, and modelling and preparing temporaries for immediate loading [11, 12].

The purpose of this study is to demonstrate guided implant placement and the application of fixed, implant-supported prosthetic restorations carried out with fully digital workflow. For this purpose, intraoral scanning techniques, virtual planning, computer guided surgery, and immediate loading protocol for the temporary prostheses have been used.

2. Materials and Methods

2.1. Selection of Patients. In the period between January 2014 and January 2015, all patients seen at two private dental clinics who presented with partially edentulous posterior maxilla and requested restoration of masticatory efficiency with an implant-supported fixed prosthesis were considered for inclusion in this study. The criteria for inclusion consisted of (1) partially edentulous posterior areas (premolars/molars) of the maxilla, (2) sufficient bone for the placing of implants at least 3.75 mm in diameter and 8.0 mm in length, and (3) willingness to participate fully in the protocol. Excluded from the study were (1) patients with systemic diseases having contraindications to implant surgery (e.g., uncontrolled diabetes, blood diseases, and psychiatric illnesses), (2) patients undergoing chemotherapy and/or radiotherapy, (3) patients receiving immunosuppressive therapies, (4) patients being treated with bisphosphonates orally and/or parenterally, (5) patients with active oral or periodontal infections (pus, fistulas, and periodontal abscesses), (6) patients with other oral diseases (vesiculobullous and ulcerative diseases, red and white lesions, and diseases of the salivary glands and cystic lesions), (7) patients with a poor oral hygiene, (8) patients with restricted mouth openings, functional limitations, or temporomandibular disorders, (9) smokers, and (10) bruxists. The protocol for this study was explained in detail to each patient, who signed an informed consent to the implant treatment. The study was carried out in accordance with the protocols established by the 1975 Helsinki Declaration (2008 review).

2.2. Image Acquisition. A full examination of soft and hard tissue was performed on each patient. Specifically, in a single appointment designated exclusively to image acquisition, each patient underwent optical scanning with a powerful intraoral scanner (Trios®, 3-Shape, Copenhagen, Denmark) and X-ray examination with CBCT (CS 9300®, Carestream Health, Rochester, NY, USA). In detail, the first examination that patients underwent was an intraoral scan of both arches, including scanning of the bite. This scan was performed after placing a number of moderately radiopaque markers (at least 3) on the teeth adjacent to the edentulous section, using a modified glass ionomer cement (Ketac Cem Radiopaque®, 3M ESPE, St Paul, MN, USA). Particular care was taken when scanning the teeth adjacent to the edentulous section and surrounding soft tissue. The patient underwent a CBCT scan immediately after, with the radiopaque markers still in place. A field of view (FOV) of 10 × 5 cm was adopted, to enable a sufficient amount of data to be collected that could also be superimposed. At this point, the owners' files generated by the intraoral scan and the Digital Imaging and Communication in Medicine (DICOM) files generated by the CBCT were transformed into solid-to-layer files (STL) and sent to a service centre (BTK Guided Surgery®, BTK, Dueville, Vicenza, Italy), for the case to be planned. The patient was then discharged after removal of the radiopaque markers.

2.3. Image Processing and the Guided Surgery Project. The STL files obtained from intraoral scanning were superimposed on the STL files obtained from the reconstruction of CBCT with proprietary software (BTK Guided Implant Planning®, BTK, Dueville, Vicenza, Italy) for guided surgery planning. Superimposition was obtained as follows. First, the intraoral scan model was roughly superimposed to the CBCT model using a "three-point" registration tool. After this first rough alignment, the final registration was performed using a "best fit alignment" function. The resulting superimposed models were then used to design teeth-supported surgical templates. The placing of the implants was thus planned virtually, taking into account the position, depth, and angle inside the residual bone crest, and we then proceeded to model the immediate temporary prostheses to be placed *in situ* on the day of the surgery. The planning was sent to the dentist for approval and implementation of any modifications required. Once the plan was confirmed and checked, the service centre physically fabricated the templates for the guided surgery in transparent acrylic resin using 3D printing; the temporary prostheses were milled from polymethylmethacrylate (PMMA). The prostheses were delivered to the dentist together with the guided implant surgery kit, the provisional titanium abutments, and the surgical guides or templates for implant placement.

2.4. Surgery and Immediate Loading. Before the operation the patient's mouth was rinsed with a solution of chlorhexidine digluconate 0.2% for 2 minutes. A local anesthetic was obtained with mepivacaine (4% infiltration with epinephrine 1 : 100,000). The teeth-supported surgical template was positioned and the intervention was ready to begin. The surgery was performed with a minimally invasive flapless procedure, without lifting the mucoperiosteal flap. The first step was to remove tissue overgrowth with a punch to allow access to the underlying bony crest, proceeding to preparation of the implant sites using drills of increasing diameters, guided in terms of placement, angle, and depth by the surgical guide. In particular, control of the angle and depth was achieved with a series of diameter reducers positioned inside the drill bushing. In effect, as the size of the drill increased, the diameter reducers were changed until the final diameter was reached, as determined in the surgery planning. Only internal hex implants were used (BTK Safe, BTK, Dueville, Vicenza, Italy), with a diameter of 3.75 mm and length of 8.0 mm, 10.0 mm, or 12.0 mm. Insertion of the implant, clamping, and tightening were performed with a torque wrench through the template, hence with the surgical guide in position. On completion of implant placement the guide was removed from the oral cavity. The dentist was able to check the depth of the implants

in relation to the mucosa. X-rays of the intraoral implants were taken straight away and the temporary titanium abutments and temporary PMMA restorations were adjusted. The restorations were positioned without the need for relining. Once any slight frictions were removed, the restorations were polished and screwed onto the abutments. The occlusal access hole was provisionally closed with composite resin. The occlusion was carefully checked using occlusal registration paper. The patient was then discharged with a prescription for antibiotics (amoxicillin clavulanic acid, 1 g every 12 hours for a total of 6 days) and analgesic (ibuprofen 600 mg for a total of three days). The patient was asked to rinse with chlorhexidine gluconate 0.2% 2-3 times a day for 4-5 days following the surgery and to avoid chewing hard foods for a period of 1 week.

2.5. Final Prosthesis. The PMMA temporaries were left in place for a total period of 3 months; after this, the patients were recalled for a second round of intraoral imaging, required for modelling and fabrication of the final prostheses. This scan was performed after removing the temporary restorations and abutments and subsequent positioning of scanbodies in polyether-ether-ketone (PEEK). These transfer devices were employed for their ideal optical characteristics, since they do not reflect light as metals do and therefore allow the exact position of the implants to be detected. The abutments and temporary prostheses were then replaced and the patient was discharged. The final scan was then converted into an STL file which was sent to the laboratory and used to determine the exact spatial location of the implants and planning of the final prosthetic structure (zirconia framework). The framework was milled in zirconia, tried in a model of the patient's mouth created with a 3D printer, and sent to the clinician for trying in the oral cavity. The model was 3D-printed in resin. During the trial, the dentist was able to assess the quality of marginal fit of the zirconia framework on the final abutments. At this point the framework was sent back to the laboratory for finalisation, that is, veneering with ceramic. The patient was called in one week later to have the final, zirconia-ceramic restoration delivered. Occlusion was checked using registration papers, and the patient was then discharged with his/her final restoration, which was cemented onto the screw-in abutments with a small amount of zinc oxide eugenol cement.

3. Results

Fifteen patients (10 males and 5 females, aged between 26 and 70 years, average age 51.5 ± 12.0) requesting oral rehabilitation with fixed, implant-supported prostheses in the posterior region of the maxilla were selected and recruited to participate in this prospective clinical study. Following an image-capturing procedure using intraoral scanning and CBCT, the surgical planning was done with dedicated software. Surgical guides were then fabricated for placing the implants using 3D printing; temporary protheses for immediate loading were milled in PMMA. Each patient received two implants through a guided surgical procedure, with placement of the temporary prosthesis at the same surgical session and immediate loading. The surgical guides were easily positioned on the supporting teeth and were sufficiently stable. In all, 30 implants were placed using a flapless procedure. The implants were immediately loaded with fixed partial prostheses made of PMMA. These prostheses were easily adjusted on temporary titanium abutments, which were screwed in and remained *in situ* for a total period of three months. In the week following the intervention, the patients did not report any postsurgical discomfort or pain and were extremely pleased with both the aesthetic and functional aspects of the loaded restorations. At the end of the temporary period, the final optical impression was taken and frameworks were milled from zirconia, and 3D-printed resin models were fabricated. The frameworks were found to be sufficiently accurate at an intraoral test and were returned to the technician for ceramic coating and aesthetic finalisation. After 1 week, the zirconia-ceramic prostheses were delivered to the patient and cemented onto the permanent titanium abutments. At a follow-up check 6 months later, no patient reported having had any problems or biological or functional complications resulting from the implant-supported restorations. All the prostheses were functioning and patients were all extremely satisfied (Figures 1–4).

4. Discussion

The ability to plan the insertion of dental implants virtually and subsequently place the fixtures in the exact position at the desired depth and angle using accurately milled or 3D-printed surgical guides has long been a clinical reality [2, 3, 5, 12]. Guided surgery has been a successful procedure for over 10 years, as evidenced by several clinical studies [12, 13] and systematic reviews [3, 14, 15]. Initially, the use of guided surgery techniques was limited to complex cases (patients who were fully edentulous, with manufacture of bone-supported or mucosa-supported templates); in fact, in order to obtain bone anatomy information, the patient had to be subjected to conventional computerised axial tomography (CT scanning), involving exposure to significant amounts of ionising radiation [3, 14, 15].

This is all changed now. The introduction of cone beam computed tomography (CBCT), which can capture 3D information on bone anatomy with low doses of radiation, has greatly expanded the potential applications of guided surgery [4, 16]. These applications now extend to teeth-supported surgical guides and therefore to cases where the planning requires placement of a lower number of fixtures. The introduction of intraoral scanners, powerful tools for obtaining dental and gingival information, is a further development in available techniques for capturing images for surgical planning [6–9]. In fact these machines enable all the dental and gingival information required to be obtained with a beam of light [7, 8] and with an accuracy, precision, and image resolution significantly higher than that obtained from CT (and even CBCT). The information obtained can be easily combined and superimposed on bone architecture information, thanks to open reverse-engineering software or proprietary software [11, 12]. It is therefore possible to create a virtual model of the patient, containing all the information required

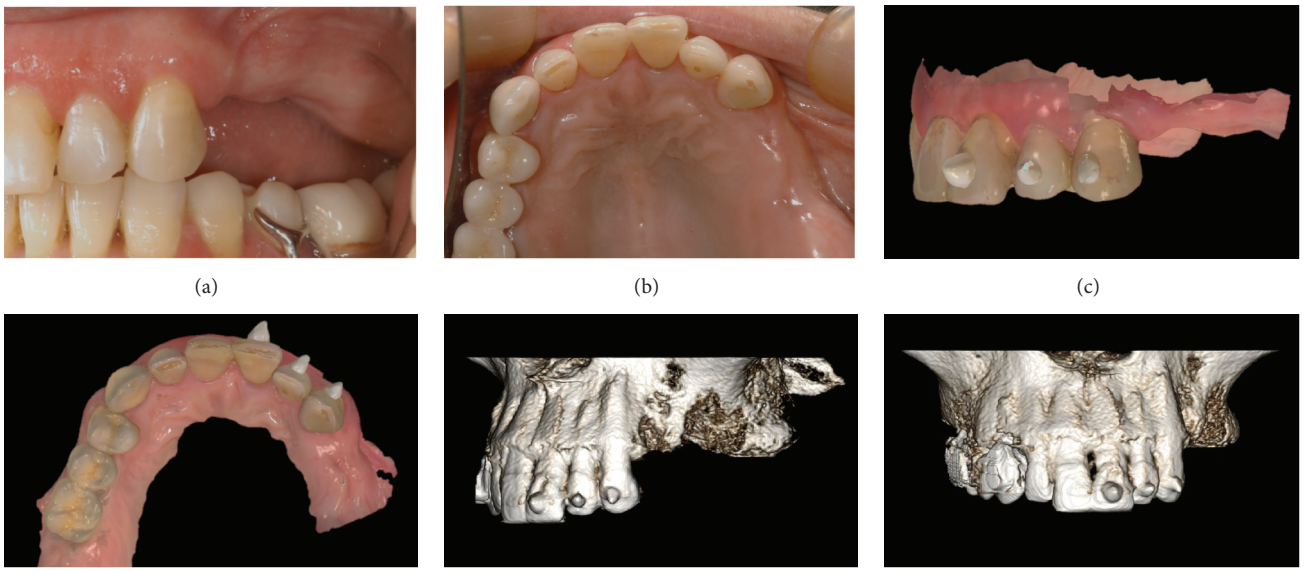

(a) (b) (c)

(d) (e) (f)

Figure 1: Image acquisition: (a) preoperative clinical picture, side view; (b) preoperative clinical picture, occlusal view; (c) intraoral scan with references, side view; (d) intraoral scan with references, occlusal view; (e) CBCT volume rendering with references, side view; (f) CBCT volume rendering with references, frontal view.

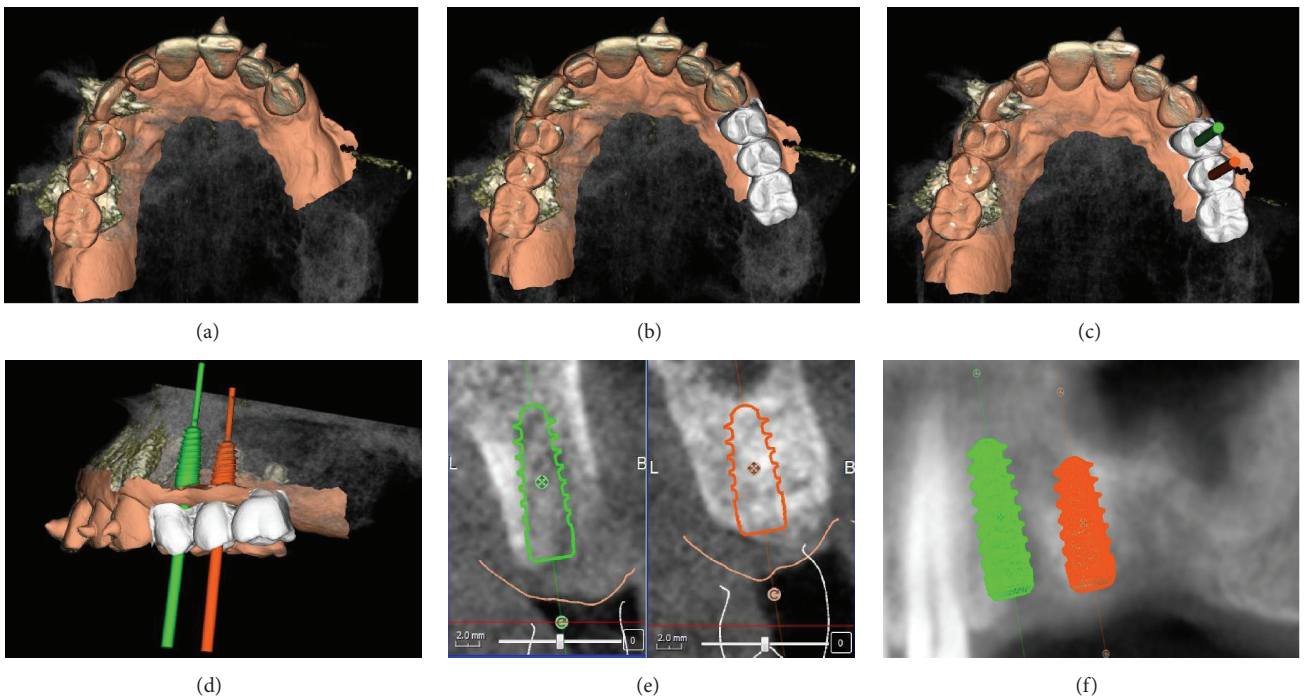

(a) (b) (c)

(d) (e) (f)

Figure 2: Surgical and prosthetic 3D planning: (a) overlapping of intraoral scan and CBCT; (b) overlapping of intraoral scan and CBCT with modelled provisional restorations; (c) overlapping of intraoral scan and CBCT with modelled provisional restoration and implant planning (occlusal view); (d) overlapping of intraoral scan and CBCT with modelled provisional restoration and implant planning (side view); (e) implant planning (cross sections); (f) implant planning (panorex).

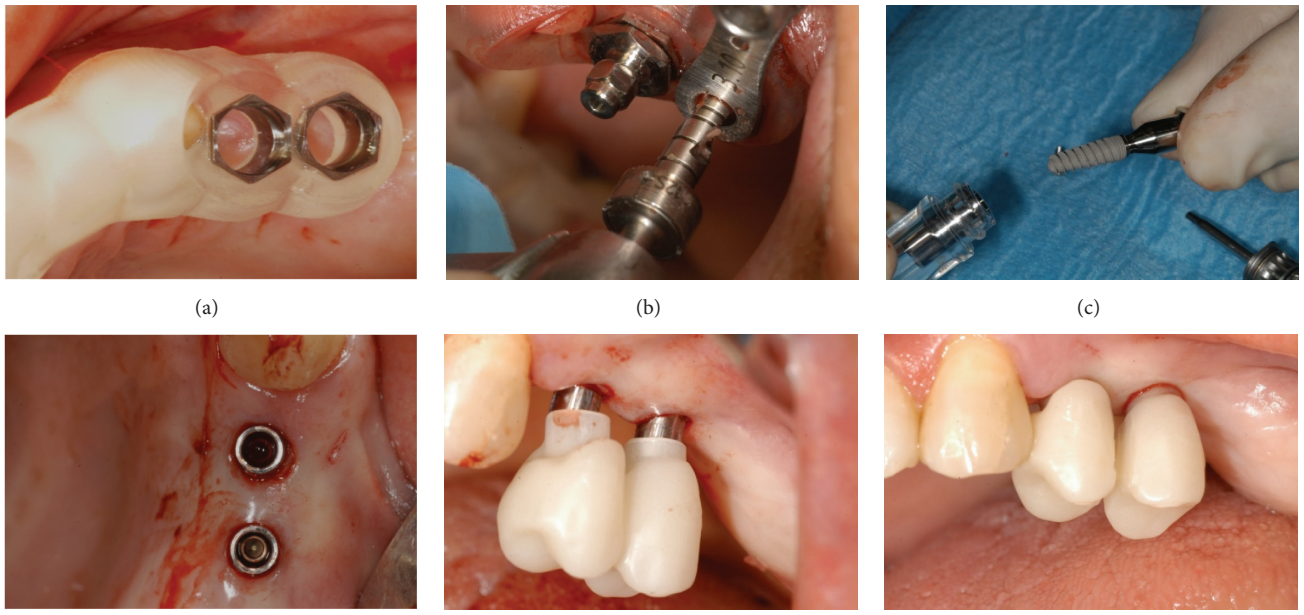

(a) (b) (c)

(d) (e) (f)

Figure 3: Surgery and immediate provisionalization: (a) the surgical guide in position; (b) preparation of the surgical sites; (c) implant placement; (d) all implants are placed with a flapless procedure; (e) the provisional PMMA restoration is placed on the temporary titanium abutments; (f) the provisional PMMA is screwed on the implants.

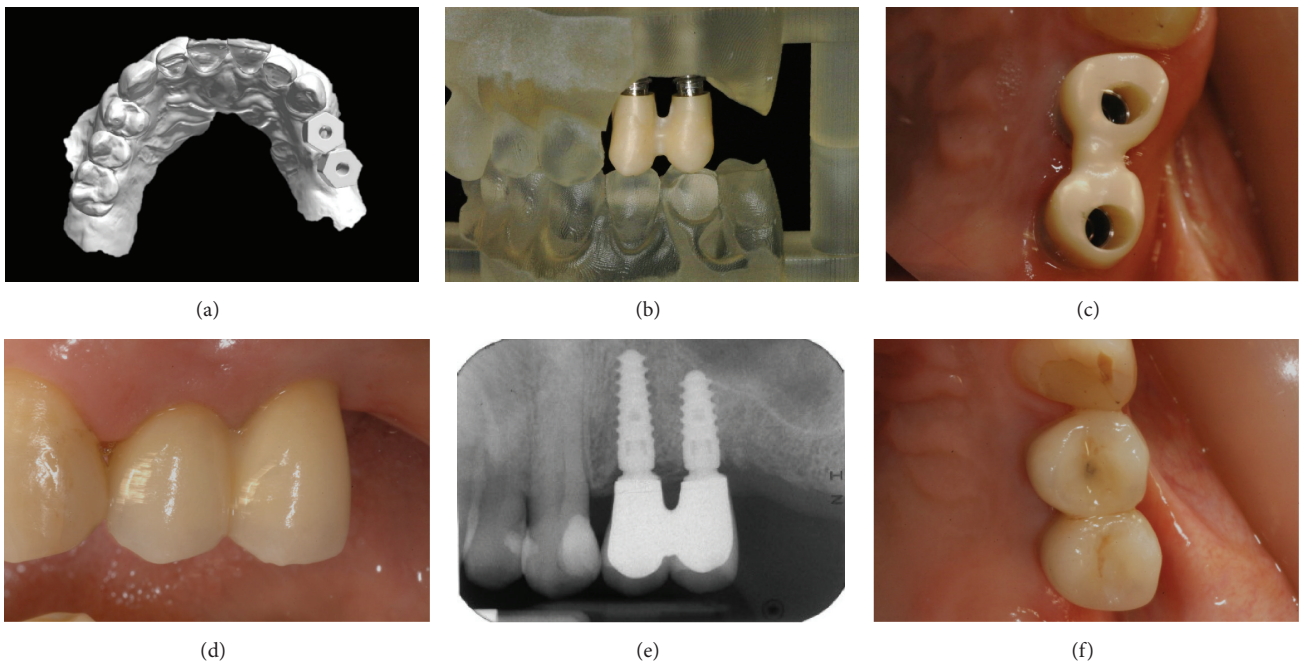

(a) (b) (c)

(d) (e) (f)

Figure 4: Three months after implant placement, the definitive intraoral impression is taken, and the definitive implant-supported restoration is fabricated and delivered to the patient: (a) digital impression with PEEK scanbodies; (b) the 3D-printed model with the zirconia framework; (c) the zirconia framework is seated on the definitive titanium abutments and checked for accuracy/precision (occlusal view); (d) delivery of the final zirconia-ceramic restoration, cemented on the final titanium abutments (side view); (e) periapical radiograph at the delivery of the final implant-supported restoration; (f) 6-month control of the final zirconia-ceramic restoration (occlusal view).

(bone, tooth, and gum) to carry out the intervention for implant placement using surgical guides supported on the teeth [12].

For this prospective study, 15 patients were selected and treated with insertion of 30 implant fixtures using guided surgical procedures. The 3D-printed surgical guides were sufficiently stable, and the interventions proceeded quickly and smoothly using a flapless technique. The potential to operate without lifting the flap is the major biological advantage to guided surgery, resulting in immediate benefit for the patient [17, 18]. Postoperative inconvenience and discomfort are substantially reduced, even eliminated entirely, using the flapless method [18]. The implants were placed without difficulty and immediately loaded with temporary PMMA prostheses obtained by milling; these prostheses were sent to the dentist before surgery and placement of the implants. The ability to load implants immediately is a further major advantage of the method used in this study. The adjustment of preformed shells and temporaries can be time-consuming in conventional procedures for immediate loading [19]; the time it takes to reline, adapt, refine, and polish the temporary restorations necessarily entails discomfort for the patient, who needs to go home and rest after the surgery [20, 21]. Modern implant and prosthetic planning techniques can greatly reduce operating times, as in this study, where the temporary PMMA restorations were placed easily with no need for relining and often requiring only minor adjustment. The temporaries remained *in situ* for a total period of 3 months and were subsequently replaced with permanent ceramic-zirconia prostheses.

The implants were manufactured using a fully digital process. A second round of intraoral imaging was carried out after positioning modern transfer devices (scanbodies) made of an opaque material [22–24] in the mouth. These devices allowed the exact location of the implants to be transmitted to the virtual plan, to enable computer-assisted design (CAD) of the prosthetic structures (frameworks) in zirconia. Subsequently the zirconia structures were milled [25] and then tried in the mouth. After the trial, the technician could then apply ceramic to the structures with the aid of a 3D-printed resin model. The devices were delivered and adjusted for aesthetic and functional requirements, to the complete satisfaction of the patients. At the 6-month check-up, no problems of any biological or prosthetic nature were reported and all restorations were functional and under load.

This study is subject to limitations. First, the number of treated patients (and consequently the number of implants placed) was rather restricted; also, the patients were only checked 6 months after placing the permanent restorations. Further studies are certainly required to validate this technique for planning implants. Last but not least, the use of this technique for guided surgery is limited by the size of the mouth opening. It was not possible to apply the technique to all patients since the surgical instrumentation is bulky, and not all patients have a large enough opening to allow implants to be placed, especially in the molar area, and for this reason they were excluded from the study. New methods will no doubt be developed that are not restricted by problems of space, which will therefore enable the application of guided surgery techniques to be extended to all patients. Finally, the stability of 3D-printed surgical guides can still be a problem. Although their stability was satisfactory in this analysis, at least ideally, the surgical teeth-supported guides should rest on the teeth at certain points; the greater the area of support, in fact, the more complex it can be to obtain the perfect fit (e.g., on the occlusal surface). The elimination of undercuts is of great importance, and the size of the guide should be as reduced as possible, to avoid problems caused by contraction of the material over time, which can cause problematic misfits.

Nevertheless, this study has shown that it is now possible to plan and implement short-span prostheses supported by implants with a fully digital process, using surgical planning. This allows optimum placing of implants, reducing the risks linked with surgical intervention and the time it takes. Postoperative discomfort for the patient is greatly reduced by using the flapless method. The full digital process also allows significant time savings for the patient and the practitioner, resulting in reduced [26, 27] costs.

5. Conclusions

In this study we have presented a fully digital method for the guided placing of implants in the posterior region of the maxilla of 15 patients and the subsequent fabrication of implant-supported fixed prostheses. In all, 30 implants were placed using a flapless procedure. The surgical guides were easily positioned on the supporting teeth and were sufficiently stable. The implants were immediately loaded with fixed partial prostheses made of PMMA. These prostheses were easily adjusted on temporary titanium abutments, which were screwed in and remained *in situ* for a total period of three months. At the end of the temporary period, a final optical impression was taken, frameworks were milled from zirconia, and 3D-printed resin models were fabricated. The frameworks were then coated with ceramic and delivered to the patients. At a follow-up check 6 months later, no patient reported having had any problems or biological or functional complications resulting from the implant-supported restorations. All the prostheses were functioning and patients were all extremely satisfied. The study is subject to limitations (small number of patients and implants, short follow-up period), and further studies will be needed to validate the method presented here.

Competing Interests

The authors report no conflict of interests for the present study.

References

[1] T. Joda and U. Brägger, "Complete digital workflow for the production of implant-supported single-unit monolithic crowns," *Clinical Oral Implants Research*, vol. 25, no. 11, pp. 1304–1306, 2014.

[2] M. A. Mora, D. L. Chenin, and R. M. Arce, "Software tools and surgical guides in dental-implant-guided surgery," *Dental Clinics of North America*, vol. 58, no. 3, pp. 597–626, 2014.

[3] R. E. Jung, D. Schneider, J. Ganeles et al., "Computer technology applications in surgical implant dentistry: a systematic review," *The International Journal of Oral & Maxillofacial Implants*, vol. 24, pp. 92–109, 2009.

[4] W. J. van der Meer, F. S. Andriessen, D. Wismeijer, and Y. Ren, "Application of intra-oral dental scanners in the digital workflow of implantology," *PLoS ONE*, vol. 7, no. 8, Article ID e43312, 2012.

[5] J. Neugebauer, G. Stachulla, L. Ritter et al., "Computer-aided manufacturing technologies for guided implant placement," *Expert Review of Medical Devices*, vol. 7, no. 1, pp. 113–129, 2010.

[6] M. Zimmermann, A. Mehl, W. H. Mörmann, and S. Reich, "Intraoral scanning systems—a current overview," *International Journal of Computerized Dentistry*, vol. 18, no. 2, pp. 101–129, 2015.

[7] E. Yuzbasioglu, H. Kurt, R. Turunc, and H. Bilir, "Comparison of digital and conventional impression techniques: evaluation of patients' perception, treatment comfort, effectiveness and clinical outcomes," *BMC Oral Health*, vol. 14, article 10, 2014.

[8] S. B. M. Patzelt, C. Lamprinos, S. Stampf, and W. Att, "The time efficiency of intraoral scanners: an in vitro comparative study," *Journal of the American Dental Association*, vol. 145, no. 6, pp. 542–551, 2014.

[9] S. Ting-shu and S. Jian, "Intraoral digital impression technique: a review," *Journal of Prosthodontics*, vol. 24, no. 4, pp. 313–321, 2015.

[10] S. P. Arunyanak, B. T. Harris, G. T. Grant, D. Morton, and W. S. Lin, "Digital approach to planning computer-guided surgery and immediate provisionalization in a partially edentulous patient," *The Journal of Prosthetic Dentistry*, 2016.

[11] J.-H. Lee, "Intraoral digital impression for fabricating a replica of an implant-supported interim prosthesis," *Journal of Prosthetic Dentistry*, vol. 115, no. 2, pp. 145–149, 2016.

[12] N. van Assche, M. Vercruyssen, W. Coucke, W. Teughels, R. Jacobs, and M. Quirynen, "Accuracy of computer-aided implant placement," *Clinical Oral Implants Research*, vol. 23, supplement 6, pp. 112–123, 2012.

[13] M. Daas, A. Assaf, K. Dada, and J. Makzoumé, "Computer-guided implant surgery in fresh extraction sockets and immediate loading of a full arch restoration: a 2-year follow-up study of 14 consecutively treated patients," *International Journal of Dentistry*, vol. 2015, Article ID 824127, 10 pages, 2015.

[14] J. D'Haese, T. van de Velde, A. Komiyama, M. Hultin, and H. de Bruyn, "Accuracy and complications using computer-designed stereolithographic surgical guides for oral rehabilitation by means of dental implants: a review of the literature," *Clinical Implant Dentistry and Related Research*, vol. 14, no. 3, pp. 321–335, 2012.

[15] S. D. Ganz, "Three-dimensional imaging and guided surgery for dental implants," *Dental Clinics of North America*, vol. 59, no. 2, pp. 265–290, 2015.

[16] A. Al-Okshi, C. Lindh, H. Salé, M. Gunnarsson, and M. Rohlin, "Effective dose of cone beam CT (CBCT) of the facial skeleton: a systematic review," *British Journal of Radiology*, vol. 88, no. 1045, Article ID 20140658, 2015.

[17] M. Vercruyssen, T. Fortin, G. Widmann, R. Jacobs, and M. Quirynen, "Different techniques of static/dynamic guided implant surgery: modalities and indications," *Periodontology 2000*, vol. 66, no. 1, pp. 214–227, 2014.

[18] T. Fortin, J. L. Bosson, M. Isidori, and E. Blanchet, "Effect of flapless surgery on pain experienced in implant placement using an image-guided system," *International Journal of Oral and Maxillofacial Implants*, vol. 21, no. 2, pp. 298–304, 2006.

[19] D. Farronato, F. Mangano, F. Briguglio, V. Iorio-Siciliano, F. Riccitiello, and R. Guarnieri, "Influence of Laser-Lok surface on immediate functional loading of implants in single-tooth replacement: a 2-year prospective clinical study," *The International Journal of Periodontics & Restorative Dentistry*, vol. 34, no. 1, pp. 79–89, 2014.

[20] F. Mangano, S. Pozzi-Taubert, P. A. Zecca, G. Luongo, R. L. Sammons, and C. Mangano, "Immediate restoration of fixed partial prostheses supported by one-piece narrow-diameter selective laser sintering implants: a 2-year prospective study in the posterior jaws of 16 patients," *Implant Dentistry*, vol. 22, no. 4, pp. 388–393, 2013.

[21] H.-L. Wang, Z. Ormianer, A. Palti, M. L. Perel, P. Trisi, and G. Sammartino, "Consensus conference on immediate loading: the single tooth and partial edentulous areas," *Implant Dentistry*, vol. 15, no. 4, pp. 324–333, 2006.

[22] T. Joda, J.-G. Wittneben, and U. Brägger, "Digital implant impressions with the 'Individualized Scanbody Technique' for emergence profile support," *Clinical Oral Implants Research*, vol. 25, no. 3, pp. 395–397, 2014.

[23] T. Wimmer, A. M. Huffmann, M. Eichberger, P. R. Schmidlin, and B. Stawarczyk, "Two-body wear rate of PEEK, CAD/CAM resin composite and PMMA: effect of specimen geometries, antagonist materials and test set-up configuration," *Dental Materials*, vol. 32, no. 6, pp. e127–e136, 2016.

[24] S. Najeeb, M. S. Zafar, Z. Khurshid, and F. Siddiqui, "Applications of polyetheretherketone (PEEK) in oral implantology and prosthodontics," *Journal of Prosthodontic Research*, vol. 60, no. 1, pp. 12–19, 2016.

[25] C. F. Selz, J. Bogler, K. Vach, J. R. Strub, and P. C. Guess, "Veneered anatomically designed zirconia FDPs resulting from digital intraoral scans: preliminary results of a prospective clinical study," *Journal of Dentistry*, vol. 43, no. 12, pp. 1428–1435, 2015.

[26] T. Joda and U. Brägger, "Patient-centered outcomes comparing digital and conventional implant impression procedures: a randomized crossover trial," *Clinical Oral Implants Research*, 2015.

[27] T. Joda and U. Brägger, "Digital vs. conventional implant prosthetic workflows: a cost/time analysis," *Clinical Oral Implants Research*, vol. 26, no. 12, pp. 1430–1435, 2015.

Hindawi Publishing Corporation
International Journal of Dentistry
Volume 2016, Article ID 6282587, 5 pages
http://dx.doi.org/10.1155/2016/6282587

Clinical Study

A New Total Digital Smile Planning Technique (3D-DSP) to Fabricate CAD-CAM Mockups for Esthetic Crowns and Veneers

F. Cattoni,[1] F. Mastrangelo,[1] E. F. Gherlone,[1] and G. Gastaldi[1,2]

[1]*Dental School, Vita Salute University, 20132 Milan, Italy*
[2]*Dental and Maxillofacial Surgery Unit, San Rocco Clinical Institute, Ome, 25050 Brescia, Italy*

Correspondence should be addressed to F. Cattoni; cattonif@tiscalinet.it

Received 5 April 2016; Revised 31 May 2016; Accepted 1 June 2016

Academic Editor: Jamil A. Shibli

Purpose. Recently, the request of patients is changed in terms of not only esthetic but also previsualization therapy planning. The aim of this study is to evaluate a new 3D-CAD-CAM digital planning technique that uses a total digital smile process. *Materials and Methods.* Study participants included 28 adult dental patients, aged 19 to 53 years, with no oral, periodontal, or systemic diseases. For each patient, 3 intra- and extraoral pictures and intraoral digital impressions were taken. The digital images improved from the 2D Digital Smile System software and the scanner stereolithographic (STL) file was matched into the 3D-Digital Smile System to obtain a virtual previsualization of teeth and smile design. Then, the mockups were milled using a CAM system. Minimally invasive preparation was carried out on the enamel surface with the mockups as position guides. *Results.* The patients found both the digital smile design previsualization (64.3%) and the milling mockup test (85.7%) very effective. *Conclusions.* The new total 3D digital planning technique is a predictably and minimally invasive technique, allows easy diagnosis, and improves the communication with the patient and helps to reduce the working time and the errors usually associated with the classical prosthodontic manual step.

1. Introduction

In recent years, the concept of what makes a smile beautiful has changed significantly [1, 2]. Nowadays, patients expect complex functional rehabilitations that are esthetically appealing [2–5]. An important goal in prosthodontic is to use minimally invasive treatment to improve the appearance of the smile [3–6] as a way to valorize the entire image of the patient [7] while maintaining the health and function of teeth and soft tissue [8, 9].

Porcelain laminate veneers (PLVs), minimally invasive solutions to dental esthetic problems, have the most long-term success [7, 10–14]. There are a number of stages in rehabilitative dental treatment, from making the impression and developing the model to creating the diagnostic wax-up and to constructing the laboratory mockup. The planning associated with creating a mockup is a very important as it affects patients' understanding of the expected result [15, 16]. Whether the patient is happy with the overall treatment depends on how similar the prosthesis is to the mockup [17, 18]. The shape of the teeth, the adaptation of the prosthesis, and the size and the color of the new elements in relation to the soft tissue, lips, and the whole face are very important in the decision-making [19].

A large number of errors can occur at the various stages of the traditional prosthetic workflow, each stage requires a transfer of two-dimensional and three-dimensional (3D) data between operators. As computer-aided design and computer-aided manufacturing (CAD/CAM) and new materials are leading to a paradigm shift in what many practitioners regard as standard care for patients, a priority is to drastically reduce operator error [20].

The aim of this research was to evaluate new total 3D digital smile planning technique (3D-DSP) used in the previsualization stage prior to milling poly(methyl methacrylate) (PMMA) mockups in the process of creating PLVs using a CAD/CAM system.

Table 1: Number of the patient veneers restorations.

	Number of treated patients	%
Males	9	32.2
Female	19	67.8
Total	28	100

Table 2: Distribution of porcelain laminate veneers according to location.

		Veneers	
		Number (n)	Percentage (%)
Maxilla	Anterior	54	50
	Posterior	30	27.8
	Total	84	77.8
Mandible	Anterior	10	9.3
	Posterior	14	12.9
	Total	24	22.2
Total		108	100

2. Materials and Methods

Between September 2012 and July 2015, 28 patients (9 male and 19 female) aged 19 to 53 years (mean age of 36 years) took part in this study at the dental clinic at San Raffaele University, Milan, Italy. None of the patients had any oral, periodontal, or systemic diseases (Tables 1 and 2).

After radiological, phonetic, and static and dynamic occlusal evaluation, each patient had three intra- and extraoral digital images taken while wearing special eyewear (Digital Smile System Srl, Italy) (Figures 1 and 2). An intraoral scanner (Scanner 3D Progress, MHT, Italy) was used to get intraoral digital impressions of the maxilla and mandible arches in open and occlusal states. All the digital images, obtained from the processing of the pictures into the software 2D-Digital Smile System (Digital Smile System Srl, Italy) (Figure 3) and the STL file from the intraoral scans, were combined into the 3D-Digital Smile System (EGS Srl, Italy) to display the patient's teeth and, from this, a virtual design of the potential dental prosthesis was created. When the patient agreed to this virtual 3D view of their planned-for prosthetics, a PMMA mockup (Bredent Srl, Italy) was milled using a CAM system (Zirkonzahn Srl, Italy) (Figure 4). Each mockup was tested in the patient's oral cavity to make sure they would consent to the esthetic therapy and be satisfied with the end result (Figure 5). The newly milled mockups, cemented using spot-etch technique [21, 22], were used to guide the position of the prosthetics and maintain the margins on the enamel surface of the teeth [23–25] (Figure 6). The double cord techniques with the intraoral scanner (Scanner 3D Progress, MHT, Italy) was used to make all the definitive impression of the prepared teeth (Figure 7). The PLVs (IPS e.max System, Ivoclar Vivadent Srl, Italy) were produced using CAD/CAM technique (Zirkonzahn Srl, Italy). A total of 78 Variolink veneers (Ivoclar Vivadent Corp., Liechtenstein) and 30 Clearfil Esthetic Cement veneers (Kuraray America Inc., USA) were cemented onto vital teeth (Table 3) (Figure 8).

Figure 1: Initial clinical case intraoral photography.

Figure 2: Initial clinical case extraoral photography.

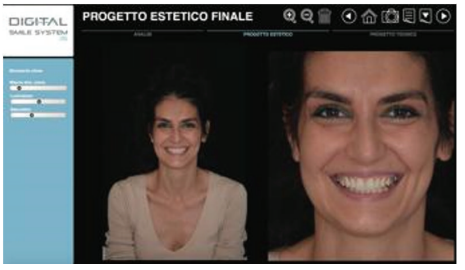

Figure 3: Digital smile design into Digital Smile System 2D.

Each patient had final intra- and extraoral digital images taken (Figures 9 and 10). Follow-up took place after 2 years.

3. Results

The preoperative patient parameters showed bruxism (22.2%), tooth trauma (14.8%), abrasion (11.2%), discoloration (22.2%), crowding (14.8%), diastema (7.4%), and caries (7.4%) (Table 4). The follow-up 2 years later revealed 1 total fracture, 2 sensitive teeth, and 1 gingival recession (0.9%). None of the 108 PLVs showed debonding,

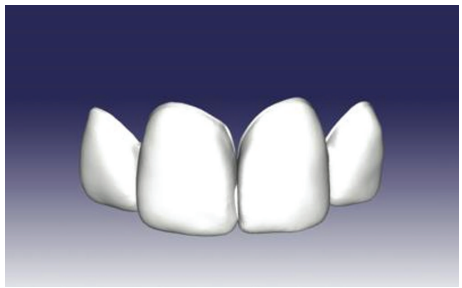

Figure 4: CAD design of the mockup.

Figure 5: Intraoral evaluation of milling CAD-CAM mockup.

Figure 6: Mockup guide for teeth preparation.

Figure 7: Double cord retraction technique.

Figure 8: Adhesive cementation of the definitive veneers.

Table 3: Distribution of PLVs according to bonding material.

Veneers (CAD-CAM)	108	100
Variolink veneers (Ivoclar Vivadent)	78	72.2
Clearfil esthetic cement (Kuraray)	30	27.8
Total	108	100

chipping, microleakage, discoloration, or secondary caries, and no root canal therapy was necessary (Table 5).

Patients responded to a questionnaire to determine their satisfaction with the digital smile design planning and the test in the form of the mockup. They graded both the planning and the test as effective, very effective, or ineffective. For the digital smile design previsualization, with visual analogical scale (VAS scale), 18 (64%) of patients found it very effective and 10 (36%) effective; 24 (86%) found the milling mockup very effective and 4 (14%) effective (Table 6).

4. Discussion

In all prosthodontic aesthetic treatment, the accurate design planning and the basic communication phase with the patient play a crucial role in the therapy. The best previsual means most widely used as a measure of explanation with a patient is the therapeutic planning, associated with the creation of a mockup [17, 19]. With contemporary digitalized techniques, it is possible to redesign a patient's smile [15, 16]. Effective previsualization followed by a mockup is the ideal way to explain changes to a patient and receive their approval [17–19]. Traditional "analogical techniques" are based on a planning process that involves radiological and clinical evaluation, intra- and extraoral photographic analysis, static and dynamic occlusal evaluation, and traditional impressions [21]. The more traditional techniques that use the free-hand "composite technique" before the wax-up do not evaluate the design of the smile [25, 26].

A secondary evolution of digital prosthetic planning is limited to bidimensional digital work flow [21] and requires, after digital smile design protocol, the stone model, the manual processing of a laboratory diagnostic wax-up, and the printing of the classic mockup in the patient's oral cavity through the use of silicone keys. In traditional planning techniques, the data transfer from virtual design to laboratory is difficult and potentially full of errors because it uses a manual process to obtain the computer design of canine zenith lines for the laboratory stone model [21]. This manual process is necessary to transfer all the measurements of the teeth to the new smile project design. Another difficult and unpredictable process is the mockup printing in the patient's

Figure 9: Final result: intraoral photography.

Figure 10: Final result: extraoral photography.

Table 4: Preoperative parameters.

	Patients		Teeth	
	Number (*n*)	Percentage (%)	Number (*n*)	Percentage (%)
Trauma	2	7.2	16	14.8
Bruxism	4	14.3	24	22.2
Abrasion	6	21.4	12	11.2
Discoloration	6	21.4	24	22.2
Crowding	4	14.3	16	14.8
Diastema	2	7.1	8	7.4
Caries	4	14.3	8	7.4
Total	28	100	108	100

Table 5: Distribution of failures according to preparation design.

	Among 28 patients	%	Among 108 veneers	%
Fracture	1	3.6	1	0.9
Chipping	0	0	0	0
Debonding	0	0	0	0
Microleakage	0	0	0	0
Secondary caries	0	0	0	0
Sensitivity	2	7.1	2	1.8
Root canal treatment	0	0	0	0
Gingival recession	1	3.6	1	0.9
Discoloration	0	0	0	0

oral cavity with a silicone mask (made on a wax-up) [10–21]. Our new planning technique allows a new totally digital and CAD-CAM process, from the initial photo shoot to CAD/CAM-milling mockup, to reduce the errors usually associated with the classical manual steps and to improve the accuracy of the prosthetic procedure. All digital data transfer from the clinical 3D planning to the laboratory CAD/CAM process is simpler, faster, and more predictable. However, having photographs plays a crucial role: the patient-approved virtual smile is used to guide the final design of the teeth, which are usually made with the CAD/CAM process.

Table 6: Appreciation of the previsualization with VAS scale.

Test with smile design	Very effective	18	64.3%
	Effective	10	35.7%
	Ineffective	0	0%
	Total	28	100%
Test with mockup	Very effective	24	85.7%
	Effective	4	14.3%
	Ineffective	0	0%
	Total	28	100%

5. Conclusions

A 2-year follow-up of prosthetic PLVs created using the new total digital smile planning technique in vital teeth in the esthetic zone showed that it is possible to obtain excellent results in both functional and esthetic rehabilitation and high patient satisfaction. The new procedure also reduces the amount of time spent in the clinic and laboratory, increases the predictability of data matching to build CAD/CAM-milling mockups, reduces trauma caused by handling hard dental tissues, and improves accuracy and reproducibility of the final mockup. The total new digital smile planning technique is minimally invasive and facilitates diagnosis, improves communication with the patient, reduces processing times, and increases predictability of the results with very little discomfort and very high esthetic final results. The present study has limits, such as the limited number of patients enrolled: further studies on a larger sample of patients are therefore needed to confirm our present results.

Competing Interests

The authors declare that they have no competing interests.

Acknowledgments

The authors are grateful to Laboratorio Latezera Srl, Savona, Italy, and Dr. Fabio Manazza, for their valuable help and support.

References

[1] C. R. Rufenacht, *Fundamentals of Esthetics*, Quintessence, Chicago, Ill, USA, 1990.

[2] M. Peumans, B. Van Meerbeek, P. Lambrechts, and G. Vanherle, "Porcelain veneers: a review of the literature," *Journal of Dentistry*, vol. 28, no. 3, pp. 163–177, 2000.

[3] M. R. Mack, "Perspective of facial esthetics in dental treatment planning," *Journal of Prosthetic Dentistry*, vol. 75, no. 2, pp. 169–176, 1996.

[4] F. G. Mangano, C. Mangano, M. Ricci, R. L. Sammons, J. A. Shibli, and A. Piattelli, "Esthetic evaluation of single-tooth morse taper connection implants placed in fresh extraction sockets or healed sites," *Journal of Oral Implantology*, vol. 39, no. 2, pp. 172–181, 2013.

[5] F. Mangano, C. Mangano, M. Ricci, R. L. Sammons, J. A. Shibli, and A. Piattelli, "Single-tooth Morse taper connection implants placed in fresh extraction sockets of the anterior maxilla: an aesthetic evaluation," *Clinical Oral Implants Research*, vol. 23, no. 11, pp. 1302–1307, 2012.

[6] G. L. Patzer, *The Physical Attractiveness Phenomena*, Plenum Publishing, New York, NY, USA, 1985.

[7] G. Gürel, "Predictable, precise, and repeatable tooth preparation for porcelain laminate veneers," *Practical Procedures & Aesthetic Dentistry*, vol. 15, no. 1, pp. 17–26, 2003.

[8] R. E. Goldstein, *Esthetics in Dentistry*, Lippincott, Philadelphia, Pa, USA, 1976.

[9] P. Richer, *Artistic Anatomy*, Watson Guptill, New York, NY, USA, 1971.

[10] G. Gürel, "Porcelain laminate veneers: minimal tooth preparation by design," *Dental Clinics of North America*, vol. 51, no. 2, pp. 419–431, 2007.

[11] D. Dieschi and R. Spreafico, *Adhesive Metal-Free Restorations: Current Concepts for the Esthetic Treatment of Posterior Teeth*, Quintessence, Chicago, Ill, USA, 1997.

[12] J.-H. Chen, C.-X. Shi, M. Wang, S.-J. Zhao, and H. Wang, "Clinical evaluation of 546 tetracycline-stained teeth treated with porcelain laminate veneers," *Journal of Dentistry*, vol. 33, no. 1, pp. 3–8, 2005.

[13] M. Granell-Ruiz, A. Fons-Font, C. Labaig-Rueda, A. Martínez-González, J.-L. Román-Rodríguez, and M. F. Solá-Ruiz, "A clinical longitudinal study 323 porcelain laminate veneers. Period of study from 3 to 11 years," *Medicina Oral, Patologia Oral y Cirugia Bucal*, vol. 15, no. 3, pp. e531–e537, 2010.

[14] M. F. Land and C. D. Hopp, "Survival rates of all-ceramic systems differ by clinical indication and fabrication method," *Journal of Evidence-Based Dental Practice*, vol. 10, no. 1, pp. 37–38, 2010.

[15] D. Little, "The impact of aesthetics in restorative treatment planning," *Dentistry Today*, vol. 34, no. 5, pp. 475–491, 2015.

[16] J.-H. Chen, H.-L. Huang, Y.-C. Lin, T.-M. Chou, J. Ebinger, and H.-E. Lee, "Dentist-patient communication and denture quality associated with complete denture satisfaction among Taiwanese elderly wearers," *The International Journal of Prosthodontics*, vol. 28, no. 5, pp. 531–537, 2015.

[17] J. Gurrea and A. Bruguera, "Wax-up and mock-up. A guide for anterior periodontal and restorative treatments," *The International Journal of Esthetic Dentistry*, vol. 9, no. 2, pp. 146–162, 2014.

[18] P. Magne, "A new approach to the learning of dental morphology, function, and esthetics: the '2D-3D-4D' concept," *The International Journal of Esthetic Dentistry*, vol. 10, no. 1, pp. 32–47, 2015.

[19] H. Simon and P. Magne, "Clinically based diagnostic wax-up for optimal esthetics: the diagnostic mock-up," *Journal of the California Dental Association*, vol. 36, no. 5, pp. 355–362, 2008.

[20] F. Beuer, J. Schweiger, and D. Edelhoff, "Digital dentistry: an overview of recent developments for CAD/CAM generated restorations," *British Dental Journal*, vol. 204, no. 9, pp. 505–511, 2008.

[21] E. A. McLaren, "Bonded functional esthetic prototype: an alternative pre-treatment mock-up technique and cost-effective medium-term esthetic solution," *Compendium of Continuing Education in Dentistry*, vol. 34, no. 8, pp. 596–607, 2013.

[22] L. Grütter and F. Vailati, "Full-mouth adhesive rehabilitation in case of severe dental erosion, a minimally invasive approach following the 3-step technique," *European Journal of Esthetic Dentistry*, vol. 8, no. 3, pp. 358–375, 2013.

[23] M. G. Buonocore, "A simple method of increasing the adhesion of acrylic filling materials," *Journal of Dental Research*, vol. 34, no. 6, pp. 849–853, 1955.

[24] A. Aykor and E. Ozel, "Five-year clinical evaluation of 300 teeth restored with porcelain laminate veneers using total-etch and a modified self-etch adhesive system," *Operative Dentistry*, vol. 34, no. 5, pp. 516–523, 2009.

[25] G. Gurel, S. Morimoto, M. A. Calamita, C. Coachman, and N. Sesma, "Clinical performance of porcelain laminate veneers: outcomes of the aesthetic pre-evaluative temporary (APT) technique," *The International Journal of Periodontics & Restorative Dentistry*, vol. 32, no. 6, pp. 625–635, 2012.

[26] M. Reshad, D. Cascione, and P. Magne, "Diagnostic mock-ups as an objective tool for predictable outcomes with porcelain laminate veneers in esthetically demanding patients: a clinical report," *Journal of Prosthetic Dentistry*, vol. 99, no. 5, pp. 333–339, 2008.

Hindawi Publishing Corporation
International Journal of Dentistry
Volume 2016, Article ID 7692387, 5 pages
http://dx.doi.org/10.1155/2016/7692387

Clinical Study

The Antimicrobial Photodynamic Therapy in the Treatment of Peri-Implantitis

Umberto Romeo,[1] Gianna Maria Nardi,[1] Fabrizio Libotte,[1] Silvia Sabatini,[1] Gaspare Palaia,[1] and Felice Roberto Grassi[2]

[1]*Department of Oral and Maxillofacial Sciences, "Sapienza" University of Rome, Via Caserta 6, 00161 Rome, Italy*
[2]*University of Bari, Piazza Umberto I, 70121 Bari, Italy*

Correspondence should be addressed to Gaspare Palaia; gaspare.palaia@uniroma1.it

Received 9 February 2016; Revised 5 April 2016; Accepted 17 April 2016

Academic Editor: Jamil A. Shibli

Introduction. The aim of this study is to demonstrate the effectiveness of addition of the antimicrobial photodynamic therapy to the conventional approach in the treatment of peri-implantitis. *Materials and Methods*. Forty patients were randomly assigned to test or control groups. Patients were assessed at baseline and at six (T1), twelve (T2), and twenty-four (T3) weeks recording plaque index (PlI), probing pocket depth (PPD), and bleeding on probing (BOP); control group received conventional periodontal therapy, while test group received photodynamic therapy in addition to it. *Result*. Test group showed a 70% reduction in the plaque index values and a 60% reduction in PD values compared to the baseline. BOP and suppuration were not detectable. Control group showed a significative reduction in plaque index and PD. *Discussion*. Laser therapy has some advantages in comparison to traditional therapy, with faster and greater healing of the wound. *Conclusion*. Test group showed after 24 weeks a better value in terms of PPD, BOP, and PlI, with an average pocket depth value of 2 mm, if compared with control group (3 mm). Our results suggest that antimicrobial photodynamic therapy with diode laser and phenothiazine chloride represents a reliable adjunctive treatment to conventional therapy. Photodynamic therapy should, however, be considered a coadjuvant in the treatment of peri-implantitis associated with mechanical (scaling) and surgical (grafts) treatments.

1. Introduction

Peri-implant disease may be defined as a pathologic condition including inflammatory and other kinds of lesions affecting the soft and/or hard tissues surrounding a dental implant [1].

Peri-implantitis is characterized by a severe inflammatory process involving both mucosa and bone around the implant [2]. This represents the most diffuse cause of long-term implant failure. Bone destruction, peri-implant pockets, bleeding on probing, the possible presence of exudate, and loss of supporting tissue are involved in peri-implantitis [3].

Peri-implantitis is due to bacterial contamination or technical problems, related to the implant surface itself or to implant support placement and the subsequent osseointegration process. Osseointegration may be influenced by mistakes or complications occurring in the surgical phase or masticatory overload.

The bacterial biofilm on the implant surfaces is similar to the one in periodontal disease. The microflora includes microorganisms such as *Aggregatibacter actinomycetemcomitans*, *Peptostreptococcus micros*, *Campylobacter rectus*, *Capnocytophaga* spp., *Porphyromonas gingivalis*, and *Tannerella forsythia*. However, it should be stressed that the residual teeth could influence the composition of microflora. Bacterial species observed in edentulous patients differ from those of partially edentulous subjects. On this basis, the idea that the presence of bacteria involved in periodontal disease could contribute to development of peri-implantitis seems to be plausible [4].

During the surgical stage, the treatment in the initial stage included elimination and of plaque and calculus, decontamination of the implant surface, and maintenance of healthy conditions [5].

Decontamination of implant surfaces is a challenging goal. Several different treatments have been proposed in the literature [6, 7]. Cleaning the surfaces can be through mechanical (dental curettes, ultrasonic scalers, and air-powder abrasive) and chemical (citric acid, H_2O_2, chlorhexidine digluconate, and EDTA) procedures, in association with local or systemic antibiotics [8, 9].

Lasers can be used in decontamination of implant surfaces. The most frequently used include diode, erbium lasers, and CO_2 due to their hemostatic properties, selective calculus ablation, and bactericidal effects [10].

An alternative approach to dental implant decontamination is the association of the conventional treatment with photodynamic therapy (PDT).

Photodynamic therapy includes the use of a low-power diode laser in combination with photosensitizing compounds. These components are linked to the bacterial membrane and, when excited, react with the substrate. The photosensitizer binds to the target cells and when it is irradiated with light of specific wavelength, in the presence of oxygen, it undergoes a transition from a low-energy ground state to an excited singlet state; then singlet oxygen and other very reactive agents are produced, which are toxic to these target cells [11].

Photodynamic therapy (PDT) has received more attention in dentistry in recent years. The application of photosensitive dyes into pockets and their activation with light promote killing of periodontal pathogens. Outcomes of clinical studies in subjects with chronic periodontitis show beneficial effects of PDT on the reduction in gingival inflammation [12].

The effects of PDT on the treatment of ligature-induced peri-implantitis were investigated in dogs. The results revealed a reduction in bacterial counts of *Prevotella intermedia/nigrescens*, *Fusobacterium* spp., and beta-haemolytic *Streptococcus* [13].

Several studies have demonstrated bacteria destruction can be achieved without any damage to the treated titanium surfaces [14].

The aim of this experimental study is to demonstrate the efficacy of antimicrobial photodynamic therapy in addition to the traditional approach.

2. Materials and Methods

40 subjects were involved in the study ranging in age from 34 to 68 years, referred to the Periodontology Department of the Dentistry Unit at Bari University Hospital. The subjects had given their consent to treatment. The study was conducted following the Declaration of Helsinki, according to the local Ethical Committee.

The patients were selected with these inclusion criteria: overall plaque index (PlI) ≥40% and at least one implant site with the following characteristics: probing depth (PD) ≥4 mm, bleeding on probing (BOP), and presence of suppuration. A full mouth series for each patient was performed to confirm diagnosis. Six sites for each implant were analyzed.

Exclusion criteria included decompensated systemic disease, degenerative bone disease, chronic immune-based mucomembranous disorders (e.g., lichen planus, pemphigoid, pemphigus, and systemic lupus erythematosus), chemotherapy or radiotherapy to the head and neck area, pregnancy, presence of teeth with periodontitis adjacent to sites affected by peri-implantitis, implants placed in fresh extraction sockets, smoking >10 cigarettes daily, and alcoholism.

Figure 1: Ultrasonic debridement has been performed.

The null hypothesis was that nonstatistically significant differences are observed with respect to the clinical parameters (e.g., PPD, BOP, and PlI) between the two treatment modalities (i.e., adjunctive PDT test group versus control group).

The primary outcome variable was the reduction of PD in peri-implant sites with probing depth ≥4 mm. Secondary outcome variables were the changes in BOP and PlI.

The ratio of this study was based on the capacity of photodynamic therapy to promote bacterial inactivation by light and not by heat. This is achieved with 40-milliwatt laser beam power, with no heat being developed. 360° light irradiation is obtained by means of special probes ensuring optimal light beam diffusion.

123 dental implants were analyzed. The patients were randomly assigned to two groups, that is, a test group (63 implants) and a control group (59 implants), using a software to create a randomization list (https://www.random.org/) and assigning a code to each patient.

For both groups of patients the following indices were measured by means of a plastic probe: the plaque index (PlI), based on the Plaque Control Record (PCR, [15]), bleeding on probing (BOP) with or without suppuration, and probing depth (PD).

Mechanical and manual decontamination of the oral cavity was performed using air polishing with micronized glycine powder to remove plaque and discolorations and expose the underlying calculus (Figure 1). The latter was removed with a piezoelectric ablator in combination with a universal tip for the scaling of natural teeth and a special nonmetal tip for implant scaling. Root debridement at sites with PD ≥4 mm was performed with a periodontal ultrasonic unit and implant debridement at sites with PD ≥4 mm was done with carbon-fiber-reinforced plastic curettes.

At the end of the procedure, according to the code of the envelope, the dental hygienist considered in the test group the addition of laser-assisted antimicrobial photodynamic therapy based on the HELBO Protocol at implant sites with PD ≥4 mm.

Figure 2: The special HELBO® Blue Photosensitizer is applied within the peri-implant pocket starting from the bottom.

Figure 3: Rinsing the fluid off the pocket.

Figure 4: Exposure to HELBO TheraLite diode laser for about 1 minute of the implant surface.

Figure 5: Final probing.

The treatment of PDT was performed using HELBO TheraLite (Bredent medical), diode laser battery powered with a wavelength of 670 nm and output of 75 mW/cm^2, with a spot size of 0.06 cm in diameter. HELBO Blue photosensitizer was used, a liquid containing methylene blue (methylthioninium hydrochloride, also known as 3,7-bis phenothiazine-5-ium chloride). The concentration of photosensitizer was 10 mg/mL with absorbance peak at 670 nm. Its use as a chromophore in photodynamic therapy is justified by its relative stability in the light, which makes it an important generator of singlet oxygen (ET = 142.1 kJ/mol with $\Phi\Delta = 0.60$ in water).

The photosensitizer was applied inside the peri-implant pocket starting from the bottom and moving in apical-coronal direction (Figure 2). Care was taken to avoid the formation of air bubbles, allowing the fluid to dye all bacteria by leaving it in situ for 60 seconds. After rinsing the fluid off the pocket and suctioning excess liquid (Figure 3), the previously dyed implant surface was exposed to HELBO TheraLite diode laser for 1 minute (Figure 4). The fluence was 25.54 J/cm^2, while the total energy applied was 1592 J/cm^2. TheraLite illumination was applied using circular movements. This type of movement promotes the best activation of the dye molecules with the laser light and transfers their energy to local oxygen. The resulting singlet oxygen is highly aggressive and capable of destroying bacterial cells.

Both groups of patients received home oral hygiene instruction. They were advised to brush their teeth for two minutes, twice a day, using an oscillating-rotating electric toothbrush with little toothpaste and a special brush for interproximal hygiene.

T1 (6 Weeks). In both groups the same clinical measurements were taken as those at baseline and home oral hygiene instruction was provided again.

T2 (12 Weeks). In both groups the same clinical measurements were taken as those at baseline and home oral hygiene instruction was provided again. This was followed by a deplaquing session with glycine air polishing.

T3, End of the Study (24 Weeks). The same clinical measurements were taken as those at baseline (Figure 5).

A weighted arithmetic mean was taken to calculate average values for each group in terms of PD, BOP, and PlI at 6, 12, and 24 weeks using a computer software (Graph Pad Prism 5®).

3. Results

As early as at the 6th week of the study, reductions in clinical parameters were observed in both groups compared with baseline values. The reductions were more marked in the test group.

PD average values were calculated. Average values were lower than the baseline. The reduction was first seen as early as at 6 weeks, to be confirmed at 12 weeks, when the values further declined. The readings remained constant at 24 weeks. Test group showed a better value of PD, with an average value of 2 mm if compared with control group (3 mm).

With regard to the plaque index, average value was calculated for each group. In this case, a significant score reduction was recorded as early as at the 6th week. Despite improving of daily oral hygiene practices, the plaque index variations were not constant. Test group showed a PlI of 17% after 24 weeks. Control group showed a PlI of 25%. There were no significant differences between the two groups (Table 2).

Regarding BOP, at baseline, all patients had bleeding on probing and suppuration at the peri-implant sites under investigation. In the test group patients, these signs of inflammation had gradually improved to disappear completely by the 24th week. In the control group, however, some improvements were recorded, but not all of the patients achieved complete remission (Table 3).

4. Discussion and Conclusion

Peri-implantitis has been defined as an inflammatory process that affects the soft tissues surrounding an osseointegrated implant in function with concomitant loss of supporting marginal bone. Peri-implant mucositis, in contrast, is a reversible inflammatory reaction of the mucosa adjacent to an implant without bone loss. Colonization of oral implant surfaces with bacterial biofilms occurs rapidly and the biofilm development seems to play an important role in altering the biocompatibility of the implant surface and, thus, enhancing peri-implant disease development [16].

Since photodynamic therapy has been introduced in dentistry, several advantages of laser and PDT in the many fields of dentistry have been described in the literature. An increasing interest is recently growing regarding PDT in implant dentistry and as a coadjuvant treatment for peri-implantitis [17]. It employs visible light (laser) and a dye (photosensitizer), the combination of which leads to the release of free oxygen radicals, which in turn can selectively destroy bacteria and their products. Although PDT has been used in the field of medicine since 1904 for light-induced inactivation of cells, microorganisms, and molecules, Branemark's discovery of osseointegration in 1965 was extremely important to restorative treatments and, particularly, functional oral rehabilitation. A large number of patients have been rehabilitated with dental implants, and, consequently, more cases of success and failure have appeared over the years. Thus, peri-implantitis has become an increasingly frequent problem in dentistry.

Laser therapy has some advantages in comparison to traditional therapy. It is well known that laser has the ability to modify dentin so as to obtain the exposition of collagen fibers. The exposition of collagen may facilitate the attachment of blood clot and its stabilization. This, in turn, may favor a speedy healing and the obtainment of a new collagen attachment in spite of long junctional epithelium. This fact could explain the faster and greater healing of the wound and the results in the test group. It is clear that further histological analysis should be carried out to demonstrate this idea [18].

Thus, photodynamic therapy (PDT) may be one such treatment alternative. Only in the last 10 years or so clinical studies have examined its application in the oral cavity.

Table 1: Probing depth average values in test and control group after 6, 12, and 24 weeks.

PD	Test	Control
Baseline	5 mm	5 mm
6 weeks	3 mm	3 mm
12 weeks	2 mm	2 mm
24 weeks	2 mm	3 mm

Table 2: Plaque index values in test and control group after 6, 12, and 24 weeks.

PlI	Test	Control
Baseline	60%	62%
6 weeks	11%	12%
12 weeks	17%	21%
24 weeks	17%	25%

Table 3: BOP and suppuration values in test and control group after 6, 12, and 24 weeks.

BOP/suppuration	Test	Control
Baseline	100%	100%
6 weeks	20%	35%
12 weeks	10%	20%
24 weeks	0%	10%

The current data show that treating chronic periodontitis with PDT alone versus conventional SRP treatment has no additional benefit [19]. In contrast, combining PDT and SRP does provide an additional benefit, particularly in lesions with unfavorable anatomic conditions. A clinical controlled study compared the effect of PDT alone (without subgingival SRP) with SRP in the treatment of aggressive periodontitis [20, 21].

In addition to this, during peri-implantitis treatment, HELBO technology offers the advantage of a noninvasive, painful, rapid bacterial inactivation thanks to liberation of oxygen. Oxygen allows the destruction of bacteria membrane, and on the other hand its sparkling effect permits dangerous enzymes and collagenosis to be quickly removed from the pocket, for a better bacterial removal and, as a consequence, could facilitate healing.

The improvement of values analyzed was more marked in the test group (Table 1). Test group showed a better value of PD, with an average value of 2 mm if compared with control group (3 mm).

Regarding PlI the significant reduction recorded at the 6th week was followed by a slight increase at 12 weeks, with values remaining constant up to the 24th week. However, the plaque index score for each patient at 24 weeks was anyway lower than at baseline.

Finally, a comparison between baseline and final average bleeding on probing (BOP) and suppuration values also shows substantial improvement.

Thus, the results obtained in this study suggest that photodynamic therapy could be considered an effective method for bacterial reduction on implant surfaces [17–22].

Our study also confirms its effectiveness in reducing clinical indices and the bacterial load at sites affected by peri-implantitis, with significant bacterial detoxification being achieved.

Photodynamic therapy should, however, be considered a coadjuvant in the treatment of peri-implantitis and associated with mechanical (scaling) and surgical (grafts) treatments in order to control peri-implant disease.

Competing Interests

The authors declare that they have no competing interests.

References

[1] A. Mombelli, M. Marxer, T. Gaberthüel, U. Grunder, and N. P. Lang, "The microbiota of osseointegrated implants in patients with a history of periodontal disease," *Journal of Clinical Periodontology*, vol. 22, no. 2, pp. 124–130, 1995.

[2] K. Warrer, D. Buser, N. P. Lang, and T. Karring, "Plaque-induced peri-implantitis in the presence or absence of keratinized mucosa. An experimental study in monkeys," *Clinical Oral Implants Research*, vol. 6, no. 3, pp. 131–138, 1995.

[3] S. Renvert and I. N. Polyzois, "Clinical approaches to treat peri-implant mucositis and peri-implantitis," *Periodontology 2000*, vol. 68, no. 1, pp. 369–404, 2015.

[4] M. Esposito, M. G. Grusovin, P. Coulthard, and H. V. Worthington, "The efficacy of interventions to treat peri-implantitis: a Cochrane systematic review of randomised controlled clinical trials," *European Journal of Oral Implantology*, vol. 1, no. 2, pp. 111–125, 2008.

[5] V. Ntrouka, M. Hoogenkamp, E. Zaura, and F. van der Weijden, "The effect of chemotherapeutic agents on titanium-adherent biofilms," *Clinical Oral Implants Research*, vol. 22, no. 11, pp. 1227–1234, 2011.

[6] F. Schwarz, N. Sahm, G. Iglhaut, and J. Becker, "Impact of the method of surface debridement and decontamination on the clinical outcome following combined surgical therapy of peri-implantitis: a randomized controlled clinical study," *Journal of Clinical Periodontology*, vol. 38, no. 3, pp. 276–284, 2011.

[7] C. M. Faggion Jr. and M. Schmitter, "Using the best available evidence to support clinical decisions in implant dentistry," *The International Journal of Oral & Maxillofacial Implants*, vol. 25, no. 5, pp. 960–969, 2010.

[8] P. A. Norowski Jr. and J. D. Bumgardner, "Biomaterial and antibiotic strategies for peri-implantitis: a review," *Journal of Biomedical Materials Research Part B: Applied Biomaterials*, vol. 88, no. 2, pp. 530–543, 2009.

[9] J. Marotti, P. T. Neto, T. Toyota de Campos et al., "Recent patents of lasers in implant dentistry," *Recent Patents on Biomedical Engineering*, vol. 4, no. 2, pp. 103–109, 2011.

[10] S. Sarkar and M. Wilson, "Lethal photosensitization of bacteria in subgingival plaque from patients with chronic periodontitis," *Journal of Periodontal Research*, vol. 28, no. 3, pp. 204–210, 1993.

[11] M. Wilson, J. Dobson, and S. Sarkar, "Sensitization of periodontopathogenic bacteria to killing by light from a low-power laser," *Oral Microbiology and Immunology*, vol. 8, no. 3, pp. 182–187, 1993.

[12] R. Andersen, N. Loebel, D. Hammond, and M. Wilson, "Treatment of periodontal disease by photodisinfection compared to scaling and root planing," *Journal of Clinical Dentistry*, vol. 18, no. 2, pp. 34–38, 2007.

[13] J. A. Shibli, M. C. Martins, L. H. Theodoro, R. F. M. Lotufo, V. G. Garcia, and E. J. Marcantonio, "Lethal photosensitization in microbiological treatment of ligature-induced peri-implantitis: a preliminary study in dogs," *Journal of Oral Science*, vol. 45, no. 1, pp. 17–23, 2003.

[14] O. Dörtbudak, R. Haas, T. Bernhart, and G. Mailath-Pokorny, "Lethal photosensitization for decontamination of implant surfaces in the treatment of peri-implantitis," *Clinical Oral Implants Research*, vol. 12, no. 2, pp. 104–108, 2001.

[15] T. J. O'Leary, R. B. Drake, and J. E. Naylor, "The plaque control record," *Journal of Periodontology*, vol. 43, no. 1, p. 38, 1972.

[16] R. R. A. Hayek, N. S. Araújo, M. A. Gioso et al., "Comparative study between the effects of photodynamic therapy and conventional therapy on microbial reduction in ligature-induced peri-implantitis in dogs," *Journal of Periodontology*, vol. 76, no. 8, pp. 1275–1281, 2005.

[17] G. M. Nardi, S. Sabatini, F. Scarano et al., "Utilizzo della terapia fotodinamica Helbo nel trattamento delle perimplantiti: case report," *Dental Hygiene*, 2012.

[18] J. F. O'Neill, C. K. Hope, and M. Wilson, "Oral bacteria in multi-species biofilms can be killed by red light in the presence of toluidine blue," *Lasers in Surgery and Medicine*, vol. 31, no. 2, pp. 86–90, 2002.

[19] F. Sgolastra, A. Petrucci, R. Gatto, G. Marzo, and A. Monaco, "Photodynamic therapy in the treatment of chronic periodontitis: a systematic review and meta-analysis," *Lasers in Medical Science*, vol. 28, no. 2, pp. 669–682, 2013.

[20] M. A. Atieh, "Photodynamic therapy as an adjunctive treatment for chronic periodontitis: a meta-analysis," *Lasers in Medical Science*, vol. 25, no. 4, pp. 605–613, 2010.

[21] R. Malik, A. Manocha, and D. K. Suresh, "Photodynamic therapy—a strategic review," *Indian Journal of Dental Research*, vol. 21, no. 2, pp. 285–291, 2010.

[22] N. Kömerik, H. Nakanishi, A. J. MacRobert, B. Henderson, P. Speight, and M. Wilson, "In vivo killing of *Porphyromonas gingivalis* by toluidine blue-mediated photosensitization in an animal model," *Antimicrobial Agents and Chemotherapy*, vol. 47, no. 3, pp. 932–940, 2003.

Hindawi Publishing Corporation
International Journal of Dentistry
Volume 2016, Article ID 7186140, 5 pages
http://dx.doi.org/10.1155/2016/7186140

Research Article

Color Stability of the Bulk-Fill Composite Resins with Different Thickness in Response to Coffee/Water Immersion

Sayna Shamszadeh,[1] Seyedeh Mahsa Sheikh-Al-Eslamian,[1] Elham Hasani,[1] Ahmad Najafi Abrandabadi,[2] and Narges Panahandeh[1]

[1]*Dental Research Center, Research Institute of Dental Sciences, Shahid Beheshti University of Medical Sciences, Tehran 19839 63113, Iran*
[2]*Preventive Dentistry Research Centre, Research Institute of Dental Sciences, Shahid Beheshti University of Medical Sciences, Tehran 19839 63113, Iran*

Correspondence should be addressed to Narges Panahandeh; nargespanahandeh@yahoo.com

Received 6 February 2016; Revised 9 April 2016; Accepted 23 May 2016

Academic Editor: Jamil A. Shibli

We aimed to evaluate the color stability of bulk-fill and conventional composite resin with respect to thickness and storage media. Twenty specimens of a conventional composite resin (6 mm diameter and 2 mm thick) and 40 specimens of the bulk-fill Tetric EvoCeram composite resin at two different thicknesses (6 mm diameter and 2 mm thick or 4 mm thick, $n = 20$) were prepared. The specimens were stored in distilled water during the study period (28 d). Half of the specimens were remained in distilled water and the other half were immersed in coffee solution 20 min/d and kept in distilled water between the cycles. Color changes (ΔE) were measured using the CIE $L^*a^*b^*$ color space and a digital imaging system at 1, 7, 14, and 28 days of storage. Data were analyzed using Two-way ANOVA and Tukey's HSD post hoc test ($P < 0.05$). Composite resins showed significant increase in color changes by time (bulk-fill > conventional; $P < 0.001$). Coffee exhibited significantly more staining susceptibility than that of distilled water ($P < 0.001$). There was greater color changes with increasing the increment thickness, which was significant at 14 ($P < 0.001$) and 28 d ($P < 0.01$). Color change of bulk-fill composite resin was greater than that of the conventional one after coffee staining and is also a function of increment thicknesses.

1. Introduction

Color stability of composite resin is an important property influencing its clinical longevity, which continues as a challenge inherent to material [1]. Color changes can occur due to various etiologic factors; extrinsic discoloration can occur due to staining in the superficial layer of resin composite, water absorption, surface roughness, smoking, and diet [2, 3]. Intrinsic discoloration could occur as a result of physicomechanical reaction within the material (e.g., the filler and the resin matrix properties) [4].

In oral conditions, composite resins are exposed to different dietary beverages such as coffee which might result in absorption and adsorption of colorants in coffee into the resin surface [5] and consequently undesirable color change. Previous investigations reported the influence of coffee on the color stability of composite resins [6–10].

Generally, it is recommended that the resins should be placed in 2 mm increments to obtain sufficient light transmittance and complete curing of composite resins [11]. Placing the resin in 2 mm increments has some merits including the reduction of the polymerization shrinkage and the voids incorporation between the layers [12]. However, the application of composite resins in an incremental technique and light curing each increment individually is a time-consuming procedure. There is also an increasing possibility of air bubble inclusion or moisture contamination between individual increments of resin composite restorations [13].

To overcome such fallibility, bulk-fill composite resins are introduced. According to the manufactures, these materials

Table 1: Composition of the materials.

Materials	Composition	Filler amount, wt%, vol%	Manufacturer
Tetric EvoCeram universal	Bis-GMA, UDMA, Ba-Al-Si glass prepolymer filler (monomer, glass filler, ytterbium trifluoride, and mixed oxide), and prepolymer	55–57	Ivoclar Vivadent (Schaan, Liechtenstein)
Tetric EvoCeram bulk-fill	Dimethacrylates: Bis-GMA, Bis-EMA, UDMA, barium glass, ytterbium trifluoride, mixed oxide, and prepolymer; additives, catalysts, stabilizers, and pigments	81–61	Ivoclar-Vivadent (Schaan, Liechtenstein)

UDMA, urethane dimethacrylate; Bis-GMA, bisphenol A diglycidyl ether dimethacrylate; Ba-Al-Si glass, barium-aluminum-silicate glass.

can be sufficiently light cured up to 4 mm in a single increment, without influencing the polymerization shrinkage, degree of conversion, or cavity adaptation [14]. In addition, it is claimed that these materials have lower polymerization shrinkage compared to conventional composite resins [15]. Thus, some postoperative problems, such as gap formation and the incidence of recurrent carries, may be diminished. Such merits are probably due to the increased translucency of the bulk-fill composites, which permits greater light transmission. Additionally, the formulation of these materials allows for modulation of the polymerization reaction by applying the stress-relieving monomers, the use of more reactive photoinitiators, and the incorporation of different types of fillers, such as prepolymer particles and fiberglass rod segments [12].

While the manufacturers recommend bulk-filling of these materials up to 4 mm, many clinicians suspect that the depth of cure and mechanical properties might not be suitable for clinical use.

There are few reports on of the effect of increment thickness and the storage media on the discoloration of these bulk-fill resin composites. Since color changes are a concern that affects the population and one of the main reasons for replacing resin-based restorations, this study investigated the effects of the increment thickness and the storage media on the discoloration of one of these bulk-fill resin composites.

2. Materials and Methods

2.1. Materials. Two A3 shade light cured composite resins, conventional and bulk-fill Tetric EvoCeram, were selected for this study. Characteristics of the materials are presented in Table 1.

2.2. Methods. The specimens of conventional (6 mm diameter and 2 mm thickness, $n = 20$) and bulk-fill composite resins at two different thicknesses (6 mm diameter and 2 mm and 4 mm thickness, $n = 20$) were prepared using a polyethylene mold. After applying the composite resin, a Mylar strip was placed and pressed with a glass slide to obtain a flat surface. The glass slide was removed and the specimens were cured for 40 s using a halogen light curing unit (1086.67 mW/cm^2, Demetron L.C; Kerr Corporation, Orange, CA, USA).

After removing the specimens from the molds, baseline color was measured using a digital image analysis method as described later. Specimens were stored at 37°C in distilled water for 28 d.

Half of the specimens remained in distilled water and the other half were immersed in coffee solution 20 min/d and remained in distilled water in the interval between cycles. To prepare the coffee solution, 25 g of coffee (Taster's Choice, Nestlé USA, Inc., Glendale, CA, USA) was poured in 250 mL of boiling water, and after 10 min of stirring, the solution was filtered through a filter paper.

The color of the specimens was assessed in the Commission International de l'Eclairege $L^*a^*b^*$ (CIELAB) color space using a digital image analysis method. The CIELAB system is a chromatic value color space that measures chroma and value in three coordinates: L^*, the lightness measured from 0 (black) to 100 (white), a^*, color in the red ($a < 0$) and green ($a > 0$) axis, and b^*, color in the blue ($b < 0$) and yellow ($b > 0$) axis.

A setup was designed in a dark room while two 60 w light sources were positioned from the sides (45-degree angle to the samples). At each interval, the specimens were rinsed with distilled water for 5 seconds, blotted dried with tissue paper, and placed on a dark background. 18% grey card was placed next to the specimens to achieve neutral background. The digital images connected with the computer running Adobe Photoshop CS5 (Adobe, San Jose, CA, USA) as color assessment software. The color change (ΔE) was calculated using the following equation:

$$\Delta E = \left(\Delta L^2 + \Delta a^2 + \Delta b^2\right)^{1/2}. \quad (1)$$

See [16].

2.3. Statistical Analysis. The results were statistically analyzed using Repeated Measures Two-way ANOVA with factors including materials (conventional, 2 mm and 4 mm bulk-fill resin composite) and immersion media (coffee and distilled water) for each time interval. For multiple comparisons, Tukey's HSD post hoc test was used to compare different materials ($P < 0.05$) (SPSS v12.0; SPSS Inc., Chicago, IL, USA).

Table 2: Mean (SD) of ΔE values at different time intervals and storage media.

Material (thickness)	Time interval	Storage media	
		Water	Coffee
Conventional (2 mm)	$\Delta E_{1\,d}$	2.1 (0.21)^{Aa}	2.86 (0.34)^{Ab}
	$\Delta E_{7\,d}$	3.26 (0.22)^{Aa}	4.97 (0.54)^{Ab}
	$\Delta E_{14\,d}$	4.41 (0.20)^{Aa}	8.11 (0.46)^{Ab}
	$\Delta E_{28\,d}$	5.59 (0.26)^{Aa}	11.34 (0.56)^{Ab}
Bulk-fill (2 mm)	$\Delta E_{1\,d}$	3.39 (0.36)^{Ba}	7.64 (0.58)^{Bb}
	$\Delta E_{7\,d}$	4.03 (0.33)^{Ba}	11.26 (0.61)^{Bb}
	$\Delta E_{14\,d}$	5.14 (0.24)^{Ba}	13.84 (0.75)^{Bb}
	$\Delta E_{28\,d}$	7.57 (0.34)^{Ba}	17.02 (0.86)^{Bb}
Bulk-fill (4 mm)	$\Delta E_{1\,d}$	3.12 (0.22)^{Ba}	8.00 (0.53)^{Bb}
	$\Delta E_{7\,d}$	4.52 (0.24)^{Ba}	11.77 (0.44)^{Bb}
	$\Delta E_{14\,d}$	5.61 (0.28)^{Ca}	17.11 (0.52)^{Cb}
	$\Delta E_{28\,d}$	7.50 (0.35)^{Ca}	21.31 (0.40)^{Cb}

$\Delta E_{1\,d}$, ΔE between 1 day and baseline; $\Delta E_{7\,d}$, ΔE between 7 days and baseline; $\Delta E_{14\,d}$, ΔE between 14 days and baseline; $\Delta E_{28\,d}$, ΔE between 28 days and baseline. Different lowercase letters indicate statistically significant differences between the media ($P \leq 0.05$). Different uppercase letters indicate statistically significant differences between materials ($P \leq 0.05$).

3. Results

The mean ΔE values of specimens at different thicknesses and media are shown in Table 2. The results of this study showed the significant color changes among all groups ($P < 0.001$). Tukey's HSD test revealed that bulk-fill composite resins showed the significantly greater ΔE values compared to those of conventional resins in all time intervals ($P < 0.001$).

Regarding color changes of bulk-fill composite resin at increasing depths, 4 mm thick specimens showed a significant increase in mean ΔE values at 14 d ($P < 0.001$) and 28 d ($P < 0.001$). However, the difference was not significant at 1 d and 7 d.

Immersion in coffee and distilled water provided significant color changes. Immersion in coffee solution resulted in greater and significant discoloration over time, when compared to that of water storage ($P < 0.001$).

4. Discussion

Color stability of dental restorations is one of the most important characteristics of composite resin materials in terms of longevity [17]. Although there have been several studies on the effect of different beverages on the color stability of resin composites, there is little information regarding the color stability of a new bulk-fill resin composite, which has been introduced for applying in thicker layers.

In the present study the effect of coffee staining on the color stability of bulk-fill (with different thicknesses) and conventional composite resins was evaluated over a period of 28 days. Coffee (20 minutes daily) and distilled water were chosen as the storage media in this study since they mimic the liquids that are constituently in contact with resin composite restorations in the oral environment.

The CIELAB color system was chosen for the color assessment in a current study. This system is a standard method for measuring color differences based on human perception. The ΔE value presents relative color differences of dental materials or tooth surfaces before and after an intervention. According to literature, values of $\Delta E < 1$ are regarded as not appreciable by the human eye. Values $1 < \Delta E < 3.3$ are considered appreciable by skilled operators but clinically acceptable, whereas values of $\Delta E > 3.3$ are considered appreciable by nonskilled persons and are, hence, not clinically acceptable [18]. Therefore, color changes above a value of $\Delta E = 3.3$ were considered clinically unacceptable.

In this study significant differences in ΔE values were found among materials for both storage media. Coffee staining produced higher color changes in the specimens than those of water storage, which was in line with the previous investigations; Ertaş et al. and Villalta et al. immersed composite resin into the different beverages and reported that coffee showed greater color changes compared to water storage [6, 7]. The present result seems reasonable because when specimens were submitted to coffee staining, discoloration occurred due to the adsorption and absorption of pigments into the organic phase of resin-based materials [19]. Additionally, coffee contains significant amounts of staining agents such as gallic acid, which facilitate staining.

The findings of our study present that water storage can also lead to slight discoloration, slightly perceptible, which is in line with the other investigations. The staining susceptibility of specimens after being immersed in distilled water might be due to their degree of water absorption and the hydrophilic/hydrophobic nature of the resin matrix. Water absorption occurs mainly as direct absorption by the resin matrix [20]. Excessive water absorption can decrease the life of a composite resin by plasticizing and expanding the resin component, causing microcrack formation. As a result, microcracks or interfacial gaps at the interface between the filler and matrix allow stain penetration and discoloration [21]. In addition, discoloration might be due to the differences in the refractive index of filler and matrix which might increase after water absorption [22].

Others factors that have been shown to have a significant impact on the color stability of material are the composition of composite resins and the characteristics of filler particle [23]. In this study the color susceptibility of bulk-fill composite resin was significantly higher than that of conventional composite resin after immersion in storage media; it is claimed that bulk-fill Tetric EvoCeram resins consist of a variety of fillers, prepolymer shrinkage stress reliever, different photoinitiator system, and light sensitivity system. These differences might influence the staining susceptibility [24]. The mechanism of the interaction between the bulk-fill composite resin and the storage media is unknown and requires further investigation.

Altering the resin thickness is one of the other variables that can affect the final appearance of composite restoration. In the present study we tested the different thicknesses (2 and 34 mm) on the color stability of bulk-fill composite resin. We found that bulk-fill materials showed significantly greater discoloration at increasing increment thickness at 14 d and

28 d. This can be explained by the polymerization process of resin-based composites. Depth of cure can be influenced by different factors such as the monomer composition, filler content, and photoinitiator system. Light exposure can lead to causing activation of the photoinitiator which is attenuated by composite absorption and scattering. Thus, depth of cure relies on the material's capacity to transfer light into its depths, as well as on the polymerization kinetics. A previous study showed that, in the case of applying composite resin incrementally, no significant difference was observed in values of depth of cure at different depths. But a bulk-fill technique might result in a greater number of particle/resin matrix interfaces and increased light scattering due to the differences in their refractive indices. Therefore, lesser amount of photons would reach deeper layers of composite resin and consequently a lower depth of cure value would be obtained at the deepest depths. In accordance with these results, Flury et al. reported lower depths of cure of the bulk-fill specimens with 4 mm thickness compared to the values asserted by the manufacturers [25]. In part, differences in the depth of cure, and even the overall degree of conversion, might affect the uncured monomer released and influence the composite discoloration [26]. As a consequence, mechanical properties are deteriorated leading to greater monomer elution which can result in more water absorption and, hence, discoloration.

5. Conclusions

Our findings demonstrated that bulk-fill composite resin had greater color susceptibility after immersion in coffee than conventional composites. Considering the increment thickness it can be noted that the discoloration is increased with greater increment thickness. We demonstrated that greater staining susceptibility of thicker specimens might be due to their lower depth of cure when placing bulk-fill materials.

Competing Interests

The authors declare that there are no competing interests.

Acknowledgments

The authors would like to thank Dr. Mina Mahdian for her contribution in revising the English version of the text.

References

[1] I. E. Ruyter, K. Nilner, and B. Möller, "Color stability of dental composite resin materials for crown and bridge veneers," *Dental Materials*, vol. 3, no. 5, pp. 246–251, 1987.

[2] I. Nasim, P. Neelakantan, R. Sujeer, and C. V. Subbarao, "Color stability of microfilled, microhybrid and nanocomposite resins—an in vitro study," *Journal of Dentistry*, vol. 38, no. 2, pp. e137–e142, 2010.

[3] N. Gönülol and F. Yılmaz, "The effects of finishing and polishing techniques on surface roughness and color stability of nanocomposites," *Journal of Dentistry*, vol. 40, no. 2, pp. e64–e70, 2012.

[4] R. I. Vogel, "Intrinsic and extrinsic discoloration of the dentition. (A literature review)," *Journal of Oral Medicine*, vol. 30, no. 4, pp. 99–104, 1975.

[5] C. M. Um and I. E. Ruyter, "Staining of resin-based veneering materials with coffee and tea," *Quintessence International*, vol. 22, no. 5, pp. 377–386, 1991.

[6] E. Ertaş, A. U. Güler, A. Ç. Yücel, H. Köprülü, and E. Güler, "Color stability of resin composites after immersion in different drinks," *Dental Materials Journal*, vol. 25, no. 2, pp. 371–376, 2006.

[7] P. Villalta, H. Lu, Z. Okte, F. Garcia-Godoy, and J. M. Powers, "Effects of staining and bleaching on color change of dental composite resins," *Journal of Prosthetic Dentistry*, vol. 95, no. 2, pp. 137–142, 2006.

[8] Z. A. Khokhar, M. E. Razzoog, and P. Yaman, "Color stability of restorative resins," *Quintessence International*, vol. 22, no. 9, 1991.

[9] M. D. Gross and J. B. Moser, "A colorimetric study of coffee and tea staining of four composite resins," *Journal of Oral Rehabilitation*, vol. 4, no. 4, pp. 311–322, 1977.

[10] M. Hasani-Tabatabaei, E. Yassini, S. Moradian, and N. Elmamooz, "Color stability of dental composite materials after exposure to staining solutions: a spectrophotometer analysis," *Majallah i Dandanpizishki*, vol. 21, no. 1, pp. Pe69–Pe78, 2009.

[11] R. Pilo, D. Oelgiesser, and H. S. Cardash, "A survey of output intensity and potential for depth of cure among light-curing units in clinical use," *Journal of Dentistry*, vol. 27, no. 3, pp. 235–241, 1999.

[12] S. Bucuta and N. Ilie, "Light transmittance and micromechanical properties of bulk fill vs. conventional resin based composites," *Clinical Oral Investigations*, vol. 18, no. 8, pp. 1991–2000, 2014.

[13] Z. Tarle, T. Attin, D. Marovic, L. Andermatt, M. Ristic, and T. T. Tauböck, "Influence of irradiation time on subsurface degree of conversion and microhardness of high-viscosity bulk-fill resin composites," *Clinical Oral Investigations*, vol. 19, no. 4, pp. 831–840, 2015.

[14] N. Ilie, S. Bucuta, and M. Draenert, "Bulk-fill resin-based composites: an in vitro assessment of their mechanical performance," *Operative Dentistry*, vol. 38, no. 6, pp. 618–625, 2013.

[15] P. Czasch and N. Ilie, "In vitro comparison of mechanical properties and degree of cure of bulk fill composites," *Clinical Oral Investigations*, vol. 17, no. 1, pp. 227–235, 2013.

[16] F. D. Jarad, M. D. Russell, and B. W. Moss, "The use of digital imaging for colour matching and communication in restorative dentistry," *British Dental Journal*, vol. 199, no. 1, pp. 43–49, 2005.

[17] F. M. Mundim, F. D. C. P. Pires-de-Souza, L. D. F. R. Garcia, and S. Consani, "Colour stability, opacity and cross-link density of composites submitted to accelerated artificial aging," *The European Journal of Prosthodontics and Restorative Dentistry*, vol. 18, no. 2, pp. 89–93, 2010.

[18] A. U. Yap, C. P. Sim, W. L. Loh, and J. H. Teo, "Human-eye versus computerized color matching," *Operative Dentistry*, vol. 24, no. 6, pp. 358–363, 1999.

[19] G. Van Groeningen, W. Jongebloed, and J. Arends, "Composite degradation *in vivo*," *Dental Materials*, vol. 2, no. 5, pp. 225–227, 1986.

[20] H. Øysæd and I. E. Ruyter, "Water sorption and filler characteristics of composites for use in posterior teeth," *Journal of Dental Research*, vol. 65, no. 11, pp. 1315–1318, 1986.

[21] R. Bagheri, M. J. Tyas, and M. F. Burrow, "Subsurface degradation of resin-based composites," *Dental Materials*, vol. 23, no. 8, pp. 944–951, 2007.

[22] A. C. Shortcill, W. M. Palin, and P. Burtscher, "Refractive index mismatch and monomer reactivity influence composite curing depth," *Journal of Dental Research*, vol. 87, no. 1, pp. 84–88, 2008.

[23] N. Azzopardi, K. Moharamzadeh, D. J. Wood, N. Martin, and R. van Noort, "Effect of resin matrix composition on the translucency of experimental dental composite resins," *Dental Materials*, vol. 25, no. 12, pp. 1564–1568, 2009.

[24] M. Orłowski, B. Tarczydło, and R. Chałas, "Evaluation of marginal integrity of four bulk-fill dental composite materials: in vitro study," *The Scientific World Journal*, vol. 2015, Article ID 701262, 8 pages, 2015.

[25] S. Flury, S. Hayoz, A. Peutzfeldt, J. Hüsler, and A. Lussi, "Depth of cure of resin composites: is the ISO 4049 method suitable for bulk fill materials?" *Dental Materials*, vol. 28, no. 5, pp. 521–528, 2012.

[26] R. Janda, J.-F. Roulet, M. Kaminsky, G. Steffin, and M. Latta, "Color stability of resin matrix restorative materials as a function of the method of light activation," *European Journal of Oral Sciences*, vol. 112, no. 3, pp. 280–285, 2004.

Hindawi Publishing Corporation
International Journal of Dentistry
Volume 2016, Article ID 7094056, 6 pages
http://dx.doi.org/10.1155/2016/7094056

Research Article

The Reinforcement Effect of Nano-Zirconia on the Transverse Strength of Repaired Acrylic Denture Base

Mohammed Gad,[1] Aws S. ArRejaie,[1] Mohamed Saber Abdel-Halim,[1] and Ahmed Rahoma[2,3]

[1]*Department of Substitutive Dental Sciences, College of Dentistry, University of Dammam, P.O. Box 1982, Dammam 31411, Saudi Arabia*
[2]*Department of Biomaterial Dental Sciences, College of Dentistry, University of Dammam, P.O. Box 1982, Dammam 31411, Saudi Arabia*
[3]*Department of Dental Materials, College of Dentistry, Al-Azhar University, P.O. Box 11117, Assiut, Egypt*

Correspondence should be addressed to Mohammed Gad; dr.gad@hotmail.com

Received 18 March 2016; Accepted 9 May 2016

Academic Editor: Jamil A. Shibli

Objective. The aim of this study was to evaluate the effect of incorporation of glass fiber, zirconia, and nano-zirconia on the transverse strength of repaired denture base. *Materials and Methods.* Eighty specimens of heat polymerized acrylic resin were prepared and randomly divided into eight groups ($n = 10$): one intact group (control) and seven repaired groups. One group was repaired with autopolymerized resin while the other six groups were repaired using autopolymerized resin reinforced with 2 wt% or 5 wt% glass fiber, zirconia, or nano-zirconia particles. A three-point bending test was used to measure the transverse strength. The results were analyzed using SPSS and repeated measure ANOVA and post hoc least significance (LSD) test ($P \leq 0.05$). *Results.* Among repaired groups it was found that autopolymerized resin reinforced with 2 or 5 wt% nano-zirconia showed the highest transverse strength ($P \leq 0.05$). Repairs with autopolymerized acrylic resin reinforced with 5 wt% zirconia showed the lowest transverse strength value. There was no significant difference between the groups repaired with repair resin without reinforcement, 2 wt% zirconia, and glass fiber reinforced resin. *Conclusion.* Reinforcing of repair material with nano-zirconia may significantly improve the transverse strength of some fractured denture base polymers.

1. Introduction

Denture fracture is a common problem in prosthodontic practice that troubles both patients and prosthodontists. Inordinate masticatory forces or denture deformation during use can result in bending forces that contribute to fatigue of the material and subsequent fracture [1]. A new denture construction increases the cost and is time consuming, so denture repair is preferred [2]. Satisfactory repair should be easy and rapid and match the original color of the denture base while maintaining the dimensional accuracy [3]. Denture repair depends on many variables including material type, material reinforcement, surface design, and surface treatment [2]. Several materials have been used to repair fractured denture bases, including autopolymerized, visible light polymerized, heat polymerized, or microwave polymerized acrylic resin [4, 5]. Most (86%) of denture base repairs are made with autopolymerized acrylic resin [6] because it is easy to manipulate and fast and can be used chair-side [7]. Unfortunately, its strength has been shown to range from 18 to 81% of intact heat polymerized denture resin [3, 8]. Many attempts have been made to overcome this shortcoming via using reinforced repair material and/or modification of repair surface design and treatment. Hanna et al. investigated the effect of 45° bevel of the repair surface on the transverse strength of the repaired denture base and found that higher values were obtained [9]. Beveling of the repair surface changed the fracture type from weak adhesive to strong cohesive fracture [10]. It is appropriate to treat the repair surface with repair monomer as it modifies the surface structure and increases its bond to repair material [11–13].

Glass fiber is one of the most common reinforcement materials and many investigations of its effect on repaired

Table 1: Tested groups and coding according to repair material reinforcement.

Group code	Repair material
HC	Intact heat polymerized specimens (control)
AP	Autopolymerized acrylic resin
2GF	Autopolymerized acrylic resin reinforced with 2 wt% glass fiber
5GF	Autopolymerized acrylic resin reinforced with 5 wt% glass fiber
2ZR	Autopolymerized acrylic resin reinforced with 2 wt% zirconia
5ZR	Autopolymerized acrylic resin reinforced with 5 wt% zirconia
2NZR	Autopolymerized acrylic resin reinforced with 2 wt% nano-zirconia
5NZR	Autopolymerized acrylic resin reinforced with 5 wt% nano-zirconia

denture base have been performed. Addition of glass fiber to repair material improves the strength of a denture base repair and may decrease the occurrence of future fracture [3, 14, 15]. This may be attributed to the fact that glass fiber has a high resilience which allows the stresses to be received by them without deformation [16].

Zirconia (ZrO_2) is a metal oxide and may be used as a reinforcement material to improve the transverse strength of denture base resin [17, 18]. Reinforcement of acrylic denture base with zirconia significantly increases its transverse strength [19]. Recently, nanotechnology invaded the prosthodontic field for medical and material enhancement purposes. The properties of the reinforced resin by nanoparticles depend on the size, shape, type, and concentration of the added particles [20]. Additions of nano-zirconia to polymethylmethacrylate (PMMA) denture base have been reported to increase the transverse strength due to its small size and homogenous distribution [21].

The disadvantage of commonly used repair materials is that they have poor strength. The current research in the field of dental materials is focused on finding the appropriate repair material with adequate strength and prolonged shelf life. Till date, the effect of nano-ZrO_2 on repair strength has not been investigated. Therefore, this study was conducted to evaluate the reinforcement effect of different concentrations of glass fiber, zirconia, and nano-zirconia on the transverse strength of a repaired denture base. The null hypothesis was that the addition of different concentrations of zirconia or nano-zirconia will not improve the transverse strength of repaired denture base.

2. Materials and Methods

In accordance with ANSI/ADA specification number 12, eighty rectangular specimens of heat polymerized acrylic resin with dimensions ($65 \times 10 \times 2.5$ mm $\pm$ 0.1) were prepared using customized molds [22]. Molds were waxed up (Cavex Set Up Wax, Cavex, Netherlands) and then wax patterns were invested in type III dental stone (GC Fujirock EP, Belgium) within a flask (61B Two Flask Compress, Handler Manufacturing, USA) and then dewaxed to create the mold space. According to the manufacturer's instructions, heat polymerized acrylic resin (Major Base 20, Major Prodotti Dentari SPA, Italy) was mixed and packed in the dough stage into the mold cavity and trial closure was done and then flask was closed and kept under bench press for 30 min. Flask with acrylic resin specimens was processed for 8 hours in water bath at 74°C and then temperature was increased to 100°C for 1 hour into thermal curing unit (KaVo Elektrotechnisches Werk GmbH, D-88299, Germany). After curing, the flasks were bench cooled to room temperature prior to deflasking. The excess resin of deflasked specimens was removed with a tungsten carbide bur (HM251 FX 040 HP, Meisinger, USA), polished with acrylic polisher (HM251FX-060, Meisinger, USA), and then stored in distilled water at 37°C for 48 hours. All specimens were randomly divided into eight groups: one intact and seven repaired groups (Table 1). To create 3 mm repair gap, repair specimens were placed into the mold and numbered on both ends for reassembling. Mark was drawn at the specimen center and then at 1.5 mm distance from this mark two lines were drawn on both sides and perpendicular to the long edge of specimen. These two lines were extended on the surfaces of the mold as a guide for all specimens. At these lines the specimens were cut with low speed diamond disc (DeguDent, GmbH, REF 59903107, Dentsply, Germany) under profuse irrigation. Standardized 45° bevel joint was prepared by measuring a 2.5 mm and drawing a line parallel to the prepared edge. In the same manner, the mold sides were cut at the center measuring 8 mm from the upper surface and 3 mm from the lower surface preserving the mold base intact. Specimens were placed in the mold and cut in bevel direction by diamond disc guided by lines and mold surfaces to create a repair gap of 3 mm $\times$ 10 mm $\times$ 2.5 mm with a 45° bevel joint. Glass fiber (E-glass; length = 3 mm, Shanghai Richem International Co., Ltd., China), zirconia (99.5%, 5 um, 1314-23-4, Shanghai Richem International Co., Ltd., China), and nano-zirconia powder (99.9%, <100 nm, 1314-23-4, Shanghai Richem International Co., Ltd., China) were weighed using an electronic balance (S-234; Denver Instrument, Germany) in a concentration of 2 wt% and 5 wt% of autopolymerized acrylic resin powder (Major Repair; Major Prodotti Dentari SPA, Italy). Preweighed glass fiber, zirconia, and nano-zirconia powder were separately added to the autopolymerized acrylic resin powder and thoroughly mixed using a mortar and pestle to achieve an equal distribution of particles and uniform color. According to numbering, specimen sections were reassembled into the original mold and fixed creating 3 mm between reassembled sections. The repair surfaces were treated with the methyl methacrylate monomer for three minutes. Repair was done using the sprinkle-on monomer-polymer method and slightly overfilling the repair

gap to compensate polymerization shrinkage and finishing procedures. Once the surface of the repair material lost its glaze, the molds and their contents were placed in the pressure chamber containing water at (40°C) and at pressure 30 IB/inch^2 (pound-force per square inch) for 15 minutes. After curing, the specimens were removed from the mold, finished, polished, and then put into distilled water and incubated at 37°C for 48 hours and then tested [3, 23]. To determine transverse strength, fracture load was measured using the three-point bending test on a universal testing machine (INSTRON 8871, Servo Hydraulic system, Merlin 2 software). The specimens were placed on a 3-point flexure apparatus and the support span was 50 mm. Load was applied at the midpoint of the repaired area with crosshead speed of 5 mm/min until the specimen fractured and fracture load was recorded. The formula

$$\left(\mathrm{TS} = \frac{3WL}{2bd^2}\right) \quad (1)$$

was used to calculate the transverse strength values of each specimen, where TS is the transverse strength (in MPa), W is the fracture load (N), L is the distance between the two supports, b is the specimen width, and d is the specimen thickness [24, 25].

3. Statistical Analysis

Data analysis was performed by using SPSS-20.0, IBM software, Chicago (USA). The results were presented as mean and standard deviations. Repeated measure ANOVA was applied to see the statistical significance of the variables in comparison with control group and AP. Post hoc least significance (LSD) test was used to see the pairwise comparison of the variables. P value ≤0.05 was considered statistically significant result.

4. Results

The mean value and standard deviation of transverse strength are summarized in Table 2. The statistical analysis revealed that the transverse strength of the HC was the highest strength value between tested groups (Figure 2). There were statistically significant differences in transverse strength between the repaired groups 5NZR, 2NZR, 2GF, and 5ZR as compared to AP ($P \leq 0.05$). The higher transverse strength values were in groups 5NZR, 2NZR, and 2GF, respectively. Meanwhile 5ZR showed a significant decrease in transverse strength value. There was no significant difference in transverse strength between 2ZR and 5GF with AP.

5. Discussion

This *in vitro* study was carried out to evaluate the reinforcing effect of different concentrations of glass fiber, zirconia, and nano-zirconia on the transverse strength of a repaired denture base. Results revealed that the HC group had the highest transverse strength values amongst all groups, which is in agreement with the results of a previous study [26]. Some

Table 2: Mean, standard deviation (SD), and P values for different concentrations of glass fiber, zirconia, and nano-zirconia reinforcement.

	Mean ± SD	Versus HC	Versus AP
HC, control	83.01 ± 3.03	—	—
AP	44.85 ± 3.68	—	—
2GF	56.98 ± 2.58**	0.0001	0.001
5GF	42.75 ± 2.45*	0.0001	0.175
2ZR	50.07 ± 2.97*	0.0001	0.064
5ZR	40.21 ± 3.31**	0.0001	0.035
2NZR	65.43 ± 2.62**	0.001	0.0001
5NZR	70.77 ± 2.80**	0.001	0.0001

*Statistical significance of the material with control group only at $P \leq 0.05$.
**Statistical significance of the material with control as well as AP at $P \leq 0.05$.

reinforced repaired specimens exhibited an increase in transverse strength compared to AP; hence, the null hypothesis was rejected. The transverse strength of AP decreased up to half the value of HC group, which is in agreement with the results of previous studies [3, 27, 28]. The decrease in transverse strength may be due to lower strength of autopolymerized acrylic resin; insufficient polymerization process; and the residual monomer retained at the repair site [29–31] (Figure 1). Glass fiber addition to repair material was found to improve the transverse strength of the repaired denture base and may be more acceptable for use because of aesthetics and ease of use [32]. Findings of the current study revealed an increase in the transverse strength of 2GF compared to AP, which is in agreement with the results of a previous study [32]. This increase may be attributed to the fact that glass fiber has a high resilience which allows the stresses to be received by them without permanent deformation [16]. 5GF showed a decrease in transverse strength, which is in agreement with a previous study [33]. This could be explained due to the high fiber content which might affect the bond strength between the repair material and the denture base [34]. The results of this study showed that the addition of 2ZR improved the transverse strength of the repaired specimens. This increase in transverse strength might be resulting from the transformation of zirconia from the tetragonal to monoclinic phase resulting in absorbing the energy of crack propagation in a process called transformation toughening. Also, in this process, expansion of ZrO_2 crystals occurs and places the crack under a state of compressive stress and arresting the crack propagation [35]. The results of the present study showed that the transverse strength decreased in proportion to zirconia concentration. 5ZR additions resulted in a significant decrease in transverse strength compared to AP. This reduction in transverse strength may be caused by many reasons including higher filler percentage which resulted in more defects that affect the material strength; clustering of the particles within the resin; and more filler particles after reaching saturation of matrix leads to interruption in the resin matrix continuity [36, 37]. In contrast, one study reported that the transverse strength increased as zirconia content increased [19]. Results of this study showed that the transverse strength significantly increased after incorporation of 2NZR [38]. This increase in the transverse strength

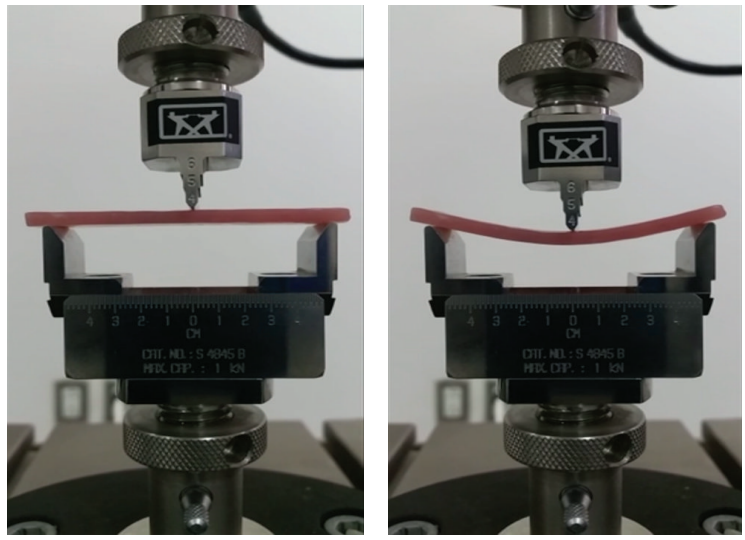

Figure 1: Acrylic resin specimen loaded on universal testing machine and subjected to fracture load.

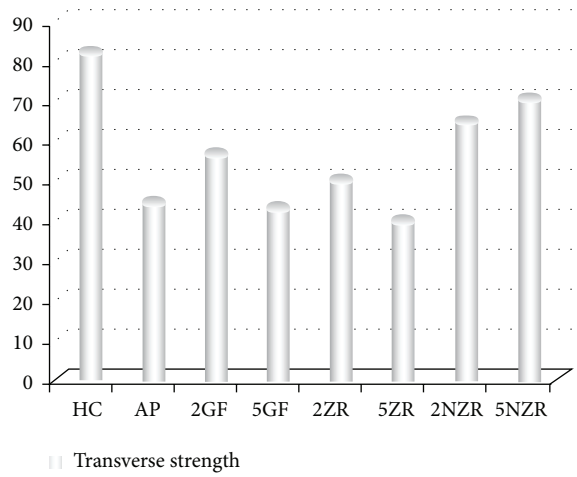

Figure 2: Mean value of transverse strength for all tested groups.

may be due to good distribution of the nanosize particles which enable them to enter and fill the spaces between polymeric chains resulting in increased interfacial shear strength between the nanoparticles and polymeric chains which improve the transverse strength [39]. It was also observed that the maximal transverse strength was recorded with 5NZR [21, 39], and the increase in nano-zirconia percentage increases the transverse strength, which is in agreement with a previous study [39] while being in disagreement with other studies [21, 40]. Clinical implication of the present study is that the incorporation of nano-zirconia into autopolymerized repair resin enhances the strength repaired denture base. The study design could not mimic the clinical conditions; hence this limitation affected the testing procedures and mechanical property investigated. Future research to study these materials should focus on simulation of clinical conditions with existing prosthesis and implementation of appropriate tests.

6. Conclusion

According to the results and limitations of this *in vitro* study, it could be concluded that nano-zirconia may be considered as a new approach for denture base repair. The repairs resulted in significantly higher transverse strength as compared to unreinforced repaired resin.

Competing Interests

The authors declare that they have no competing interests regarding the publication of this paper.

Acknowledgments

The authors would like to thank Deanship of Scientific Research, University of Dammam, for providing a research grant for this study (Grant no. 2014142). The authors would also like to deeply thank Dr. Lindsey Mateo and Mr. Intisar Siddiqui for their assistance with the mechanical testing and statistical analysis.

References

[1] U. R. Darbar, R. Huggett, and A. Harrison, "Denture fracture: a survey," *British Dental Journal*, vol. 176, no. 9, pp. 342–345, 1994.

[2] R. S. Seó, K. H. Neppelenbroek, and J. N. A. Filho, "Factors affecting the strength of denture repairs: topics of interest," *Journal of Prosthodontics*, vol. 16, no. 4, pp. 302–310, 2007.

[3] G. L. Polyzois, P. A. Tarantili, M. J. Frangou, and A. G. Andreopoulos, "Fracture force, deflection at fracture, and toughness of repaired denture resin subjected to microwave polymerization or reinforced with wire or glass fiber," *Journal of Prosthetic Dentistry*, vol. 86, no. 6, pp. 613–619, 2001.

[4] J. N. Arioli Filho, L. E. Butignon, R. D. P. Pereira, M. G. Lucas, and F. D. A. Mollo Jr., "Flexural strength of acrylic resin repairs processed by different methods: water bath, microwave energy

and chemical polymerization," *Journal of Applied Oral Science*, vol. 19, no. 3, pp. 249–253, 2011.

[5] S. Suvarna, T. Chhabra, D. Raghav, D. Singh, P. Kumar, and S. Sahoo, "Residual monomer content of repair autopolymerizing resin after microwave postpolymerization treatment," *European Journal of Prosthodontics*, vol. 2, no. 1, pp. 28–32, 2014.

[6] A. I. Zissis, G. L. Polyzois, and S. A. Yannikakis, "Repairs in complete dentures: results of a survey," *Quintessence of Dental Technology*, vol. 20, pp. 149–155, 1997.

[7] C. Bural, G. Bayraktar, I. Aydin, I. Yusufoğlu, N. Uyumaz, and M. Hanzade, "Flexural properties of repaired heat-polymerising acrylic resin after wetting with monomer and acetone," *Gerodontology*, vol. 27, no. 3, pp. 217–223, 2010.

[8] I. Kostoulas, V. T. Kavoura, M. J. Frangou, and G. L. Polyzois, "Fracture force, deflection, and toughness of acrylic denture repairs involving glass fiber reinforcement," *Journal of Prosthodontics*, vol. 17, no. 4, pp. 257–261, 2008.

[9] E. A. Hanna, F. K. Shah, and A. A. Gebreel, "Effect of joint surface contours on the transverse and impact strength of denture base resin repaired by various methods: an in vitro study," *Journal of American Science*, vol. 6, no. 9, pp. 115–125, 2010.

[10] S. Kirti, M. R. Dhakshaini, and A. K. Gujjari, "Evaluation of transverse bond strength of heat cured acrylic denture base resin repaired using heat polymerizing, autopolymerizing and fiber reinforced composite resin—an in vitro study," *International Journal of Clinical Cases and Investigations*, vol. 4, no. 2, pp. 33–43, 2012.

[11] P. K. Vallittu, V. P. Lassila, and R. Lappalainen, "Wetting the repair surface with methyl methacrylate affects the transverse strength of repaired heat-polymerized resin," *The Journal of Prosthetic Dentistry*, vol. 72, no. 6, pp. 639–643, 1994.

[12] M. Vojdani, S. Rezaei, and L. Zareeian, "Effect of chemical surface treatments and repair material on transverse strength of repaired acrylic denture resin," *Indian Journal of Dental Research*, vol. 19, no. 1, pp. 2–5, 2008.

[13] H. Minami, S. Suzuki, Y. Minesaki, H. Kurashige, and T. Tanaka, "In vitro evaluation of the influence of repairing condition of denture base resin on the bonding of autopolymerizing resins," *Journal of Prosthetic Dentistry*, vol. 91, no. 2, pp. 164–170, 2004.

[14] H. D. Stipho, "Repair of acrylic resin denture base reinforced with glass fiber," *The Journal of Prosthetic Dentistry*, vol. 80, no. 5, pp. 546–550, 1998.

[15] E. Nagai, K. Otani, Y. Satoh, and S. Suzuki, "Repair of denture base resin using woven metal and glass fiber: effect of methylene chloride pretreatment," *The Journal of Prosthetic Dentistry*, vol. 85, no. 5, pp. 496–500, 2001.

[16] G. Uzun, N. Hersek, and T. Tinçer, "Effect of five woven fiber reinforcements on the impact and transverse strength of a denture base resin," *The Journal of Prosthetic Dentistry*, vol. 81, no. 5, pp. 616–620, 1999.

[17] N. V. Asar, H. Albayrak, T. Korkmaz, and I. Turkyilmaz, "Influence of various metal oxides on mechanical and physical properties of heat-cured polymethylmethacrylate denture base resins," *Journal of Advanced Prosthodontics*, vol. 5, no. 3, pp. 241–247, 2013.

[18] A. O. Alhareb and Z. A. Ahmad, "Effect of Al_2O_3/ZrO_2 reinforcement on the mechanical properties of PMMA denture base," *Journal of Reinforced Plastics and Composites*, vol. 30, no. 1, pp. 86–93, 2011.

[19] N. M. Ayad, M. F. Badawi, and A. A. Fatah, "The effect of reinforcement of high-impact acrylic resin with zirconia on some physical and mechanical properties," *Cairo Dental Journal*, vol. 24, no. 2, pp. 245–250, 2008.

[20] I. N. Safi, "Evaluation the effect of nano—fillers (TiO_2 , AL_2O_3 , SiO_2) addition on glass transition temperature, E-moudulus and coefficient of thermal expansion of acrylic denture base material," *Journal of Baghdad College of Dentistry*, vol. 26, no. 1, pp. 37–41, 2014.

[21] N. S. Ihab and M. Moudhaffar, "Evaluation the effect of modified nano-fillers addition on some properties of heat cured acrylic denture base material," *Journal of Baghdad College of Dentistry*, vol. 23, no. 3, pp. 23–29, 2011.

[22] American Dental Association, "Revised American Dental Association Specification no. 12 for denture base polymers," *Journal of the American Dental Association*, vol. 90, no. 2, pp. 451–458, 1975.

[23] R. N. Rached, J. M. Powers, and A. A. Del Bel Cury, "Efficacy of conventional and experimental techniques for denture repair," *Journal of Oral Rehabilitation*, vol. 31, no. 11, pp. 1130–1138, 2004.

[24] M. Alkurt, Z. Yeşil Duymuş, and M. Gundogdu, "Effect of repair resin type and surface treatment on the repair strength of heat-polymerized denture base resin," *Journal of Prosthetic Dentistry*, vol. 111, no. 1, pp. 71–78, 2014.

[25] R. Zbigniew and D. Nowakowska, "Mechanical properties of hot curing acrylic resins after reinforced with different kinds of fibers," *International Journal of Biomedical Materials Research*, vol. 1, no. 1, pp. 9–13, 2013.

[26] F. Keyf and G. Uzun, "The effect of glass fibre-reinforcement on the transverse strength, deflection and modulus of elasticity of repaired acrylic resins," *International Dental Journal*, vol. 50, no. 2, pp. 93–97, 2000.

[27] H. D. Stipho and A. S. Stipho, "Effectiveness and durability of repaired acrylic resin joints," *The Journal of Prosthetic Dentistry*, vol. 58, no. 2, pp. 249–253, 1987.

[28] F. Faot, W. J. da Silva, R. S. da Rosa, A. A. Del Bel Cury, and R. C. M. R. Garcia, "Strength of denture base resins repaired with auto- and visible light-polymerized materials," *Journal of Prosthodontics*, vol. 18, no. 6, pp. 496–502, 2009.

[29] R. N. Rached, J. M. Powers, and A. A. Del Bel Cury, "Repair strength of autopolymerizing, microwave, and conventional heat-polymerized acrylic resins," *Journal of Prosthetic Dentistry*, vol. 92, no. 1, pp. 79–82, 2004.

[30] P. K. Vallittu, "The effect of surface treatment of denture acrylic resin on the residual monomer content and its release into water," *Acta Odontologica Scandinavica*, vol. 54, no. 3, pp. 188–192, 1996.

[31] J. A. Kenneth, C. Shen, and H. R. Rawls, *Phillips' Science of Dental Materials*, Elsevier Saunders, Philadelphia, Pa, USA, 12th edition, 2013.

[32] G. S. Solnit, "The effect of methyl methacrylate reinforcement with silane-treated and untreated glass fibers," *The Journal of Prosthetic Dentistry*, vol. 66, no. 3, pp. 310–314, 1991.

[33] N. Anasane, Y. Ahirrao, D. Chitnis, and S. Meshram, "The effect of joint surface contours and glass fiber reinforcement on the transverse strength of repaired acrylic resin: an in vitro study," *Dental Research Journal*, vol. 10, no. 2, pp. 214–219, 2013.

[34] M. M. Gad, M. A. Helal, M. E. Abdel-Nasser, and M. I. Seif-Elnassr, "Effect of the microwave and reinforcement of repaired acrylic resin on some mechanical properties," *Al-Azhar Journal of Dental Science*, vol. 12, no. 1, pp. 65–72, 2009.

[35] J. A. Kenneth, *Phillips' Science of Dental Materials*, Saunders, Philadelphia, Pa, USA, 11th edition, 2003.

[36] T. Nejatian, A. Johnson, and R. Van Noort, "Reinforcement of denture base resin," *Advances in Science and Technology*, vol. 49, pp. 124–129, 2006.

[37] M. Braden, "Some aspects of the chemistry and physics of dental resins," *Advances in Dental Research*, vol. 2, no. 1, pp. 93–97, 1988.

[38] X.-J. Zhang, X.-Y. Zhang, B.-S. Zhu, and C. Qian, "Effect of nano ZrO_2 on flexural strength and surface hardness of polymethylmethacrylate," *Shanghai Kou Qiang Yi Xue*, vol. 20, no. 4, pp. 358–363, 2011.

[39] M. A. Ahmed and M. I. Ebrahim, "Effect of zirconium oxide nano-fillers addition on the flexural strength, fracture toughness, and hardness of heat-polymerized acrylic resin," *World Journal of Nano Science and Engineering*, vol. 4, no. 2, pp. 50–57, 2014.

[40] H. K. Hameed and H. A. Rahman, "The effect of addition nano particle ZrO2 on some properties of autoclave processed heat cure acrylic denture base material," *Journal of Baghdad College of Dentistry*, vol. 27, no. 1, pp. 32–39, 2015.

Hindawi Publishing Corporation
International Journal of Dentistry
Volume 2016, Article ID 8590971, 9 pages
http://dx.doi.org/10.1155/2016/8590971

Clinical Study

3D Printing/Additive Manufacturing Single Titanium Dental Implants: A Prospective Multicenter Study with 3 Years of Follow-Up

Samy Tunchel,[1] Alberto Blay,[2] Roni Kolerman,[3] Eitan Mijiritsky,[4] and Jamil Awad Shibli[5]

[1]*Private Practice, Rua Asia 173, Cerqueira Cesar, 05413-030 Sao Paulo, SP, Brazil*
[2]*Private Practice, Rua Inacio Pereira da Rocha 147, 05432-010 Sao Paulo, SP, Brazil*
[3]*Department of Periodontology, The Maurice and Gabriela Goldschleger School of Dental Medicine, University of Tel Aviv, Ramat-Aviv, 6997801 Tel Aviv, Israel*
[4]*Department of Oral Rehabilitation, The Maurice and Gabriela Goldschleger School of Dental Medicine, University of Tel Aviv, Ramat-Aviv, 6997801 Tel Aviv, Israel*
[5]*Department of Periodontology and Oral Implantology, Dental Research Division, Guarulhos University, Praca Teresa Cristina 229, 07023070 Guarulhos, SP, Brazil*

Correspondence should be addressed to Samy Tunchel; stunchel@gmail.com

Received 20 February 2016; Revised 14 April 2016; Accepted 5 May 2016

Academic Editor: Spiros Zinelis

This prospective 3-year follow-up clinical study evaluated the survival and success rates of 3DP/AM titanium dental implants to support single implant-supported restorations. After 3 years of loading, clinical, radiographic, and prosthetic parameters were assessed; the implant survival and the implant-crown success were evaluated. Eighty-two patients (44 males, 38 females; age range 26–67 years) were enrolled in the present study. A total of 110 3DP/AM titanium dental implants (65 maxilla, 45 mandible) were installed: 75 in healed alveolar ridges and 35 in postextraction sockets. The prosthetic restorations included 110 single crowns (SCs). After 3 years of loading, six implants failed, for an overall implant survival rate of 94.5%; among the 104 surviving implant-supported restorations, 6 showed complications and were therefore considered unsuccessful, for an implant-crown success of 94.3%. The mean distance between the implant shoulder and the first visible bone-implant contact was 0.75 mm (±0.32) and 0.89 (±0.45) after 1 and 3 years of loading, respectively. 3DP/AM titanium dental implants seem to represent a successful clinical option for the rehabilitation of single-tooth gaps in both jaws, at least until 3-year period. Further, long-term clinical studies are needed to confirm the present results.

1. Introduction

Dental implants available for clinical uses are conventionally produced from rods of commercially pure titanium (cpTi) or its alloy Ti-6Al-4V (90% titanium, 6% aluminium, and 4% vanadium). Manufacturing processes involve machining, at a later stage, postprocessing with application of surface treatments, with the aim of enhancing healing processes, and osseointegration around dental implants [1, 2].

Over the last years, several surface treatments have been proposed, such as sandblasting, grit-blasting, acid-etching, and anodization; deposition of hydroxyapatite, calcium-phosphate crystals, or coatings with other biological molecules are all examples of attempts to obtain better implant surfaces [2–4]. In fact, several *in vitro* studies have identified that rough implant surfaces can positively influence cell behaviour and therefore bone apposition, when compared to smooth surfaces [3, 5]. Rough surfaces show superior molecules adsorption from biological fluids, improving early cellular responses, including extracellular matrix deposition, cytoskeletal organization, and tissues maturation. This implant surface topography can finally lead to a better and faster bone response around rough surfaced dental implants [3, 5]. Histological studies clearly show that rough surfaces, when compared to smooth ones, can stimulate a faster and effective

osseointegration [6–8]. These features were ratified by several clinical studies, proving excellent long-term survival/success rates for implants with modified rough surfaces [9, 10].

Traditional manufacturing and postprocessing methods, however, provide us with fixtures characterized by a high-density titanium core with different micro- or nanorough surfaces [2–4]. Using these methods, it is not possible to fabricate implants with structure possessing a gradient of porosity perpendicular to the long axis and therefore with a highly porous surface and a highly dense core [11, 12].

However, structures with controlled variable porosity can balance the mismatch between different elastic modulus of bone tissues and titanium implants, thus reducing stresses under functional loading and promoting long-term fixation stability and clinical success [11, 12]. Conventionally, cpTi implants present a higher rigidity than surrounding bone because of Young's modulus (elastic modulus) of the material and the geometry of the structure [12]. Elastic modulus of cpTi (112 GPa) and titanium alloy Ti-6Al-4V (115 GPa) are both higher than those of cortical bone (10–26 GPa) [12]. In addition, osseointegration of the dental implant can be biologically improved by a porous structure with an open interconnected pore system; this system can promote bone ingrowth into the metal framework, giving a strong mechanical interlocking between the fixture and the bone [12, 13].

Because of these considerations, there is a demand for new fabrication methods, with the aim of obtaining porous titanium framework, with controlled porosity, pore size, and localization [13, 14].

Porous titanium implants have been introduced in orthopaedics and dental practice since the end of the 1960s with interesting results [15, 16]; however, these were generally obtained using sprays techniques and coating on implant surfaces [16]. However, fatigue resistance of coated implants fabricated with this method may be reduced up to 1/3 when compared with standard uncoated implants [17]. More recently, different fabrication methods to obtain porous titanium frameworks have been proposed including cosintering precursor particles, powder plasma spraying over a high-density core, titanium fibers sintering, and solid-state foaming by expansion of argon-filled pores [17–19]. However, none of these methods can realize titanium scaffolds allowing complete control on the external shape geometry as well as interconnected pore system [12].

In the last few decades, 3D printing/additive manufacturing (3DP/AM) technologies have become more and more important in the world of industry: these allow realizing physical objects starting from virtual 3D data project, without intermediate production steps, saving time and money [12, 20, 21]. With 3DP/AM, porous titanium implants for medical applications can be fabricated. In fact, a high power focused laser beam fuses metal particles arranged in a powder bed and generates the implant layer-by-layer, with no postprocessing steps required [20, 21].

The physical and chemical properties of 3DP/AM titanium have been extensively studied [11, 12, 21]. At a later stage, different *in vitro* studies have investigated the cell response to the surface of 3DP/AM implants, examining the formation of human fibrin clot [22] and the behaviour of human mesenchymal stem cells and human osteoblasts [22, 23]. Several animal [24, 25] and human [26–28] histologic/histomorphometric studies have documented the bone response after the placement of 3DP/AM titanium implants. However, only a few clinical studies have investigated the performance of 3DP/AM titanium dental implants: these are based on a limited number of patients with a short follow-up [29–32].

Hence, the aim of the present prospective clinical study with 3 years of follow-up was to evaluate the survival and success rates of single 3DP/AM titanium dental implants placed in both jaws.

2. Materials and Methods

2.1. Inclusion and Exclusion Criteria. The present investigation was designed as a prospective multicenter clinical study. Between January 2010 and January 2012, all patients with a single-tooth gap or in need of replacement of a failing, nonrecoverable single tooth, who were referred to 4 different private practices for treatment with dental implants, were considered for enrollment in the present study. Inclusion criteria were good oral health and sufficient bone availability to receive a fixture of at least 3.3 mm in diameter and 8.0 mm in length. Exclusion criteria were poor oral hygiene, nontreated periodontal disease, smoking, and bruxism. The study protocol was exposed to each subject before enrollment: everybody accepted it and signed an informed consent form. The work was performed in accordance with the principles outlined in the Declaration of Helsinki on experimentation involving human subjects, as revised in 2008.

2.2. Additive Manufacturing Implants and Characterization. The implants used in this study (Tixos®, Leader Implants, Milan, Italy) were fabricated with an additive manufacturing (AM) technology, starting from powders of titanium alloy (Ti-6Al-4V) with a particle size of 25–45 μm. The implants were fabricated layer-by-layer by an Yb (ytterbium) fiber laser system (EosyntM270®, EOS GmbH, Munich, Germany), operating in an argon controlled atmosphere, using a wavelength of 1,054 nm with a continuous power of 200 W at a scanning rate of 7 m/s and with the capacity to build a volume of 250 × 250 × 215 mm. Laser spot size was 0.1 mm. Postproduction steps consisted of sonication for 5 min in distilled water at 25°C, immersion in NaOH (20 g/L) and hydrogen peroxide (20 g/L) at 80°C for 30 min, and then further sonication for 5 min in distilled water. The implants were then acid-etched in a mixture of 50% oxalic acid and 50% maleic acid, at 80°C for 45 min, and washed for 5 min in a sonic bath of distilled water. These procedures were needed to remove any residual nonadherent titanium particle. The AM implants featured a porous surface with R_a value of 66.8 μm, R_q value of 77.55 μm, and R_z value of 358.3 μm, respectively.

The implant surface microstructure consisted of roughly spherical particles ranging between 5 and 50 μm. After exposure to hydrofluoric acid some of these were removed and the microsphere diameter then ranged from 5.1 μm to 26.8 μm. Particles were replaced by grooves with 14.6 to 152.5 μm in

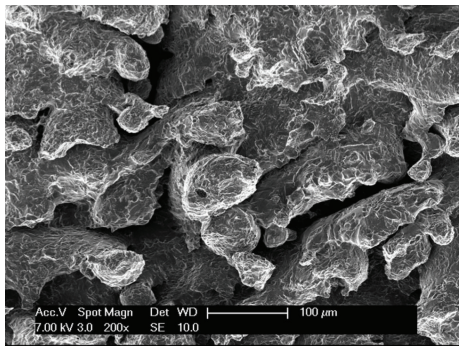

Figure 1: Scanning electron microscopy (SEM) of the 3DP/AM porous implant surface.

width and 21.4 to 102.4 μm in depth after an organic acid treatment. The metal core consisted of prior beta grains. The titanium alloy was composed of titanium (90.08%), aluminium (5.67%), and vanadium (4.25%) (Figure 1). Young's modulus of the inner core material was 104 ± 7.7 GPa, while that of the outer porous material was 77 ± 3.5 GPa. The fracture face showed a dimpled appearance typical of ductile fracture [12].

2.3. Preoperative Evaluation. An accurate preoperative evaluation of the oral hard and soft tissue was performed in each patient. Preoperative procedures included the clinical and radiographic examination of the single-tooth gaps. Panoramic and periapical radiographs were taken as primary investigation. In some cases, cone-beam computed tomography (CBCT) was required. CBCT data were processed by dedicated DICOM (Digital Imaging and Communications in Medicine) viewer softwares in order to realize a 3D reconstruction of maxillary bones. With these types of software, it is possible to navigate between maxillary structures and to correctly assess bone features for each implant site, such as thickness, density of the cortical plates and of the cancellous bone, and ridge angulations. Finally, impressions were taken and stone casts were made for the diagnostic wax-up.

2.4. Implant Placement. Local anaesthesia was obtained, infiltrating 4% articaine with 1 : 100.000 adrenaline. In patients with a missing single tooth, a crestal incision and two releasing incisions, on mesial and distal sides, were made at surgical site. Full-thickness flaps were elevated depicting alveolar ridge. The preparation of fixture sites was realized with spiral drills of increasing diameter, under constant irrigation with sterile saline. Cover screws were screwed on the implants; then flaps were repositioned using interrupted sutures. In patients with a failing, nonrecoverable single tooth, a flapless approach was followed. A gentle extraction was performed, avoiding any damage of the socket bone walls, using a periotome. Then, the preparation of the surgical site was based on the receiving site's bone quality. The preparation was deepened 3-4 mm apically to the end of the postextraction socket in order to better engage the implant. The implant was placed in position with its cover screw; then particulate bone grafts were placed to fill the space between the implant and the socket walls. Finally, platelet rich in growth factors (PRGF) was prepared, positioned, and sutured to cover the socket in order to protect the surgical site and to accelerate soft tissue healing.

2.5. Postoperative Treatment. Pharmacological postsurgery procedures consisted of oral antibiotics 2 g each day for 6 days (Augmentin®, GlaxoSmithKline Beecham, Brentford, UK). Any postoperative pain was managed by administering 100 mg nimesulide (Aulin®, Roche Pharmaceutical, Basel, Switzerland) every 12 h for 2 days. In addition, patients were educated about oral hygiene maintenance with mouth rinses with 0.12% chlorhexidine (Chlorexidine®, OralB, Boston, MA, USA) administered for 7 days. Sutures were removed at 8–10 days after surgery.

2.6. Healing Period. Implants were placed with a two-stage technique, waiting a healing period of at least 2-3 months in the mandible and 3-4 months in the maxilla. During the second-stage surgery, underlying fixtures were exposed with a small crestal incision and healing transmucosal abutments were screwed replacing the cover screws. Flaps were stabilized around healing abutment by suturing. Two weeks later, the final impressions were taken, and therefore the final abutments and the provisional crowns were delivered to patients. Provisional crowns, made in acrylic resin, had the task of evaluating the stability of implants under a progressive functional load and influencing the maturation of soft tissues around fixtures before the implementation of final restorations. The provisional crowns were left *in situ* for three months; then the final metal-ceramic crowns were delivered and cemented with zinc phosphate cement or zinc-eugenol oxide cement.

2.7. Clinical, Prosthetic, and Radiographic Evaluation. All patients were enrolled in a follow-up recall program, with sessions of professional oral hygiene every 6 months. During these sessions, every year, the implant-supported restorations were carefully checked. Static and dynamic occlusion was controlled, and periapical radiographs were taken using a Rinn alignment system (Rinn®, Dentsply, Elgin, IL, USA). Customized positioners were also used for correct repositioning and stabilization of radiographic template.

At the end of the study, after three years of functional loading, the following clinical, prosthetic, and radiographic parameters were evaluated for each implant.

Clinical Parameters

(i) Presence/absence of pain, sensitivity.

(ii) Presence/absence of suppuration, exudation.

(iii) Presence/absence of implant mobility.

Prosthetic Parameters

(i) Presence/absence of mechanical complications (i.e., complications of prefabricated implant components,

such as abutment screw loosening, abutment screw fracture, abutment fracture, and implant fracture).

(ii) Presence/absence of technical complications (i.e., complications related to superstructures, such as loss of retention and ceramic/veneer fracture).

Radiographic Parameters

(i) Presence/absence of continuous peri-implant radiolucency.

(ii) Distance between the implant shoulder and the first visible bone-implant contact (DIB).

This last value, measured with the aim of an ocular grid (4.5x), represented the quantification of crestal bone reabsorption after 3 years of functional loading, and it was measured on mesial and distal side of implant. To compensate for radiographic distortion, the actual (known) fixture length was compared to the radiographic length, using a proportion.

2.8. Implant Survival and Implant-Crown Success Criteria. An implant was categorized as survival if it was still in function after three years of functional loading. On the contrary, implant losses were all categorized as failures. Implant mobility in the absence of clinical signs of infection, persistent and/or recurrent infections (with pain, suppuration, and bone loss), progressive marginal bone loss caused by mechanical overload, and implant body fracture were conditions for which implant removal could be indicated. Implant failures were divided into "early" (before the abutment connection) or "late" (after the abutment connection) failures.

An implant-supported restoration was considered successful when the following clinical, prosthetic, and radiographic success criteria were fulfilled:

(i) Absence of pain, sensitivity.

(ii) Absence of suppuration, exudation.

(iii) Absence of clinically detectable implant mobility.

(iv) Absence of continuous peri-implant radiolucency.

(v) DIB < 1.5 mm after the first year of functional loading (and not exceeding 0.2 mm in each subsequent year).

(vi) Absence of prosthetic (mechanical or technical) complications.

3. Results

Eighty-two patients (44 males, 38 females; age range 26–67 years), who were recruited in 4 different clinical centers, fulfilled the inclusion criteria and did not present any of the conditions enlisted in the exclusion criteria: therefore, they were enrolled in the present study. In total, 110 implants (65 maxilla, 45 mandible) were installed: 75 in healed ridges and 35 in postextraction sockets. The prosthetic restorations included 110 single crowns (SCs): 32 of these were in the anterior areas (incisors, cuspids, and first premolars), while 78 were in the posterior areas (second premolars, molars). Lengths and diameters of used implants were summarized in Table 1.

Table 1: Implant distribution by length and diameter.

	8.0 mm	10.0 mm	11.5 mm	13.0 mm	
3.3 mm	—	5	5	5	15
3.75 mm	2	40	23	3	68
4.5 mm	4	10	13	—	27
	6	55	41	8	110

At the end of the study, after 3 years of functional loading, six implants failed (four during the healing period and before the abutment connection, because of implant mobility in the absence of clinical signs of infection, two after the abutment connection, one for persistent/recurrent peri-implant infection, and another one for implant body fracture) for an overall implant survival rate of 94.5% (Figures 2–5). Four implants failed in healed ridges, whereas two implants failed in extraction sockets. In the maxilla, four implants failed (3 implants showed mobility and lack of osseointegration in absence of infection, in the posterior maxilla, and had to be removed; an implant body fracture occurred in the anterior maxilla) for a survival rate of 93.8%; in the mandible, two implants failed (one for lack of osseointegration and another one for persistent/recurrent infection, both in the posterior mandible) and were removed, for a survival rate of 95.6%.

With regard to the implant-crown success, no implants showed pain or sensitivity, suppuration or exudation, or continuous peri-implant radiolucency. However, two implants showed a DIB > 1.5 mm during the first year of functional loading and were therefore considered not successful; in addition, three prosthetic abutments became loose, in the posterior areas of the mandible. These abutments were reinserted and screwed again; however, these were considered prosthetic complications. Another prosthetic complication registered was a ceramic chipping in a maxillary molar. At the end of the study, among the 104 surviving implant-supported restorations, 6 showed complications and were therefore considered unsuccessful, for a 3-year implant-crown success of 94.3%. Finally, the mean DIB was 0.75 mm (±0.32) and 0.89 (±0.45) after 1 year and 3 years of functional loading, respectively.

4. Discussion

A porous structure has many biological advantages. In fact, it facilitates the diffusion of biological fluids and nutrients for the maturation of the tissues and the removal of waste products of metabolism; moreover, it allows cell ingrowth and reorganization as well as neovascularization from surrounding tissues. A scaffold with well-defined porosity characteristics (pores size, geometry, distribution, and interconnectivity) can therefore enhance bone ingrowth [12, 13, 20, 33]. In this context the size of the interconnections between pores, according to several researchers, seems to be one of the most important parameters influencing the bone growth in its structure [20].

According to some researchers, pore size between 200 and 400 μm seems to be the ideal measure to positively

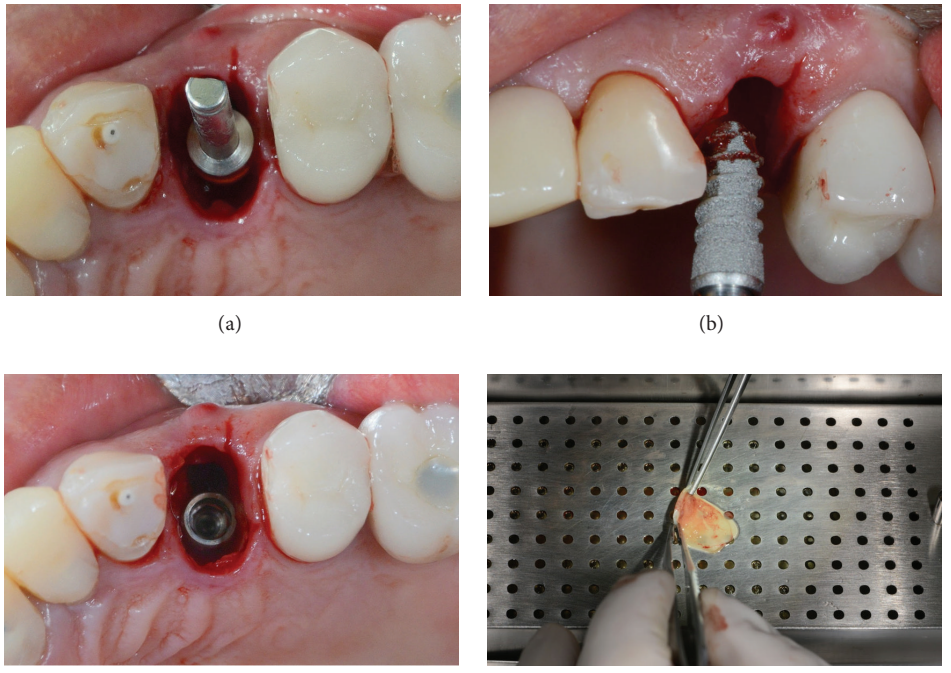

(a) (b)

(c) (d)

Figure 2: Placement of a single 3DP/AM titanium dental implant in a postextraction socket of the posterior maxilla: surgical phases. (a) Preparation of the implant site. (b) Placement of the 3DP/AM porous implant in the postextraction socket. (c) The implant in position. (d) Preparation of the biological membrane-platelet rich in growth factors (PRGF).

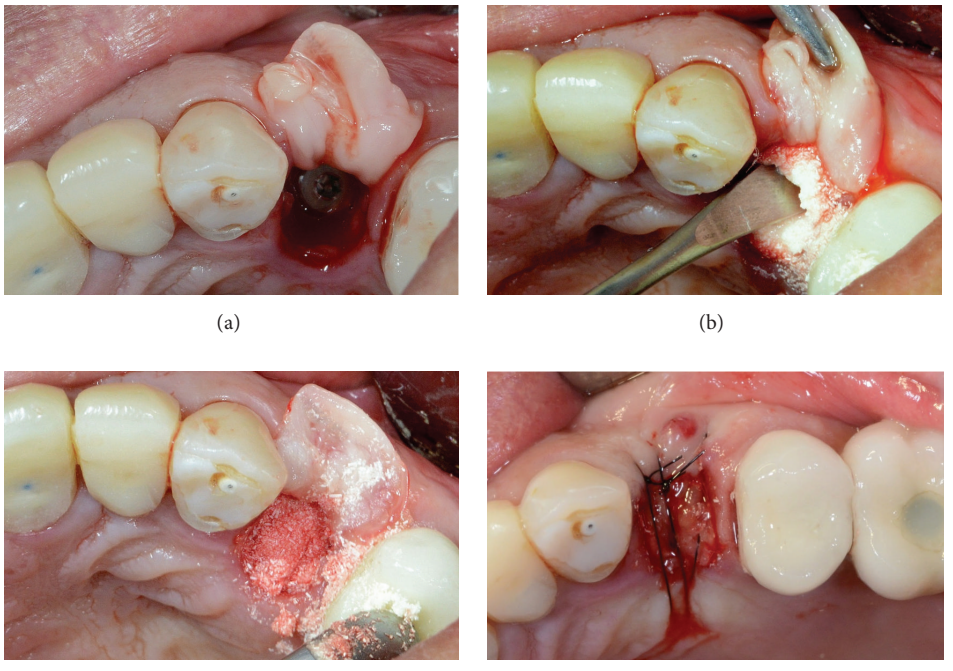

(a) (b)

(c) (d)

Figure 3: Placement of a single 3DP/AM titanium dental implant in a postextraction socket of the posterior maxilla: surgical phases. (a) The biological membrane is ready to be sutured for protecting the socket. (b) Socket preservation with particulate bone grafts. (c) The socket is completely filled with particulate bone grafts before the sutures. (d) Sutures.

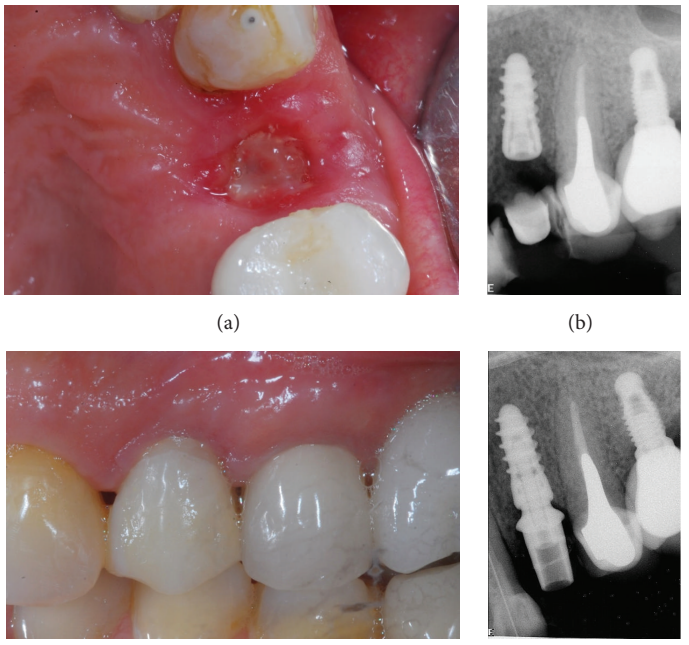

(a) (b)

(c) (d)

Figure 4: A single 3DP/AM titanium dental implant in a postextraction socket of the posterior maxilla: healing phases. (a) Ten days after surgery, sutures are removed. (b) Periapical rx 10 days after implant placement. (c) Three months later, a provisional restoration is placed. (d) Periapical rx at placement of the provisional restoration.

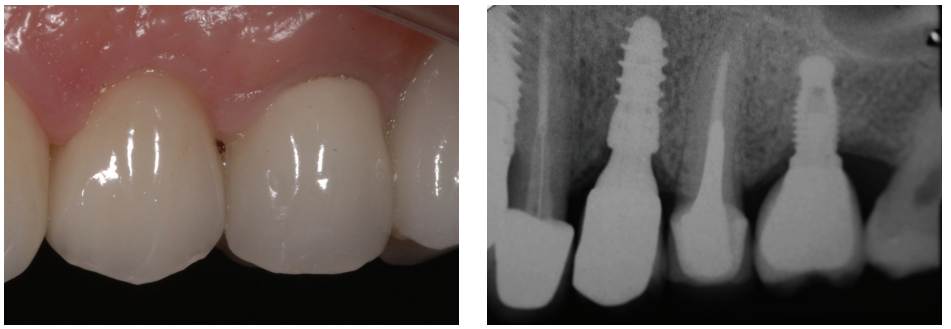

(a) (b)

Figure 5: A single 3DP/AM titanium dental implant in a postextraction socket of the posterior maxilla: 3-year follow-up control. (a) Clinical picture after 3 years of functional loading. (b) Periapical rx after 3 years of functional loading.

influence the behaviour of bone cells [20, 33], whereas Sachlos and Czernuszka [34] have achieved excellent results using a scaffold with 500 μm pores size. Xue et al. [35, 36] have recently assessed the *in vitro* reaction of bone cells in presence of a porous titanium AM scaffold. The authors have highlighted how osteoblasts spread on the surface, migrate into the cavities of these porous scaffolds (pore sizes of 200 μm or higher are recommended), and produce new bone matrix [35, 36]. The *in vivo* physiological response to these porous scaffolds includes the formation of new tissue that infiltrates the network, with capillaries, perivascular tissues, and progenitor cells migrating into the pore system and supporting the healing processes [35, 36]. Because of the considerable amount of data in the current literature, there is still no agreement on the optimal size of the pores for endosseous implants; however, pore sizes between 100 and 400 μm seem to be able to support the formation of mineralized bone inside porous scaffolds [37, 38].

Although the benefits of an open-pore structure with controlled porosity at the implant surface have been elucidated [38], it was very difficult to realize implants with these characteristics using standard production methods.

3DP/AM techniques have been recently proposed in order to overcome these obstacles and to fabricate endosseous implants (including dental implants) with controlled and functionally graded porosity [11–13]. 3DP/AM is able to control the porosity of each layer and consequently the porous structure of the whole implant by simply modifying

some processing parameters (such as power and diameter of the focused laser beam, layer thickness and distance between them, the size of the original titanium powders, and processing atmosphere) [11, 12]. With this method, it is also possible to control the size, distribution, and interconnectivity of pores [13], giving a controlled, open-pore network. In addition, 3DP/AM allows implants with a gradient of porosity along the main axis to be fabricated [12]. Finally, 3DP/AM implants do not require postfabrication process: they do not require decontamination, since they are not machined and therefore no oils or contaminants are employed. Moreover, they do not need surface treatments, and this may further reduce the costs.

One of early steps of osseointegration process involves migration of osteoprogenitor cells into fibrin network established on the implant surface [12, 13, 20]. A recent *in vitro* study [22] reported that human fibrin can quickly realize, around porous AM titanium surface, a stable three-dimensional network. Moreover, AM porous titanium surfaces are able to recruit osteoprogenitor cells that, when differentiated into osteoblasts, produce woven bone under the influence of bone morphogenetic proteins, vascular endothelial growth factor, and other specific bone proteins [22, 23]. Research has partially clarified some of the mechanisms that regulate cell functions and differentiation. Cells interact with their substrates through specific adhesion membrane proteins, called integrins, which are responsible for the formation of focal adhesion plaque [38–40]. Moreover, integrins are linked to specific cytoskeleton adaptor proteins through their cytoplasmic domain. The formation of focal adhesion plaques and subsequent cell adhesion generate mechanical forces that are converted into biochemical signals within cells by integrins and other mechanoreceptors [38–40]. Thus, the geometry of substrates can affect a wide spectrum of cellular responses [38–40]. Geometric properties of implant surface are then able to induce modification in cell shape, inducing changes on genes expression [39].

The surface generated with 3DP/AM technology, characterized by pores, cavities, and interconnections, could represent a powerful stimulus for osteogenic phenotype expression, as demonstrated in different *in vitro* studies [21, 22]. Cells in contact with AM surfaces are forced to take specific three-dimensional shape according to scaffold pores and cavities, generating mechanical stresses that induce osteogenic phenotype expression [22, 23].

All these findings have been confirmed in a series of histologic and histomorphometric studies, in animals [24, 25] and humans [26–28]. However, until now, only a few clinical studies have dealt with 3DP/AM titanium implants [29–32].

In a first multicenter clinical study evaluating the survival and success of 201 3DP/AM porous titanium implants supporting fixed restorations (single crowns, fixed partial prostheses, and fixed full arches), 201 implants were inserted in 62 subjects [29]. Most of the implants (122) were placed in the posterior areas of jaws. After 1 year of loading, an overall implant survival rate of 99.5% was reported, with only one failed and removed fixture [29]. In this first study, among the surviving fixtures implants (200), only 5 could not satisfy the success criteria, for an implant-crown success of 97.5% [29]; moreover, a mean distance between the implant shoulder and the first bone-to-implant contact of 0.4 mm (±0.2) was reported [29].

Another clinical study aimed at evaluating survival, complications, and peri-implant marginal bone loss of 3DP/AM porous titanium implants used to support bar-retained maxillary overdentures [30]. Over a 2-year period, 120 fixtures were installed in the maxilla of 30 subjects to support bar-retained overdentures. Each denture was supported by 4 splinted implants, by means of a rigid cobalt chrome bar. The patient-based implant survival and incidence of biologic and prosthetic complications were registered. At the 3-year follow-up examination, three implants failed and had to be removed, for an overall survival rate of 92.9% [30]. The biologic complications amounted to 7.1%, whereas the prosthetic complications were more frequent (17.8%) [30]. At the 3-year examination, the peri-implant marginal bone loss amounted to 0.62 mm (±0.28); therefore the authors concluded that the use of 4 3DP/AM titanium implants to support bar-retained maxillary overdentures can be considered a safe and successful treatment procedure [30].

Finally, in a recent previous clinical study, 231 one-piece 3DP/AM porous titanium mini-implants (2.7 and 3.2 mm diameter) were inserted in 62 patients to support immediately loaded mandibular overdentures [31]. In this study, six fixtures failed after a period of 4 years of functional loading, giving an overall cumulative survival rate of 96.9% [31]. The biologic complications amounted to 6.0%, while the prosthetic complications were more frequent (12.9%). Finally, a mean DIB of 0.38 mm (±0.25) and 0.62 mm (±0.20) was reported at the 1-year and 4-year follow-up examinations, respectively [31].

These results seem to be in accordance with those of our present 3-year follow-up prospective clinical study, in which the clinical behaviour of 110 single implants produced with 3DP/AM technology and placed in both jaws was evaluated. A satisfactory survival rate was observed (94.5%), with only six failed and removed implants. Among the 104 implants still in function at the end of the follow-up period, 98 were categorized as successful, giving an implant-crown success rate of 94.3%. Only six implants could not attain implant-crown success criteria: two fixtures displayed a DIB > 1.5 mm after 1 year of functional loading, three implants presented loosening of prosthetic abutment during follow-up period, and another implant-supported restoration had a ceramic chipping. Furthermore, radiographic evaluation showed an excellent bone stability around single 3DP/AM implants. The mean distances between the implant shoulder and the first visible bone-to-implant contact (DIB) were 0.75 mm (±0.32) and 0.89 (±0.45) after 1 year and 3 years of functional loading, respectively.

5. Conclusions

In this 3-year follow-up prospective clinical study, single 3DP/AM implants have shown 94.5% of survival rate and 94.3% of implant-crown success rate. Considering these results, dental implants produced with 3DP/AM technologies seem to represent a successful clinical option for the

rehabilitation of single-tooth gaps in both jaws, at least after a 3-year follow-up. However, the present study has clear limits (such as limited number of patients treated and fixtures installed and short follow-up period); therefore further long-term clinical studies will be necessary to evaluate the long-term performance as well as the mechanical resistance of single 3DP/AM implants placed in both jaws. In addition, real potential of 3DP/AM implants in restoring partially or completely edentulous arches still needs to be elucidated.

Competing Interests

The authors declare that they have no financial relationship with any company or commercial entity that may pose competing interests for the present work.

References

[1] M. M. Shalabi, A. Gortemaker, M. A. Van't Hof, J. A. Jansen, and N. H. J. Creugers, "Implant surface roughness and bone healing: a systematic review," *Journal of Dental Research*, vol. 85, no. 6, pp. 496–500, 2006.

[2] A. Wennerberg and T. Albrektsson, "Effects of titanium surface topography on bone integration: a systematic review," *Clinical Oral Implants Research*, vol. 20, no. 4, pp. 172–184, 2009.

[3] A. B. Novaes Jr., S. L. S. de Souza, R. R. M. de Barros, K. K. Y. Pereira, G. Iezzi, and A. Piattelli, "Influence of implant surfaces on osseointegration," *Brazilian Dental Journal*, vol. 21, no. 6, pp. 471–481, 2010.

[4] A. Jemat, M. J. Ghazali, M. Razali, and Y. Otsuka, "Surface modifications and their effects on titanium dental implants," *BioMed Research International*, vol. 2015, Article ID 791725, 11 pages, 2015.

[5] D. Buser, "Titanium for dental applications (II): implants with roughened surfaces," in *Titanium in Medicine. Material Science, Surface Science, Engineering, Biological Responses and Medical Applications*, D. M. Brunette, P. Tengvall, M. Textor, and P. Thomsen, Eds., pp. 875–888, Springer, Berlin, Germany, 2001.

[6] H. Chiang, H. Hsu, P. Peng et al., "Early bone response to machined, sandblasting acid etching (SLA) and novel surface-functionalization (SLAffinity) titanium implants: characterization, biomechanical analysis and histological evaluation in pigs," *Journal of Biomedical Materials Research Part A*, vol. 104, no. 2, pp. 397–405, 2016.

[7] J. A. Shibli, S. Grassi, L. C. de Figueiredo et al., "Influence of implant surface topography on early osseointegration: a histological study in human jaws," *Journal of Biomedical Materials Research—Part B: Applied Biomaterials*, vol. 80, no. 2, pp. 377–385, 2007.

[8] J. A. Shibli, S. Grassi, A. Piattelli et al., "Histomorphometric evaluation of bioceramic molecular impregnated and dual acid-etched implant surfaces in the human posterior maxilla," *Clinical Implant Dentistry and Related Research*, vol. 12, no. 4, pp. 281–288, 2010.

[9] D. L. Cochran, J. M. Jackson, J.-P. Bernard et al., "A 5-year prospective multicenter study of early loaded titanium implants with a sandblasted and acid-etched surface," *The International Journal of Oral & Maxillofacial Implants*, vol. 26, no. 6, pp. 1324–1332, 2011.

[10] F. Mangano, A. Macchi, A. Caprioglio, R. L. Sammons, A. Piattelli, and C. Mangano, "Survival and complication rates of fixed restorations supported by locking-taper implants: a prospective study with 1 to 10 years of follow-up," *Journal of Prosthodontics*, vol. 23, no. 6, pp. 434–444, 2014.

[11] D. A. Hollander, M. von Walter, T. Wirtz et al., "Structural, mechanical and in vitro characterization of individually structured Ti-6Al-4V produced by direct laser forming," *Biomaterials*, vol. 27, no. 7, pp. 955–963, 2006.

[12] T. Traini, C. Mangano, R. L. Sammons, F. Mangano, A. Macchi, and A. Piattelli, "Direct laser metal sintering as a new approach to fabrication of an isoelastic functionally graded material for manufacture of porous titanium dental implants," *Dental Materials*, vol. 24, no. 11, pp. 1525–1533, 2008.

[13] G. E. Ryan, A. S. Pandit, and D. P. Apatsidis, "Porous titanium scaffolds fabricated using a rapid prototyping and powder metallurgy technique," *Biomaterials*, vol. 29, no. 27, pp. 3625–3635, 2008.

[14] S. Fujibayashi, M. Neo, H.-M. Kim, T. Kokubo, and T. Nakamura, "Osteoinduction of porous bioactive titanium metal," *Biomaterials*, vol. 25, no. 3, pp. 443–450, 2004.

[15] R. A. Lueck, J. Galante, W. Rostoker, and R. D. Ray, "Development of an open pore metallic implant to permit attachment to bone," *Surgical Forum*, vol. 20, no. 1, pp. 456–457, 1969.

[16] R. P. Welsh, R. M. Pilliar, and I. Macnab, "Surgical implants. The role of surface porosity in fixation to bone and acrylic," *The Journal of Bone & Joint Surgery—AmericanVolume*, vol. 53, no. 5, pp. 963–977, 1971.

[17] H. Gruner, "Thermal spray coatings on titanium," in *Titanium in Medicine: Material Science, Surface Science, Engineering, Biological Responses and Medical Applications*, D. M. Brunette, P. Tengvall, M. Textor, and P. Thomsen, Eds., Engineering Materials, pp. 375–416, Springer, Berlin, Germany, 2001.

[18] J. Galante, W. Rostoker, R. Lueck, and R. D. Ray, "Sintered fiber metal composites as a basis for attachment of implants to bone," *The Journal of Bone & Joint Surgery—American Volume*, vol. 53, no. 1, pp. 101–114, 1971.

[19] J. P. Li, J. R. De Wijn, C. A. Van Blitterswijk, and K. De Groot, "Porous Ti6Al4V scaffold directly fabricating by rapid prototyping: preparation and in vitro experiment," *Biomaterials*, vol. 27, no. 8, pp. 1223–1235, 2006.

[20] X. Wang, S. Xu, S. Zhou et al., "Topological design and additive manufacturing of porous metals for bone scaffolds and orthopaedic implants: a review," *Biomaterials*, vol. 83, no. 6, pp. 127–141, 2016.

[21] F. Mangano, L. Chambrone, R. van Noort, C. Miller, P. Hatton, and C. Mangano, "Direct metal laser sintering titanium dental implants: a review of the current literature," *International Journal of Biomaterials*, vol. 2014, Article ID 461534, 11 pages, 2014.

[22] C. Mangano, M. Raspanti, T. Traini, A. Piattelli, and R. Sammons, "Stereo imaging and cytocompatibility of a model dental implant surface formed by direct laser fabrication," *Journal of Biomedical Materials Research Part A*, vol. 88, no. 3, pp. 823–831, 2009.

[23] C. Mangano, A. De Rosa, V. Desiderio et al., "The osteoblastic differentiation of dental pulp stem cells and bone formation on different titanium surface textures," *Biomaterials*, vol. 31, no. 13, pp. 3543–3551, 2010.

[24] L. Witek, C. Marin, R. Granato et al., "Characterization and in vivo evaluation of laser sintered dental endosseous implants in dogs," *Journal of Biomedical Materials Research Part B: Applied Biomaterials*, vol. 100, no. 6, pp. 1566–1573, 2012.

[25] S. Stübinger, I. Mosch, P. Robotti et al., "Histological and biomechanical analysis of porous additive manufactured implants made by direct metal laser sintering: a pilot study in sheep," *Journal of Biomedical Materials Research Part B: Applied Biomaterials*, vol. 101, no. 7, pp. 1154–1163, 2013.

[26] C. Mangano, A. Piattelli, M. Raspanti et al., "Scanning electron microscopy (SEM) and X-ray dispersive spectrometry evaluation of direct laser metal sintering surface and human bone interface: a case series," *Lasers in Medical Science*, vol. 26, no. 1, pp. 133–138, 2011.

[27] C. Mangano, A. Piattelli, F. Mangano et al., "Histological and synchrotron radiation-based computed microtomography study of 2 human-retrieved direct laser metal formed titanium implants," *Implant Dentistry*, vol. 22, no. 2, pp. 175–181, 2013.

[28] J. A. Shibli, C. Mangano, F. Mangano et al., "Bone-to-implant contact around immediately loaded direct laser metal-forming transitional implants in human posterior maxilla," *Journal of Periodontology*, vol. 84, no. 6, pp. 732–737, 2013.

[29] C. Mangano, F. Mangano, J. A. Shibli et al., "Prospective clinical evaluation of 201 direct laser metal forming implants: results from a 1-year multicenter study," *Lasers in Medical Science*, vol. 27, no. 1, pp. 181–189, 2012.

[30] F. Mangano, F. Luongo, J. A. Shibli, S. Anil, and C. Mangano, "Maxillary overdentures supported by four splinted direct metal laser sintering implants: a 3-year prospective clinical study," *International Journal of Dentistry*, vol. 2014, Article ID 252343, 9 pages, 2014.

[31] F. G. Mangano, A. Caprioglio, L. Levrini, D. Farronato, P. A. Zecca, and C. Mangano, "Immediate loading of mandibular overdentures supported by one-piece, direct metal laser sintering mini-implants: a short-term prospective clinical study," *Journal of Periodontology*, vol. 86, no. 2, pp. 192–200, 2015.

[32] F. Mangano, S. Pozzi-Taubert, P. A. Zecca, G. Luongo, R. L. Sammons, and C. Mangano, "Immediate restoration of fixed partial prostheses supported by one-piece narrow-diameter selective laser sintering implants: a 2-year prospective study in the posterior jaws of 16 patients," *Implant Dentistry*, vol. 22, no. 4, pp. 388–393, 2013.

[33] K. F. Leong, C. M. Cheah, and C. K. Chua, "Solid freeform fabrication of three-dimensional scaffolds for engineering replacement tissues and organs," *Biomaterials*, vol. 24, no. 13, pp. 2363–2378, 2003.

[34] E. Sachlos and J. T. Czernuszka, "Making tissue engineering scaffolds work. Review: the application of solid freeform fabrication technology to the production of tissue engineering scaffolds," *European Cells & Materials*, vol. 5, no. 4, pp. 29–40, 2003.

[35] T. Yoshikawa, H. Ohgushi, and S. Tamai, "Immediate bone forming capability of prefabricated osteogenic hydroxyapatite," *Journal of Biomedical Materials Research*, vol. 32, no. 3, pp. 481–492, 1996.

[36] W. Xue, B. V. Krishna, A. Bandyopadhyay, and S. Bose, "Processing and biocompatibility evaluation of laser processed porous titanium," *Acta Biomaterialia*, vol. 3, no. 6, pp. 1007–1018, 2007.

[37] V. Karageorgiou and D. Kaplan, "Porosity of 3D biomaterial scaffolds and osteogenesis," *Biomaterials*, vol. 26, no. 27, pp. 5474–5491, 2005.

[38] U. Ripamonti, "Soluble, insoluble and geometric signals sculpt the architecture of mineralized tissues," *Journal of Cellular and Molecular Medicine*, vol. 8, no. 2, pp. 169–180, 2004.

[39] D. E. Ingber, "From cellular mechanotrasduction to biologically inspired engineering: 2009 Pritzker Award Lecture. BMES Annual Meeting October 10, 2009," *BMES Annual Meeting October*, vol. 38, no. 3, pp. 1148–1161, 2009.

[40] E. Cretel, A. Pierres, A. Benoliel, and P. Bongrand, "How cells feel their environment: a focus on early dynamic events," *Cellular and Molecular Bioengineering*, vol. 1, no. 1, pp. 5–14, 2008.

Hindawi Publishing Corporation
International Journal of Dentistry
Volume 2016, Article ID 1473918, 8 pages
http://dx.doi.org/10.1155/2016/1473918

Research Article

Correlation Assessment between Three-Dimensional Facial Soft Tissue Scan and Lateral Cephalometric Radiography in Orthodontic Diagnosis

Piero Antonio Zecca, Rosamaria Fastuca, Matteo Beretta, Alberto Caprioglio, and Aldo Macchi

Department of Surgical and Morphological Sciences, University of Insubria, 21100 Varese, Italy

Correspondence should be addressed to Rosamaria Fastuca; rosamariaf@hotmail.it

Received 21 February 2016; Accepted 12 April 2016

Academic Editor: Thomas Fortin

Purpose. The aim of the present prospective study was to investigate correlations between 3D facial soft tissue scan and lateral cephalometric radiography measurements. *Materials and Methods*. The study sample comprised 312 subjects of Caucasian ethnic origin. Exclusion criteria were all the craniofacial anomalies, noticeable asymmetries, and previous or current orthodontic treatment. A cephalometric analysis was developed employing 11 soft tissue landmarks and 14 sagittal and 14 vertical angular measurements corresponding to skeletal cephalometric variables. Cephalometric analyses on lateral cephalometric radiographies were performed for all subjects. The measurements were analysed in terms of their reliability and gender-age specific differences. Then, the soft tissue values were analysed for any correlations with lateral cephalometric radiography variables using Pearson correlation coefficient analysis. *Results*. Low, medium, and high correlations were found for sagittal and vertical measurements. Sagittal measurements seemed to be more reliable in providing a soft tissue diagnosis than vertical measurements. *Conclusions*. Sagittal parameters seemed to be more reliable in providing a soft tissue diagnosis similar to lateral cephalometric radiography. Vertical soft tissue measurements meanwhile showed a little less correlation with the corresponding cephalometric values perhaps due to the low reproducibility of cranial base and mandibular landmarks.

1. Introduction

Skeletal and dental components are of great importance in craniofacial diagnosis and orthodontic treatment planning [1]. Hard tissue is routinely evaluated by means of lateral cephalometric radiography collected by clinicians prior to orthodontic therapy. Besides skeletal evaluation, facial soft tissue analysis is assuming a relevant role in orthodontic diagnosis and treatment planning, since clinicians need to carefully assess the effects of dental and skeletal changes on the soft tissue profile when managing orthodontic treatment in order to estimate facial changes along with occlusal improvements [2]. Therefore, soft tissue analysis might represent an important source of treatment outcome evaluation and additional information for diagnosis.

Although cephalometric analysis of lateral radiography is spreading among orthodontists, its role in diagnosis and treatment planning is still debated [3]. Moreover, the fundamental *principles of justification*, optimization, and dose limitation should always be considered when radiographic examinations are performed at the beginning of the orthodontic treatment.

The growing interest in noninvasive diagnosis has allowed the development of new imaging tools which could enhance the role of soft tissue in diagnosis. Nevertheless, the difficulty of performing facial examinations reliably is probably responsible for the secondary role of soft tissue analysis in supporting diagnosis compared with skeletal analysis [4, 5].

Several analyses have been proposed for the evaluation of facial soft tissue. Most of them include photographic images

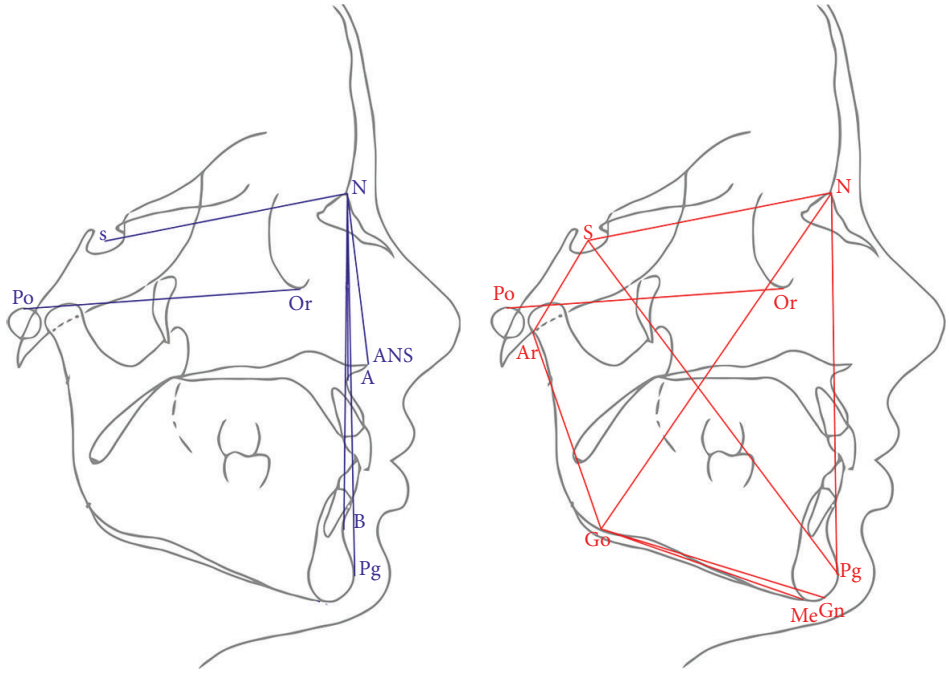

Figure 1: 2D tracings and cephalometric analysis performed with lateral cephalometric radiography. (a) Sagittal measurements and (b) vertical measurements.

in lateral position [6–9]. Some authors [4, 5] have also proposed soft tissue evaluation with frontal pictures and underlined the importance of reproducible head position during image acquisition.

Among the recently introduced noninvasive imaging techniques, stereophotogrammetry and laser scanning allow accurate acquisition of three-dimensional (3D) facial soft tissue with the possibility of locating landmarks and measuring angles, distances, surfaces, and volumes [10–13]. Even though normative values of 3D facial soft tissue are not available for the general population, some proposals have been made for specific sagittal and vertical measurements [14, 15] but further studies are needed to improve their reliability.

The difficulties related to the use of the appropriate equipment and software and the absence of reliable normative values for 3D facial soft tissue measurements might prevent their adoption by clinicians, who are still using lateral cephalometric radiography to perform their diagnosis.

The relationships between facial soft tissue and underlying hard tissue should be considered and investigated for any correspondences that might improve noninvasive orthodontic diagnosis and thus reduce patients' exposure to ionizing radiation.

The soft tissue profile may reflect the underlying skeletal and hard tissue, and it would be possible to estimate the skeletal configuration by visual inspection of the soft tissue profile alone, as suggested by previous studies [16]. Validation of the anatomy of facial soft tissue is fundamental for an objective analysis of craniofacial morphologies.

The aim of the present study was therefore to investigate correlations between facial soft tissue scans and lateral cephalometric radiography measurements.

2. Materials and Methods

2.1. Patient Selection. Signed informed consent to the release of diagnostic records for scientific purposes was obtained from patients prior to enrolment in the present prospective study. The protocol was reviewed and approved by the Ethical Committee (Approval number 6154) and procedures followed adhered to the Declaration of Helsinki. The final study sample comprised 312 subjects: 155 males (mean age of 24.3) and 157 females (mean age of 25.8). Inclusion criteria were Caucasian ethnic origin, age between 20 and 30 years to avoid errors arising from soft tissue laxity which might increase with age, and normal body mass index (BMI) [17]. Subjects were selected from those patients seeking orthodontic treatment for whom a diagnostic lateral cephalometric radiograph had been recorded within the previous six months. Exclusion criteria were craniofacial syndromes or anomalies, noticeable asymmetries, and previous or current orthodontic treatment that might affect the homogeneity of the sample.

Lateral cephalometric radiographs were then collected for all subjects and cephalometric measurements were performed with Deltadent software (Outside Format, Milan, Italy) (Figure 1).

A facial scanner (Primesense Carmine 1.09, Subsidiary of Apple Inc., Israel, 2005) was employed for acquisition of

Figure 2: Facial soft tissue scan. Frontal, prospective, and right lateral 3D views of facial soft tissue scan of female patient.

the facial soft tissue of the subjects. The subject-to-scanner distance was set at 80 cm and scan time was 30 s on average. The scanner depth sensor data were 640 × 480 pixels. Data were recorded on a desktop workstation with a 2.6 GHz i7 Intel processor (Dell, Wicklow, Ireland).

Light conditions were set in order for reliable data capture. The subjects were seated with the lips relaxed and with the head in natural head position (NHP) (self-balance "mirror" position) as described by previous authors [18–20]. If a subject moved between scans, the procedure was repeated and the data of the first scan were eliminated from the study.

The data were acquired by dedicated Skanect software (developed by the ManCTL Company, 2011, Madrid) (Figure 2). Mimics software (version 10.11, Materialise Medical Co., Leuven, Belgium) was used to import the surface model and to perform 3D cephalometric analysis.

All the lateral cephalometric radiographs underwent reposition of the head on the basis of the orientation of the soft tissue scan position by superimposition on the right lateral view of the 3D facial scan using Deltadent software.

A set of reproducible landmarks was developed to compute the soft tissue cephalometric analysis (Figure 3). Fourteen sagittal (Figures 4, 5, and 6) and 14 vertical (Figures 7, 8, and 9) angular measurements were selected and performed for good anatomical correspondence between hard tissue and soft tissue structures and reference landmarks. The average of the angles was computed for symmetric structures.

Then, every skeletal measurement was coupled and assigned to one or more soft tissue measurement (Table 1) for the correlation analysis.

2.2. Statistical Analysis. A pilot study was executed on 20 patients (12 males and 8 females) for the power analysis.

One sagittal and three vertical measurements were employed as main outcome for the power analysis as follows: SsN′Sl, TrOr′^Go′Gn′, TrN′^Go′Gn′, and ObsN′^Go′Gn′. No differences in gender were included in the power analysis.

According to the power analysis, 300 subjects were required in order to obtain power of 0.80 for the present study.

SPSS software, version 22.0 (SPSS® Inc., Chicago, Illinois, USA), was used to run statistical analyses. The Shapiro-Wilk test revealed a normal distribution of tested variables. The mean and standard deviation (SD) of each of the variables were then calculated. Independent t-test was used to compare

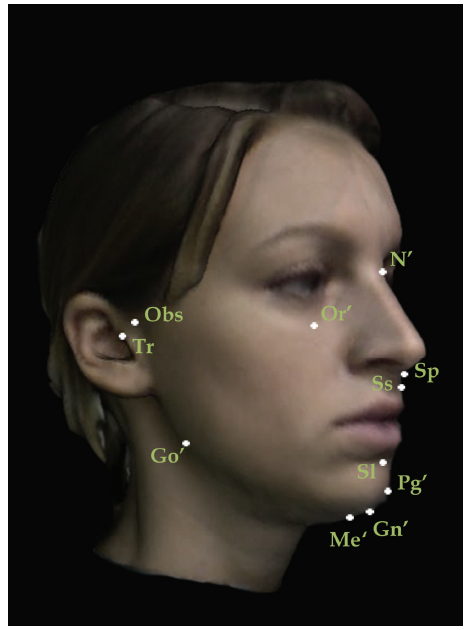

Figure 3: Set of reproducible landmarks employed to perform sagittal and vertical soft tissue 3D measurements: N′ Nasion; Obs Otobasion; Tr Tragus; Or′ Orbitale; Sp Spinal; Ss Subspinal; Go′ Gonion; Sl Sublabial; Pg′ Pogonion; Me′ Menton; Gn′ Gnation.

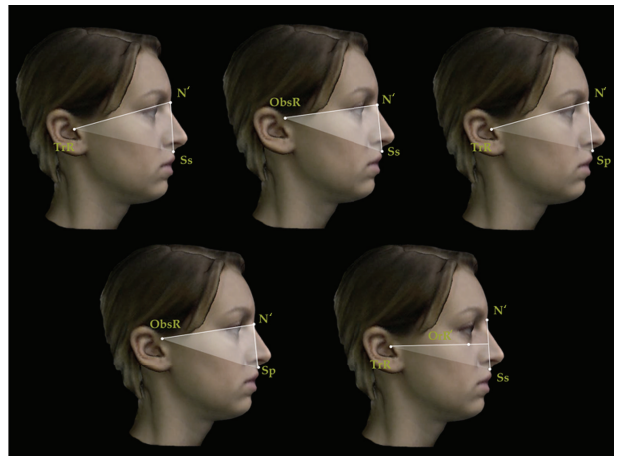

Figure 4: Sagittal angular measurements for 3D facial soft tissue. R: right. Maxillary sagittal measurements.

the mean differences between females and males and $P < 0.05$ was set as the level of significance. All the variables were then further analysed for any correlations with corresponding lateral cephalometric radiography measurements with the Pearson correlation coefficient (r) with the level of significance set at $P < 0.05$.

2.3. Method Error. All the measurements were performed by the same trained operator. Thirty of the 3D facial scans were repeated two weeks after the first recording and measurements were performed. The Dahlberg coefficient [21] was used to test the reproducibility of all the soft tissue landmarks

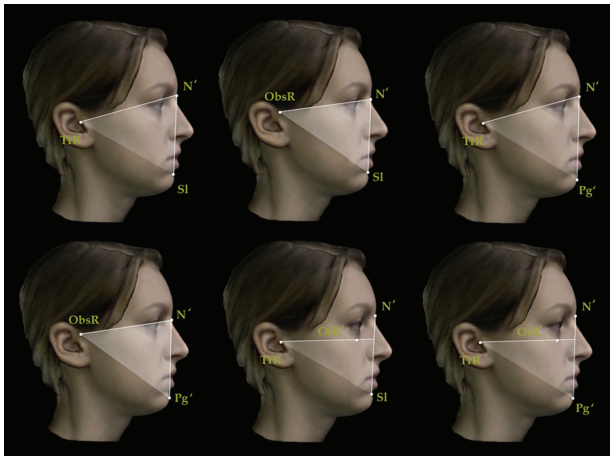

Figure 5: Sagittal angular measurements for 3D facial soft tissue. R: right. Mandibular sagittal measurements.

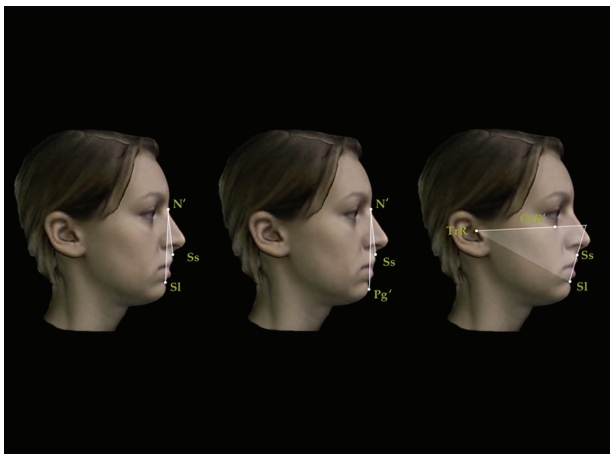

Figure 6: Sagittal angular measurements for 3D facial soft tissue. R: right. Maxillomandibular sagittal measurements.

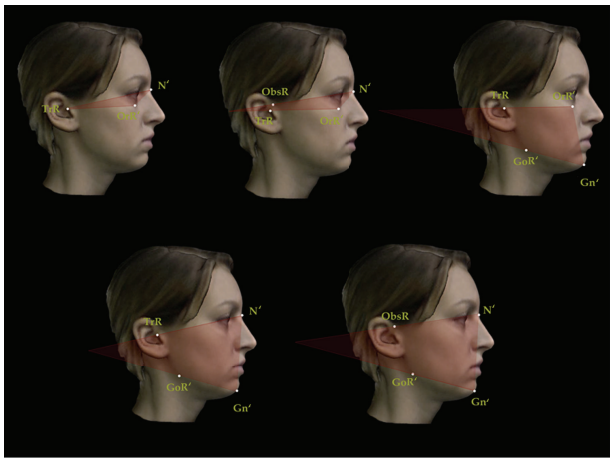

Figure 7: Vertical angular measurements for 3D facial soft tissue. R: right. Part 1.

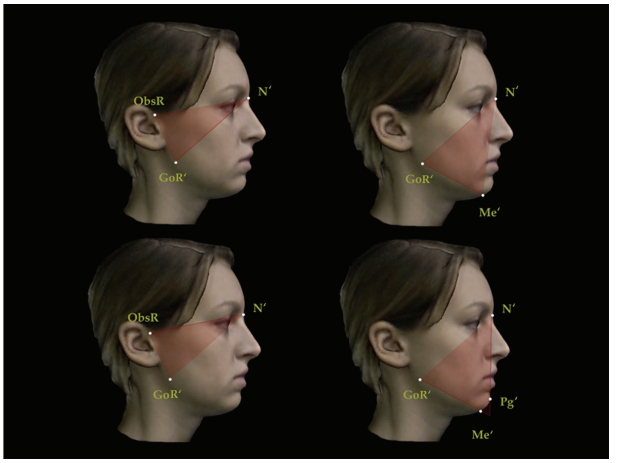

Figure 8: Vertical angular measurements for 3D facial soft tissue. R: right. Part 2.

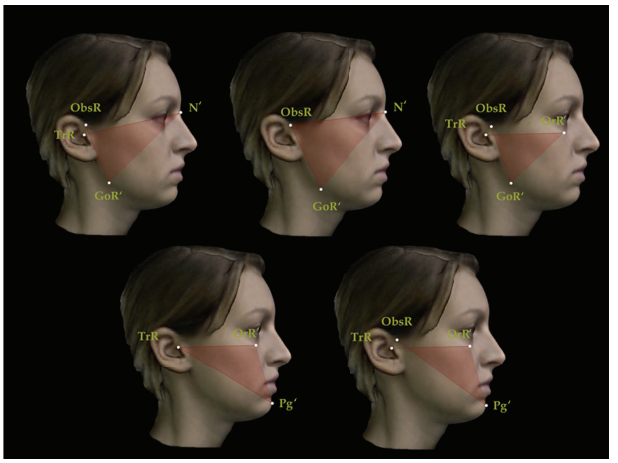

Figure 9: Vertical angular measurements for 3D facial soft tissue. R: right. Part 3.

employed. All the parameters displayed a method error < 1°, which is considered clinically irrelevant.

3. Results

Mean and standard deviations were calculated for each lateral cephalometric radiograph and soft tissue measurement.

The tested variables such as mean and SD did not show significant differences in terms of gender-specific differences (Table 2), and the following statistical analyses were performed for the total sample.

Medium, low, and high correlations were found for sagittal parameters and vertical parameters in assessment of correlation with the corresponding lateral cephalometric radiography measurements previously assigned (Tables 3 and 4).

ANB, ANPg, and FH^AB were the only sagittal variables which showed high correlation coefficients compared with

Table 1: 2D and 3D cephalometric analyses. Cephalometric sagittal and vertical analyses and corresponding 3D soft tissue measurements.

Cephalometrics	3D soft tissue
Sagittal	
SNA	TrN′Ss
	ObsN′Ss
SNans	TrN′Sp
	ObsN′Sp
FH^NA	TrOr′^N′Ss
SNB	TrN′Sl
	ObsN′Sl
SNPg	TrN′Pg′
	ObsN′Pg′
FH^NB	TrOr′^N′Sl
FH^NPg	TrOr′^N′Pg′
ANB	SsN′Sl
ANPg	SsN′Pg′
FH^AB	TrOr′^SsSl
Vertical	
SN^FH	TrN′^TrOr′
	ObsN′^TrOr′
FMA	TrOr′^Go′Gn′
SN^GoGn	TrN′^Go′Gn′
	ObsN′^Go′Gn′
Gonial s ArGoN	ObsGo′N′
Gonial i NGoMe	N′Go′Me′
Articulare SArGo	N′ObsGo′
NPg-GoMe	N′Pg′^Go′Me′
SN^ArGo	TrN′^ObsGo′
	ObsN′^ObsGo′
FH^ArGo	TrOr′^ObsGo′
FH^SPg	TrOr′^TrPg′
	TrOr′^ObsPg′

the respective soft tissue variables. Conversely, FH^NA and SNans showed low correlation coefficients (Table 3).

No high correlations coefficients were found for the vertical parameters which showed medium correlation coefficients except for SN^FH that exhibited low correlation compared with the respective soft tissue variables (Table 4).

4. Discussion

The purpose of this study was to compare facial soft tissue analysis, obtained from facial scans, with lateral cephalometric radiography, in order to highlight possible correspondences between hard tissue and soft tissue diagnoses. The growing role of noninvasive imaging tools could be of great importance in orthodontic diagnosis since 3D facial soft tissue might be employed as the first screening examination for guiding clinicians through skeletal diagnosis and performance of further radiological exams only when needed.

Table 2: Sex differences. Data are shown as mean (in bold) and standard deviation (SD) (in italic) for the whole sample for females and for males. P values resulting from t-test to explore gender-specific differences are shown.

3D soft tissue	Mean female	SD female	Mean male	SD male	P value
		Sagittal			
TrN′Ss	**79.75**	*2.53*	**81.46**	*3.41*	0.08
ObsN′Ss	**82.03**	*2.73*	**84.02**	*3.74*	0.06
TrN′Sp	**82.66**	*2.59*	**84.08**	*3.39*	0.12
ObsN′Sp	**84.94**	*2.43*	**86.63**	*3.83*	0.08
TrOr′^N′Ss	**86.67**	*1.82*	**85.83**	*2.47*	0.17
TrN′Sl	**71.63**	*3.39*	**71.74**	*3.93*	0.47
ObsN′Sl	**73.91**	*3.48*	**74.30**	*4.29*	0.41
TrN′Pg′	**71.16**	*3.69*	**71.86**	*3.79*	0.33
ObsN′Pg′	**73.44**	*3.81*	**74.42**	*4.21*	0.28
TrOr′^N′Sl	**84.24**	*3.63*	**83.92**	*3.53*	0.42
TrOr′^N′Pg′	**83.71**	*3.97*	**84.02**	*3.38*	0.43
SsN′Sl	**8.11**	*1.99*	**9.72**	*2.43*	0.06
SsN′Pg′	**8.59**	*2.45*	**9.60**	*2.14*	0.17
TrOr′^SsSl	**70.10**	*5.77*	**65.74**	*7.82*	0.06
		Vertical			
TrN′^TrOr′	**12.65**	*2.29*	**12.43**	*1.09*	0.41
ObsN′^TrOr′	**10.41**	*3.06*	**9.68**	*1.47*	0.28
TrOr′^Go′Gn′	**30.52**	*6.10*	**28.22**	*4.12*	0.18
TrN′^Go′Gn′	**43.17**	*6.19*	**40.65**	*4.02*	0.16
ObsN′^Go′Gn′	**40.92**	*6.41*	**37.91**	*3.72*	0.13
ObsGo′N′	**64.09**	*6.03*	**65.40**	*2.63*	0.29
N′Go′Me′	**70.19**	*5.84*	**70.36**	*5.51*	0.47
N′ObsGo′	**84.09**	*3.94*	**82.15**	*4.66*	0.14
N′Pg′^Go′Me′	**65.72**	*4.63*	**67.76**	*6.46*	0.18
TrN′^ObsGo′	**85.56**	*3.70*	**84.58**	*3.79*	0.27
ObsN′^ObsGo′	**84.09**	*3.94*	**82.15**	*4.66*	0.14
TrOr′^ObsGo′	**76.24**	*5.23*	**72.47**	*4.52*	0.05
TrOr′^TrPg′	**38.31**	*2.85*	**36.62**	*1.86*	0.08
TrOr′^ObsPg′	**44.47**	*3.01*	**43.99**	*1.80*	0.35

The tested infrared scanner showed good reliability and reproducibility in facial morphology acquisition. Moreover, the facial scans proved appropriate for landmark location and the method error for soft tissue cephalometric analysis was acceptable. The possibility of evaluating soft tissue components in 3D allowed us to relocate the head and did not present the limitation of bidimensional (2D) photographic pictures where head position errors can be of great importance in landmark identification.

The sample was first tested for any gender-specific differences. Kochel et al. [14] employed stereophotogrammetry for the evaluation of facial soft tissue focusing on sagittal measurements and found significant differences between males and females with the mean age (25.4 years) similarly to the sample in the present study. According to the present results, no significant differences in facial soft tissue sagittal

Table 3: Sagittal measurement correlations. Pearson correlation coefficients (r) are shown for sagittal measurements as low (in italic), medium (lightface), and high (in bold). $^{*}P < 0.05$.

Cephalometrics			3D soft tissue			r
Variable	Mean	SD	Variable	Mean	SD	
SNA	81.43	3.35	TrN′Ss	80.08	2.81	0.36*
			ObsN′Ss	82.41	3.05	0.34
SNans	85.55	3.84	TrN′Sp	82.94	2.82	0.31*
			ObsN′Sp	85.27	2.84	*0.27*
FH^NA	87.13	1.93	TrOr′^N′Ss	86.51	1.99	*0.16**
SNB	76.79	3.02	TrN′Sl	71.66	3.50	0.59*
			ObsN′Sl	73.99	3.66	0.62*
SNPg	77.47	3.02	TrN′Pg′	71.30	3.72	0.54*
			ObsN′Pg′	73.63	3.91	0.56*
FH^NB	86.46	2.63	TrOr′^N′Sl	84.17	3.61	0.67*
FH^NPg	86.70	2.20	TrOr′^N′Pg′	83.77	3.87	0.66*
ANB	4.65	2.36	SsN′Sl	8.42	2.18	**0.74***
ANPg	4.03	2.61	SsN′Pg′	8.79	2.43	**0.74***
FH^AB	79.92	6.12	TrOr′^SsSl	69.26	6.46	**0.81***

Table 4: Vertical measurement correlations. Pearson correlation coefficients (r) are shown for vertical measurements as low (in italic) and medium (lightface). $^{*}P < 0.05$.

Cephalometrics			3D soft tissue			r
Variable	Mean	SD	Variable	Mean	SD	
SN^FH	10.38	2.76	TrN′^TrOr′	12.60	2.11	*0.25**
			ObsN′^TrOr′	10.26	2.84	*0.15**
FMA	25.00	4.42	TrOr′^Go′Gn′	30.07	5.84	0.59*
SN^GoGn	35.38	5.06	TrN′^Go′Gn′	42.68	5.92	0.54*
			ObsN′^Go′Gn′	40.34	6.10	0.53*
Gonial s ArGoN	53.46	4.06	ObsGo′N′	64.35	5.56	0.42*
Gonial i NGoMe	75.66	4.56	N′Go′Me′	70.22	5.78	0.45*
Articular SArGo	142.06	6.62	N′ObsGo′	83.72	4.16	0.45*
NPg-GoMe	67.15	4.28	N′Pg′^Go′Me′	66.12	5.10	0.61*
SN^ArGo	84.69	3.97	TrN′^ObsGo′	85.37	3.74	0.33
			ObsN′^ObsGo′	83.72	4.16	0.43
FH^ArGo	75.87	5.38	TrOr′^ObsGo′	75.51	5.32	0.45
FH^SPg	57.16	3.13	TrOr′^TrPg′	37.98	2.77	0.57
			TrOr′^ObsPg′	44.38	2.82	0.59

and vertical dimensions were found between the genders, even though a tendency toward statistical significance ($P < 0.08$) was reported for TrN′Ss and ObsN′Ss measurements (Table 2). These measurements indicated maxillary protrusion and were reported to be smaller in females. Although similar samples were tested, the results of the present study were not in agreement with those of Kochel et al. [14]. Indeed, the methods of facial scanning and the soft tissue analysis employed should be considered as possible reasons for the different results in the variability of sagittal dimensions between genders. Moreover, in the present sample, gender differences seemed to have no influence on vertical dimensions in agreement with previous investigations [15].

Since no differences were assessed between genders, the sample was considered as a whole and Pearson correlation coefficients were computed for each variable in order to check for any correlations between sagittal and vertical soft tissue measurements and corresponding skeletal measurements in lateral cephalometric radiography. Little previous evidence has been presented for correspondences between soft tissue and skeletal measurements with 3D and 2D image acquisition tools [22, 23] but they showed high correlations between the tested variables. The present results were analysed for sagittal and vertical measurements, separately.

Most of the sagittal parameters showed medium correlation coefficients (between 0.31 and 0.67) (Table 3). ANB,

ANPg, and FH^AB showed high correlation coefficients ($r > 0.7$) when compared with the respective soft tissue variables. These angles are usually applied in the evaluation of sagittal relationships between maxilla and mandible and account for the diagnosis of skeletal malocclusion. According to the present results, the diagnosis performed on soft tissue seemed to be reliable in predicting skeletal cephalometric outcomes since the coefficients showed high values and reached the level of significance. Kochel et al. [14] evaluated sagittal soft tissue measurements and their correspondences with lateral cephalometric radiography, describing a set of variables defined on the basis of common skeletal cephalometric measurements. Their findings are in agreement with the present investigation. The selection of the corresponding landmarks between skeletal and soft tissue seemed very important in the outcomes of correlation coefficients. Previous studies [24] found no correlation between soft tissue measurements of facial profile and cephalometric ANB angle, employing the landmarks subnasal and skin pogonion as correspondent of skeletal landmarks A and B, respectively. The present investigation used the landmarks subspinal (Ss) and sublabial (Sl) and high correlation between soft tissue and ANB skeletal angle was found, showing that different outcomes might be owing to the selection of different landmarks.

The measurements of maxillary sagittal position (SNA, SNans, and FH^NA) showed the lowest r values (ranging from 0.16 to 0.36) in relation to soft tissue corresponding measurements. On the other hand, the converse was the case for measurements of mandible sagittal position such as SNB, SNPg, FH^NPg, and FH^NB with r values ranging from 0.54 to 0.81. This result suggested that stronger sagittal relations between soft tissue and underlying hard tissue involved the lower third of the face compared with the middle third of the face.

Medium correlation coefficients were found for the vertical parameters (Table 4) in agreement with other studies [15]. Only SN^FH exhibited low correlation with the respective soft tissue variables ($r = 0.15$ and $r = 0.25$). This may be because of the difficulty of locating corresponding soft tissue landmarks for the middle cranial base and the Go′ landmark that might have a small correspondence with the external soft tissues.

All the facial scans in the present study were performed with relaxed lips and this position was considered accurate in terms of diagnosis and treatment planning [4, 5] and allowed comparison with lateral cephalometric radiographs that are routinely performed with relaxed lips.

Unfortunately, the collected lateral cephalometric radiographs were not all performed with the same X-ray machine and this could be seen as a limitation of the present study. Moreover, only selected cephalometric landmarks were employed and only one operator analysed the data. Also, the inclusion of Caucasian patients only could be considered a limitation of the present investigation.

Even though encouraging results were obtained from the present study, they are still limited to our sample and methods. Also, the selected sample showed normal BMI, possibly the ideal condition for the present investigations since excessive BMI was reported to have significant effects on the ratio between skeleton and overlying soft tissue, so the results should not be extended to altered BMI conditions where the correspondences between hard and soft tissues may be less precise. Further studies are needed in order to clarify the complex relationships between soft and hard tissues and help clinicians and researchers with diagnosis and treatment planning with noninvasive tools.

5. Conclusions

From the results of the present study, the following facts can be stated:

(i) No statistically significant differences were found for sagittal and vertical soft tissue measurements between females and males in the tested sample.

(ii) Sagittal measurements seemed to be more reliable in terms of providing a soft tissue diagnosis than lateral cephalometric radiography measurements (ANB and ANPg), especially for the lower third of the face (SNB, SNPg, FH^NPg, and FH^NB).

(iii) Vertical soft tissue measurements showed weaker correlation with the corresponding lateral cephalometric radiography variables.

The present soft tissue analysis proposal based on 3D facial scans showed good reliability and reproducibility even though further studies are needed in order to confirm the findings of the research.

Competing Interests

The authors report no competing interests related to this study.

Authors' Contributions

Piero Antonio Zecca acquired the clinical data and processed all the images for the analyses; Rosamaria Fastuca performed the statistical analysis and drafted the paper; Matteo Beretta supervised drafting the paper and revising it critically for important intellectual content; Alberto Caprioglio supervised acquiring clinical data, drafting the paper, and revising it critically for important intellectual content; Aldo Macchi supervised the entire research project, drafting the paper, and revising it critically for important intellectual content.

References

[1] P. G. Nijkamp, L. L. M. H. Habets, I. H. A. Aartman, and A. Zentner, "The influence of cephalometrics on orthodontic treatment planning," *European Journal of Orthodontics*, vol. 30, no. 6, pp. 630–635, 2008.

[2] N. Kilic, G. Catal, A. Kiki, and H. Oktay, "Soft tissue profile changes following maxillary protraction in Class III subjects," *European Journal of Orthodontics*, vol. 32, no. 4, pp. 419–424, 2010.

[3] L. Devereux, D. Moles, S. J. Cunningham, and M. McKnight, "How important are lateral cephalometric radiographs

in orthodontic treatment planning?" *American Journal of Orthodontics and Dentofacial Orthopedics*, vol. 139, no. 2, pp. e175–e181, 2011.

[4] G. W. Arnett and R. T. Bergman, "Facial keys to orthodontic diagnosis and treatment planning. Part I," *American Journal of Orthodontics and Dentofacial Orthopedics*, vol. 103, no. 4, pp. 299–312, 1993.

[5] G. W. Arnett and R. T. Bergman, "Facial keys to orthodontic diagnosis and treatment planning. Part II," *American Journal of Orthodontics and Dentofacial Orthopedics*, vol. 103, no. 5, pp. 395–411, 1993.

[6] W. B. Downs, "Analysis of the dentofacial profile," *Angle Orthodontist*, vol. 26, pp. 191–212, 1956.

[7] R. A. Holdaway, "A soft-tissue cephalometric analysis and its use in orthodontic treatment planning. Part I," *American Journal of Orthodontics*, vol. 84, no. 1, pp. 1–28, 1983.

[8] R. M. Ricketts, "Esthetics, environment, and the law of lip relation," *American Journal of Orthodontics*, vol. 54, no. 4, pp. 272–289, 1968.

[9] L. L. Merrifield, "The profile line as an aid in critically evaluating facial esthetics," *American Journal of Orthodontics*, vol. 52, no. 11, pp. 804–822, 1966.

[10] V. F. Ferrario, C. Sforza, V. Ciusa, C. Dellavia, and G. M. Tartaglia, "The effect of sex and age on facial asymmetry in healthy subjects: a cross-sectional study from adolescence to mid-adulthood," *Journal of Oral and Maxillofacial Surgery*, vol. 59, no. 4, pp. 382–388, 2001.

[11] C. H. Kau and S. Richmond, "Three-dimensional analysis of facial morphology surface changes in untreated children from 12 to 14 years of age," *American Journal of Orthodontics and Dentofacial Orthopedics*, vol. 134, no. 6, pp. 751–760, 2008.

[12] E. Nkenke, E. Vairaktaris, M. Kramer et al., "Three-dimensional analysis of changes of the malar-midfacial region after LeFort I osteotomy and maxillary advancement," *Oral and Maxillofacial Surgery*, vol. 12, no. 1, pp. 5–12, 2008.

[13] F. Ras, L. L. M. H. Habets, F. C. Van Ginkel, and B. Prahl-Andersen, "Quantification of facial morphology using stereophotogrammetry—demonstration of a new concept," *Journal of Dentistry*, vol. 24, no. 5, pp. 369–374, 1996.

[14] J. Kochel, P. Meyer-Marcotty, F. Strnad, M. Kochel, and A. Stellzig-Eisenhauer, "3D soft tissue analysis—part 1: sagittal parameters," *Journal of Orofacial Orthopedics*, vol. 71, no. 1, pp. 40–52, 2010.

[15] J. Kochel, P. Meyer-Marcotty, M. Kochel, S. Schneck, and A. Stellzig-Eisenhauer, "3D soft tissue analysis—part 2: vertical parameters," *Journal of Orofacial Orthopedics*, vol. 71, no. 3, pp. 207–220, 2010.

[16] A. M. McCance, J. P. Moss, W. R. Fright, A. D. Linney, and James, "Three-dimensional analysis techniques—part 3: color-coded system for three-dimensional measurement of bone and ratio of soft tissue to bone: the analysis," *The Cleft Palate-Craniofacial Journal*, vol. 34, no. 1, pp. 52–57, 1997.

[17] M. L. Riolo, R. E. Moyers, T. R. TenHave, and C. A. Mayers, "Facial soft tissue changes during adolescence," in *Craniofacial Growth during Adolescence*, D. S. Carlson and K. A. Ribbens, Eds., Monograph 20, Craniofacial Growth Series, Center for Human Growth and Development, University of Michigan, Ann Arbor, Mich, USA, 1987.

[18] C. S. W. Chiu and R. K. F. Clark, "Reproducibility of natural head position," *Journal of Dentistry*, vol. 19, no. 2, pp. 130–131, 1991.

[19] B. Solow and A. Tallgren, "Natural head position in standing subjects," *Acta Odontologica Scandinavica*, vol. 29, no. 5, pp. 591–607, 1971.

[20] A. Lundström, F. Lundström, L. M. L. Lebret, and C. F. A. Moorrees, "Natural head position and natural head orientation: basic considerations in cephalometric analysis and research," *European Journal of Orthodontics*, vol. 17, no. 2, pp. 111–120, 1995.

[21] G. Dahlberg, *Statistical Methods for Medical and Biological Students*, Interscience Publications, New York, NY, USA, 1940.

[22] A. K. Incrapera, C. H. Kau, J. D. English, K. McGrory, and D. M. Sarver, "Soft tissue images from cephalograms compared with those from a 3D surface acquisition system," *Angle Orthodontist*, vol. 80, no. 1, pp. 58–64, 2010.

[23] M. A. Shamlan and A. M. Aldrees, "Hard and soft tissue correlations in facial profiles: a canonical correlation study," *Clinical, Cosmetic and Investigational Dentistry*, vol. 7, pp. 9–15, 2015.

[24] A. M. Schwarz, *Die Röntgenostatik*, Urban & Schwarzenberg, Munich, Germany, 1958.

Hindawi Publishing Corporation
International Journal of Dentistry
Volume 2016, Article ID 9393219, 9 pages
http://dx.doi.org/10.1155/2016/9393219

Clinical Study

Soft Tissue Stability around Single Implants Inserted to Replace Maxillary Lateral Incisors: A 3D Evaluation

F. G. Mangano,[1] F. Luongo,[2] G. Picciocchi,[3] C. Mortellaro,[4] K. B. Park,[5] and C. Mangano[6]

[1]*Department of Surgical and Morphological Science, Dental School, University of Varese, 21100 Varese, Italy*
[2]*Private Practice, 00193 Rome, Italy*
[3]*Private Practice, 20154 Milan, Italy*
[4]*Department of Health Sciences, University of Eastern Piedmont, 28100 Novara, Italy*
[5]*Mir Dental Hospital, 149-132 Samduk 2Ga, Jung-Gu, Daegu 700 412, Republic of Korea*
[6]*Department of Dental Sciences, Vita Salute San Raffaele University, 20132 Milan, Italy*

Correspondence should be addressed to F. G. Mangano; francescomanganol@mclink.net

Received 16 February 2016; Revised 27 March 2016; Accepted 24 April 2016

Academic Editor: Andreas Stavropoulos

Purpose. To evaluate the soft tissue stability around single implants inserted to replace maxillary lateral incisors, using an innovative 3D method. *Methods*. We have used reverse-engineering software for the superimposition of 3D surface models of the dentogingival structures, obtained from intraoral scans of the same patients taken at the delivery of the final crown (S1) and 2 years later (S2). The assessment of soft tissues changes was performed via calculation of the Euclidean surface distances between the 3D models, after the superimposition of S2 on S1; colour maps were used for quantification of changes. *Results*. Twenty patients (8 males, 12 females) were selected, 10 with a failing/nonrestorable lateral incisor (*test* group: immediate placement in postextraction socket) and 10 with a missing lateral incisor (*control* group: conventional placement in healed ridge). Each patient received one immediately loaded implant (Anyridge®, Megagen, Gyeongbuk, South Korea). The superimposition of the 3D surface models taken at different times (S2 over S1) revealed a mean (±SD) reduction of 0.057 mm (±0.025) and 0.037 mm (±0.020) for *test* and *control* patients, respectively. This difference was not statistically significant ($p = 0.069$). *Conclusions*. The superimposition of the 3D surface models revealed an excellent peri-implant soft tissue stability in both groups of patients, with minimal changes registered along time.

1. Introduction

In recent years, aesthetics has become increasingly important: everyone wants to be beautiful, according to modern society's concept of beauty. Since a beautiful smile can make the difference, dental and oral implantology are no exception: patients have high aesthetic expectations of implant-prosthetic treatment and require cosmetic restorations that are indistinguishable from natural teeth [1, 2]. This is why the reconstruction of single missing teeth in the aesthetic areas of the maxilla with dental implants is currently a challenge for the surgeon and the prosthodontist [2–4].

The loss of a tooth actually results in a contraction of the hard and soft tissues [5–7]. The gradual involution and reduction of alveolar bone volume begin immediately after extraction and are accompanied by a contraction of the overlying soft tissues [6–8]. As demonstrated in various animal [9–12] and human [13–16] studies, a major contraction of the alveolar bone volume occurs after extraction of natural teeth, during the first six months and up to 2 years after extraction. A marked reduction in the buccopalatal width and the height of the alveolar ridge is already evident in the first year after the extraction [7, 8, 14] and is accompanied by a contraction of the overlying soft tissues [6, 8, 17, 18]. These phenomena are particularly evident in the anterior maxilla [7, 8, 14, 16], since in this area tooth extraction compromises the vascularization of the delicate vestibular bone plate, mainly provided by the vascular plexus of the periodontal ligament. The immediate consequence of reduced vascularization in the anterior maxilla is the physiological horizontal and vertical resorption of the vestibular bone plate, with contraction of the overlying soft tissues [7, 8, 14, 17, 18]. This contraction

can make implant-prosthetic treatment unpredictable when restoring and maintaining a cosmetic appearance identical to that of a natural tooth are our purpose [17, 18].

The long-term stability of the peri-implant soft tissues in the anterior maxilla is of fundamental importance for the success of implant treatment [17, 18]. For this reason, over the years, a whole series of indexes for describing the aesthetic outcome of implants and for monitoring the stability of the peri-implant soft tissues over time have been proposed in the literature [19–24]. Although these indexes, particularly some of them [21, 22], have been used by various authors [2, 4, 25–27] and have represented the standard for evaluating the aesthetic success of reconstructions with single implants in the anterior maxilla [21, 22, 25–27], until now it was not possible to perform an exact quantitative evaluation of the stability of the peri-implant soft tissues over time [28]. In fact, the indexes proposed in the literature are based on a two-dimensional photographic assessment (2D) and on the comparison of photographs taken at different times (usually at the delivery of the final restoration and over the following years) through the application of established criteria [28]. This does not allow the actual loss or the three-dimensional contraction (3D) of the peri-implant tissues over time to be exactly quantified [28]. To date, only one clinical work has tried to quantitatively assess the modifications of the soft tissues around individual implants in the aesthetic area over time [29]; however, this study employed reconstructions from cone beam computed tomography (CBCT), which is not ideal for the purpose.

Various surgical techniques have been proposed for placing of implants in the anterior maxilla [4, 25–27]. Amongst them, we should mention the immediate placement of implants in postextraction sockets, early implant placement in sites where bone healing is still ongoing (4–8 weeks after extraction), and conventional implant placement in fully healed sites (6–8 months after extraction) [4, 25–27]. Although all of these techniques can provide high implant survival, it is not yet clear which of these may give the best aesthetic result [4, 25–28].

Recent advances in the field of digital dentistry, and in particular the introduction of intraoral scanners which are powerful devices for taking optical impressions [30, 31], could help clinicians to fully understand the dynamics and transformations of the peri-implant soft tissue over time: this is of particular interest for single implants positioned in the anterior maxilla. In fact, the patient can undergo various scans with the intraoral scanner in the course of the treatment (e.g., at the time of placement of the final restoration and during subsequent check-ups). The patient's 3D models can then be loaded into reverse-engineering software and superimposed over each other [32, 33], in order to exactly quantify the stability of the peri-implant soft tissues over time.

Hence, the aim of this study was to compare the stability of peri-implant soft tissues around single implants positioned in the anterior maxilla, over time, with two different surgical protocols (immediate implants versus conventional implants), using an innovative 3D technique.

2. Materials and Methods

2.1. Study Population. The present study was designed as a prospective investigation based on data from patients recruited/treated in two different private practices (Gravedona, Como and Rome, Italy), under a standardized protocol, over a two-year period (September 2011–2013).

Inclusion criteria were patients in good oral/systemic health, in need for replacement of failing/nonrestorable maxillary lateral incisors (immediate implants in postextraction sockets: *test* group) or missing lateral incisors (conventional implants in healed ridges: *control* group), with sufficient bone height/width to place an implant of at least 3.5 mm in diameter and 10.0 mm in length, and with natural teeth adjacent to the implant site. In the *control* group, both patients with congenitally missing lateral incisors and patients who had previously lost a lateral incisor (with at least 4 months of healing after tooth extraction) were included.

Exclusion criteria were patients with active oral infections, chronic periodontitis with advanced loss of support (defined by periodontal pocking depth > 6 mm with clinical attachment loss > 4 mm, radiographic evidence of bone loss and increased tooth mobility), and patients with severe systemic diseases that would not allow a surgical intervention (immunocompromised patients, patients who underwent radiotherapy and/or chemotherapy, and patients in treatment with intravenous and/or oral amino-bisphosphonates). Smoking was not an exclusion criterion, although all patients were informed that smoking is associated with an increased risk of implant failure [34]. All patients received full explanation about the surgical and prosthetic protocol and signed an informed consent form prior to being enrolled in the present study; all patients accepted to fully participate in surveys. The Ethics Committee for Human Studies of the Hospital of Varese approved the present study, which was conducted in accordance with the principles outlined in the Declaration of Helsinki of 1975, as revised in 2008.

2.2. Surgical and Prosthetic Protocol. The surgical and prosthetic protocol was as previously reported [35]. In brief, all patients received one single implant (Anyridge, Megagen, Gyeongbuk, South Korea), placed to replace a failing/nonrestorable or a missing maxillary lateral incisor.

The fixtures used in the present have a tapered design with aggressive threads and a calcium-incorporated nanostructured surface (Xpeed®, Megagen, Gyeongbuk, South Korea) with the potential to accelerate healing processes and to promote osseointegration [36]. In addition, they have a conical connection (10°), which offers a tight seal and a built-in platform switching, ideal for preventing crestal bone resorption and for maintaining soft tissue volume along time [35].

Prior to surgery, a careful preoperative clinical and radiographic assessment was made in each patient, with the aim of better understanding the anatomy of implant sites; moreover, impressions were taken, casts were developed, and a diagnostic wax-up was performed, in order to better understand the patient's prosthetic needs.

In postextraction sockets, after local anaesthesia, an intrasulcular incision was made, extended to the neighboring teeth, and the failing/nonrestorable tooth was gently extracted, avoiding any movement that could damage the buccal bone wall. The postextraction socket was carefully debrided and the integrity of the socket walls was checked. After that, the surgical site was prepared, by deepening the socket for 3-4 mm, and the implant was placed; finally, particles of synthetic bone grafts were used to fill the gap between the implant body and the buccal bone wall and to overbuild the buccal bone wall, for protection against bone resorption.

In healed sites, after local anaesthesia, a crestal incision was made, connected with two lateral (vertical) releasing incisions, and a full-thickness surgical flap was raised to expose the alveolar crest; then, the surgical site was prepared according to the manufacturer's recommendations, and the implant was placed.

The surgeons were free to choose between different implant lengths (10.0 mm, 11.5 mm, and 13.0 mm) and diameters (3.5 mm and 4.0 mm). In both postextraction sockets and healed sites, the implants were placed slightly palatally, in order to avoid contact with the buccal bone wall. The implant stability was checked manually at placement. Sutures were placed. All implants were functionally loaded immediately after placement, with a provisional crown. Patients were prescribed with oral antibiotics (amoxicillin plus clavulanic acid, 2 gr/day for 6 days) and analgesics (ibuprofen, 600 mg/day for 3 days). Ice packs were provided, and a soft diet was recommended for the first week. After one week, sutures were removed.

The provisional crown remained *in situ* for a period of 3 months; after that final impressions were taken and the final metal-ceramic crown was provided. All crowns were cemented with a temporary zinc-eugenol cement. All patients were enrolled in a 6-month postoperative control program.

2.3. Intraoral Scans. Each patient underwent two different intraoral scans of the full mouth: three months after implant placement, at the delivery of the final implant-supported restoration (S1), and two years later (S2). All scans were performed by two calibrated operators, with proven experience in the use of intraoral scanners. All scans were performed with a powerful, modern intraoral scanner (Trios, 3-Shape, Copenhagen, Denmark). This structured-light device works under the principle of confocal microscopy and ultrafast optical scanning, and it produces in-color 3D surface models in a proprietary (.DCM) format [33]. These files were then converted into solid-to-layer (.STL) files, using proprietary software.

2.4. 3D Soft Tissues Evaluation. The 3D surface models of the two different scans (S1 and S2) from each patient were imported into powerful reverse-engineering software (Geomagic Studio 2012, Geomagic, Morrisville, NC, USA) [36]. All scans were checked and cleaned using the "mesh doctor" function, so that small artifacts identified as independent polygons could be automatically removed. After that, the scans were cut and trimmed using the "cut with planes" function, in order to obtain uniform surface models, representing the implant-supported restoration and the adjacent natural teeth only, with related soft tissues. Subsequently, the function "cut with lines" was used to isolate the soft tissues from the implant-supported restoration and the adjacent natural teeth. The obtained uniform 3D surface models represented the region of interest for this study: they were saved in specific folders and were ready for superimposition. Superimposition was obtained as follows. First, the S2 model was roughly superimposed to the S1 model (reference dataset) using the "three-point" registration tool. The three points were identified on the final implant-supported crown, two on the crown margin and one on the cervical area, in order to facilitate this alignment. After this first rough alignment, the final registration was performed using the "best fit alignment" function. This final registration was obtained using an iterative closest point algorithm, also called "robust iterative closest point" (RICP). The distances between the S1 and the S2 models were minimized using the point-to-plane method. For each case, approximately 65.000 triangles were superimposed. Congruence between specific corresponding structures was calculated at this stage, for testing the accuracy of the procedure. Finally, the distances between corresponding areas of S1 and S2 were color-coded on the superimposed models for visualization of the results; a color map was generated, where the distances between specific points of interest were quantified overall and in all three planes of space. The modifications of peri-implant soft tissues along time were therefore visualized and calculated as mean (± standard deviations, SD). The color maps indicated inward (blue) or outward (orange, red) displacement between overlaid structures, while an absence of changes was indicated by the green color. The analysis was repeated with four different settings (50 μm, 25 μm, 10 μm, and 5 μm), in order to help the reader to highlight the 3D deviations at different resolution/magnification. With the first two settings (50 μm and 25 μm), in fact, only the biggest variations affecting the tissues (>50 and >25 micrometers, resp.) could be visualized; with the last two (10 μm and 5 μm), it was possible to visually assess even little tissue variations along time (variations >10 and >5 micrometers, resp.). All the aforementioned procedures for 3D soft tissue evaluation along time were made by the same calibrated operator, with extensive experience with reverse-engineering software and software for overlapping of digital images.

2.5. Statistical Analysis. All collected data were inserted in a sheet for statistical analysis (Excel 2003®, Microsoft, Redmond, WA, USA). Mean ± SD of the modifications of peri-implant soft tissues along time were calculated for each patient and then for each group of patients (*test* versus *control* patients). The t-test for independent samples was used to evaluate the differences between the two groups. The level of significance was set at 0.05. All computations were carried out with statistical analysis software (SPSS 17.0®, SPSS Inc., Chicago, IL, USA).

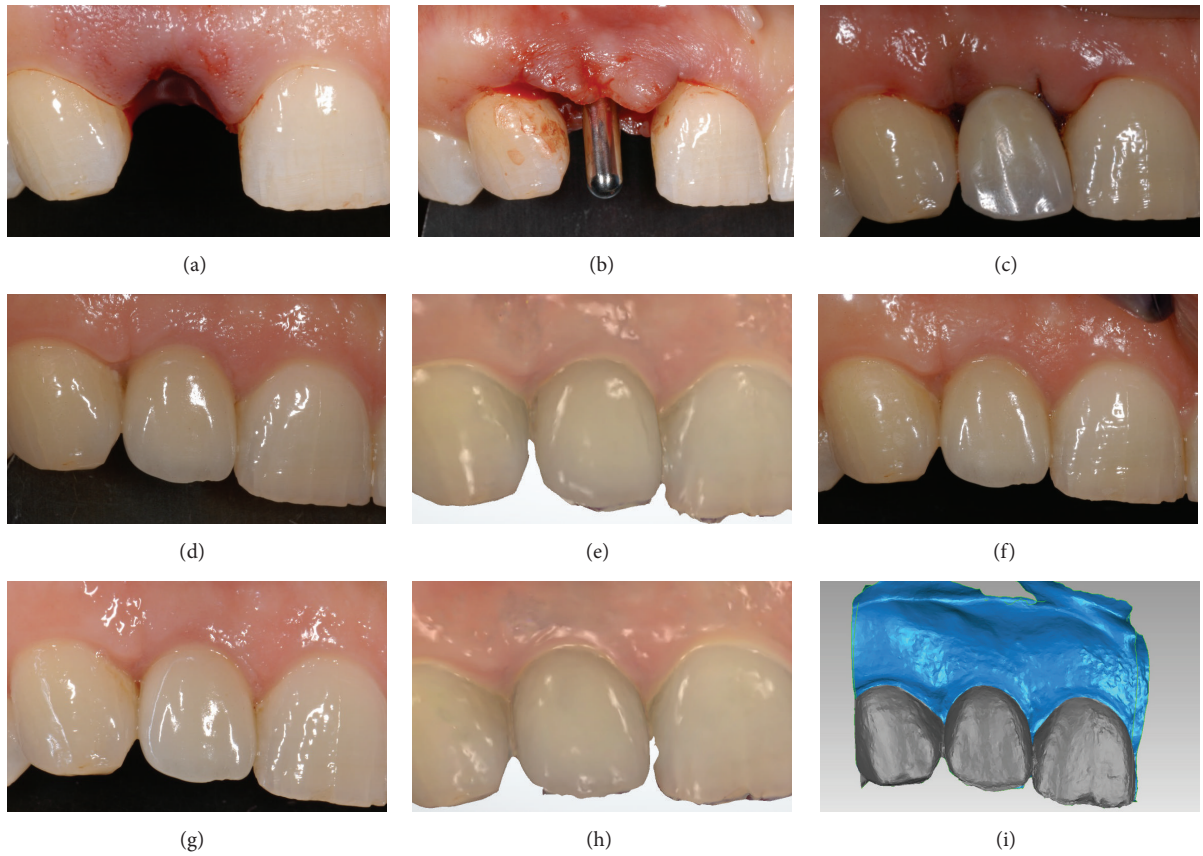

Figure 1: Immediate implant placement in postextraction socket (*test* group) of an adult female patient (34 years old): (a) the socket immediately after extraction; (b) the implant (Anyridge, Megagen, Gyeongbuk, South Korea) was placed in the fresh extraction socket; (c) the implant was immediately loaded with a provisional resin crown; (d) three months later, the final metal-ceramic crown was delivered to the patient; (e) first scan (S1) of the peri-implant soft tissues with a powerful intraoral scanner (Trios®, 3-Shape, Copenhagen, Denmark), at the delivery of the final crown; (f) 1-year clinical control; (g) 2-year clinical control; (h) second scan (S2) of the peri-implant soft tissues 2 years after the delivery of the final crown; (i) overlapping of digital images (S2 over S1) in powerful reverse-engineering software (Geomagic Studio 2012®, Geomagic, Morrisville, NC, USA).

3. Results

Six patients did not match the inclusion criteria and were therefore excluded from the study. Twenty patients (8 males, 12 females; aged between 17 and 54 years) with failing/nonrestorable or missing lateral incisors presented no conditions enlisted in the exclusion criteria and were enrolled in the present study. Ten patients (5 males, 5 females; aged between 19 and 54) had a failing/nonrestorable lateral incisor and were subjected to immediate implant placement (*test* group); among these patients, root fracture was the most frequent reason for tooth loss (5 patients), followed by caries (3 patients) and recurrent nontreatable endodontic lesions (2 patients). The other 10 patients (5 males, 5 females; aged between 17 and 34 years) had a missing lateral incisor (8 of them congenitally) and were therefore subjected to conventional implant placement (*control* group). Each patient received one single implant. All implants were functionally loaded immediately after placement. All implant-supported restorations were followed up for a period of 2 years after delivery (Figures 1 and 3). The superimposition of the 3D surface models taken at different times (S2 on S1) revealed a mean (±SD) reduction of 0.057 mm (±0.025) and 0.037 mm (±0.020) for *test* and *control* patients, respectively (Table 1, Figures 2 and 4). This difference was not statistically significant ($p = 0.069$). The changes evidenced between S1 and S2 were minimal, so that an excellent 3D peri-implant soft tissue stability along time was found in both groups of patients.

4. Discussion

Currently, the placement of single implants in the aesthetic area of the anterior maxilla is a difficult challenge for the surgeon and the prosthodontist [2–4]. On the one hand, in a world where a beautiful smile is becoming increasingly important, the patient's aesthetic expectations are in fact higher than ever [2, 4]; on the other, it is known that the loss of a tooth inevitably results in resorption of alveolar bone, with consequent contraction of the overlying soft tissues [5–7].

A recent systematic review on clinical studies by Tan and colleagues [7] has confirmed that, after tooth extraction, a pronounced horizontal dimensional reduction (3.79 ± 0.23 mm) combined with a vertical reduction (1.24±0.11 mm

Table 1: Soft tissue contraction around single implants inserted to replace failing/nonrestorable (*test* group: immediate implant placement in postextraction socket) and missing (*control* group: conventional implant placement in healed ridge) lateral incisors. The assessment of soft tissue contraction was performed via calculation of the Euclidean surface distances between the 3D models, after the superimposition of S2 on S1, in mm, over a 2-year period.

Immediate implant placement in postextraction sockets (*test* group)	Conventional implant placement in healed ridges (*control* group)
0.024	0.091
0.048	0.044
0.09	0.025
0.065	0.038
0.051	0.022
0.042	0.037
0.028	0.025
0.044	0.028
0.099	0.033
0.079	0.028
Overall: 0.057 (±0.025)	Overall: 0.037 (±0.020)

on buccal, 0.84 ± 0.62 mm on mesial and 0.80 ± 0.71 mm on distal sites) occurs at 6 months; percentage horizontal and vertical dimensional changes were comprised between 29–63% and 11–22% at 6 months, respectively [7]. The amount of bone resorption is usually greater at the buccal aspect than at its palatal/lingual counterpart, particularly in the anterior maxilla [7, 8, 13, 15, 16]. In fact, most tooth sites in the anterior maxilla exhibit very thin (≤1 mm) buccal bone walls that are frequently made up of only bundle bone [13, 15, 16, 37, 38]. As the bundle bone is a tooth-dependent structure, such a thin bone wall may undergo marked resorption following tooth extraction [37, 38]. Chappuis and colleagues have identified a buccal bone wall thickness of ≤1 mm as a critical factor associated with the extent of bone resorption [14]. Thin-wall phenotypes displayed pronounced vertical bone resorption, with a median bone loss of 7.5 mm, as compared with thick-wall phenotypes, which decreased by only 1.1 mm [14].

Various treatment modalities have been described for implant therapy in the anterior zone such as conventional (4–6 months after tooth extraction), early (typically 4–8 weeks after extraction), and immediate implant placement (placement of a dental implant at the time of tooth extraction) [1, 2, 4, 25, 26]. Immediate implant placement has several advantages over the other treatment modalities, since it reduces the number of dental appointments, the time of treatment, and the number of surgeries, improving patient acceptance, with the psychological benefit of simultaneously replacing a lost tooth with an implant [4, 25, 26].

However, it is not yet clear which of these techniques will ensure the best aesthetic results in the anterior maxilla [1, 2, 4, 25–28]. In fact, few studies have compared the aesthetic outcome of these different therapies and consequently the stability over time of the soft tissues around single implants placed in the aesthetic areas using the different surgical protocols mentioned above [4, 25–28].

In addition, almost all of these studies were based on 2D evaluation of photographs taken at different times during the course of therapy (usually at the time of delivery of the final restoration and at the time of subsequent follow-ups) [2, 4, 25–28]. In fact, the criteria introduced so far for evaluating the cosmetic success of the placement of single implants in the anterior maxilla are only 2D [19–24, 28]. Though these criteria can be useful for determining whether an implant-prosthetic restoration is cosmetically acceptable, they do not allow us to quantify changes in the peri-implant soft tissues over time [28, 29].

In order to quantify these changes with certainty, we must in fact have 3D models, obtained at different times during the course of therapy, so that we can overlay them with each other [29]. In this sense, the digital revolution, by introducing a series of powerful tools for capturing 3D images (cone beam computed tomography-CBCT, intraoral, extraoral, and face scanners) and reverse-engineering software for the processing/superimposition of images, can be of help [29–33].

In the last few years, various methods have been described for superimposition of 3D datasets, including landmark-based superimposition, surface-based superimposition, or voxel-based superimposition of form-stable anatomical structures [32, 33]. The validity of the first two superimposition techniques depends on the accuracy of landmark identification and on the precision of the 3D surface models, respectively [32]. The recent study by Chappuis and colleagues was the first ever to propose a technique for the 3D evaluation of the stability over time of the soft tissues around single implants placed in the anterior maxilla [29]. For this paper, the authors used a voxel-based overlay technique, reconstructing the peri-implant soft tissues from CBCT images [29]. Although this overlay method is safe and effective, the need of several CBCT scans, with consequent exposure to ionizing radiations, represents a major limitation of the procedure [29].

The introduction of the intraoral scanners, powerful tools for taking an optical impression [30], allows these problems to be overcome. Intraoral scanners actually allow us to obtain highly accurate 3D models of dentoalveolar tissue, using only a beam of light [30–33]. The scans can therefore be repeated at different times, without harming the patient. The purpose of the present prospective clinical study was to investigate the 3D stability of peri-implant soft tissues along time, in patients treated with a single implant for replacement of a maxillary lateral incisor. In order to quantitatively evaluate the 3D soft tissues dynamics, we have superimposed .STL files of intraoral scans taken at different time (at the delivery of the final restoration, S1; and 2 years later, S2), using powerful reverse-engineering software. With this software, the 3D differences of the superimposed models (S2 on S1) were quantified and translated into color codes, representing the distance between corresponding points. Ten patients with a failing/nonrestorable lateral incisor (*test* group) and 10 with

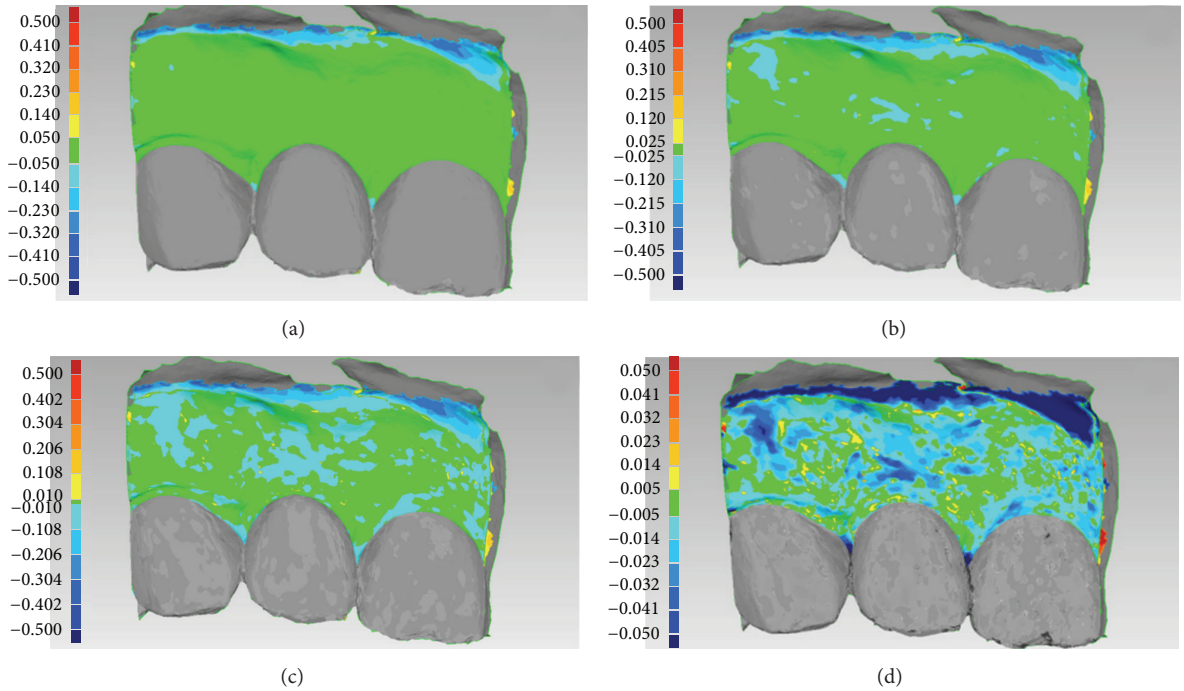

Figure 2: Immediate implant placement in postextraction socket (*test* group) of an adult female patient (34 years old): (a) overlapping of digital images (S2 over S1): colorimetric map, first setting (50 μm). Since the variations in soft tissue volume over 2 years did not exceed 50 μm, the only color visualized was green; (b) overlapping of digital images (S2 over S1): colorimetric map, second setting (25 μm). Only in a few restricted areas was a variation/reduction in soft tissue volume > 25 μm registered: therefore, the predominant color was still green; (c) overlapping of digital images (S2 over S1): colorimetric map, third setting (10 μm). Overall, the soft tissues were stable and did not show contractions > 10 μm, but the soft tissues overlying the vestibular (bundle) bone showed some kind of variation/reduction over time, as they were depicted in light blue; (d) overlapping of digital images (S2 over S1): colorimetric map, fourth setting (5 μm). The area of the vestibular mucosa overlying the vestibular (bundle) bone was clearly the most affected by tissue contraction over time, although the mean (±SD) soft tissue reduction in the whole inspected area amounted to 0.024 mm (±0.048) only.

a missing lateral incisor (*control* group) were selected for the present study. Each patient received one single, immediately loaded implant. The final crowns were provided 3 months after surgery and monitored for a period of 2 years. At the end of the study, a mean loss of tissue of 0.057 mm (±0.025) and 0.037 mm (±0.020) was reported for *test* and *control* patients, respectively. This difference was not statistically significant ($p = 0.069$). The changes evidenced between S1 and S2 were minimal, so that an excellent 3D peri-implant soft tissue stability along time was found. In general, the contraction of the tissues mostly affected the vestibular mucosa over the implant, as expected; this decrease was more pronounced in the case of immediate implants (*test* group); implants placed in healed ridges (*control* group) showed a lesser modification in this area and major changes in the papillae. The overall best results obtained in the present study with immediate implants (*test* group) may be in some way related to the use of bone grafting material for the protection of the buccal bone. However, these issues are worthy of further investigation and analysis: in fact, factors affecting soft tissue level around anterior maxillary single-tooth implants still need to be elucidated [39].

This study has limits. A limited number of patients were selected and evaluated; most of them (8) had a congenitally missing lateral incisor [40]. The intraoral scans were taken by two operators (although experienced and calibrated) at different times, with different environment conditions (room temperature, light, and more). Moreover, the assessment of tissue stability was only possible from the delivery of the final crown, which was used as a reference for the overlapping of 3D models; in this way, an evaluation of the tissues dynamics during provisionalization, and immediately following placement of the implant, was not possible. The only possible solution to evaluate soft tissues stability in the first 3 months after implant placement would be the use of the provisional restorations as references for the overlapping. In fact, the adjacent (natural) teeth cannot be used as references: they may be subject to movements, and these changes may render the overlapping of digital images rather inaccurate, jeopardizing the final 3D evaluation. However, the use of provisional restorations as references has limits: soft tissues are subjected to some kind of edema immediately after surgery, and this may introduce a bias in the study. Moreover, only modifications in a limited timeframe (3 months) can be registered, if provisional restorations are used as references for the overlapping procedures. It is very important to select proper landmarks for the overlapping of 3D models: these landmarks/reference points should be identified on

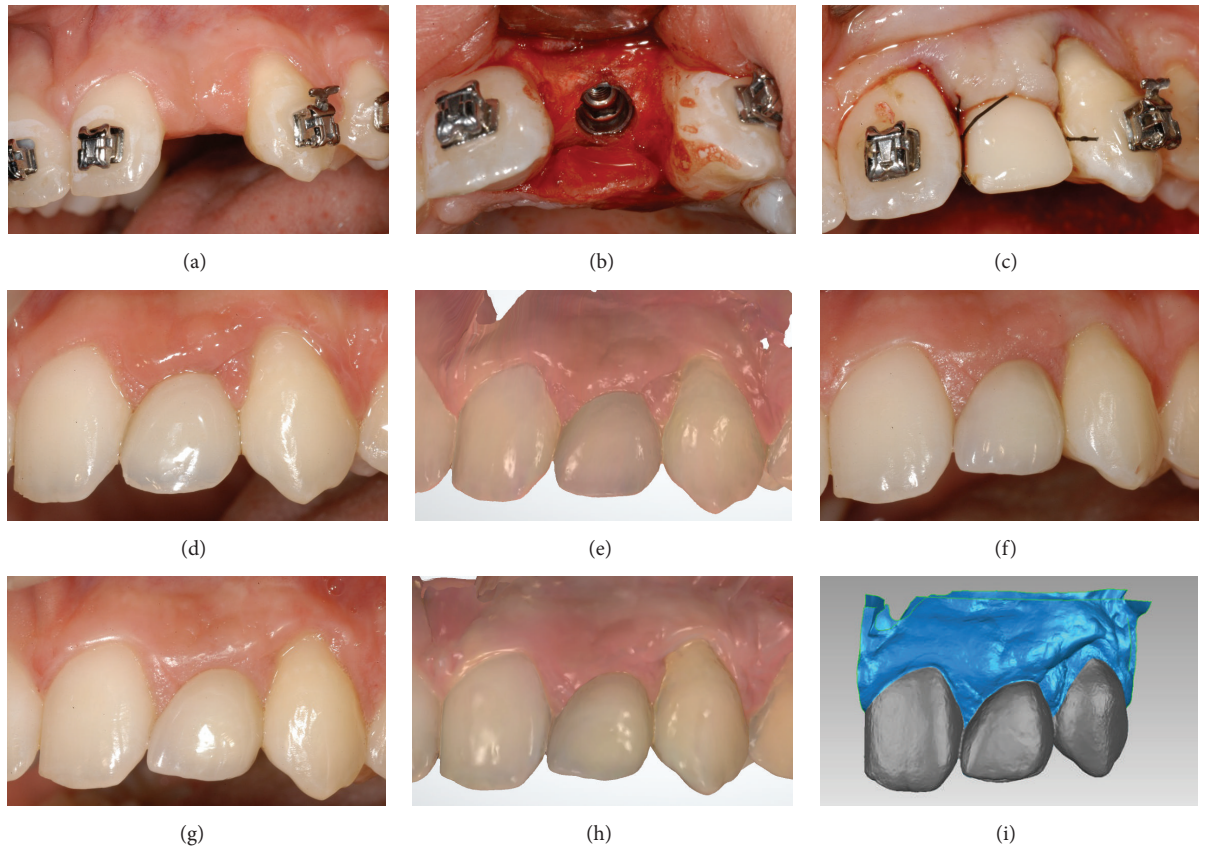

Figure 3: Conventional implant placement in healed ridge (*control* group) of a young female patient (19 years old) who underwent orthodontic treatment: (a) preoperative situation; (b) the mucoperiosteal flap was raised, the alveolar bone was exposed and the implant (Anyridge, Megagen, Gyeongbuk, South Korea) was placed in the healed ridge; (c) the implant was immediately loaded with a provisional resin crown; (d) three months later, the final metal-ceramic crown was delivered to the patient; (e) first scan (S1) of the peri-implant soft tissues with a powerful intraoral scanner (Trios, 3-Shape, Copenhagen, Denmark), at the delivery of the final crown; (f) 1-year clinical control; (g) 2-year clinical control; (h) second scan (S2) of the peri-implant soft tissues 2 years after the delivery of the final crown; (i) overlapping of digital images (S2 over S1) in powerful reverse-engineering software (Geomagic Studio 2012, Geomagic, Morrisville, NC, USA).

the implant-supported restorations only, and not on the adjacent (natural) teeth. A possible solution for future studies should be the identification of two different timeframes, with a short-term evaluation of soft tissue stability during the provisionalization (first scan, S1, two weeks after implant placement; second scan, S2, 3 months later, before replacing the provisional with the final restoration) and then a long-term evaluation of soft tissues stability after the placement of final restoration (third scan, S3, immediately after the final restoration is placed; fourth scan, S4, 2 years later). Finally, the procedure for the overlapping of digital images is not easy, as it requires experience with the use of reverse-engineering software.

Beyond these considerations, the new method presented in this paper allows a detailed quantitative 3D evaluation of peri-implant soft tissue modifications along time. This could help to evaluate treatment results in the aesthetic areas of the anterior maxilla and therefore to identify the best treatment modalities (immediate versus early versus conventional implant placement) in different clinical situations, for achieving and maintaining aesthetic success in the long-term.

5. Conclusions

In the present study, we have introduced a new 3D method for the quantitative evaluation of soft tissue stability around single implants inserted to replace failing/nonrestorable and missing lateral incisors. This method is based on the overlapping of 3D models obtained from intraoral scans of the same patient taken at different times (at the delivery of the final crown and 2 years later). Within the limits of this study (limited number of patients treated and scans taken by different operators at different time) the new method introduced here can help to evaluate treatment results in the aesthetic areas of the anterior maxilla; therefore it could help to identify the best treatment modalities (immediate versus early versus conventional implant placement) for achieving and maintaining aesthetic success.

Competing Interests

The authors report no competing interests for the present work.

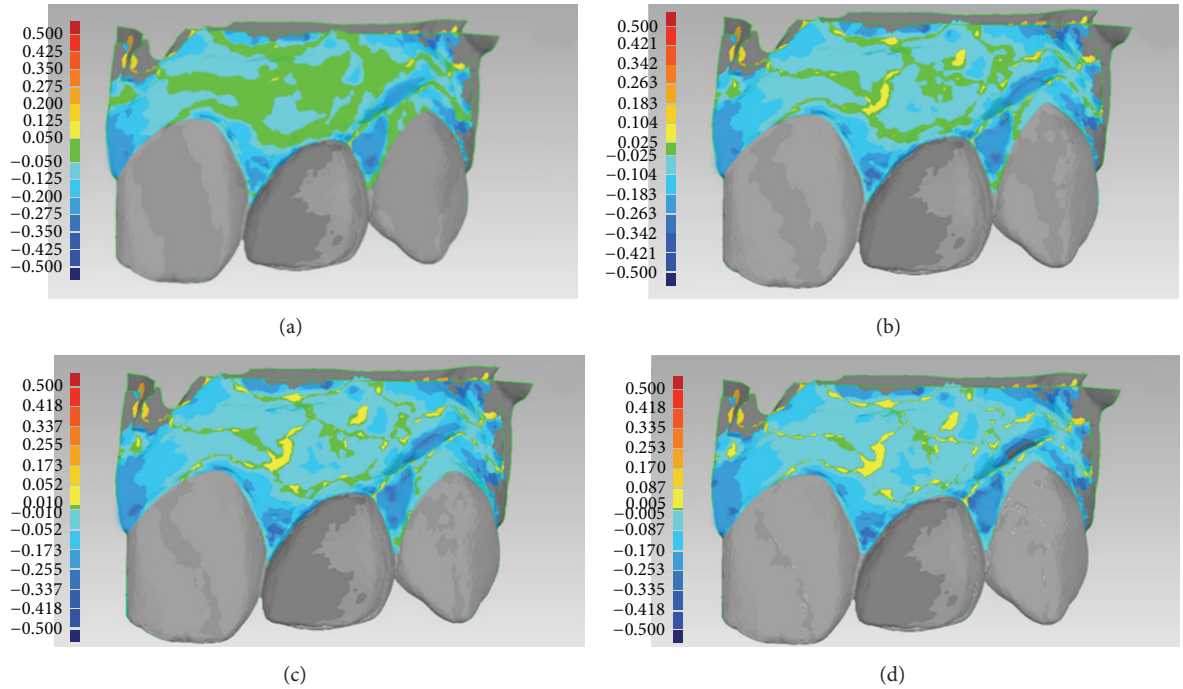

Figure 4: Conventional implant placement in healed ridge (*control* group) of a young female patient (19 years old) who underwent orthodontic treatment: (a) overlapping of digital images (S2 over S1): colorimetric map, first setting (50 μm). The soft tissues overlying the vestibular (bundle) bone appeared stable, while the papillae showed some kind of contraction; however, this could be related to the movements of the natural teeth adjacent to the implant-supported restoration; (b) overlapping of digital images (S2 over S1): colorimetric map, second setting (25 μm). The predominant color was light blue, since in most areas a variation/reduction in soft tissue volume > 25 μm was registered; (c) overlapping of digital images (S2 over S1): colorimetric map, third setting (10 μm). Only a few areas showed contraction < 10 μm; (d) overlapping of digital images (S2 over S1): colorimetric map, fourth setting (5 μm). The area of the vestibular mucosa overlying the vestibular (bundle) bone was the least affected by tissue contraction over time, whereas the papillae were the most affected. Overall, the mean (±SD) soft tissue contraction/reduction in the whole inspected area amounted to 0.091 mm (±0.073).

References

[1] S. T. Chen and D. Buser, "Esthetic outcomes following immediate and early implant placement in the anterior maxilla—a systematic review," *The International Journal of Oral & Maxillofacial Implants*, vol. 29, supplement, pp. 186–215, 2014.

[2] F. Mangano, C. Mangano, M. Ricci, R. L. Sammons, J. A. Shibli, and A. Piattelli, "Single-tooth Morse taper connection implants placed in fresh extraction sockets of the anterior maxilla: an aesthetic evaluation," *Clinical Oral Implants Research*, vol. 23, no. 11, pp. 1302–1307, 2012.

[3] J. Y. K. Kan, K. Rungcharassaeng, K. Umezu, and J. C. Kois, "Dimensions of peri-implant mucosa: an evaluation of maxillary anterior single implants in humans," *Journal of Periodontology*, vol. 74, no. 4, pp. 557–562, 2003.

[4] D. Buser, V. Chappuis, M. M. Bornstein, J.-G. Wittneben, M. Frei, and U. C. Belser, "Long-term stability of contour augmentation with early implant placement following single tooth extraction in the esthetic zone: a prospective, cross-sectional study in 41 patients with a 5- to 9-year follow-up," *Journal of Periodontology*, vol. 84, no. 11, pp. 1517–1527, 2013.

[5] U. Covani, M. Ricci, G. Bozzolo, F. Mangano, A. Zini, and A. Barone, "Analysis of the pattern of the alveolar ridge remodelling following single tooth extraction," *Clinical Oral Implants Research*, vol. 22, no. 8, pp. 820–825, 2011.

[6] G. Juodzbalys and H.-L. Wang, "Soft and hard tissue assessment of immediate implant placement: a case series," *Clinical Oral Implants Research*, vol. 18, no. 2, pp. 237–243, 2007.

[7] W. L. Tan, T. L. T. Wong, M. C. M. Wong, and N. P. Lang, "A systematic review of post-extractional alveolar hard and soft tissue dimensional changes in humans," *Clinical Oral Implants Research*, vol. 23, supplement 5, pp. 1–21, 2012.

[8] M. G. Araújo, C. O. Silva, M. Misawa, and F. Sukekava, "Alveolar socket healing: what can we learn?" *Periodontology 2000*, vol. 68, no. 1, pp. 122–134, 2015.

[9] M. G. Araujo and J. Lindhe, "Dimensional ridge alterations following tooth extraction. An experimental study in the dog," *Journal of Clinical Periodontology*, vol. 32, no. 2, pp. 212–218, 2005.

[10] M. G. Araújo and J. Lindhe, "Ridge alterations following tooth extraction with and without flap elevation: an experimental study in the dog," *Clinical Oral Implants Research*, vol. 20, no. 6, pp. 545–549, 2009.

[11] S. Fickl, O. Zuhr, H. Wachtel, M. Kebschull, and M. B. Hürzeler, "Hard tissue alterations after socket preservation with additional buccal overbuilding: a study in the beagle dog," *Journal of Clinical Periodontology*, vol. 36, no. 10, pp. 898–904, 2009.

[12] J. Blanco, S. Mareque, A. Linares, and F. Munoz, "Vertical and horizontal ridge alterations after tooth extraction in the dog:

flap vs. flapless surgery," *Clinical Oral Implants Research*, vol. 22, no. 11, pp. 1255–1258, 2011.

[13] D. Botticelli, T. Berglundh, and J. Lindhe, "Hard-tissue alterations following immediate implant placement in extraction sites," *Journal of Clinical Periodontology*, vol. 31, no. 10, pp. 820–828, 2004.

[14] V. Chappuis, O. Engel, M. Reyes, K. Shahim, L.-P. Nolte, and D. Buser, "Ridge alterations post-extraction in the esthetic zone: a 3D analysis with CBCT," *Journal of Dental Research*, vol. 92, supplement 12, pp. 195s–201s, 2013.

[15] M. Farmer and I. Darby, "Ridge dimensional changes following single-tooth extraction in the aesthetic zone," *Clinical Oral Implants Research*, vol. 25, no. 2, pp. 272–277, 2014.

[16] M. G. Araújo, J. C. C. da Silva, A. F. de Mendonça, and J. Lindhe, "Ridge alterations following grafting of fresh extraction sockets in man: a randomized clinical trial," *Clinical Oral Implants Research*, vol. 26, no. 4, pp. 407–412, 2015.

[17] G. E. Romanos, "Tissue preservation strategies for fostering long-term soft and hard tissue stability," *The International Journal of Periodontics & Restorative Dentistry*, vol. 35, no. 3, pp. 363–371, 2015.

[18] D. S. Thoma, S. Mühlemann, and R. E. Jung, "Critical soft-tissue dimensions with dental implants and treatment concepts," *Periodontology 2000*, vol. 66, no. 1, pp. 106–118, 2014.

[19] T. Jemt, "Regeneration of gingival papillae after single-implant treatment," *The International Journal of Periodontics and Restorative Dentistry*, vol. 17, no. 4, pp. 326–333, 1997.

[20] H. J. A. Meijer, K. Stellingsma, L. Meijndert, and G. M. Raghoebar, "A new index for rating aesthetics of implant-supported single crowns and adjacent soft tissues—the implant crown aesthetic index: a pilot study on validation of a new index," *Clinical Oral Implants Research*, vol. 16, no. 6, pp. 645–649, 2005.

[21] R. Fürhauser, D. Florescu, T. Benesch, R. Haas, G. Mailath, and G. Watzek, "Evaluation of soft tissue around single-tooth implant crowns: the pink esthetic score," *Clinical Oral Implants Research*, vol. 16, no. 6, pp. 639–644, 2005.

[22] U. C. Belser, L. Grütter, F. Vailati, M. M. Bornstein, H.-P. Weber, and D. Buser, "Outcome evaluation of early placed maxillary anterior single-tooth implants using objective esthetic criteria: a cross-sectional, retrospective study in 45 patients with a 2- to 4-year follow-up using pink and white esthetic scores," *Journal of Periodontology*, vol. 80, no. 1, pp. 140–151, 2009.

[23] M. Hosseini and K. Gotfredsen, "A feasible, aesthetic quality evaluation of implant-supported single crowns: an analysis of validity and reliability," *Clinical Oral Implants Research*, vol. 23, no. 4, pp. 453–458, 2012.

[24] V. H. Vilhjálmsson, K. S. Klock, K. Størksen, and A. Bårdsen, "Aesthetics of implant-supported single anterior maxillary crowns evaluated by objective indices and participants' perceptions," *Clinical Oral Implants Research*, vol. 22, no. 12, pp. 1399–1403, 2011.

[25] F. G. Mangano, C. Mangano, M. Ricci, R. L. Sammons, J. A. Shibli, and A. Piattelli, "Esthetic evaluation of single-tooth morse taper connection implants placed in fresh extraction sockets or healed sites," *Journal of Oral Implantology*, vol. 39, no. 2, pp. 172–181, 2013.

[26] F. Raes, J. Cosyn, and H. De Bruyn, "Clinical, aesthetic, and patient-related outcome of immediately loaded single implants in the anterior maxilla: A Prospective Study in Extraction Sockets, Healed Ridges, and Grafted Sites," *Clinical Implant Dentistry and Related Research*, vol. 15, no. 6, pp. 819–835, 2013.

[27] J. Cosyn, A. Eghbali, L. Hanselaer et al., "Four modalities of single implant treatment in the anterior maxilla: a clinical, radiographic, and aesthetic evaluation," *Clinical Implant Dentistry and Related Research*, vol. 15, no. 4, pp. 517–530, 2013.

[28] G. I. Benic, K. Wolleb, M. Sancho-Puchades, and C. H. F. Hämmerle, "Systematic review of parameters and methods for the professional assessment of aesthetics in dental implant research," *Journal of Clinical Periodontology*, vol. 39, supplement 12, pp. 160–192, 2012.

[29] V. Chappuis, O. Engel, K. Shahim, M. Reyes, C. Katsaros, and D. Buser, "Soft tissue alterations in esthetic postextraction sites: a 3-dimensional analysis," *Journal of Dental Research*, vol. 94, supplement 9, pp. 187s–193s, 2015.

[30] M. Zimmermann, A. Mehl, W. H. Mörmann, and S. Reich, "Intraoral scanning systems—a current overview," *International Journal of Computerized Dentistry*, vol. 18, no. 2, pp. 101–129, 2015.

[31] S. Ting-Shu and S. Jian, "Intraoral digital impression technique: a review," *Journal of Prosthodontics*, vol. 24, no. 4, pp. 313–321, 2015.

[32] L. H. C. Cevidanes, A. E. F. Oliveira, D. Grauer, M. Styner, and W. R. Proffit, "Clinical application of 3D imaging for assessment of treatment outcomes," *Seminars in Orthodontics*, vol. 17, no. 1, pp. 72–80, 2011.

[33] N. Gkantidis, M. Schauseil, P. Pazera, B. Zorkun, C. Katsaros, and B. Ludwig, "Evaluation of 3-dimensional superimposition techniques on various skeletal structures of the head using surface models," *PLoS ONE*, vol. 10, no. 2, article e118810, 2015.

[34] B. R. Chrcanovic, T. Albrektsson, and A. Wennerberg, "Smoking and dental implants: a systematic review and meta-analysis," *Journal of Dentistry*, vol. 43, no. 5, pp. 487–498, 2015.

[35] G. Luongo, C. Lenzi, F. Raes, T. Eccellente, M. Ortolani, and C. Mangano, "Immediate functional loading of single implants: a 1-year interim report of a 5-year prospective multicentre study," *European Journal of Oral Implantology*, vol. 7, no. 2, pp. 187–199, 2014.

[36] S.-Y. Lee, D.-J. Yang, S. Yeo, H.-W. An, K. H. Ryoo, and K.-B. Park, "The cytocompatibility and osseointegration of the Ti implants with XPEED® surfaces," *Clinical Oral Implants Research*, vol. 23, no. 11, pp. 1283–1289, 2012.

[37] G. Huynh-Ba, B. E. Pjetursson, M. Sanz et al., "Analysis of the socket bone wall dimensions in the upper maxilla in relation to immediate implant placement," *Clinical Oral Implants Research*, vol. 21, no. 1, pp. 37–42, 2010.

[38] A. L. Januário, W. R. Duarte, M. Barriviera, J. C. Mesti, M. G. Araújo, and J. Lindhe, "Dimension of the facial bone wall in the anterior maxilla: a cone-beam computed tomography study," *Clinical Oral Implants Research*, vol. 22, no. 10, pp. 1168–1171, 2011.

[39] K. Nisapakultorn, S. Suphanantachat, O. Silkosessak, and S. Rattanamongkolgul, "Factors affecting soft tissue level around anterior maxillary single-tooth implants," *Clinical Oral Implants Research*, vol. 21, no. 6, pp. 662–670, 2010.

[40] C. Mangano, L. Levrini, A. Mangano, F. Mangano, A. MacChi, and A. Caprioglio, "Esthetic evaluation of implants placed after orthodontic treatment in patients with congenitally missing lateral incisors," *Journal of Esthetic and Restorative Dentistry*, vol. 26, no. 1, pp. 61–71, 2014.

Hindawi Publishing Corporation
International Journal of Dentistry
Volume 2016, Article ID 5926941, 6 pages
http://dx.doi.org/10.1155/2016/5926941

Research Article

ATP Bioluminometers Analysis on the Surfaces of Removable Orthodontic Aligners after the Use of Different Cleaning Methods

Luca Levrini,[1] Alessandro Mangano,[2] Silvia Margherini,[2] Camilla Tenconi,[2] Davide Vigetti,[3] Raffaele Muollo,[2] and Gian Marco Abbate[2]

[1]*Department of Surgical and Morphological Sciences, Oro Cranio Facial Disease and Medicine Research Center, Dental Hygiene School, University of Insubria, Via Giuseppe Piatti 10, 21100 Varese, Italy*
[2]*Oro Cranio Facial Disease and Medicine Research Center, University of Insubria, 21100 Varese, Italy*
[3]*Department of Surgical and Morphological Sciences, University of Insubria, 21100 Varese, Italy*

Correspondence should be addressed to Luca Levrini; luca.levrini@uninsubria.it

Received 20 February 2016; Accepted 14 April 2016

Academic Editor: Thomas Fortin

Purpose. The aim was to quantify the bacteria concentration on the surface of orthodontic clear aligners using three different cleaning methods. Furthermore the objective was to validate the efficacy of the bioluminometer in assessing the bacteria concentration. *Materials and Methods*. Twenty subjects (six males and fourteen females) undergoing orthodontic therapy with clear aligners (Invisalign® Align Technology, Santa Clara, California) were enrolled in this study. The observation time was of six weeks. The patients were instructed to use different cleaning methods (water, brushing with toothpaste, and brushing with toothpaste and use of sodium carbonate and sulphate tablet). At the end of each phase a microbiological analysis was performed using the bioluminometer. *Results*. The highest bacteria concentration was found on aligners cleaned using only water (583 relative light units); a value of 189 relative light units was found on aligners cleaned with brushing and toothpaste. The lowest bacteria concentration was recorded on aligners cleaned with brushing and toothpaste and the use of sodium carbonate and sulfate tablet. *Conclusions*. The mechanical removal of the bacterial biofilm proved to be effective with brushing and toothpaste. The best results in terms of bacteria concentration were achieved adding the use of sodium carbonate and sulfate tablet.

1. Introduction

Traditional fixed orthodontic appliances lead to a change in the quantity and in the composition of oral microbiota. Fixed orthodontic devices cause plaque accumulation, impede correct professional hygiene procedures, and potentially cause enamel demineralization, tooth decay, and periodontal disease [1–6]. Digital dentistry is a fast moving field and new technologies give both the clinicians and patients new treatment possibilities. In 1999 a new orthodontic appliance based on a polymer composed of a chain of organic units joined with urethane links was introduced (Invisalign, Align Technology, Santa Clara, California) and produced with a CAM (computer aided manufacturing) technology as a removable appliance able to gradually move the teeth according to a computer designed treatment plan. The introduction of this technology gave the patients the possibility to better control the oral hygiene. In fact, the use of removable orthodontic devices guarantees a normal professional hygiene cleaning, thus reducing the risk of developing plaque related diseases [7–9]. The use of removable clear aligners showed, also, a better patient compliance in terms of oral hygiene procedures [10]. In the case of removable aligners it is important that before use they are cleaned and without bacteria. A correct hygiene is able to impede the accumulation of bacteria on the surfaces, thus avoiding the potential risk of spreading bacteria on teeth surfaces and periodontium. Therefore, it is important to clean and disinfect the removable aligners, but information given to patients is often incomplete and unclear. This could be attributable to a lack of evidence in the

scientific literature; the same problem could be related also to other removable orthodontic appliances [11, 12]. The aim of this study was to evaluate the efficacy in removing the bacterial biofilm on clear aligners using three different cleaning methods. Furthermore the reliability of bioluminometer was tested.

2. Materials and Methods

2.1. Patient Population. Twenty (6 males and 14 females) consecutive patients undergoing orthodontic treatment with clear aligners (Invisalign, Align Technology, Santa Clara, California) referring to the Department of Orthodontics of the University of Insubria with age ranging from 18 to 30 years were enrolled in this study. All patients were informed of the nature of the study to be carried out on an individual basis and read and signed a written consent form. The study protocol was conducted in accordance with the Helsinki Declaration of 1975, as revised in 2007. The study protocol was approved by the Ospedale di Circolo e Fondazione Macchi Ethics Committee, Varese.

2.2. Inclusion and Exclusion Criteria. Inclusion criteria were as follows: Class I skeletal relationship, normodivergent Frankfort mandibular-plane angle, age > 18, and no active periodontal disease.

Exclusion criteria were as follows: smoking habit, presence of fixed bridges/crowns or partial dentures, previous periodontal nonsurgical treatment (such as full-mouth disinfection, quadrant-by-quadrant therapy, and full-mouth debridement) within the past year, and medications such as antibiotics, steroids, or nonsteroidal anti-inflammatory drugs within the past 6 months.

2.3. Study Design, Evaluation of Total Biofilm, and Statistical Analysis. Before taking part in the study all subjects were motivated and instructed to a correct oral hygiene by one operator (CT). All patients were instructed to use a manual toothbrush with a rolling technique. To reduce bias patients were provided with the same oral hygiene products (anticaries toothpaste, mouthrinse, and interdental floss). All subjects underwent professional dental cleaning by one operator (CT) before the study period. Each patient received three series of aligners, each to be worn for 2 weeks, and was asked to use different cleaning procedures over the 6 weeks of their application. At the end of each two-week stage a microbiological sample was obtained from the aligners by means of sterile swab. The patients were asked to clean the clear aligners using three different cleaning methods described as follows:

T1 (water—W): during the first two weeks patients were asked to remove the clear aligners before eating and to rinse the aligners in cold running water for 15 seconds.

T2 (toothbrush—TB): for the second two weeks before eating patients were asked to remove the aligners and to brush them for at least 30 seconds with a soft toothbrush and toothpaste with a relative dentin abrasion value of less than 100.

T3 (tablet and toothbrush—TBT): all the subjects were asked to clean their appliances daily for at least 20 minutes by soaking them in cold water in which effervescent tablets containing sodium carbonate and sulfate (Invisalign Cleaning System, Align Technology, San Jose, CA, USA) had been dissolved. Before wearing the aligners, the patients were also instructed to brush them for at least 30 seconds with a soft toothbrush and toothpaste with a relative dentin abrasion value of less than 100. At the end of each 2-week stage, bioluminometer analysis was carried out. A Wilcoxon match paired test was used. The level of significance was set at 0.05. All statistical analyses were run on the MedCalc® software (MedCalc Software bvba, Ostend, Belgium).

2.4. Bioluminometer Validation. A crossed analysis was carried out in order to evaluate the reliability of the bioluminometer values. A microbiological sample was obtained and analysed. The total biofilm value was evaluated using two different methods. A sample of saliva was obtained for both analyses. The traditional LB Agar culture was carried out counting the CFU (colony-forming unit). The bioluminometer gives a bacteria concentration value expressed in RLU (relative light units). A comparison of the values obtained with the two different methods was done.

2.5. Bioluminometer Microbiological Analysis. A microbiological analysis was carried out using the Bioluminometer System Sure II Plus (RG Strumenti, Parma, Italy) with the SuperSnap kit (RG Strumenti, Parma, Italy) according to the manufacturer's instructions. The sample was collected passing the SuperSnap kit on the aligners from molar to molar; a round movement was performed on the molars while a simple scraping was performed on the other parts of the aligners. The samples were then stored in a solution for the bacterial lysis and for the chemiluminescence. The sample was stored for 4 hours at 4°C before proceeding with the chemiluminescence analysis.

3. Results

3.1. Bioluminometer Validation. A correlation was found between the results obtained with the Bioluminometer and the LB Agar culture. A proportional relationship was found between UFC and the RLU values. A linear relationship was found until 200 UFC value (Figure 1).

3.2. Bioluminometer Microbiological Analysis. All the samples were colonized by a bacterial biofilm (Table 1). The mean values of the bacterial concentration were 583 RLU, 188 RLU, and 71 RLU for the water (W), toothbrush (TB), and toothbrush and tablets (TBT), respectively (Figure 2). The median values were 518 W (95% confidence interval 248–781), 145 TB (95% confidence interval 103–205), and 64 TBT (95% confidence interval 39–85). The highest bacterial value

Table 1: Value of the bioluminometer analysis; concentration value is expressed in RLU (relative light units).

Patient	T1 Water	T2 Toothbrush	T3 Toothbrush and tablet
1	1.292	127	38
2	1.240	82	89
3	749	325	78
4	500	146	47
5	216	46	71
6	42	145	24
7	74	23	7
8	536	45	36
9	304	69	27
10	186	160	62
11	976	451	107
12	237	187	64
13	439	324	98
14	1.403	625	152
15	343	113	51
16	704	127	220
17	788	209	16
18	635	306	82
19	851	162	86
20	154	107	65

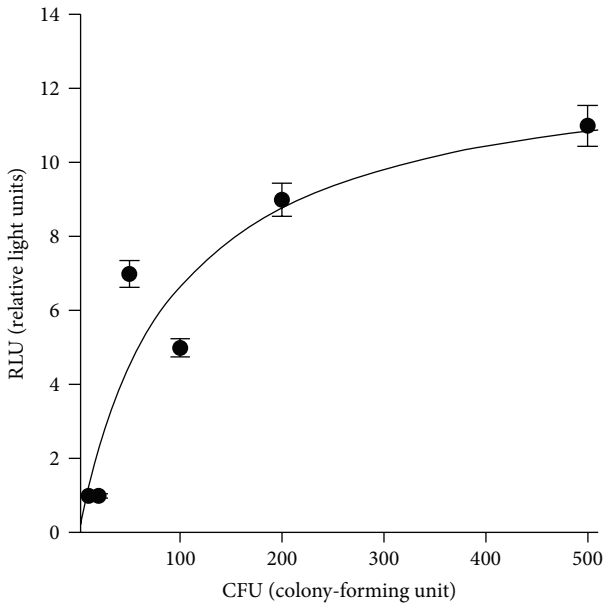

Figure 1: Linear relationship graph.

in the TBT group was lower than the lowest value of the TB value; similarly the highest value of the TB group was lower than the lowest value of the W group. A statistical significant difference was found between the TBT group and the TB group ($p = 0.0003$) (Figure 3).

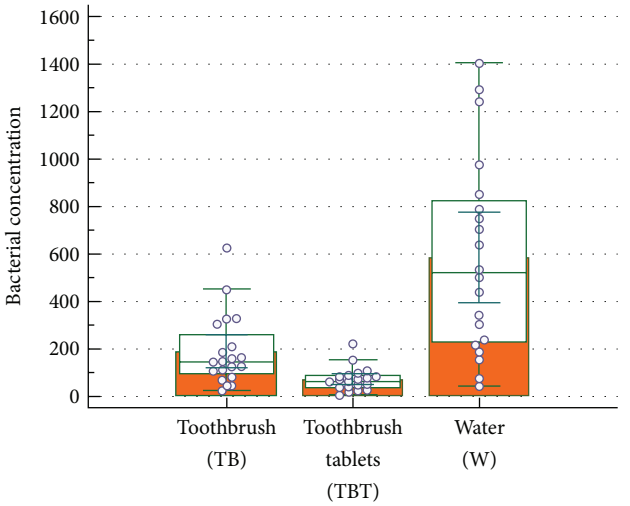

Figure 2: Box plot comparison between TB, TBT, and W. The graphical representation box and whiskers plot shown above, using the multiple comparison mode, is used to describe the distribution of a sample by means of simple measures of dispersion and location. The central box represents the values from the lower to upper quartile (25 to 75 percentile). The middle line represents the median. A line extends from the minimum to the maximum value, excluding "outside" and "far out" values which are displayed as separated points.

4. Discussion

Orthodontic treatment with clear aligners is widely accepted and used because it is a highly aesthetic and nearly invisible treatment option. A high compliance with oral hygiene procedures was found in patients treated with removable aligners, thus reducing the risk of developing plaque-related disease [10]. Several clinical [9, 13] and microbiological [8] studies showed that Invisalign appliance, even if embedded teeth and part of the keratinized gingiva nearly all day, reduces the risk of developing periodontal injury compared with fixed orthodontic appliance. This could be attributed to the fact that aligners are removable and thus allow unimpeded oral hygiene.

The fact that aligners can be removed before eating and during oral hygiene procedures does not exclude bacterial contamination and proliferation on them. Studies conducted with Scanning Electron Microscopy (SEM) highlighted the adherence of organic material and bacteria to clear aligners compromising the aesthetic aspect of them in terms of transparency. Lombardo et al. demonstrated, in vitro, using artificial saliva that the optical properties of orthodontic aligners appear to vary between brands and constituent materials but deteriorate with in vitro aging in all cases [14]. The growth of a bacterial biofilm does not only influence the aesthetic aspect of the clear aligners but also it is a potential risk factor for the development of bacteria-related disease; thus it is important to determine the most effective cleaning method. Several studies conducted on materials used in restoration procedures (such as denture materials and porcelains) showed how *S. mutans*, *C. albicans*, and

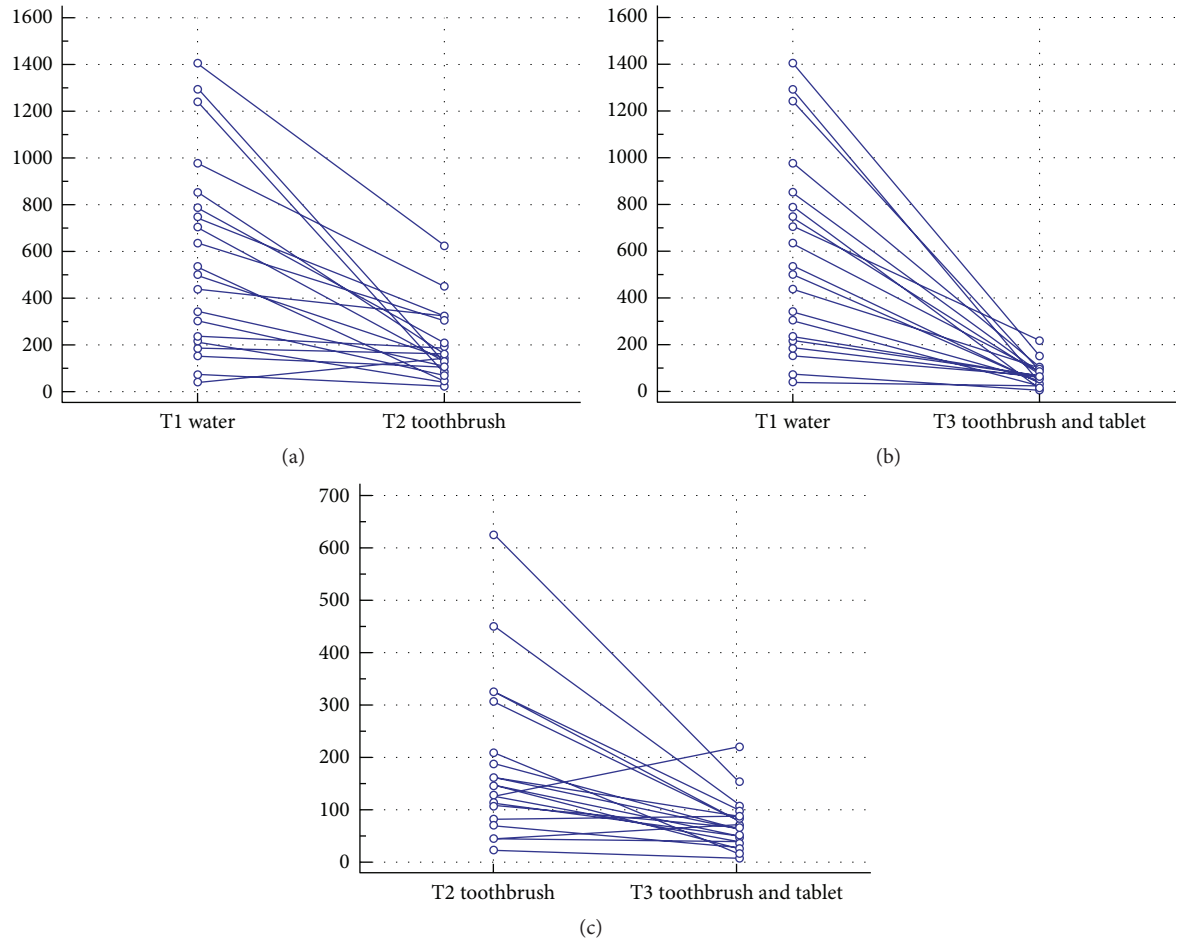

Figure 3: Wilcoxon test for paired data. W and TB (a), W and TBT (b), and TB and TBT (c).

streptococci accumulate on the surface of removable appliances [15, 16]. Li et al. highlighted that the nature of a surface is able to influence biofilm features such as biomass accumulation and susceptibility to antimicrobial treatments [17]. These studies showed how total biofilm mass can be reduced using daily correct hygiene procedures. A study was conducted on removable resin-made orthodontic devices and analysed the distribution frequency of *Streptococcus mutans* in the saliva of two groups of children: one group treated with resin-made removable appliances and one group untreated. A higher bacterial colonization was found in the treated group, showing how orthodontic devices may be potential carriers of bacterial infections [18]. A SEM study conducted by Diedrich on removable orthodontic appliances showed the microbiological colonization on these appliances. The results showed that using only a toothbrush was not able to provide an acceptable hygiene; on the contrary the use of ultrasound gave optimal results [19]. A recent SEM study conducted on clear aligners analysed the bacterial colonization using three different cleaning methods: running water, toothbrush and toothpaste, and toothbrush and toothpaste with sodium carbonate and sulfate [20]. This study suggested that brushing associated with the use of effervescent tablets containing sodium carbonate and sulfate is the most effective method of cleaning clear aligners. Our data are in accordance with these findings. These results can be attributable to the use of sodium carbonate and sulfate that reduce the bacterial colonization. The bioluminometer values recorded were in accordance with the results reported in the literature. Nevertheless biofilm continued to be present, even if in low concentration, in particular on the internal surfaces. This, potentially, could give rise to different problems: discoloration of the aligners, an unpleasant odour, and interaction with bacteria already present in the oral cavity. Low reported with SEM is the colonization of invisible aligners; this study described an organized growth of biofilm on the aligners' surfaces, in particular localized on more recessed and sheltered areas of the appliance, such as the cusp tips and attachment dimples [21]. Peixoto et al. performed a microbiological analysis to quantitatively evaluate the presence of *S. mutans* on the surfaces of removable orthodontic appliances. The study involved a 3-week cycle, with 1-week intervals between the weeks. During each week, three different groups of patients each followed three appliance-cleaning methods: (1) tooth brushing + baseplate brushing + sterile tap water spraying once a day; (2) tooth brushing + baseplate brushing + spraying with a 0.20% CHX-based solution on the seventh day after appliance placement; and (3) tooth brushing baseplate

brushing + spraying with a 0.20% CHX-based solution on the fourth and seventh days after appliance placement. At the end of each week, the bacterial load of three randomly chosen appliances, one for each cleaning protocol, was analysed under SEM. Bacterial biofilm was detected on the surfaces of all the devices; the quantity of *S. mutans* on the surfaces treated with 0.12% CHX spray was lower than the prevalence of *S. mutans* detected on the H_2O spray-treated surfaces and no significant difference was found between the two CHX spray protocols. It has been demonstrated and it is widely accepted that the most effective cleaning method must be still identified [22]. A study evaluated the feasibility of the removable thermoplastic appliance to adsorb hygienic solution and inhibit bacterial growth in culture and, in vivo, examined the efficacy of three hygiene protocols in reducing bacterial biofilm adherence (brushing, immersion in chlorhexidine mouthwash, and using a vibrating bath with cleaning solution). In vitro results showed the impossibility of thermoplastic appliance to adsorb substances that reduce the bacterial colonization, such as chlorhexidine. In vivo results showed that chlorhexidine and vibrating bath with cleaning solution significantly reduced baseline biofilm adherence [23]. Gracco et al. studied short-term chemical and physical changes in Invisalign appliance; morphological and structural variation occurred after their use [24]. Aligners worn for 14 days had microcracks, abraded and delaminated areas, localised calcified biofilm deposits, and loss of transparency. These alterations could induce the ecological contamination of aligners, such as for other removable orthodontic devices. A recent trial showed a similar result on the surface of Essix retainers, thus showing the bacterial colonization of removable orthodontic appliances [25]. Furthermore an analysis on the most appropriate modality of decontamination of appliances was carried out. The bacteria analysed in this study were *S. mutans* and *S. sanguis*, Actinomyces naeslundii, methicillin-resistant *Staphylococcus aureus*, and *Candida albicans*. The necessity of brushing Essix appliance, associated with the use of chemical antimicrobial method of sanitation, appears useful to reduce the bacterial count on appliances. Further studies should focus on the use of ultrasonic device for the hygienization of removable orthodontic appliances. In fact, according to some authors, the mechanical action of ultrasonic devices on dental devices may give good results even in the absence of any chemical action [26–29].

5. Conclusions

Within the limit of this study we can state that

(i) the use of sodium carbonate and sulphate effervescent tablets combined with the mechanical debridement resulted in being the most effective cleaning method;

(ii) the bioluminometer resulted in being a reliable tool for preliminary investigation of bacterial colonization.

Further studies should investigate the use of ultrasonic devices for the cleaning of Invisalign aligners.

Competing Interests

The authors report no financial relationship with any commercial firm that may pose a conflict of interests for this study. No grants, equipment, or other sources of support were provided. The authors do not report any conflict of interests related to this study.

References

[1] A.-M. Bollen, J. Cunha-Cruz, D. W. Bakko, G. J. Huang, and P. P. Hujoel, "The effects of orthodontic therapy on periodontal health—a systematic review of controlled evidence," *The Journal of the American Dental Association*, vol. 139, no. 4, pp. 413–422, 2008.

[2] A. O. Freitas, M. Marquezan, C. Nojima Mda, D. S. Alviano, and L. C. Maia, "The influence of orthodontic fixed appliances on the oral microbiota—a systematic review," *Dental Press Journal of Orthodontics*, vol. 19, no. 2, pp. 46–55, 2014.

[3] H. Liu, J. Sun, Y. Dong et al., "Periodontal health and relative quantity of subgingival porphyromonas gingivalis during orthodontic treatment," *Angle Orthodontist*, vol. 81, no. 4, pp. 609–615, 2011.

[4] M. Ristic, M. Vlahovic Svabic, M. Sasic, and O. Zelic, "Effects of fixed orthodontic appliances on subgingival microflora," *International Journal of Dental Hygiene*, vol. 6, no. 2, pp. 129–136, 2008.

[5] P. M. Sinclair, M. F. Cannito, L. J. Goates, L. F. Solomos, and C. M. Alexander, "Patient responses to lingual appliances," *Journal of Clinical Orthodontics*, vol. 20, no. 6, pp. 396–404, 1986.

[6] J. Van Gastel, M. Quirynen, W. Teughels, W. Coucke, and C. Carels, "Longitudinal changes in microbiology and clinical periodontal parameters after removal of fixed orthodontic appliances," *European Journal of Orthodontics*, vol. 33, no. 1, pp. 15–21, 2011.

[7] L. Levrini, G. M. Abbate, F. Migliori, G. Orrù, S. Sauro, and A. Caprioglio, "Assessment of the periodontal health status in patients undergoing orthodontic treatment with fixed or removable appliances. A microbiological and preliminary clinical study," *Cumhuriyet Dental Journal*, vol. 16, no. 4, pp. 296–307, 2013.

[8] L. Levrini, A. Mangano, P. Montanari, S. Margherini, A. Caprioglio, and G. M. Abbate, "Periodontal health status in patients treated with the Invisalign® system and fixed orthodontic appliances: a 3 months clinical and microbiological evaluation," *European Journal of Dentistry*, vol. 9, no. 3, pp. 404–410, 2015.

[9] R.-R. Miethke and K. Brauner, "A comparison of the periodontal health of patients during treatment with the Invisalign system and with fixed lingual appliances," *Journal of Orofacial Orthopedics*, vol. 68, no. 3, pp. 223–231, 2007.

[10] G. M. Abbate, M. P. Caria, P. Montanari et al., "Periodontal health in teenagers treated with removable aligners and fixed orthodontic appliances," *Journal of Orofacial Orthopedics*, vol. 76, no. 3, pp. 240–250, 2015.

[11] J. Eichenauer, C. Serbesis, and S. Ruf, "Cleaning removable orthodontic appliances—a survey," *Journal of Orofacial Orthopedics*, vol. 72, no. 5, pp. 389–395, 2011.

[12] A. S. Axe, R. Varghese, M. Bosma, N. Kitson, and D. J. Bradshaw, "Dental health professional recommendation and consumer habits in denture cleansing," *The Journal of Prosthetic Dentistry*, vol. 115, no. 2, pp. 183–188, 2016.

[13] R. R. Miethke and S. Vogt, "A comparison of the periodontal health of patients during treatment with the invisalign system and with fixed orthodontic appliances," *Journal of Orofacial Orthopedics*, vol. 66, no. 3, pp. 219–229, 2005.

[14] L. Lombardo, A. Arreghini, R. Maccarrone, A. Bianchi, S. Scalia, and G. Siciliani, "Optical properties of orthodontic aligners—spectrophotometry analysis of three types before and after aging," *Progress in Orthodontics*, vol. 16, no. 1, article 41, 2015.

[15] R. F. André, I. M. Andrade, C. H. Silva-Lovato, F. Paranhos Hde, F. C. Pimenta, and I. Y. Ito, "Prevalence of mutans streptococci isolated from complete dentures and their susceptibility to mouthrinses," *Brazilian Dental Journal*, vol. 22, no. 1, pp. 62–67, 2011.

[16] S. C. de Lucena-Ferreira, I. M. G. Cavalcanti, and A. A. Del Bel Cury, "Efficacy of denture cleansers in reducing microbial counts from removable partial dentures: a short-term clinical evaluation," *Brazilian Dental Journal*, vol. 24, no. 4, pp. 353–356, 2013.

[17] L. Li, M. B. Finnegan, S. Özkan et al., "In vitro study of biofilm formation and effectiveness of antimicrobial treatment on various dental material surfaces," *Molecular Oral Microbiology*, vol. 25, no. 6, pp. 384–390, 2011.

[18] G. Batoni, M. Pardini, A. Giannotti et al., "Effect of removable orthodontic appliances on oral colonisation by mutans streptococci in children," *European Journal of Oral Sciences*, vol. 109, no. 6, pp. 388–392, 2001.

[19] P. Diedrich, "Microbial colonization and various cleaning procedures for orthodontic appliances," *Fortschr Kieferorthop*, vol. 50, no. 3, pp. 231–239, 1989.

[20] L. Levrini, F. Novara, S. Margherini, C. Tenconi, and M. Raspanti, "Scanning electron microscopy analysis of the growth of dental plaque on the surfaces of removable orthodontic aligners after the use of different cleaning methods," *Journal of Clinical, Cosmetic and Investigational Dentistry*, vol. 15, no. 7, pp. 125–131, 2015.

[21] B. Low, W. Lee, C. J. Seneviratne, L. P. Samaranayake, and U. Hägg, "Ultrastructure and morphology of biofilms on thermoplastic orthodontic appliances in 'fast' and 'slow' plaque formers," *European Journal of Orthodontics*, vol. 33, no. 5, pp. 577–583, 2011.

[22] I. T. A. Peixoto, C. Enoki, I. Y. Ito, M. A. N. Matsumoto, and P. Nelson-Filho, "Evaluation of home disinfection protocols for acrylic baseplates of removable orthodontic appliances: a randomized clinical investigation," *American Journal of Orthodontics and Dentofacial Orthopedics*, vol. 140, no. 1, pp. 51–57, 2011.

[23] N. Shpack, R. B.-N. Greenstein, D. Gazit, R. Sarig, and A. D. Vardimon, "Efficacy of three hygienic protocols in reducing biofilm adherence to removable thermoplastic appliance," *The Angle Orthodontist*, vol. 84, no. 1, pp. 161–170, 2014.

[24] A. Gracco, A. Mazzoli, O. Favoni et al., "Short-term chemical and physical changes in invisalign appliances," *Australian Orthodontic Journal*, vol. 25, no. 1, pp. 34–40, 2009.

[25] C. S. Chang, S. Al-Awadi, D. Ready, and J. Noar, "An assessment of the effectiveness of mechanical and chemical cleaning of Essix orthodontic retainer," *Journal of Orthodontics*, vol. 41, no. 2, pp. 110–117, 2014.

[26] P. C. Cruz, I. M. de Andrade, A. Peracini et al., "The effectiveness of chemical denture cleansers and ultrasonic device in biofilm removal from complete dentures," *Journal of Applied Oral Science*, vol. 19, no. 6, pp. 668–673, 2011.

[27] Y. Nishi, K. Seto, Y. Kamashita, C. Take, A. Kurono, and E. Nagaoka, "Examination of denture-cleaning methods based on the quantity of microorganisms adhering to a denture," *Gerodontology*, vol. 29, no. 2, pp. e259–e266, 2012.

[28] H. F. O. Paranhos, C. H. Silva-Lovato, R. F. Souza, P. C. Cruz, K. M. Freitas, and A. Peracini, "Effects of mechanical and chemical methods on denture biofilm accumulation," *Journal of Oral Rehabilitation*, vol. 34, no. 8, pp. 606–612, 2007.

[29] N. Sesma, A. L. Rocha, D. C. Laganá, B. Costa, and S. Morimoto, "Effectiveness of denture cleanser associated with microwave disinfection and brushing of complete dentures: in vivo study," *Brazilian Dental Journal*, vol. 24, no. 4, pp. 357–361, 2013.

Hindawi Publishing Corporation
International Journal of Dentistry
Volume 2016, Article ID 8242535, 8 pages
http://dx.doi.org/10.1155/2016/8242535

Research Article

A Patient Specific Biomechanical Analysis of Custom Root Analogue Implant Designs on Alveolar Bone Stress: A Finite Element Study

David Anssari Moin, Bassam Hassan, and Daniel Wismeijer

Department of Oral Function and Restorative Dentistry, Academic Centre for Dentistry Amsterdam (ACTA), Research Institute MOVE, 1081 LA Amsterdam, Netherlands

Correspondence should be addressed to David Anssari Moin; danssari@acta.nl

Received 8 February 2016; Accepted 24 March 2016

Academic Editor: Thomas Fortin

Objectives. The aim of this study was to analyse by means of FEA the influence of 5 custom RAI designs on stress distribution of peri-implant bone and to evaluate the impact on microdisplacement for a specific patient case. *Materials and Methods*. A 3D surface model of a RAI for the upper right canine was constructed from the cone beam computed tomography data of one patient. Subsequently, five (targeted) press-fit design modification FE models with five congruent bone models were designed: "Standard," "Prism," "Fins," "Plug," and "Bulbs," respectively. Preprocessor software was applied to mesh the models. Two loads were applied: an oblique force (300 N) and a vertical force (150 N). Analysis was performed to evaluate stress distributions and deformed contact separation at the peri-implant region. *Results*. The lowest von Mises stress levels were numerically observed for the Plug design. The lowest levels of contact separation were measured in the Fins model followed by the Bulbs design. *Conclusions*. Within the limitations of the applied methodology, adding targeted press-fit geometry to the RAI standard design will have a positive effect on stress distribution, lower concentration of bone stress, and will provide a better primary stability for this patient specific case.

1. Introduction

With technological advances in the field of implant dentistry novel treatment modalities and more efficient options became available. The custom 3D printed root analogue implant (RAI) as defined by Anssari Moin et al. [1, 2] and Figliuzzi et al. [3] is a futuristic treatment option for immediate implantation and immediate loading cases for a soon to be removed tooth. Advantages of the RAI technique when compared to conventional screw shaped multipiece implants may encompass more cost efficiency, one-piece implant, and minimal traumatic surgical intervention [1–6].

An essential factor for realization of all implant-based prosthetic reconstructions is successful osseointegration of the implant. In particular, primary stability plays a fundamental role in one-stage implant surgery with or without immediate loading [7]. Conventional screw type implants achieve primary stability through mechanical fixation by implant threads in bone [8]. Numerous studies on the factors influencing primary stability (implant shape specifications, surface modifications, bone quality, and surgical technique) and the effect on the process of osseointegration have been performed [8–11]. However, primary stability for the RAI technique is based on the (targeted) press-fit phenomenon for achieving successful osseointegration [1–3, 6]. Since the custom RAI is based on Cone Beam Computed Tomography (CBCT), Computer Aided Design (CAD), and 3D printing technology an unlimited array of designs for this custom implant approach is available. Every RAI design option aimed at increasing initial mechanical stability for the root part of the RAI will have a different biomechanical effect on the surrounding bone and influence on the relative microdisplacement at bone-to-implant interface consequently leading to diverse osseointegration results, bone resorption, or failures.

Finite Element Analysis (FEA) has become an effective method in investigating bone stress/strain around implants

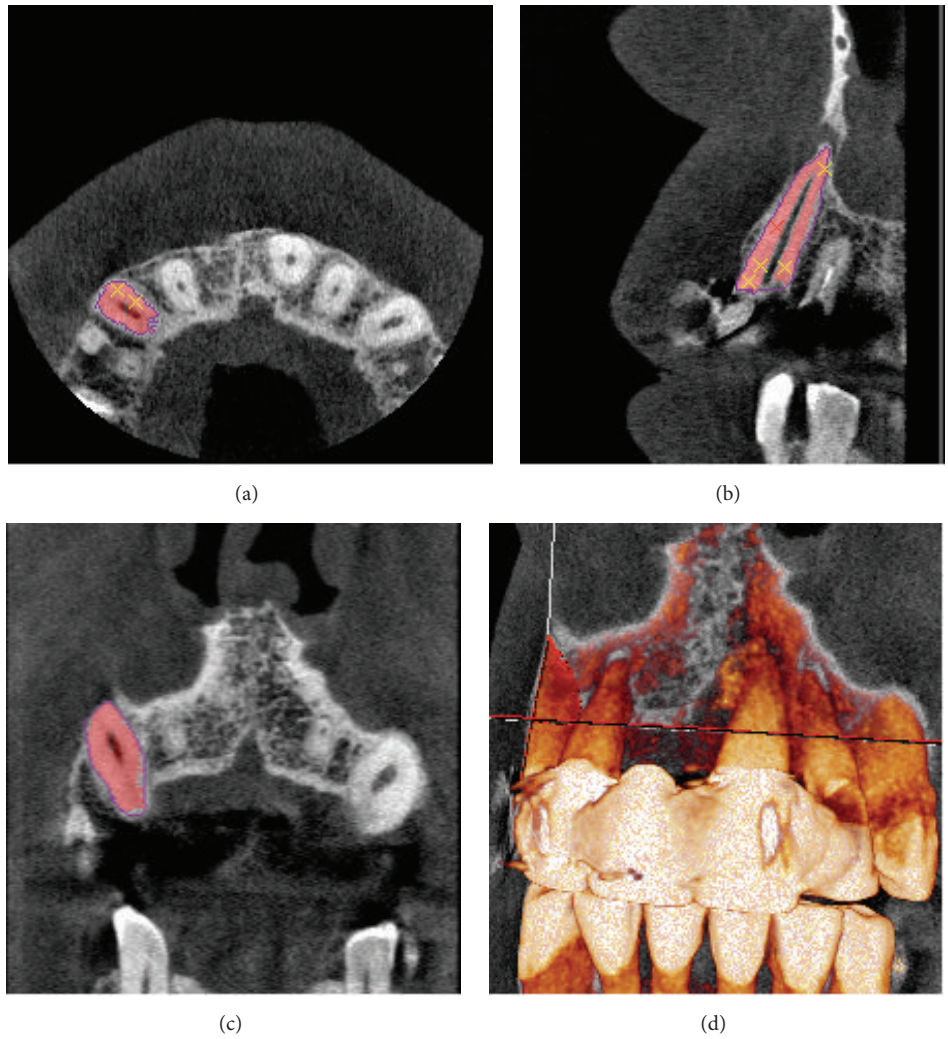

Figure 1: Segmentation and preparation of the RAI. Coronal (a), axial (b), sagittal (c), and 3D (d) views.

and relative microdisplacement between bone-to-implant interfaces [12]. However, as with all FEA studies the analysis is confined to a limited amount of factors and designs and cannot be generalised, specifically not for individual cases. Thus, the aim of this study is to analyse, with the means of FEA, the influence of 5 custom RAI designs on stress distribution of peri-implant bone and to evaluate the impact on microdisplacement for a specific patient case.

2. Materials and Methods

2.1. Model Design. A patient (male, 64 years of age) presenting a profoundly decayed upper right canine was selected and informed consent was obtained from the patient. Based on the method previously described by Anssari Moin et al. [1, 2] a 3D surface model of RAI was constructed. In brief the procedure was as follows: the patient was scanned with the 3D Accuitomo 170 CBCT system (Accuitomo 170, 90 kVp, 5 mA, 30.8 s, 4 × 4 cm Field of View [FoV], voxel 0.08 mm^3, Morita Inc., Kyoto, Japan) using the recommended scan protocol. Amira software (v4.1, Visage Imaging, Carlsbad, CA) was used for image analysis. A region of interest limited to the tooth and its surrounding was initially selected and a threshold segmentation algorithm based on histogram analysis of grey values was used to separate the tooth (root and crown) from surrounding bone and periodontium. Further semiautomated segmentation based on slice-by-slice analysis was implemented to enhance the segmentation by removing any residual artifacts (Figure 1). The segmented dataset was converted to 3D surface model using the marching cube algorithm and saved in the standardized triangulation language (STL) file format.

Based on the STL model five different (targeted) press-fit design RAI FE models have been constructed using 3D CAD software (Inventor™, Autodesk GmbH, Munich, Germany). For the five RAI models a Standard identical abutment, based on morphological expectation of the original tooth crown and measurements on neighboring teeth, was designed at 2 mm distance coronal from the expected bone level after implantation. Subsequently, the following (targeted) press-fit design modifications were constructed: (1) nonmodified Standard, (2) targeted press-fit Prism, (3) targeted press-fit

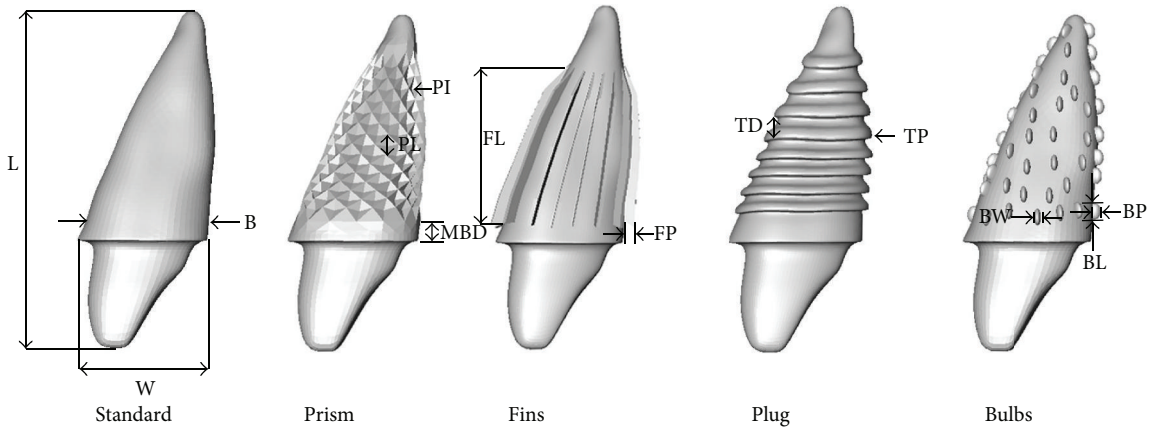

Figure 2: 3D models of the 5 designs analyzed. Dimensions and notation of geometric properties are as follows: L: total implant length 26.90 mm similar to all designs, W: maximum width of basic implant body 9.55 mm, MBD: shoulder margin to bone (B) distance 2 mm for all models, PI: Prism maximum intrusion 0.85 mm, PL: Prism maximum length 1.65 mm, FP: Fins protrusion 0.80 mm, FL: Fins length 12.90 mm, TP: thread protrusion 0.30 mm, TD: thread maximum distance 1.50 mm, BP: Bulbs protrusion 0.50 mm, BW: Bulbs width 0.55 mm, and Bl: Bulbs length 1.20 mm.

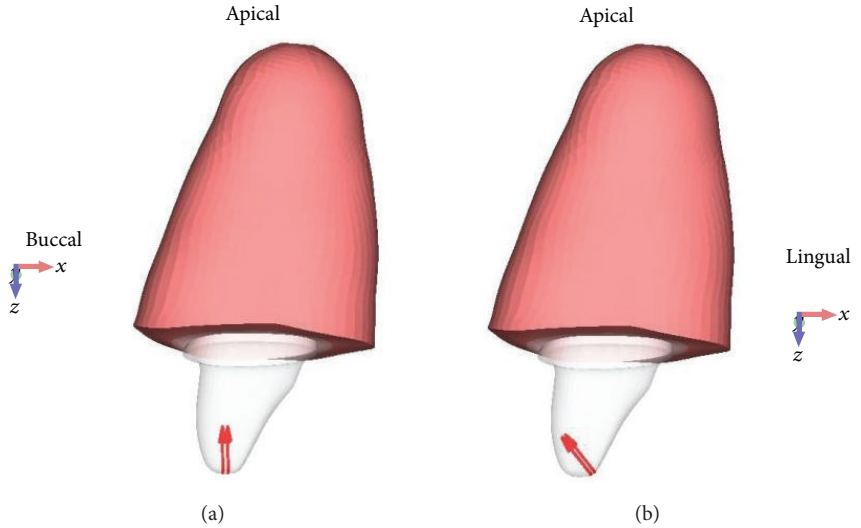

Figure 3: Overall illustration of a meshed model. The red vectors indicating the direction of the applied vertical (a) and oblique (b) forces.

Fins, (4) targeted press-fit Plug, and (5) targeted press-fit Bulbs, referred to as "Standard," "Prism," "Fins," "Plug," and "Bulbs," respectively. Figure 2 shows the five designs with description of the different geometrical characteristics.

Five bone models surrounding 3 mm congruent to the respective RAI models were built using Femap software (v. 11.0.1, Siemens PLM Software, Plano, TX, USA).

Finally, preprocessor software (Femap v. 11.0.1, Siemens PLM Software, Plano, TX, USA) was applied to mesh the models with quadratic tetrahedral solid elements (Figure 3). Mesh refinement based on convergence analysis resulted in a mesh size of 0.5 mm. Table 1 summarizes the number of elements and nodes for each model.

2.2. Material Properties, Interface, Constrains, and Loading Conditions. The following assumptions were made for the RAI FE models: composition of a titanium alloy Ti6Al4V, Young's modulus $E = 110$ GPa, and Poisson's ratio $\nu = 0.35$ with the material being homogeneous, isotropic, and linearly elastic [13, 14].

The bone models were constructed using a homogenous isotropic linearly elastic material of 1 mm inner cortical layer

Table 1: Number of elements and nodes used in the 5 FE models.

Model	Elements	Nodes
Standard	235094	336907
Prism	212965	306454
Fins	211820	309433
Plug	389742	567419
Bulbs	371570	550137

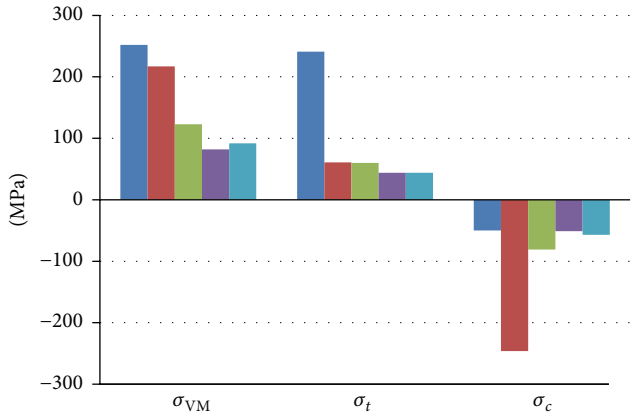

	σ_{VM}	σ_t	σ_c
Standard	252	241	−50
Prism	217	61	−246
Fins	123	60	−81
Plug	82	44	−51
Bulbs	92	44	−57

(a)

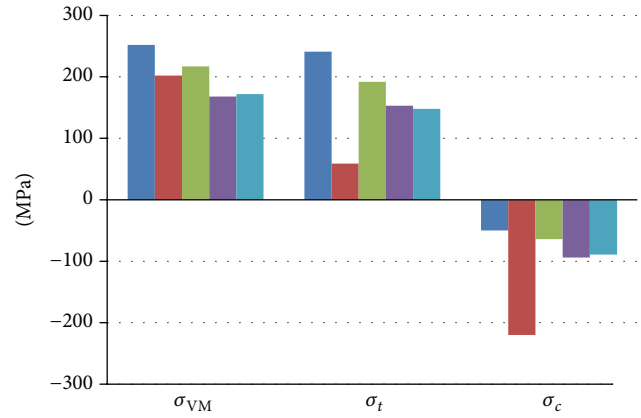

	σ_{VM}	σ_t	σ_c
Standard	252	241	−50
Prism	202	59	−220
Fins	217	192	−64
Plug	168	153	−94
Bulbs	172	148	−89

(b)

FIGURE 4: Comparison of the maximum von Mises equivalent stress (σ_{VM}) and the tensile (σ_t) and compressive (σ_c) principal stresses under vertical (a) and oblique (b) loading components in the 5 designs.

(Young's modulus $E = 12.6$ GPa, Poisson's ratio $\nu = 0.3$, and Shear modulus $G = 5.7$ GPa) and a 2 mm outer trabecular layer (Young's modulus $E = 1.1$ GPa, Poisson's ratio $\nu = 0.3$, and Shear modulus $G = 0.07$ GPa) as proposed in the reviewed literature [13, 14].

Bone-to-implant interfaces were assumed to be frictional surfaces to represent a nonosseointegrated contact situation. A Coulomb frictional method (coefficient of friction = 0.3) was adopted to define linear contact behavior [14, 15].

Two loads were applied to simulate anterior bite force: an oblique buccoapical force with a magnitude of 300 N set on 135° to the long axis of the implant and a vertical force in apical direction to the long axis of the implant with a magnitude of 150 N, as shown in Figure 3 [16, 17].

The nodes in the outer surrounding layer of trabecular bone were constrained in all directions (zero nodal displacement).

2.3. Analysis. Numerical solving (Nastran v. 8.0, Siemens PLM software, Plano, TX) and postprocessor analysis (Femap v. 11.0.1, Siemens PLM software, Plano, TX, USA) was performed on the meshed bone-implant models to evaluate stress distributions on cortical and trabecular bone and deformed contact separation (micromotion) at the peri-implant region.

Based on previous research the following measurements were recorded: the von Mises equivalent stress (σ_{VM}) at the bone peri-implant interface as a quantity of stress level for the load transfer mechanism [12, 18–21], the tensile/maximum (σ_t) and compressive/minimum (σ_c) principal stresses as a criterion to evaluate the bone overloading [19, 20], and finally deformed contact separation (micromotion in μm) as an indicator for initial implant stability [22, 23].

3. Results

Figure 4 displays the average measured stress values (in MPa) of the principal and von Mises stresses at the supporting tissues for all groups. Notably, on average the stress levels caused by oblique loading were higher when compared to vertical loading.

The Standard design RAI exhibited the highest von Mises stress and highest minimum principal stress values (highest compressive stress) under both loading conditions ($\sigma_{VM} = 252$ and $\sigma_c = -50$). The lowest von Mises stress levels were numerically observed for the Plug design under the different loading conditions (Figure 4(a), $\sigma_{VM} = 82$; Figure 4(b), $\sigma_{VM} = 168$), indicating a reduction of 67.4% and 33.3%, respectively, when compared to the Standard design. Furthermore, the highest measured tensile stress in cancellous bone was 4 MPa for the Standard design (data not shown).

Comparing behavior of von Mises stress distribution caused by vertical (Figure 5(a)) and oblique loading (Figure 5(b)), it can be observed that the cortical peri-implant bone exhibited greater stress concentration than trabecular bone. In tension stress, concentrations can be noted at the loaded side for the Standard and Prism under the oblique loading component (Figure 6).

However, under the same conditions the Plug, Fins, and Bulb designs showed tensile stress intensities on the lingual side and in the buccal area of the protrusive extensions of the design (Figure 6).

The apical peri-implant area indicated high von Mises stress concentrations in all designs (Figure 7) and tensile stress peaks under both loading conditions for the Standard, Plug, and Fin designs. Comparison of the minimum principal

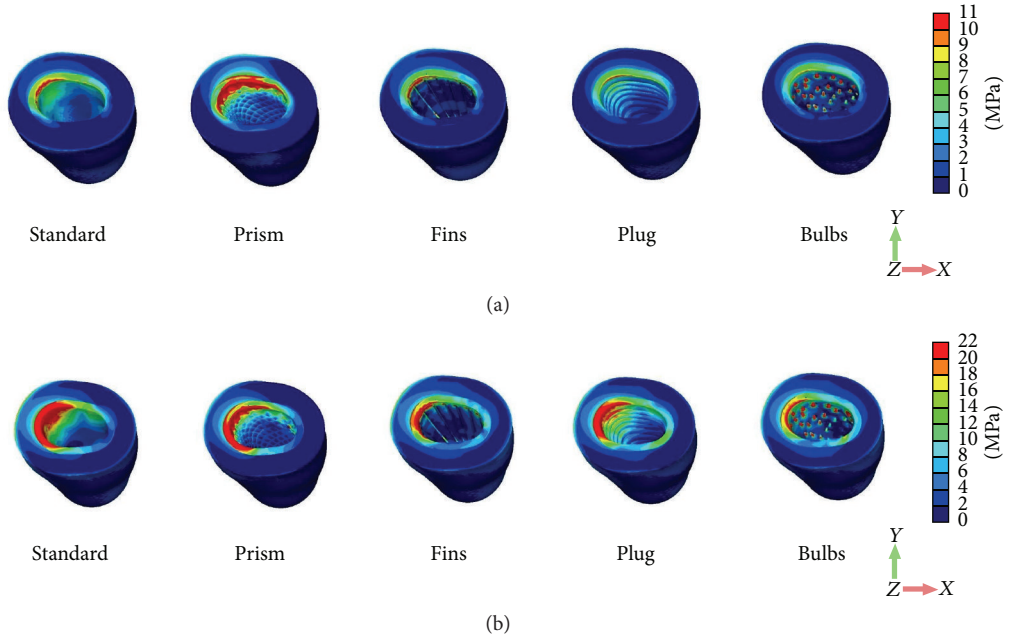

Figure 5: Distribution patterns of von Mises stress under vertical (a) and oblique (b) loading components.

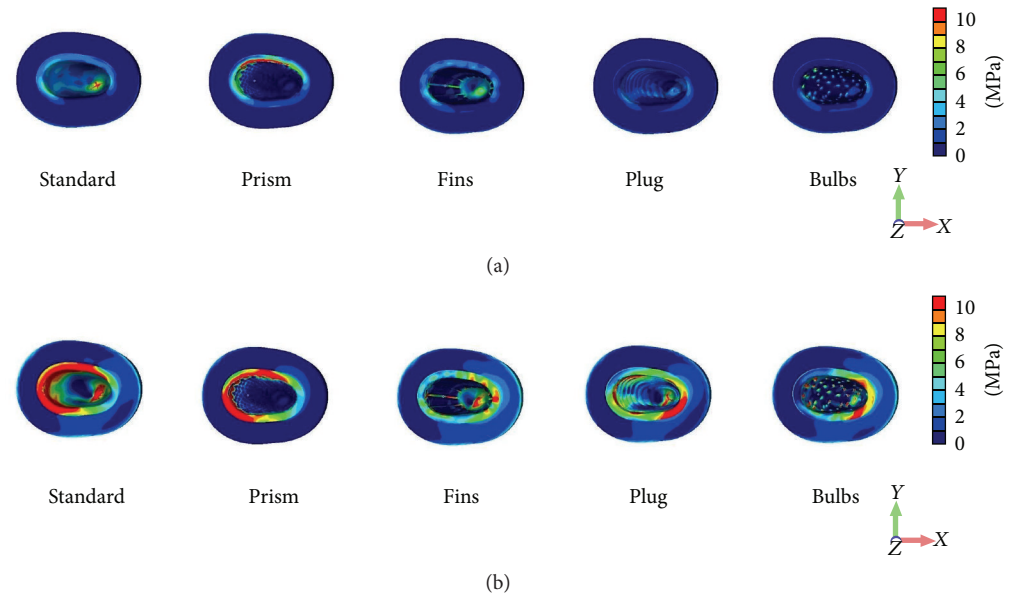

Figure 6: Distribution patterns of the tensile principal stress under vertical (a) and oblique (b) loading components.

stress illustrated in all models the highest compressive stress concentrations on the lingual side (Figure 8).

Table 2 shows the microdisplacement of the various RAI designs from the peri-implant bone with respect to the loading conditions. The highest magnitude of micromotion level was measured in the Prism design, 32.10 μm and 32.51 μm under vertical and oblique loading, respectively. Remarkably, the lowest levels of contact separation were measured in the Fins model followed by the Bulbs design under vertical and oblique forces: 5.45 μm, 6.25 μm and 6.35 μm, 6.42 μm, respectively. Microdisplacement patterns were located at

Table 2: Micromotion measures (μm) on the various models.

Model	Micromotion (μm) under vertical loading	Micromotion (μm) under oblique loading
Standard	10.90	11.72
Prism	32.10	32.51
Fins	5.45	6.25
Plug	9.88	10.69
Bulbs	6.35	6.42

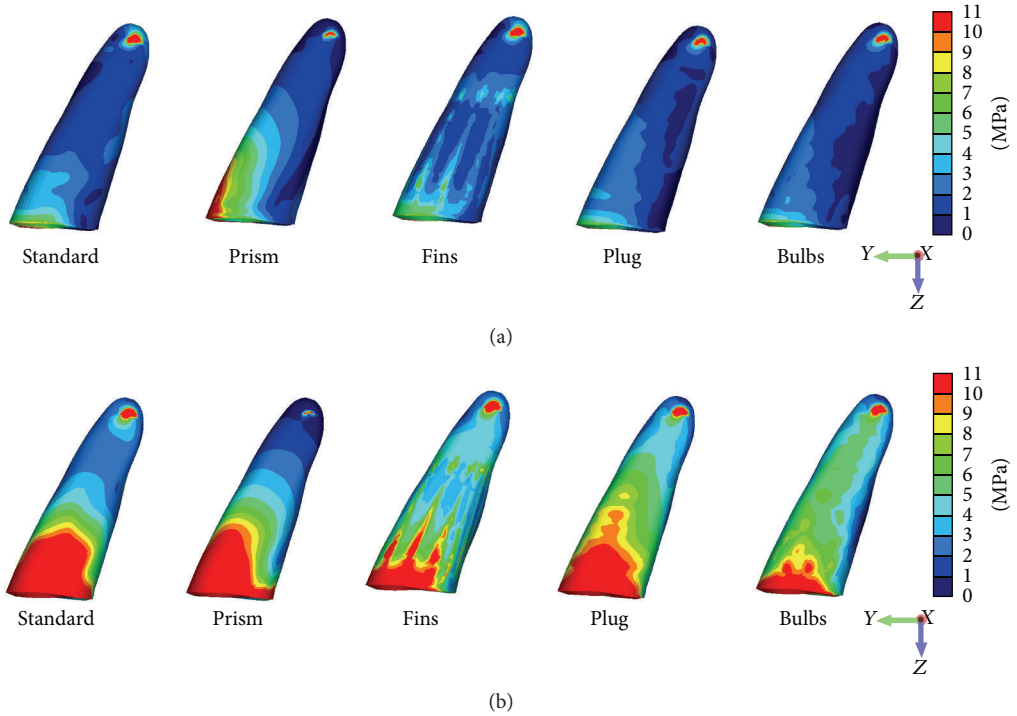

Figure 7: Distribution patterns of von Mises stress in the cortical outer layer of the surrounding bone under vertical (a) and oblique (b) loading components.

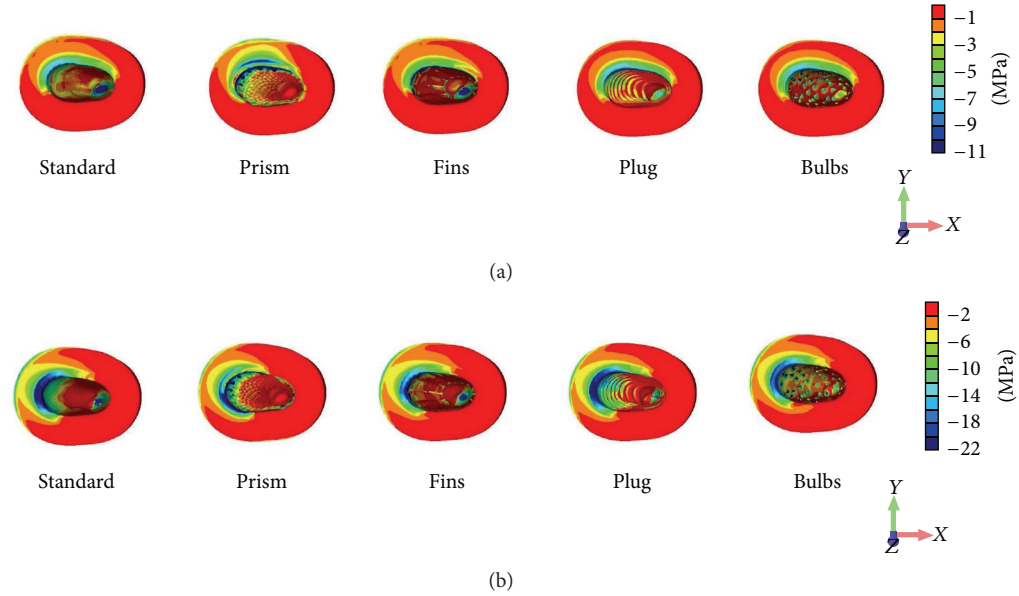

Figure 8: Distribution patterns of the compressive principal stress under vertical (a) and oblique (b) loading components.

neck area in direction of the forces and in contra lateral direction in the apical area in all designs (images not shown).

4. Discussion

In this study five different designs of RAI were analyzed for stress-based biomechanical behavior for a specific patient by means of finite element simulations. In the primary phase of endosseous healing multiple biomechanical mechanical factors play a role. The von Mises stress was used as an indicator for the load transfer mechanism, principal stresses as indicator to bone overloading and micromotion as indicator for initial stability. Numerical results from the current study suggest that adding targeted press-fit design characteristics

to the Standard RAI design will decrease the amount of maximum von Mises stress in the surrounding peri-implant bone, subsequently leading to more favorable load behavior for this patient. Previous studies have assumed maximum bone strength as biological limit to bone failure and activation of bone resorption [15, 19, 21]. Correspondingly, it has been proposed that overloading of cortical bone occurs when the maximum compressive principal stress exceeds −190 MPa and maximum tensile principal stress exceeds 130 MPa [15, 19, 21]. Likewise, trabecular bone overloading will occur when the compressive and tensile principal stresses exceed −5 MPa and 5 MPa, respectively [15, 19, 21]. According to the result of this study it has been found that solitary Prism design exceeded the maximum compressive stress criterion for cortical bone. The Standard, Fins, Plug, and Bulbs designs exceeded the tensile stress threshold in cortical bone. The threshold for trabecular bone overloading in tension was not reached. However, when observing the compressive stresses under oblique loading in trabecular bone, it can be noted that in the regions of the implant neck all implant designs exceeded the biological limit, inducing a risk to bone loss (Figure 8). The Fins and Bulbs designs showed the lowest levels of micromotion, indicating the most favorable primary stability. Nonetheless, it must be noted that the influence of micromotion on osseointegration is of scientific debate as some studies have suggested a more positive effect on the tissue differentiation and bone formation around implants under controlled micromotion up to 50 μm [24]. Additionally, in our study it has been found that the higher oblique loading component causes more stress concentrations on cortical and trabecular bone when compared to vertical loading. Therefore, oblique loading in the primary stage after implantation will have a more negative effect on bone healing and should be minimized.

In this current study multiple drawbacks and limitations should be named. The peri-implant surrounding bone was modeled and assumed as a homogeneous, isotropic, linearly elastic material. However, it is known that the biomechanical behavior of this living tissue is heterogeneous, anisotropic, and nonlinear [14, 19, 20]. Moreover, a 100% osseous contact between implant and bone was assumed. Contact relationship between implant and bone was defined as linear contact behavior by using a Coulomb frictional model. Although contact behavior should be defined in a nonlinear method, several studies are in agreement about adopting a linear frictional model since non-linear contact analysis is highly complex [14, 25]. In clinical situations the actual bone-to-implant contact directly after insertion of the RAI will be dependent on many factors, that is, accuracy of the RAI technique on multiple levels, (periapical) bone defects, and surgical handling. The quantity of in situ osseous contact after implantation of the RAI will have profound effect on primary stability and stress behavior. Furthermore, the herein applied loads were static one directional loads of amplitude of 150 N (vertical) and 300 N (oblique) whereas in clinical situations considerably variable loads can be observed depending on the location of the RAI in the oral cavity and patient characteristics. Despite the fact that simulation methods and FE modeling were beyond the scope of this investigation, the current limitations can be considered as acceptable in a numerical sense and are in agreement with multiple studies [13, 14, 16, 17, 19, 25].

Especially with the rise of custom 3D printed implants questions concerning biomechanical behavior in each specific patient surface. Ideally for future implementation of custom 3D designed and printed implants easy accessible individual patients specific FEA should be performed to get a better understanding of the biomechanical behavior of different implant designs for a specific case.

5. Conclusion

Based on the results of this study and within the limitations of the applied methodology, it has been found that adding targeted press-fit geometry to the RAI Standard design, preferably Fins or Bulbs, will have a positive effect on stress distribution and lower concentration of bone stress and will provide a better primary stability for this patient case.

Competing Interests

The authors declare that they have no competing interests.

References

[1] D. Anssari Moin, B. Hassan, P. Mercelis, and D. Wismeijer, "Designing a novel dental root analogue implant using cone beam computed tomography and CAD/CAM technology," *Clinical Oral Implants Research*, vol. 24, no. 100, pp. 25–27, 2013.

[2] D. Anssari Moin, B. Hassan, A. Parsa, P. Mercelis, and D. Wismeijer, "Accuracy of preemptively constructed, Cone Beam CT-, and CAD/CAM technology-based, individual Root Analogue Implant technique: an *in vitro* pilot investigation," *Clinical Oral Implants Research*, vol. 25, no. 5, pp. 598–602, 2014.

[3] M. Figliuzzi, F. Mangano, and C. Mangano, "A novel root analogue dental implant using CT scan and CAD/CAM: selective laser melting technology," *International Journal of Oral and Maxillofacial Surgery*, vol. 41, no. 7, pp. 858–862, 2012.

[4] W. Pirker and A. Kocher, "Immediate, non-submerged, root-analogue zirconia implant in single tooth replacement," *International Journal of Oral and Maxillofacial Surgery*, vol. 37, no. 3, pp. 293–295, 2008.

[5] W. Pirker, D. Wiedemann, A. Lidauer, and A. A. Kocher, "Immediate, single stage, truly anatomic zirconia implant in lower molar replacement: a case report with 2.5 years follow-up," *International Journal of Oral and Maxillofacial Surgery*, vol. 40, no. 2, pp. 212–216, 2011.

[6] F. G. Mangano, M. De Franco, A. Caprioglio, A. MacChi, A. Piattelli, and C. Mangano, "Immediate, non-submerged, root-analogue direct laser metal sintering (DLMS) implants: a 1-year prospective study on 15 patients," *Lasers in Medical Science*, vol. 29, no. 4, pp. 1321–1328, 2014.

[7] J. Blanco, E. Alvarez, F. Muñoz, A. Liñares, and A. Cantalapiedra, "Influence on early osseointegration of dental implants installed with two different drilling protocols: a histomorphometric study in rabbit," *Clinical Oral Implants Research*, vol. 22, no. 1, pp. 92–99, 2011.

[8] J. Steigenga, K. Al-Shammari, C. Misch, F. H. Nociti Jr., and H.-L. Wang, "Effects of implant thread geometry on percentage of

osseointegration and resistance to reverse torque in the tibia of rabbits," *Journal of Periodontology*, vol. 75, no. 9, pp. 1233–1241, 2004.

[9] J. Y. K. Kan, K. Rungcharassaeng, J. Kim, J. L. Lozada, and C. J. Goodacre, "Factors affecting the survival of implants placed in grafted maxillary sinuses: a clinical report," *The Journal of Prosthetic Dentistry*, vol. 87, no. 5, pp. 485–489, 2002.

[10] M. Akkocaoglu, S. Uysal, I. Tekdemir, K. Akca, and M. C. Cehreli, "Implant design and intraosseous stability of immediately placed implants: a human cadaver study," *Clinical Oral Implants Research*, vol. 16, no. 2, pp. 202–209, 2005.

[11] H. Abuhussein, G. Pagni, A. Rebaudi, and H.-L. Wang, "The effect of thread pattern upon implant osseointegration," *Clinical Oral Implants Research*, vol. 21, no. 2, pp. 129–136, 2010.

[12] R. C. Van Staden, H. Guan, and Y. C. Loo, "Application of the finite element method in dental implant research," *Computer Methods in Biomechanics and Biomedical Engineering*, vol. 9, no. 4, pp. 257–270, 2006.

[13] A. M. O'Mahony, J. L. Williams, and P. Spencer, "Anisotropic elasticity of cortical and cancellous bone in the posterior mandible increases peri-implant stress and strain under oblique loading," *Clinical Oral Implants Research*, vol. 12, no. 6, pp. 648–657, 2001.

[14] H.-L. Huang, J.-T. Hsu, L.-J. Fuh, M.-G. Tu, C.-C. Ko, and Y.-W. Shen, "Bone stress and interfacial sliding analysis of implant designs on an immediately loaded maxillary implant: a non-linear finite element study," *Journal of Dentistry*, vol. 36, no. 6, pp. 409–417, 2008.

[15] D. Lin, Q. Li, W. Li, and M. Swain, "Dental implant induced bone remodeling and associated algorithms," *Journal of the Mechanical Behavior of Biomedical Materials*, vol. 2, no. 5, pp. 410–432, 2009.

[16] C. M. Stanford and R. A. Brand, "Toward an understanding of implant occlusion and strain adaptive bone modeling and remodeling," *The Journal of Prosthetic Dentistry*, vol. 81, no. 5, pp. 553–561, 1999.

[17] Y. Akagawa, Y. Sato, E. R. Teixeira, N. Shindoi, and M. Wadamoto, "A mimic osseointegrated implant model for three-dimensional finite element analysis," *Journal of Oral Rehabilitation*, vol. 30, no. 1, pp. 41–45, 2003.

[18] J.-P. A. Geng, K. B. C. Tan, and G.-R. Liu, "Application of finite element analysis in implant dentistry: a review of the literature," *The Journal of Prosthetic Dentistry*, vol. 85, no. 6, pp. 585–598, 2001.

[19] A. N. Natali, R. T. Hart, P. G. Pavan, and I. Knets, Eds., *Mechanics of Bone Tissue*, Taylor & Francis, London, UK, 2003.

[20] Y. H. An and R. A. Draughn, *Mechanical Testing of Bone and the Bone-Implant Interface*, vol. 1, Taylor & Francis, 2010.

[21] A. N. Natali and P. G. Pavan, "A comparative analysis based on different strength criteria for evaluation of risk factor for dental implants," *Computer Methods in Biomechanics and Biomedical Engineering*, vol. 5, no. 2, pp. 127–133, 2002.

[22] J. B. Brunski, "Avoid pitfalls of overloading and micromotion of intraosseous implants," *Dental Implantology Update*, vol. 4, no. 10, pp. 77–81, 1993.

[23] J. B. Brunski, D. A. Puleo, and A. Nanci, "Biomaterials and biomechanics of oral and maxillofacial implants: current status and future developments," *International Journal of Oral & Maxillofacial Implants*, vol. 15, no. 1, pp. 15–46, 2000.

[24] K. Vandamme, I. Naert, L. Geris, J. V. Sloten, R. Puers, and J. Duyck, "Histodynamics of bone tissue formation around immediately loaded cylindrical implants in the rabbit," *Clinical Oral Implants Research*, vol. 18, no. 4, pp. 471–480, 2007.

[25] C.-L. Lin, Y.-H. Lin, and S.-H. Chang, "Multi-factorial analysis of variables influencing the bone loss of an implant placed in the maxilla: prediction using FEA and SED bone remodeling algorithm," *Journal of Biomechanics*, vol. 43, no. 4, pp. 644–651, 2010.

Hindawi Publishing Corporation
International Journal of Dentistry
Volume 2016, Article ID 4348325, 8 pages
http://dx.doi.org/10.1155/2016/4348325

Clinical Study

Applicative Characteristics of a New Zirconia Bracket with Multiple Slots

Koutaro Maki, Katsuyoshi Futaki, Satoru Tanabe, Mariko Takahashi, Yuta Ichikawa, and Tetsutaro Yamaguchi

Department of Orthodontics, School of Dentistry, Showa University, 2-1-1 Kitasenzoku, Ohta-Ku, Tokyo 145-8515, Japan

Correspondence should be addressed to Tetsutaro Yamaguchi; tyamaguchi@dent.showa-u.ac.jp

Received 26 February 2016; Accepted 5 April 2016

Academic Editor: Francesco Mangano

We have developed a new orthodontic bracket with three slots with lubricative properties on the working surfaces and proposed a new orthodontic treatment system employing 0.012–0.014-inch Ni-Ti arch wires. We recruited 54 patients, of which 27 received treatment with the new zirconia bracket with multiple slots system (M group), and the others received treatment with standard edgewise appliances (control group [C group]). We compared the (1) tooth movement rate at the early stage of leveling; (2) changes in the dental arch morphology before and after leveling; and (3) pain caused by orthodontic treatment. Student's t-test was used in all assessments. The tooth movement rate in the maxillomandibular dentition was higher in the M group. The basal arch width, anterior length, and the intercanine width in the maxillary dentition were not significantly different in the two groups; however, the intercanine width in the mandibular dentition was higher in the C group. In assessments of treatment-related pain, the visual analogue pain score was 56.0 mm and 22.6 mm in the C and M groups, respectively. A new zirconia bracket with multiple slots system provided better outcomes with respect to tooth movement rate, treatment period, and postoperative pain, thus indicating its effectiveness over conventional orthodontic systems.

1. Introduction

Orthodontic treatment involves the use of wires to apply loads for tooth movement. It has been reported that when the orthodontic force is weak and long-lasting, teeth move quickly with less pain [1]. In this study, we developed a new orthodontic bracket and proposed a new orthodontic treatment system, in which 0.012–0.014-inch Ni-Ti arch wires are used.

We produced an orthodontic bracket with three slots, using a zirconia firing working method that can add lubricative properties to the internal surface of the wire slots and external surface of the brackets. A new zirconia bracket with multiple slots was developed to shorten orthodontic treatment time, relieve pain and discomfort, reduce the restricted function of muscles around the oral cavity, and promote cleansability and esthetics.

The purpose of the present study was to compare this new orthodontic treatment system with conventional treatment systems to clarify differences in the tooth movement rate, clarify changes in the morphology of the dental arch at the early stage of leveling, and assess the degree of pain caused by orthodontic treatment.

2. Methods

2.1. Bracket Design (Figure 1)

2.1.1. Profile. The spherical structure of the bracket surface and the slot torque is shown in Figure 1(a). The bracket surface and the internal surface of the slots are smooth due to the zirconia firing working method (Figure 1(b)). Torque is symmetrically applied to both ends of the slot. Therefore, it is unnecessary to change brackets according to tooth type.

2.1.2. Slots (Figure 1(c)). The size of the three square slots is equal.

2.1.3. Base (Figure 1(d)). Strong bond strength can be achieved by a mechanical interlocking force.

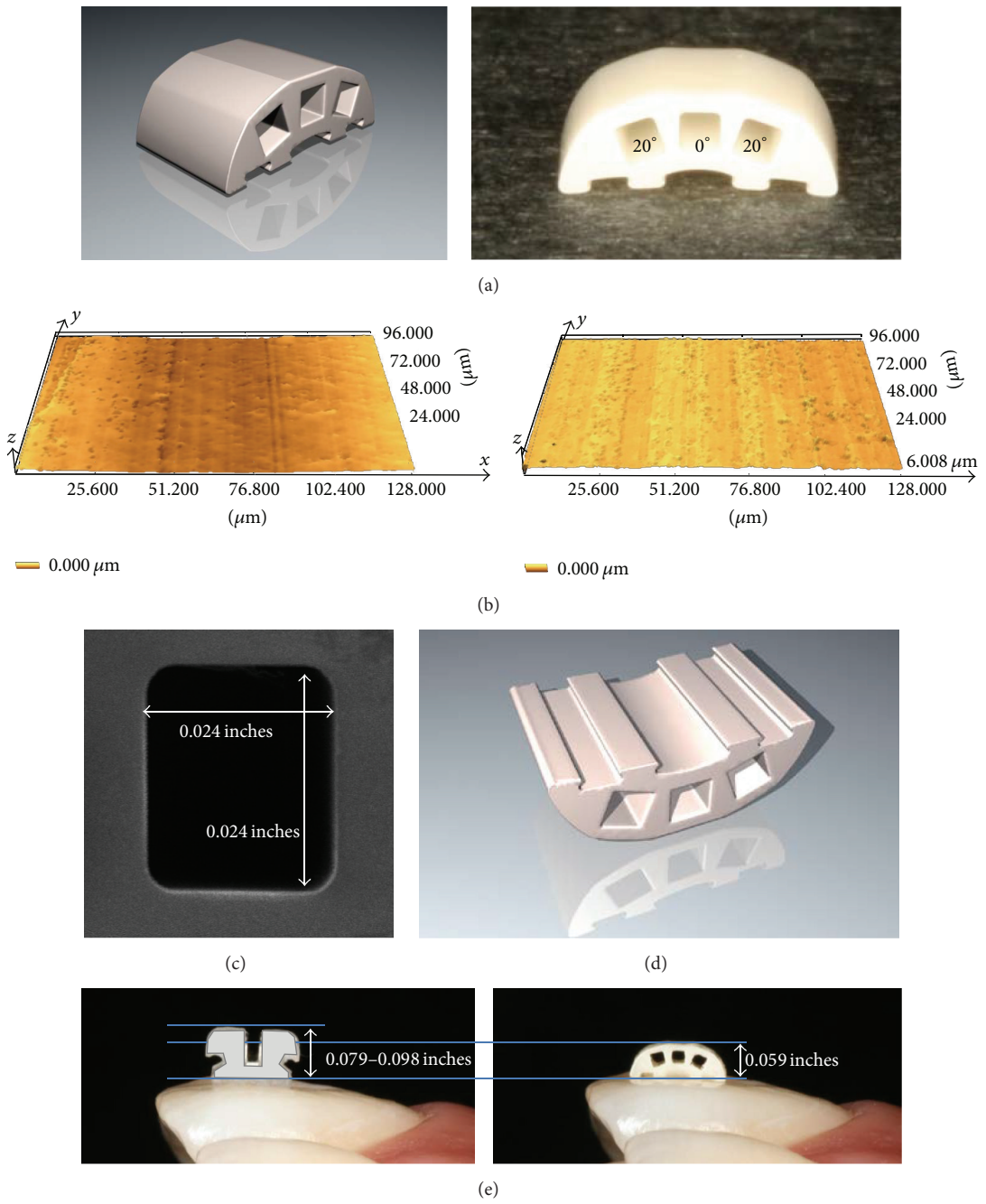

Figure 1: (a) Spherical structure of the bracket surface and slot torque; (b) bracket surface (left) and internal surface (right) of slots (laser microscope, magnification x100) (GC ORTHOLY CORPORATION, Tokyo, Japan); (c) slots (scanning electron microscope, magnification x20); (d) base; and (e) size. Conventional brackets for the anterior tooth area (left) and a new zirconia bracket with multiple slots (right).

2.1.4. Size (Figure 1(e)). Because of the excellent strength of zirconia, a small size and low profile could be used. Furthermore, we succeeded in adding three slots.

3. Materials and Methods

3.1. Subjects. The subjects were 54 patients (15 males and 39 females) who visited the Department of Orthodontics at the dental hospital attached to Showa University, from whom consent for this research was obtained. This study was performed after receiving approval from the ethics committee at Showa University Dental School (approval number: 2007-28).

Twenty-seven patients (7 males and 20 females aged 11–49 years, mean age: 21 years and 0 months), who received treatment using the new orthodontic treatment system, were classified into a new zirconia bracket with multiple slots group (M group); and 27 patients (8 males and 19 females

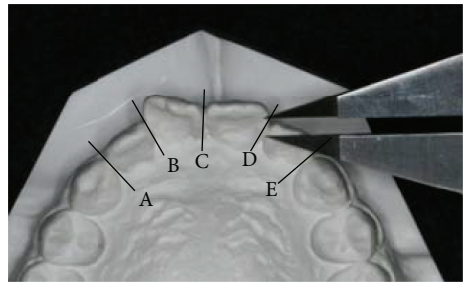

Figure 2: Irregularity index (sum of contact point displacements) (A + B + C + D + E).

aged 11–39 years, mean age: 21 years and 8 months), who received treatment using standard edge-wise appliances, were classified into a control group (C group). Regarding the M and C groups, the following three items were compared.

3.2. Measurements with Plaster Casts. For plaster casts, hard dental plaster for orthodontic treatment (ORTHO MAX, SHIMOMURA GYPSUM Co., Ltd., Saitama, Japan) was used. Measurement was performed using calipers with divisions of 1/20 mm. The mean of three measurements was calculated. The same clinician performed each measurement.

3.2.1. Tooth Movement Rate at the Early Stage of Leveling. The irregularity index before and after leveling was calculated from plaster casts (Figure 2). The completion of leveling was judged using intraoral photographs and plaster casts. A linear functional numerical expressing tooth movement was achieved from the irregularity index before and after leveling and the treatment period required until leveling completion was determined. The gradient of the formula indicates the rate of tooth movement, and when the gradient is large, the rate of tooth movement is high. Regarding the irregularity index after leveling completion, a permissible range was set at a moderate irregularity of 4–6, in reference to the criteria proposed by Little [2].

3.2.2. Changes in the Dental Arch Morphology before and after Leveling. We measured the intercanine width (Figure 3(a)), basal arch width (Figure 3(b)), and anterior length (Figure 3(c)) before and after leveling, and a comparison of the extent of change between M and C groups was performed.

3.2.3. Pain due to Orthodontic Treatment. Pain was evaluated based on individual interviews and the visual analogue scale method [3]. A line of 100 mm was drawn on an investigation form, and patients marked the line to show the level of pain they felt during the period of treatment, setting the left end as no pain at all and the right end as unbearable pain. The distance between the left end and the point indicating the level of pain was measured, and a comparison between M and C groups was performed.

3.3. Statistical Analysis. Student's t-test was used in all cases.

Table 1: Mean treatment period until leveling completion.

		Days		
Group C	Upper	127.6	(n = 27)	*
Group M	Upper	79.7	(n = 24)	
Group C	Lower	139.4	(n = 25)	*
Group M	Lower	74.2	(n = 26)	

*$P < 0.05$.

4. Results and Discussion

4.1. Tooth Movement Rate at the Early Stage of Leveling. The linear functional formula expressing tooth movement is $Y = -0.05X + 8.87$ in the C group and $Y = -0.12X + 13.36$ in the M group in the maxillary dentition; and $Y = -0.04X + 7.31$ in the C group and $Y = -0.09X + 9.47$ in the M group in the mandibular dentition (Figure 4). The gradient of the formula indicating the rate of tooth movement was higher in the M group than the C group in the maxillomandibular dentitions.

Furthermore, the mean treatment period was 127.6 days in the C group and 79.7 days in the M group in the maxillary dentition and 139.4 days in the C group and 74.2 days in the M group in the mandibular dentition (Table 1). The tooth movement rate increased in the M group in the maxillomandibular dentitions, in comparison with the C group.

4.2. Changes in the Dental Arch Morphology before and after Leveling (Figure 5). Regarding the basal arch width and anterior length, no significant differences were noted between the M and C groups. Furthermore, the intercanine width showed no significant difference between the M and C groups in the maxillary dentition; however, in the mandibular dentition, it increased in the C group in comparison with the M group, showing a significant difference (Figure 6).

4.3. Pain due to Orthodontic Treatment (Figure 7). The distance indicating the level of pain was 56.0 mm in the C group and 22.6 mm in the M group. Furthermore, 36.8% of patients in the M group answered that no pain was present, and five of 19 patients reported definite pain. Furthermore, two subjects who had experienced the insertion of conventional orthodontic appliances reported the marked alleviation of discomfort.

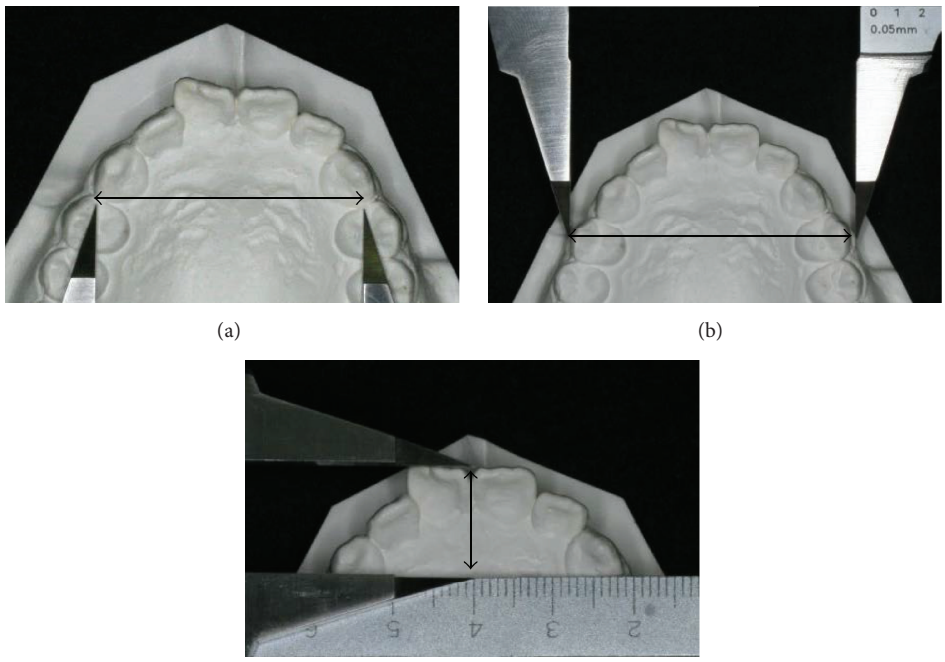

Figure 3: (a) Intercanine width; (b) basal arch width; and (c) anterior length.

The fabrication of veneers, full and partial coverage crowns, fixed partial dentures, posts and/or cores, primary double crowns, implants, implant abutments, and various other dental auxiliary components such as cutting burs, surgical drills, extracoronal attachments, and orthodontic brackets are all employed in the clinical application of zirconia [4]. The biotechnical characteristics of zirconia result in high-quality materials with excellent biocompatibility and aesthetic appearance [5]. Because patients wear orthodontic brackets for months to years, smaller brackets that look similar to natural teeth are preferred for their aesthetic, subtle appearance, which helps patients feel more confident and self-assured while undergoing treatment. Nonmetal brackets offer the attractive combination of aesthetics and performance [6]. Among dental ceramics, zirconia features superior aesthetics and strength [7] and has been applied in the fabrication of orthodontic brackets [8]. We sought to develop brackets that were as small and thin as possible, by using three slots to increase variation in mechanics. In these brackets, the maximum wire size is 0.016–0.016 in for a continuous arch wire and 0.016–0.022 in for a sectional arch wire. Mesiodistal root uprighting and labiolingual torque were achieved with Invisalign® or aligner systems [9].

To reposition teeth that have deviated from their normal position, it is considered that the new orthodontic treatment system can achieve a faster tooth movement rate than conventional methods (Figure 8). It is believed that this is because (1) a new zirconia bracket with multiple slots is nonligated, (2) the internal surface of the slots is lubricative because the bracket is produced by the zirconia firing working method, and (3) friction occurring in the wires is minimized by using 0.012–0.014-inch Ni-Ti arch wires. Furthermore, the involvement of load force applied by soft tissue in the dentition is estimated. Although it was clarified by Frederick [10] that the muscles surrounding the oral cavity and tongue have an important relationship with the position of the teeth, because the bracket surface structure of a new zirconia bracket with multiple slots is spherical, very small, and thin, it is unlikely that it hinders their function. Furthermore, Blake and Bibby [11] reported that the expansion of the mandibular intercanine width increases the risk of relapse. From the results of the present study, it is considered that because new zirconia bracket with multiple slots applies weaker forces than conventional methods, leveling is possible without expanding the mandibular intercanine width, and a more stable occlusal condition can be achieved. On the other hand, in cases requiring mesial movement of the molars and expansion, improvements in the movement period and efficiency are necessary.

Furthermore, in comparison with conventional orthodontic treatment methods, patient-reported pain did not readily occur as a result of using new zirconia bracket with multiple slots. It is considered that this was not only because the orthodontic force was low owing to the use of 0.012–0.014-inch Ni-Ti arch wires, but also because the friction occurring in the wire was minimal with new zirconia bracket with multiple slots.

In the future, it will be necessary to reconfirm the optimal load to move teeth in orthodontic treatment. This is important to prevent tooth root resorption and perform more effective tooth movement.

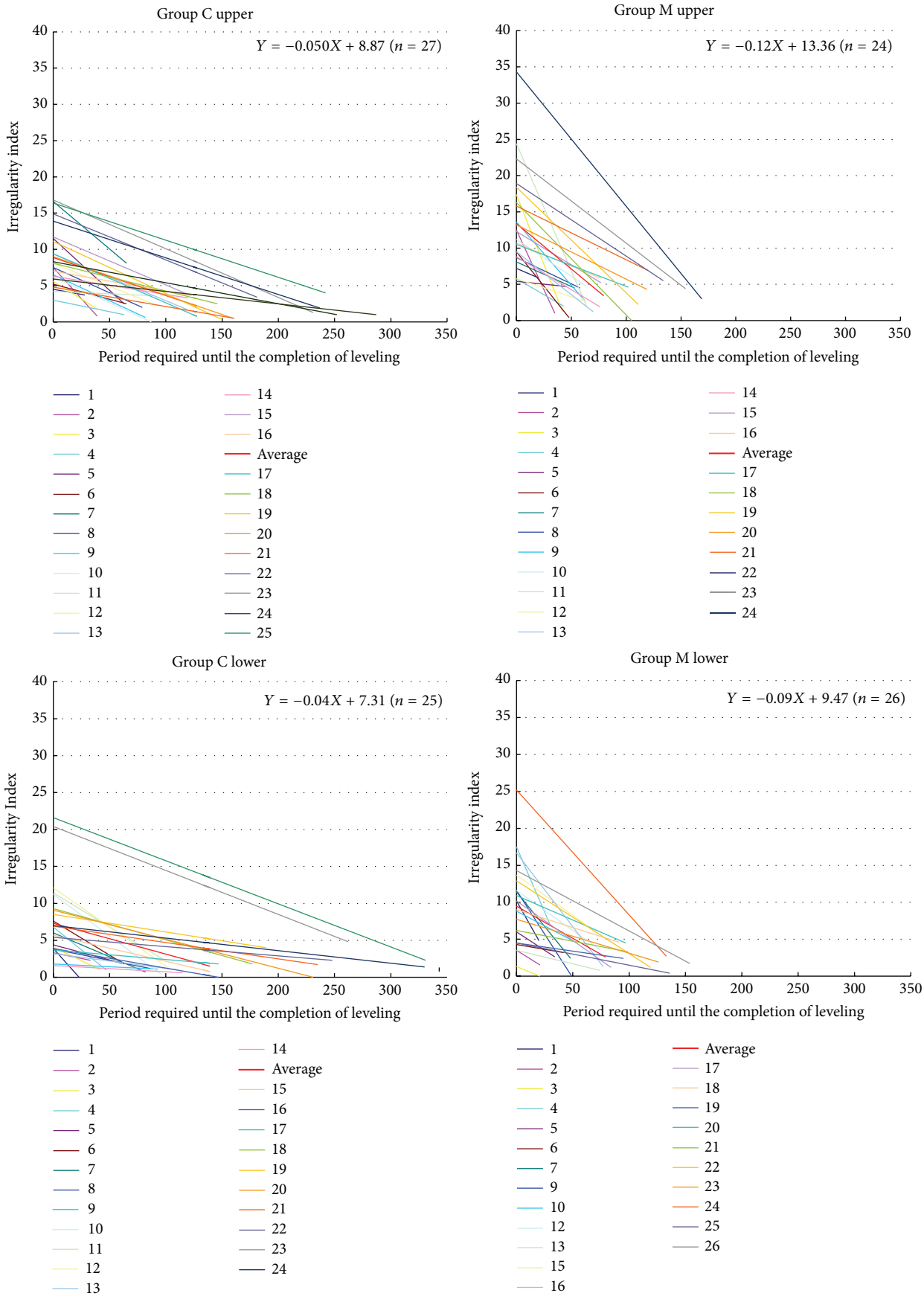

Figure 4: Linear functional formula expressing tooth movement.

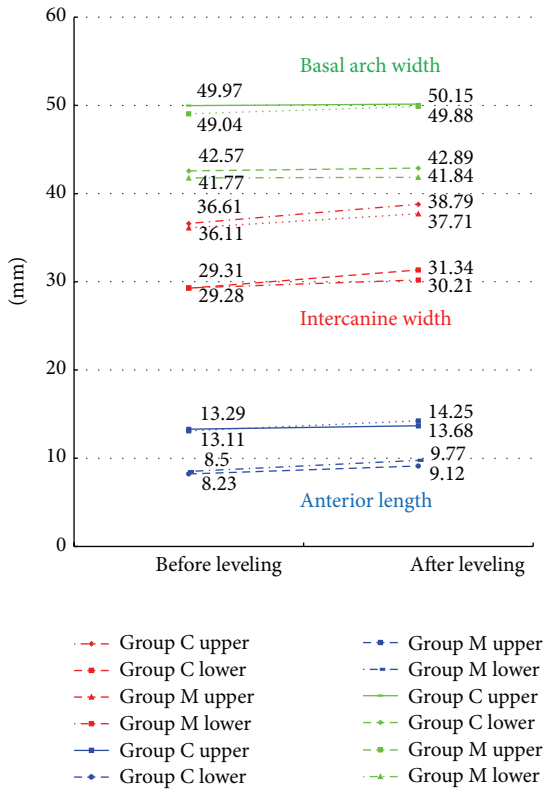

Figure 5: Changes in the dental arch morphology before and after leveling.

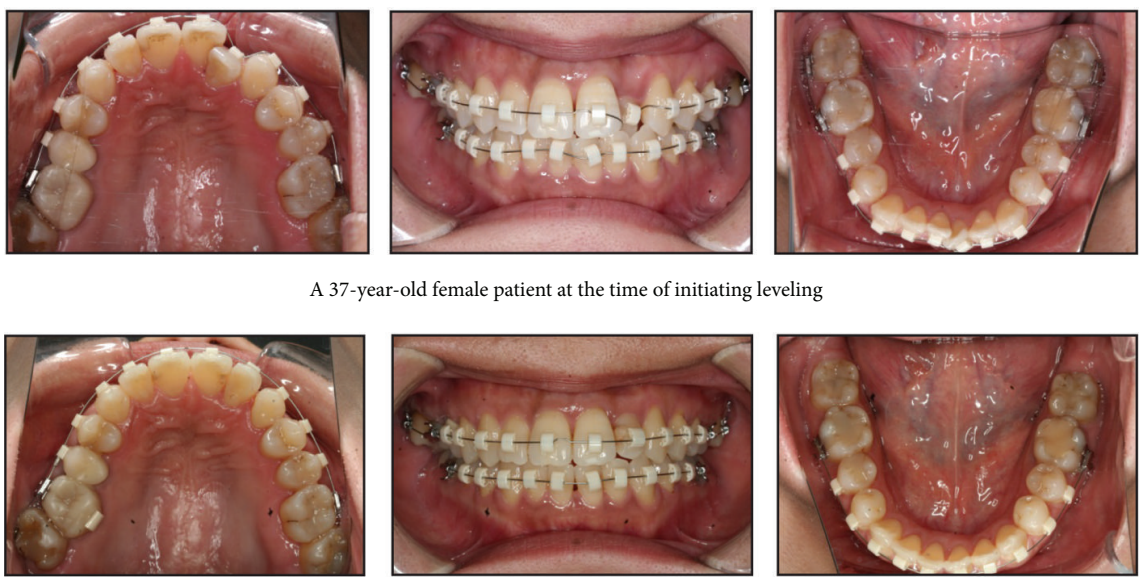

A 37-year-old female patient at the time of initiating leveling

After 4 months, at the time of leveling completion

Figure 6: Intraoral photographs before and after leveling completion in the M group.

5. Conclusion

The purpose of the present study was to clarify the properties of new zirconia bracket with multiple slots regarding the tooth movement rate, changes in the morphology of the dental arch at the early stage of leveling, and pain caused by orthodontic treatment, by comparing the new orthodontic treatment system with a conventional treatment system. The proposed new orthodontic treatment system showed a higher tooth movement rate in the early stage of leveling, and the mean treatment period until the completion of leveling was significantly shorter.

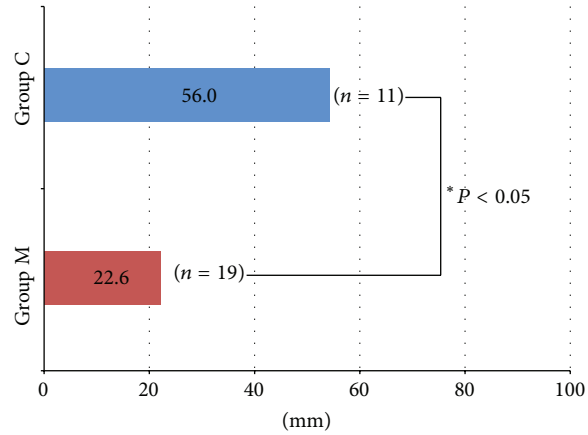

Figure 7: Pain caused by orthodontic treatment (visual analogue scale method).

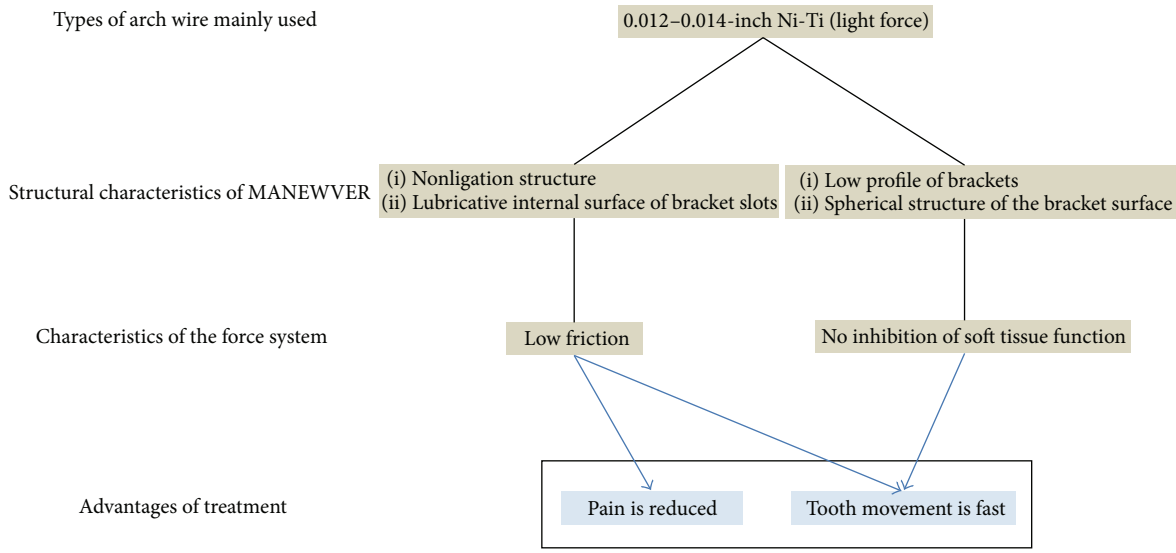

Figure 8: Properties of the new orthodontic treatment system.

Competing Interests

The authors declare that they have no competing interests.

References

[1] S. Luppanapornlarp, T. S. Kajii, R. Surarit, and J. Iida, "Interleukin-1β levels, pain intensity, and tooth movement using two different magnitudes of continuous orthodontic force," *European Journal of Orthodontics*, vol. 32, no. 5, pp. 596–601, 2010.

[2] R. M. Little, "The Irregularity index: a quantitative score of mandibular anterior alignment," *American Journal of Orthodontics*, vol. 68, no. 5, pp. 554–563, 1975.

[3] R. Melzack, Z. Rosberger, M. L. Hollingsworth, and M. Thirlwell, "New approaches to measuring nausea," *Canadian Medical Association Journal*, vol. 133, no. 8, pp. 755–758, 1985.

[4] S. O. Koutayas, T. Vagkopoulou, S. Pelekanos, P. Koidis, and J. R. Strub, "Zirconia in dentistry: part 2. Evidence-based clinical breakthrough," *The European Journal of Esthetic Dentistry*, vol. 4, no. 4, pp. 348–380, 2009.

[5] A. Vichi, C. Louca, G. Corciolani, and M. Ferrari, "Color related to ceramic and zirconia restorations: a review," *Dental Materials*, vol. 27, no. 1, pp. 97–108, 2011.

[6] H. L. Filho, L. H. Maia, M. V. Araújo, C. N. Eliast, and A. C. O. Ruellas, "Colour stability of aesthetic brackets: ceramic and plastic," *Australian Orthodontic Journal*, vol. 29, no. 1, pp. 13–20, 2013.

[7] F. Zarone, S. Russo, and R. Sorrentino, "From porcelain-fused-to-metal to zirconia: clinical and experimental considerations," *Dental Materials*, vol. 27, no. 1, pp. 83–96, 2011.

[8] O. Keith, R. P. Kusy, and J. Q. Whitley, "Zirconia brackets: an evaluation of morphology and coefficients of friction," *American Journal of Orthodontics and Dentofacial Orthopedics*, vol. 106, no. 6, pp. 605–614, 1994.

[9] M. Simon, L. Keilig, J. Schwarze, B. A. Jung, and C. Bourauel, "Treatment outcome and efficacy of an aligner technique—regarding incisor torque, premolar derotation and molar distalization," *BMC Oral Health*, vol. 14, article 68, 2014.

[10] S. Frederick, "The perioral muscular phenomenon: part II," *Australian Orthodontic Journal*, vol. 12, no. 2, pp. 83–89, 1991.

[11] M. Blake and K. Bibby, "Retention and stability: a review of the literature," *American Journal of Orthodontics and Dentofacial Orthopedics*, vol. 114, no. 3, pp. 299–306, 1998.

Hindawi Publishing Corporation
International Journal of Dentistry
Volume 2016, Article ID 3264545, 7 pages
http://dx.doi.org/10.1155/2016/3264545

Research Article

Detection of Carious Lesions and Restorations Using Particle Swarm Optimization Algorithm

Mohammad Naebi,[1] Eshaghali Saberi,[2] Sirous Risbaf Fakour,[3] Ahmad Naebi,[4] Somayeh Hosseini Tabatabaei,[5] Somayeh Ansari Moghadam,[6] Elham Bozorgmehr,[7] Nasim Davtalab Behnam,[8] and Hamidreza Azimi[3]

[1]*School of Dentistry, Zahedan University of Medical Science, Zahedan, Iran*
[2]*Oral and Dental Disease Research Center, Department of Endodontics, School of Dentistry, Zahedan University of Medical Science, Zahedan, Iran*
[3]*Oral and Dental Disease Research Center, Department of Oral and Maxillofacial Surgery, Zahedan University of Medical Science, Zahedan, Iran*
[4]*State Key Laboratory for Manufacturing Systems Engineering, Systems Institute, Xi'an Jiaotong University, Xi'an, China*
[5]*Department of Operative Dentistry, Oral and Dental Disease Research Center, Zahedan University of Medical Science, Zahedan, Iran*
[6]*Department of Periodontology, Oral and Dental Disease Research Center, Zahedan University of Medical Science, Zahedan, Iran*
[7]*Department of Public Health, Oral and Dental Disease Research Center, Zahedan University of Medical Science, Zahedan, Iran*
[8]*School of Dentistry, Tabriz University of Medical Science, Tabriz, Iran*

Correspondence should be addressed to Mohammad Naebi; mohammadnayebi2000@gmail.com

Received 10 January 2016; Revised 6 March 2016; Accepted 22 March 2016

Academic Editor: Francesco Mangano

Background/Purpose. In terms of the detection of tooth diagnosis, no intelligent detection has been done up till now. Dentists just look at images and then they can detect the diagnosis position in tooth based on their experiences. Using new technologies, scientists will implement detection and repair of tooth diagnosis intelligently. In this paper, we have introduced one intelligent method for detection using particle swarm optimization (PSO) and our mathematical formulation. This method was applied to 2D special images. Using developing of our method, we can detect tooth diagnosis for all of 2D and 3D images. *Materials and Methods*. In recent years, it is possible to implement intelligent processing of images by high efficiency optimization algorithms in many applications especially for detection of dental caries and restoration without human intervention. In the present work, we explain PSO algorithm with our detection formula for detection of dental caries and restoration. Also image processing helped us to implement our method. And to do so, pictures taken by digital radiography systems of tooth are used. *Results and Conclusion*. We implement some mathematics formula for fitness of PSO. Our results show that this method can detect dental caries and restoration in digital radiography pictures with the good convergence. In fact, the error rate of this method was 8%, so that it can be implemented for detection of dental caries and restoration. Using some parameters, it is possible that the error rate can be even reduced below 0.5%.

1. Introduction

Caries is a multifactorial disease that is induced by the interaction among three factors, tooth, microflora, and diet. Radiography is a useful technique for detecting carious lesions as the caries process causes demineralization of enamel and dentin. Lesion is observed in a diagnostic image as a radiolucent (darker) zone since the demineralized area of the tooth does not absorb as many X-ray photons as the unaffected portion. Radiography is a valuable supplement to a thorough clinical examination of the teeth for detecting caries lesions.

Various morphologic phenomena, such as pits and fissures, cervical burnout, and Mach band effect, and dental

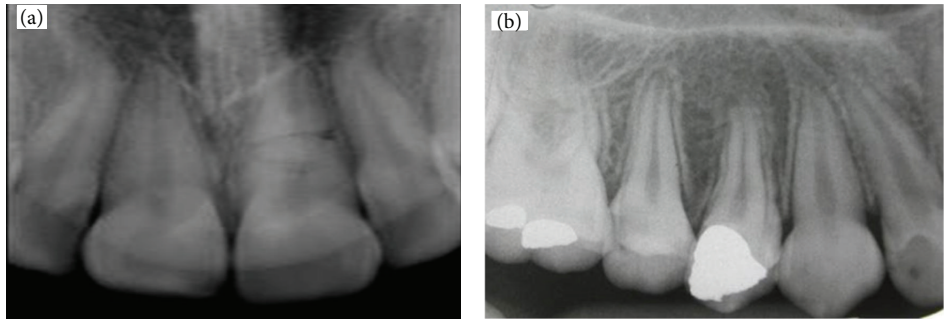

Figure 1: (a) Teeth with no decay and restoration. (b) Three teeth with decay and restoration.

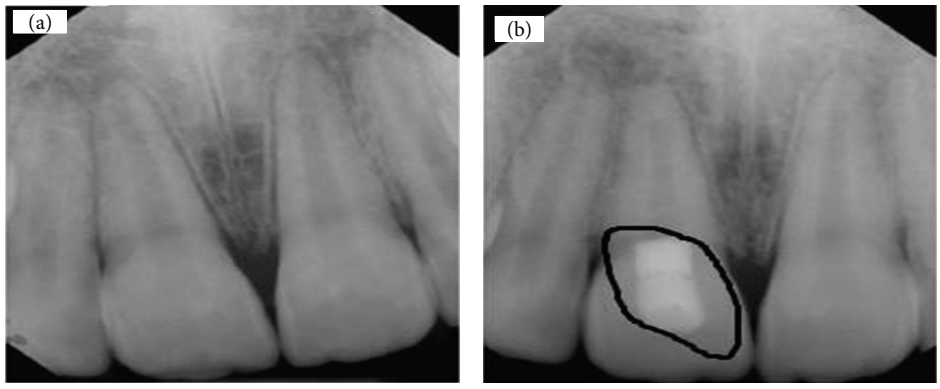

Figure 2: Detection of dental caries and restoration by dentist: (a) safe, (b) restoration.

anomalies, such as hypoplastic pits and concavities produced by wear, can mimic the appearance of a carious lesion [1–3].

Image processing has evolved since 1964. It has led to creation of digital multispectral ground surface images used in agricultural and forestry sectors. From mid-1970s to 1980s, the medicine has been evolved by invention of Computerized Axial Tomography scanners (CAT scan) and magnetic resonance imagery (MRI). Printing industry is another potential user of this technology. In addition, since entering to entrainment world at the end of 1980s, digital image processing has been common in this industry. By appearance of machine vision, the world of industry has been constantly evolving by robots. Purity in production of food vessels and their mass production has led to spending more time and cost on this technology. The high detection rate of decay and restoration of tooth by dentist require the mechanized systems with high quality and detection rate. Through such mechanized systems, it is possible to control and communicate with data in optimal databank and compare them with valid values in real-time control units to provide the optimum and fastest machine vision systems [4].

Sometimes we need to complete the detection and restoration of teeth for a moment. Using the OCR frequent images of a tooth, it is possible to detect its decay and restoration in a fraction of a second. This is related to time of a qualitative problem, and the new system stops and detection process resumes once that problem is resolved [5]. The OCR pictures show the location of tooth in mouth. A dentist starts repairing the dental caries and restoration once he/she detects its location in mouth (Figure 1) [6].

In the second section, we review the previous research conducted in detection of dental caries and restoration and image processing. In addition, we introduce works related to detection with PSO or other algorithms in other fields of study. In the third section, we explain briefly our proposed method for detection of dental caries and restoration. In the fourth section, we present the results obtained after running our proposed model. Then, in the discussion section, we describe results of experiment and limitation of PSO with our formulation for 2D and 3D. Last section is related to conclusion.

2. Materials and Methods

Based on investigating previous works, no study was found on intelligent detection of dental caries and restoration using image processing and algorithms [5, 7]. No researcher has researched in this area.

All of the detections were done by dentist, as a dentist looks at picture and detects dental caries and restoration on basis of his own experiences. Figure 2(a) illustrates detection of one spot of dental decay and restoration (Figure 2) [6].

In another study, image processing was applied for detecting liquid level in bottle using some algorithms, rather than PSO, which are not either popular or efficient (Figure 3) [6]. Figure 3 indicates detection of liquid surface level using this algorithm [8, 9].

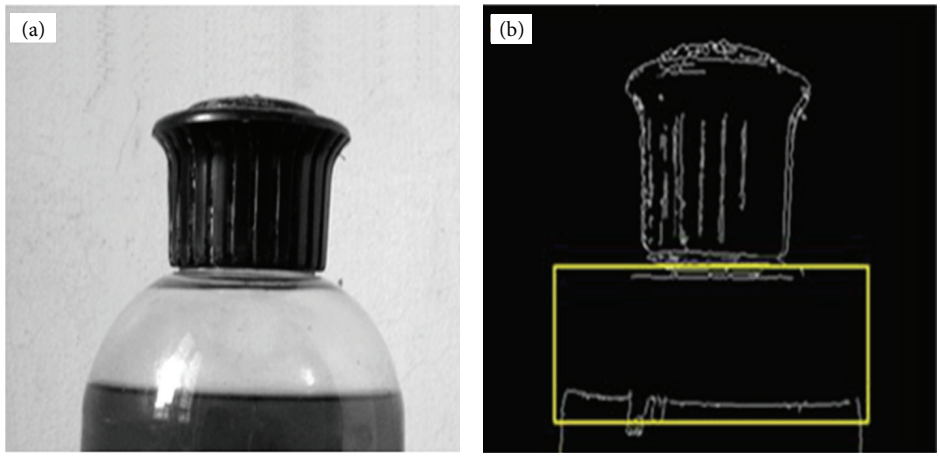

Figure 3: (a) Bottle of liquid. (b) Detection of surface level of liquid in bottle.

2.1. LOG Algorithm for Optimal Edge Recognition. The LOG algorithm shows that the location of edge occurrence is neither smooth nor thin. However, it is more efficient than previous method on low signal over noise. The steps of LOG algorithm can be summarized as follows [8, 9]: (a) convolving of image I by two-dimensional Gaussian function; (b) calculation of convolved image's Laplace; (c) edge pixel for passing from zero which is in L.

2.2. Algorithm Kani. Kani was assumed to be edge conditional to white Gaussian noise. The edge detector was considered with cannulation filter f, which distributes noise and location of edge. Here, the problem is to determine a filter that optimizes three criteria in recognition of a given edge. Algorithm Kani [10] is as follows:

(a) Reading image I.

(b) Convolving on one-dimensional Gaussian cover with I.

(c) Gaussian first derivative in the directions x and y.

(d) Convolved I with G along rows and bottom of columns to obtain I_x and I_y, respectively.

(e) Convolved I_x with G_x to reach I_x and I_y with G_y to have I_u.

(f) Finding results in any pixel.

3. Particle Swarm Optimization (PSO)

PSO algorithm was inspired from birds' behavior in their groups. This algorithm has fast and high convergence speed. Therefore, it has been efficiently used in static environments. Standard PSO algorithm has a population with m members, where each member is one potential solution in D-dimensional space of the problem [11, 12]. In the standard PSO algorithm, in the t iteration, the D-dimension of rate and situation of i member vary according to (1) and (2), respectively; w, c_1, and c_2 are nonnegative real constant parameters; and r_1 and r_2 are independent random numbers with uniform distribution in the range of 0 to 1. Consider

$$V_i^d(t+1) = \omega V_i^d(t) + c_1 r_{1,i}^d(t)\left(P_i^d(t) - X_i^d(t)\right) + c_2 r_{2i}^d(t)\left(P_g^d(t) - X_i^d(t)\right), \quad (1)$$

$$X_i^d(t+1) = X_i^d(t) + V_i^d(t+1). \quad (2)$$

In FITNESS function, to obtain the threshold value for detecting the lesions in specific point (the center of lesions) based on the experience, we calculate an average of the selected color of the whole pixels of the image of human teeth. Hence, we do not take into account the points around the image of teeth which are not considered as the part of the human tooth. We multiply this average by 20% to obtain the threshold value for detecting the point where the lesions are formed around it. Because the quality of pictures may change by receivers, we alter this 20% to 1 to 3%, indeed 17% to 23% using α variable ((3) formula). By multiplying the specified value by β instead of α, the threshold value for the points surrounding pixels can be found (formula (4)). Consider

$$\text{Threshold } X = \alpha \times \frac{20}{100} \times \frac{\sum_{i=1}^{i=\text{row}} \sum_{j=1}^{j=\text{column}} p_{i,j};\ p_{i=1,\ldots,\text{row},j=1,\ldots,\text{column}} \geq a}{\sum_{i=1}^{i=\text{row}} \sum_{j=1}^{j=\text{column}} \text{count} = \text{count} + 1;\ p_{i=1,\ldots,\text{row},j=1,\ldots,\text{column}} \geq a}, \quad (3)$$

$$\text{Threshold } X \text{ Around} = \beta \times \frac{20}{100} \times \frac{\sum_{i=1}^{i=\text{row}} \sum_{j=1}^{j=\text{column}} p_{i,j};\ p_{i=1,\ldots,\text{row},j=1,\ldots,\text{column}} \geq a}{\sum_{i=1}^{i=\text{row}} \sum_{j=1}^{j=\text{column}} \text{count} = \text{count} + 1;\ p_{i=1,\ldots,\text{row},j=1,\ldots,\text{column}} \geq a}. \quad (4)$$

The threshold value (Threshold X) for the central point is always less than the threshold value (ThresholdAround) for surrounding areas. Since this is the start point and end point of lesion, the threshold value will be always higher than that in other points, unless the lesion is improved.

For detecting the edges in four directions, we move pixel by pixel and review the threshold value of surrounding points, until a pixel is found with a threshold value higher than the threshold value of surrounding points. We save the spacing of these points to the central point (formula (5)). Then, we calculate the average of all points within a certain range around the central point (formula (6)). Consider

$$\begin{aligned}
\text{point}_A &= \text{image}\left(X_i, X_j - \text{const } 1, :\right);\\
\text{point}_B &= \text{image}\left(X_i, X_j + \text{const } 2, :\right);\\
\text{point}_C &= \text{image}\left(X_i - \text{const } 3, X_j, :\right);\\
\text{point}_D &= \text{image}\left(X_i + \text{const } 4, X_j, :\right),
\end{aligned} \tag{5}$$

$$\text{Avg point} = \frac{\sum_{i=X_i-d}^{i=X_i+d} \sum_{j=X_j-d}^{j=X_j+d} P_{i,j}}{\sum_{i=X_i-d}^{i=X_i+d} \sum_{j=X_j-d}^{j=X_j+d} \text{count avg point} = \text{count avg point} + 1}. \tag{6}$$

By investigating some conditions one can recognize that the central point can be the central point of lesion (formula (7)). The conditions are as follows: (1) the color of considered point should be lower than the threshold value. (2) The average of whole points within a certain range around the central point should be lower than the threshold value. (3) The difference between horizontal and vertical edges should be less than the threshold value separately, since this causes not going further away from the main edge of the teeth. Last part of FITNESS function is related to existence or nonexistence of preapical lesion in X point and around X point (7). Consider

$$\text{Exist\_carious\_lesion} = \begin{cases} 1; & C_x \le X_{i,j} \le \text{Threshold } X \text{ Around},\\ & C_x \le \text{Avg point} \le \text{Threshold } X \text{ Around},\\ & (|A - B| \parallel |C - D| \le \text{Threshold } X \text{ Around})\\ 0; & \text{Other.} \end{cases} \tag{7}$$

We explain some parameters below. The average points around X are Avg point. P, row, column, a and count are pixel (point) of picture, maximum row of picture, maximum column of picture, point of carious lesions and restoration teeth in picture, and number of selecting points for calculation. $P_{i,j}$ is color value of image(i, j, 1) or image(i, j, 2) or image(i, j, 3). $X_{i,j}$ is one point in place of image(X_i, X_j, $1, \ldots, 3$) and X_i is value of $1, \ldots,$ row, X_j is value of $1, \ldots,$ column, and C_x is constant value to avoid detection out of tooth.

4. Results

In this section, study results are presented. Figure 4(b) shows a tooth with no decay and restoration, while the one in Figure 4(a) shows distribution of particles for detection of dental caries and restoration. Also two pictures were taken in the same mode. Figures 5, 6, and 7 show presence of decay and restoration in one tooth.

Through the experiments conducted in this research, first the particles are distributed throughout the pictures for diagnosis. Distribution of particles can be observed in (a) of Figures 4, 5, 6, and 7. Secondly, particles start to move in any picture. During running, PSO algorithm calculates value of transferring for any particle.

After running the algorithm, if the carious lesions or restoration is in teeth, PSO algorithm can recognize it and identify its location. Figure 4 indicates a picture where there are no dental caries and restoration, while Figures 5, 6, and 7 illustrate that three other pictures have one case of dental caries and restoration. Our algorithm in Figure 4(b) does not show any dental caries and restoration. In comparison, the algorithm shows the place of dental caries and restoration for Figures 5(b), 6(b), and 7(b) through a green line crossing a yellow line.

The convergence of PSO is shown for 400 iterations in Figure 8. The algorithm converges very fast between 1 and 50 iterations. In other words, convergence occurs very fast. After that the rate of change is very slow for the next 400 iterations. The rate of change exactly is between 0.1 and 0.5.

5. Discussion

It has been shown that when six people without having any consultation with each other observe and interpret an X-ray radiographic stereotype, only 50% of them will have the same opinions; moreover, when radiographs are shown to a person at two different times, different interpretations are presented. Hence, it is recommended that, in order to interpret the radiographs, two independent people are used, and if there is disagreement between them, they should consult with each other to find an agreement, and if not so, one can ask a third person to offer his/her opinion; in this case, differences will be reduced from 50% to 25% [13].

Of mass particle swarm optimization (PSO) features, one can refer to the system memory in this system, in which the knowledge of proper solutions can be maintained by all the particles; in other words, in the algorithm of mass particle, every particle can benefit from its past information, while there are no such behaviors and features in other evolutionary algorithms. Also, in this algorithm, the populations are connected with each other and they solve their problem through the exchange of the information in a high speed convergence way. Using PSO algorithm with the help of image interpretation, the X-ray radiography processing error can be minimized. The differences in the interpretations of X-ray radiographies can be reduced from 25% to less than 8%, as well. Moreover, it saves time and increases interpretation accuracy. Our results show that this method can detect dental caries and restoration in digital radiography pictures. The error rate

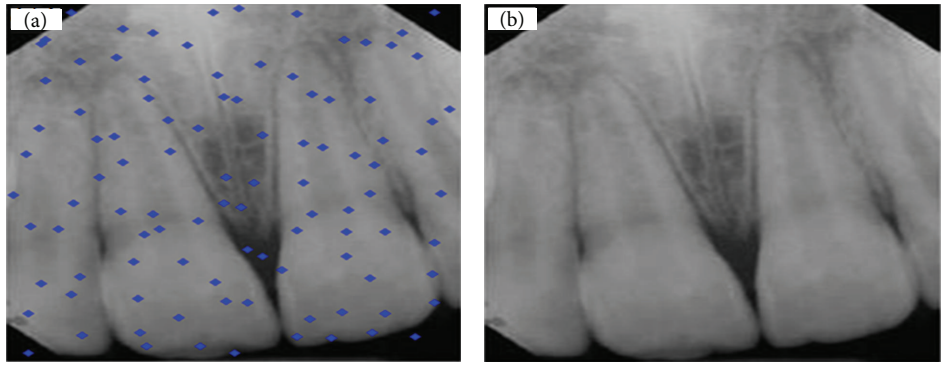

Figure 4: (a) Distribution of particles for detection of dental caries and restoration. (b) Teeth with no decay and restoration.

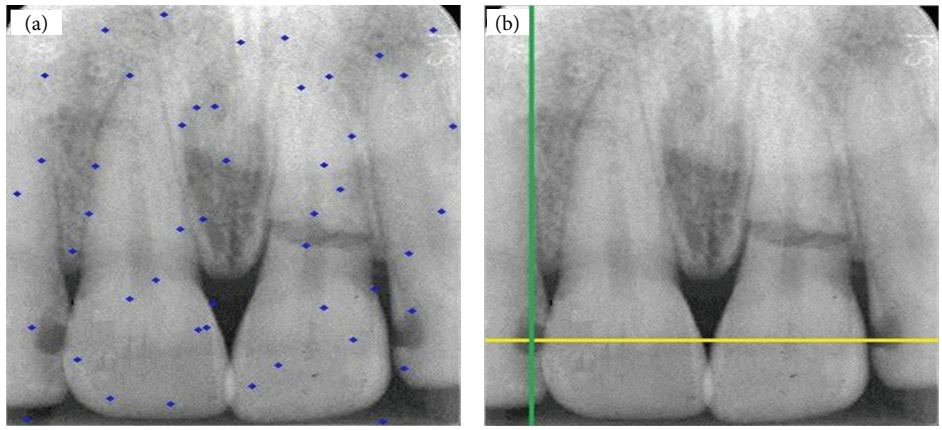

Figure 5: (a) Distribution of particles for detection of carious lesion and restoration. (b) Detection of one tooth with decay (right) depicted by green line crossed with yellow line.

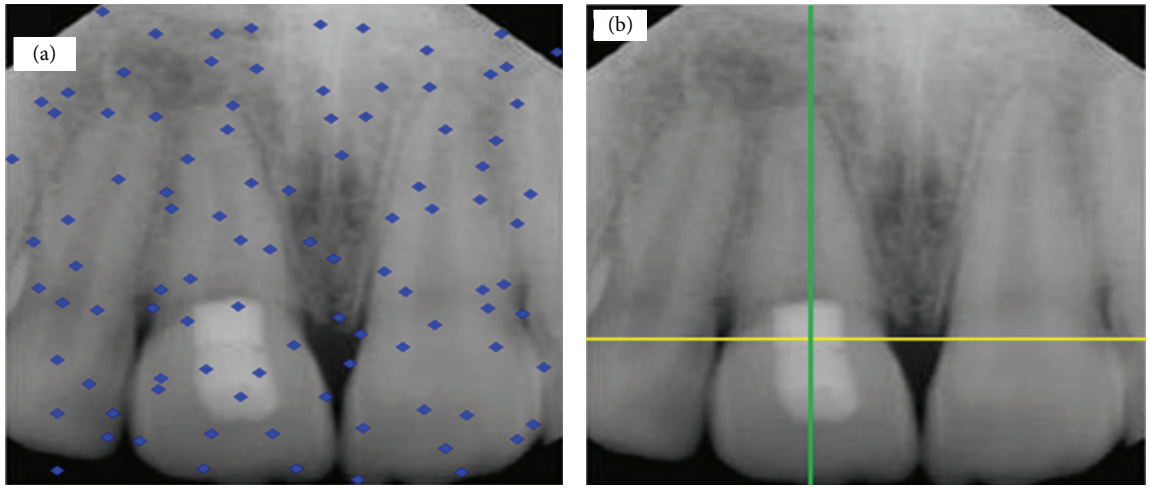

Figure 6: (a) Distribution of particles for detection of dental caries and restoration. (b) Detection of one tooth with decay and restoration, depicted by green line crossed with yellow line.

of this method was 8%, so that it can be implemented for detection of dental caries and restoration by dentist, since the error rate can be even reduced below 0.5%.

Therefore, we will do detection and repair of tooth diagnosis intelligently in the future. This method will come to help some special robots for our area with ability of dental lesions restoration without human intervention in the future. According to the authors of this paper, introducing this intelligent detecting lesions system in the future, as a result of designing the robots, will create a more prominent role, and

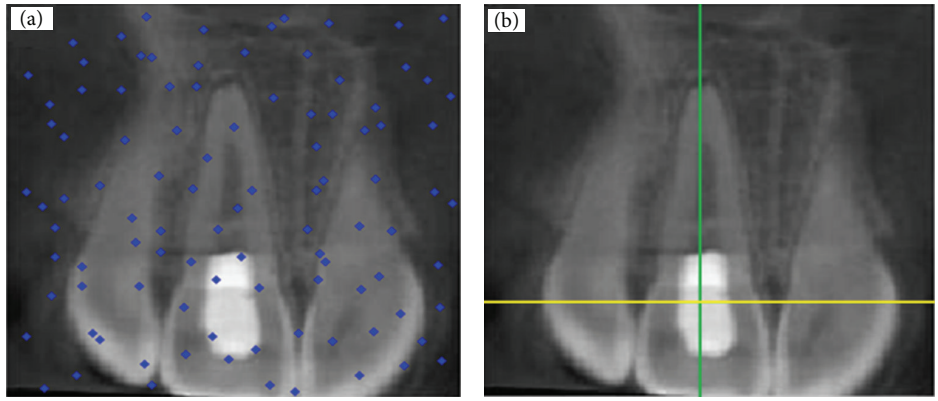

Figure 7: (a) Distribution of particles for detection of dental caries and restoration (b) and detection of one tooth with restoration, depicted by green line crossed with yellow line.

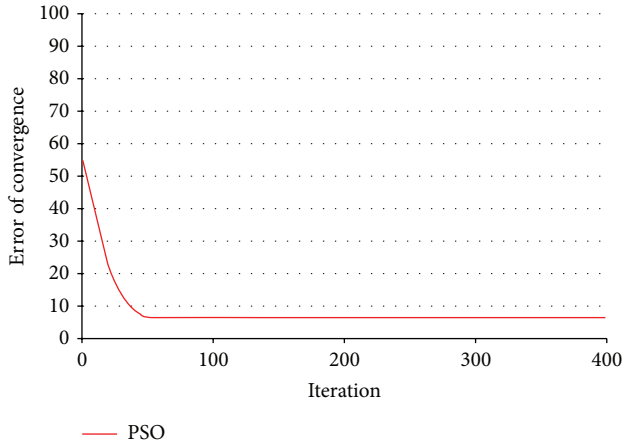

Figure 8: Converge of PSO during 400 steps.

developing of this intelligent system will support the clinicians in dental offices.

This method was used for 2D special images. At this time, it can find tooth lesions in Gary image. We also can apply color 2D image, because we just need to change detection value. But we did not apply it to 3D image for detection. We need to develop this method for 3D image. Then we will test on 3D images. If it has any problem, we will change some parameters to solve this problem. Also we need to test more different images that some different systems can take images of teeth. Our method is not a new algorithm. In fact, we use PSO algorithm and we have implemented the part of fitness by our formula.

6. Conclusion

In this paper, the image processing technique was introduced for some applications. One of these applications is the detection of dental caries and restoration. Therefore, we used both of image processing methods and particle swarm optimization (PSO) algorithm for detecting teeth decay and restoration. We implemented some mathematics formula for fitness of PSO. This idea helps us to solve this problem easily. Our results show that this method can detect dental caries and restoration in digital radiography pictures. The error rate was 8%, so that it is possible to use for detection of dental caries and restoration by dentist. Using the addition of some parameters, it is possible that the error rate can be even reduced below 0.5%. The convergence of this algorithm is good. But we can have very fast convergence using combinatorial optimization of some algorithms together. This method can be potentially used for detection of dental caries and restoration in the future. As the guideline for future works, the authors of this work recommend working on detection of dental caries and restoration using image processing and other popular algorithms.

Competing Interests

The authors have no conflict of interests relevant to this paper.

References

[1] O. Fejerskov and E. A. M. Kidd, *Dental Caries: The Disease and Its Clinical Management*, Blackwell, Munksgaard, Danmark, 2nd edition, 2008.

[2] "NIH Consensus Development Conference on Diagnosis and Management of Dental Caries Throughout Life. Bethesda, MD, March 26–28, 2001. Conference Papers," *Journal of Dental Education*, vol. 65, no. 10, pp. 935–1179, 2001.

[3] R. H. Selwitz, A. I. Ismail, and N. B. Pitts, "Dental caries," *The Lancet*, vol. 369, no. 9555, pp. 51–59, 2007.

[4] K. J. Pithadiya, C. K. Modi, and J. D. Chauhan, "Selecting the most favourable edge detection technique for liquid level inspection in bottles," *International Journal of Computer Information Systems and Industrial Management Applications*, vol. 3, pp. 34–44, 2011.

[5] E. Newbrun, *Cariology*, Williams & Wilkins, Baltimore, Md, USA, 3rd edition, 1989.

[6] K. J. Pithadiya, C. K. Modi, and J. D. Chauhan, "Machine vision based liquid level inspection systemusing isef edge detection technique," in *Proceedings of the ACM International Conference*

and Workshop on Emerging Trends in Technology (ICWET '10), pp. 601–605, Mumbai, India, February 2010.

[7] I. D. Mandel, "Caries prevention: current strategies, new directions," *Journal of the American Dental Association*, vol. 127, no. 10, pp. 1477–1488, 1996.

[8] K. J. Pithadiya, C. K. Modi, and J. D. Chauhan, "Comparison of optimal edge detection algorithms for liquid level inspection in bottles," in *Proceedings of the 2nd International Conference on Emerging Trends in Engineering and Technology (ICETET '09)*, pp. 447–452, IEEE, Nagpur, India, December 2009.

[9] J. D. Chauhan, C. K. Modi, and K. J. Pithadiya, "Location M estimator with optimal edge detector for quality inspection of surface mount device capacitor," in *Proceedings of the International Conference and Workshop on Emerging Trends in Technology (ICWET '10)*, pp. 595–600, Mumbai, India, February 2010.

[10] F. Duan, Y. Wang, and H. Liu, "A real-time machine vision system for bottle finish inspection," in *Proceedings of the 8th International Conference on Control, Automation, Robotics and Vision (ICARCV '04)*, vol. 2, pp. 842–846, Kunming, China, December 2004.

[11] J. Kennedy and R. C. Eberhart, "Particle swarm optimization," in *Proceedings of the IEEE International Conference on Neural Networks, IV*, pp. 1942–1948, Perth, Australia, 1995.

[12] R. Eberhart and J. Kennedy, "A new optimizer using particle swarm theory," in *Proceedings of the Sixth International Symposium on Micro Machine and Human Science (MHS '95)*, pp. 39–43, Nagoya, Japan, October 1995.

[13] M. Goldman, A. H. Pearson, and N. Darzenta, "Reliability of radiographic interpretations," *Oral Surgery, Oral Medicine, Oral Pathology*, vol. 38, no. 2, pp. 287–293, 1974.

Hindawi Publishing Corporation
International Journal of Dentistry
Volume 2016, Article ID 7484159, 4 pages
http://dx.doi.org/10.1155/2016/7484159

Research Article

Computer-Assisted Technique for Surgical Tooth Extraction

Hosamuddin Hamza

The Orthopaedic Department, October 6 University, Giza, Egypt

Correspondence should be addressed to Hosamuddin Hamza; hosamuddinhamza@gmail.com

Received 23 February 2016; Accepted 13 March 2016

Academic Editor: Francesco Mangano

Introduction. Surgical tooth extraction is a common procedure in dentistry. However, numerous extraction cases show a high level of difficulty in practice. This difficulty is usually related to inadequate visualization, improper instrumentation, or other factors related to the targeted tooth (e.g., ankyloses or presence of bony undercut). *Methods*. In this work, the author presents a new technique for surgical tooth extraction based on 3D imaging, computer planning, and a new concept of computer-assisted manufacturing. *Results*. The outcome of this work is a surgical guide made by 3D printing of plastics and CNC of metals (hybrid outcome). In addition, the conventional surgical cutting tools (surgical burs) are modified with a number of stoppers adjusted to avoid any excessive drilling that could harm bone or other vital structures. *Conclusion*. The present outcome could provide a minimally invasive technique to overcome the routine complications facing dental surgeons in surgical extraction procedures.

1. Introduction

Surgical extraction of broken and badly decayed teeth is routinely done through conventional technique (root sectioning, bone cutting, and removal of dental and bony undercuts) [1]. This technique has proven fast and reliable; however, ideally, it needs 3 X-rays (periapical radiographs): 1 preoperative for evaluation of root curvature, angulation, or any root fracture; 1 intraoperative to check the accuracy of the extraction procedure (e.g., complete root sectioning); 1 postoperative to confirm complete removal of any remaining tooth structure [2].

This technique still possesses some limitations; for example, excessive bone cutting could lead to bone necrosis in the related area. Also, the technique is considerably invasive in areas related to vital structures (e.g., nerves and maxillary sinuses) when applied on teeth with fused or angled roots [3].

In addition, this conventional technique relies on visualization of the surgical field, which could be hindered in case of bleeding, irritable patients, overlapping soft tissues, or malaligned or malpositioned teeth. It also has a relatively prolonged operative time and could be not applicable in patients with limited mouth opening or incompliant patients [4].

While the use of 3D imaging, scanning, virtual designing, planning, and printing in dentistry has been increasing in the past decades, especially in dental implantation, the concept of printing of hybrid objects (metal and plastics) is limitedly applied in the medical and dental fields [5].

The aim of this work is to present a computer-assisted technique (cutting guide and instruments) that could replace the conventional surgical extraction.

2. Methods

For a patient undergoing surgical extraction for single or multiple teeth, a model is firstly done (impression and gypsum pouring) to validate the accuracy of the final outcome extraorally before proceeding with the surgical procedure. Then, the patient is directed to perform digital radiograph (CT or CBCT). The 3D images are firstly segmented so that teeth, bone, and other structures are differentiated.

Treatment planning is done according to 3D data collected from the radiographs, that is, accurate determination of the position, alignment, and inclination of teeth/roots. Also, bone density overall and in targeted areas could be determined from 3D radiographs.

Figure 1: Surgical stent fabricated for extraction of remaining roots of mandibular first molar.

Figure 2: Hard stopper added to the cutting tool to determine the depth of cutting.

Finally, vital structures such as nerves and sinuses adjacent to the proposed tooth/teeth for extraction are located.

The important aspects of the roots to be extracted are their position, angulation, and proximity to bone and other structures as well as their length and bifurcation/trifurcation depth [6].

The planning is done to provide cutting slots for the surgical burs to reach the roots, bone, and root-bone interface in optimal orientation. These cutting slots are designed to allow the drills to pass exactly and accurately in the weak areas between the roots as could be obtained from the 3D radiographs [7].

The weak areas are more likely to be in the junction between roots (Figure 1): in the lower molars, one cut in the line of junction between the mesial and distal roots, while in the upper molars, 3 cuts in the lines of junction between the mesiobuccal and distobuccal roots, between the mesiobuccal and palatal roots, and between the distobuccal and palatal roots.

Moreover, in case of existing bony undercut between one or more roots with the proximal bone, more cutting slots could be designed to make the drills pass accurately and undertake osteotomy to relieve any pressure in this area.

The cutting slots are designed as empty lines, points, or areas on the virtual stent corresponding to the cutting areas. The designing could be done by specifying the areas to be fabricated of metals and the rest of the stent to be fabricated of plastics. The surgical guide is designed with assuring the stability and extension of the stent and involvement of required areas as well as smoothening of its margins to avoid injury of the soft tissue due to friction.

Designing the plastic and metal components is done as two separate parts to account for internal structures, as well as include considerations for methods of fastening (jointing) the parts together into a single component.

Then, the final design of the surgical guide is converted to stl files, which are, in turn, transferred to special 3D printer that is capable of printing plastics, milling metal, and fusing metal and plastic material into one object.

The surgical guide is made of hybrid metal-plastic material. Each material is durable enough and heat-stable to withstand the mechanical forces during drilling and the heat during preoperative sterilization. The metal components are NiTi or stainless steel; while the plastics are polyamide nylon. The materials used do not result in any debris during drilling or cutting that could contaminate the surgical field and delay healing of the extraction socket.

In another step of the technique, and according to measurements obtained from the 3D radiographs, hard plastic stoppers could be added to the drill to determine the depth of cutting (Figure 2) to avoid undesired overcutting (especially in depth dimension).

The surgical guide is adapted onto the master model to validate its fitting; then it could be sterilized preoperatively with autoclave. The cutting stent is fixed onto the patient's maxillary or mandibular arch by either pins, screws, or engagement into the dental or bone undercuts. Cutting could be done within the cutting slots by dental drills or burs with the depth stoppers. Cutting aims at freeing all possible undercuts around the targeted tooth that could resist the extraction procedure. Tooth extraction is completed safely by normal curved forceps or elevators.

3. Results

The surgical guide is specifically tailored for each patient with one or multiple teeth that need surgical extraction. The final outcome is a surgical guide that is fabricated to provide an access toward the surgical field. Visibility is not as important as the stent is capable of providing direct access to the target area. Surgical extraction using the surgical guide could minimize postoperative bleeding, tissue laceration, and pain.

4. Discussion

This work aims to exploit the currently evolving 4D printing technology which merges metallic and nonmetallic materials into one component or object. It also aims to ease surgical extraction procedure for dentists/oral surgeons and to reduce the pain that is usually associated with such procedure through planning the cutting direction, depth, and inclination on computer and then transferring these data into physical objects (templates and instrumentation) and to avoid uncalculated bone cuttings or teeth sectioning done in the procedures.

The proposed method is similar to fabricating the surgical guides routinely used for dental implants, as digital treatment plan is firstly performed with the data acquired from CT scan;

a master model is created with extraction site determined prior to planning; segmentation of bone, teeth, and soft tissues is done on the digital scan.

Other geometric features are determined, including position and size of the target tooth for extraction as well as root angulation, inclination, and depth and the preferable drilling options [8]. Virtual evaluating of the treatment plan should be done prior to printing the splint and must be discussed with the surgeon performing the extraction procedure. However, modifying the treatment plan to simulate the tooth extractions or bone modifications should be done if necessary. Optionally, the surgical guide could be manufactured based on the master model; but, in the proposed method, the master model is used only for validating the final outcome [9].

Bone structure is segmented from CT image data, and the cutting slots on the guide are virtually added onto the soft tissue, bone, and tooth structures with parameters reflecting the treatment plan. The most important vital structure related to the maxillary jaw is the maxillary sinus, while, for the mandibular jaw, the nerve channels are of importance [10].

A model of the soft tissue can be further created from CT scan or optical scan to be united with or trimmed by jaw bone structure to give more detailed description of the surgical field. The thickness of soft tissue is digitally created and visually inspected; it should be equal to the distance between the cutting guide and the patient's jaw bone; calculation of soft tissue thickness is done by computing and analyzing this distance. The final outcome (surgical guide) has 2 surfaces: one fitting surface toward the patient's anatomy and an outside surface, which have to be checked against the master model before application in the surgery [11].

It is worth mentioning that advancing CAD/CAM and imaging technologies have enabled clinicians to analyze patients' anatomy and to manipulate areas that need skeletal reconstruction. It has been used for maxillofacial and implant procedures such as maxillary-sinus augmentation with reportedly high precision [12]. Moreover, in light of sinus augmentation procedures, the present method is similar to the guided bone-grafting and bone-reconstructive surgery which aim to reduce mental navigation and to replace the conventional surgical methods. The use of CT scanning and stereolithography has produced accurate and predictable results and enhanced the outcome of dental implant procedures [13].

One limitation of this work is that it relies on sophisticated 3D designing and needs special 3D printing and milling machines. However, depending on the components' shape considerations, each part of the surgical guide could be created with a different setup. When designing such components, some major differences between 3D printing (an additive process) and CNC milling (a subtractive process) should be considered. Additive processes build layer by layer and therefore have very little problem building internal structures. So, internal mesh, cavities, tubes, and the like inside a relatively seamless, solid piece (considering overhangs and support structures, here) could be created, but some formulations of plastics will not be available in 3D printer filaments coinciding with the metal part. The subtractive process, CNC milling, will provide more material flexibility, but it will require considering the shape of the components more carefully for the fabrication method. Soft metals like brass and aluminum could be used more accurately with relative ease, and could be milled through nylon easily. As milling is a subtractive procedure, it cuts from the outside of a material to the inside; that is, the procedure will be similar to cutting from a direction, rather than building layer by layer, so it could be difficult to get at the inside of the material without clearing away more material to have access to the internal portions of the components.

Another limitation of this methodology is the fact that it needs prolonged time compared to the routine surgical extraction done in dental facilities. However, considering the accurate cutting the surgical guide could provide and the less tissue injury due to trauma, tissue laceration, or uncalculated drilling, using this technique could compensate for the long time for achieving CT scans as well as designing and fabricating the cutting guide to complete the procedure [3].

Competing Interests

The author declares that he has no competing interests.

Acknowledgments

The author would like to express his great appreciation and gratitude to Professor Mahmoud A. Hafez for his continuous support and help. The author would like also to thank the research team at the Orthopaedic Department, October 6 University, for their scientific collaboration.

References

[1] O. E. Danielson, A. C. Chinedu, E. A. Oluyemisi, B. O. Bashiru, and O. O. Ndubuisi, "Frequency, causes and pattern of adult tooth extraction in a Nigerian rural health facility," *Odonto-Stomatologie Tropicale*, vol. 34, no. 134, pp. 5–10, 2011.

[2] E. M. Rivera and R. E. Walton, "Cracking the cracked tooth code: detection and treatment of various longitudinal tooth fractures," *American Association of Endodontists Colleagues for Excellence Newsletter*, vol. 2, pp. 1–19, 2008.

[3] V. Nguyen and G. Palmer, "A review of the diagnosis and management of the cracked tooth," *Dental Update*, vol. 36, no. 6, pp. 338–346, 2009.

[4] W. S. Eakle, E. H. Maxwell, and B. V. Braly, "Fractures of posterior teeth in adults," *Journal of the American Dental Association*, vol. 112, no. 2, pp. 215–218, 1986.

[5] C. E. Misch, *Contemporary Implant Dentistry*, Mosby Publications, St. Louis, Mo, USA, 3rd edition, 2007.

[6] C. G. Petrikowski, M. J. Pharoah, and A. Schmitt, "Presurgical radiographic assessment for implants," *The Journal of Prosthetic Dentistry*, vol. 61, no. 1, pp. 59–64, 1989.

[7] C. T. Castro-Ruiz, J. Noriega, and M. E. Guerrero, "Validity of ridge mapping and cone beam computed tomography in dental implant therapy," *Journal of Indian Society of Periodontology*, vol. 19, no. 3, pp. 290–293, 2015.

[8] N. Stoppie, V. Pattijn, T. Van Cleynenbreugel, M. Wevers, J. Vander Sloten, and N. Ignace, "Structural and radiological parameters for the characterization of jawbone," *Clinical Oral Implants Research*, vol. 17, no. 2, pp. 124–133, 2006.

[9] M. Z. Kola, A. H. Shah, H. S. Khalil et al., "Surgical templates for dental implant positioning; current knowledge and clinical perspectives," *Nigerian Journal of Surgery*, vol. 21, no. 1, pp. 1–5, 2015.

[10] G. Tepper, U. B. Hofschneider, A. Gahleitner, and C. Ulm, "Computed tomographic diagnosis and localization of bone canals in the mandibular interforaminal region for prevention of bleeding complications during implant surgery," *International Journal of Oral and Maxillofacial Implants*, vol. 16, no. 1, pp. 68–72, 2001.

[11] V. Arisan, C. Z. Karabuda, and T. Özdemir, "Implant surgery using bone- and mucosa-supported stereolithographic guides in totally edentulous jaws: surgical and post-operative outcomes of computer-aided vs. standard techniques," *Clinical Oral Implants Research*, vol. 21, no. 9, pp. 980–988, 2010.

[12] F. Mangano, P. Zecca, S. Pozzi-Taubert et al., "Maxillary sinus augmentation using computer-aided design/computer-aided manufacturing (CAD/CAM) technology," *International Journal of Medical Robotics and Computer Assisted Surgery*, vol. 9, no. 3, pp. 331–338, 2013.

[13] G. A. Mandelaris and A. L. Rosenfeld, "A novel approach to the antral sinus bone graft technique: the use of a prototype cutting guide for precise outlining of the lateral wall. A case report," *International Journal of Periodontics and Restorative Dentistry*, vol. 28, no. 6, pp. 569–575, 2008.

Hindawi Publishing Corporation
International Journal of Dentistry
Volume 2015, Article ID 301796, 6 pages
http://dx.doi.org/10.1155/2015/301796

Research Article

Cone-Beam Computed Tomographic Assessment of Mandibular Condylar Position in Patients with Temporomandibular Joint Dysfunction and in Healthy Subjects

Maryam Paknahad,[1,2] Shoaleh Shahidi,[1] Shiva Iranpour,[1] Sabah Mirhadi,[1] and Majid Paknahad[3]

[1]*Oral Radiology Department, Dental School, Shiraz University of Medical Sciences, Shiraz 7145613466, Iran*
[2]*Prevention of Oral and Dental Disease Research Center, Dental School, Shiraz University of Medical Sciences, Shiraz 7145613466, Iran*
[3]*Radiology Department, Medical School, Shiraz University of Medical Sciences, Shiraz 7145613466, Iran*

Correspondence should be addressed to Maryam Paknahad; paknahadmaryam@yahoo.com

Received 1 October 2015; Accepted 27 October 2015

Academic Editor: Francesco Mangano

Statement of the Problem. The clinical significance of condyle-fossa relationships in the temporomandibular joint is a matter of controversy. Different studies have evaluated whether the position of the condyle is a predictor of the presence of temporomandibular disorder. *Purpose*. The purpose of the present study was to investigate the condylar position according to gender in patients with temporomandibular disorder (TMD) and healthy controls using cone-beam computed tomography. *Materials and Methods*. CBCT of sixty temporomandibular joints in thirty patients with TMD and sixty joints of thirty subjects without TMJ disorder was evaluated in this study. The condylar position was assessed on the CBCT images. The data were analyzed using Pearson chi-square test. *Results*. No statistically significant differences were found regarding the condylar position between symptomatic and asymptomatic groups. Posterior condylar position was more frequently observed in women and anterior condylar position was more prevalent in men in the symptomatic group. However, no significant differences in condylar position were found in asymptomatic subjects according to gender. *Conclusion*. This study showed no apparent association between condylar positioning and clinical findings in TMD patients.

1. Introduction

The temporomandibular joint (TMJ) is one of the most complex joints in the body which is located between the mandibular condyle and the temporal bone [1, 2]. The radiographic joint space is a radiolucent area between the mandibular condyle and the temporal bone [3]. Joint space measurements were introduced by Ricketts to describe condylar position [4]. The condylar position can be determined by the relative dimensions of the radiographic joint spaces between the glenoid fossa and the mandibular condyle [3].

The clinical significance of condyle-fossa relationships in the temporomandibular joint is a matter of controversy [5]. Some studies have suggested an association between eccentric condylar position and temporomandibular disorder (TMD) [6–9]. These studies have suggested therapeutic procedures to optimize the condylar position in some patients [6, 10, 11]. However, other studies failed to demonstrate significant association between the condylar positioning and the incidence of TMD [12, 13].

Various radiographic methods have been used in previous studies to determine condylar position such as plain film radiography, conventional tomography, computed tomography, cone-beam tomography, and magnetic resonance imaging [5, 14–18]. Cone-beam computed tomography (CBCT) is the modality of choice for the assessment of temporomandibular osseous structures [19]. In the present study, the observers have used CBCT to study condylar positioning.

The aim of the present study was to investigate the condylar position according to gender in patients with TMD and healthy controls using CBCT.

2. Materials and Methods

This study was carried out at the Department of Maxillofacial Radiology at Shiraz Dental University in Shiraz, Iran. An expert radiologist examined the participants and divided them into two groups including symptomatic group and asymptomatic group. The symptomatic group consisted of 30 patients (20 females and 10 males) aged 20 to 42 years (mean 33/4 years) with clinical signs and symptoms of TMD such as joint pain, muscle pain, mouth-opening limitation, joint noise (click or crepitation), and nonharmonic movements of the joint who were referred to the Department of Maxillofacial Radiology for the treatment of TMDs and required CBCT for more investigation. The asymptomatic group consisted of 30 adults (18 females and 12 males) who had no temporomandibular symptoms and no history of occlusal equilibration or masticatory disorders referred to our department for reasons other than TMJ problems. The age of the patients in the control group ranged from 15 to 34 years (mean 24 years). In the control group, the patients who had any evidence of TMD in clinical or radiological examination were excluded from the present study. In both groups, the exclusion criteria were the presence of any congenital abnormalities and/or any systemic disease which could affect joint morphology such as rheumatoid arthritis.

All the participants took part voluntarily in this study and the written consent forms were taken from each of them after being informed about the nature of the study in detail. The study was approved by the local Ethical Committee of Shiraz Dental School.

2.1. CBCT of the TMJ. The CBCT scans of bilateral TMJs were performed by a NewTom VGi (QR Srl, Italy) with a field of view 15 cm × 15 cm. The exposure factors were 120 kv, 5 mA, and exposure time of 5 seconds. The subjects were standing and biting their teeth into maximum intercuspal position. Their heads were positioned with the Frankfurt plane parallel to the floor.

2.2. Condylar Position Assessment. The axial view, in which the condylar process had the widest mediolateral diameter, was chosen as the reference view for secondary reconstruction. On this selected axial view, a line parallel to the long axis of the condylar process was drawn and lateral slices were reconstructed with 0.5 mm slice interval and 0.5 mm thickness (Figure 1(a)). On the central sagittal section, an expert maxillofacial radiologist measured the values of the narrowest posterior (P) and anterior (A) joint space accurately using NewTom NNT analysis software (Figure 1(b)). Condylar position was expressed by the following formula according to the method of Pullinger and Hollender [20]:

$$\text{condylar ratio} = \frac{P - A}{P + A} \times 100. \quad (1)$$

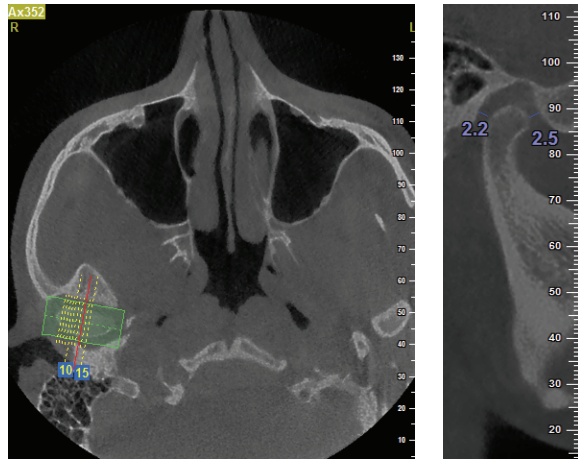

(a) (b)

Figure 1: Linear measurement of anterior (A) and posterior (P) subjective closest joint spaces in a sample patient. (a) Axial view; (b) sagittal view.

Figure 2: Posterior condylar position in a sample patient in the symptomatic group.

The position of the condyle was considered concentric if the ratio was within ±12%. If the ratio was smaller than −12%, the condylar position was considered posterior and if the ratio was greater than +12%, the condyle was considered in an anterior position (Figures 2 and 3).

2.3. Statistical Analysis. All data were analyzed with the SPSS program (SPSS 15.0, IBM, Chicago, IL, USA). The statistical analysis was performed using Pearson chi-square test to compare the condylar positions between two groups at the significance level of 0.05. To assess the significance of any errors during measurement, all images were revaluated over one-week interval. The mean difference between the first and second measurement was analyzed using paired t-test. The level for significance was set at $P < 0.05$.

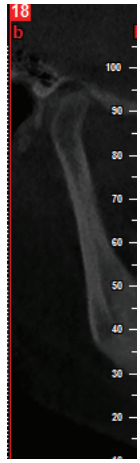

Figure 3: Anterior condylar position in a sample patient in the symptomatic group.

3. Results

There were no significant differences between dual measurements. The means of these two measurement values were used to minimize the error in identifying the reference points.

In the asymptomatic group, the frequency of posterior position was 25%, concentric position 38.5%, and anterior position 36.7%. In the symptomatic objects the incidence of posterior condylar position was 38.3%, concentric position 36.7%, and anterior position 35% (Table 1). There was no significant difference between the symptomatic and the asymptomatic groups for condylar position (P value = 0.22). Distribution of the condylar position in the symptomatic and asymptomatic groups according to gender is summarized in Table 2. No significant differences in condylar position between men and women were found in the asymptomatic subjects (P value = 0.757). The condylar position in the symptomatic group was significantly different in men and women (P value < 0.05) (Table 2). Posterior condylar position is significantly more prevalent in women (50%) and anterior condylar position more prevalent in men (55%).

4. Discussion

The clinical significance of condyle-fossa relationships in the temporomandibular joint is a matter of controversy [5]. Some studies have suggested eccentric condylar position is associated with temporomandibular disorder [6–9]. The aim of this study was to evaluate the condylar position according to gender in patients with TMD and healthy controls using CBCT.

Different radiographic techniques including conventional radiography [15], conventional tomography [18], computed tomography [1], MRI [14, 16, 17], and cone-beam computed tomography [5, 14, 21] have been used to study the condylar position in the glenoid fossa and the articular eminence morphology. Previously conventional radiography, especially transcranial radiography, has been used to assess condylar position and morphology [7]. However, transcranial

Table 1: Distribution of condyle position in the symptomatic and asymptomatic group.

Group	Condylar position			P value
	Posterior	Concentric	Anterior	
Asymptomatic	15 (25.0%)	23 (38.3%)	22 (36.7%)	0.22
Symptomatic	23 (38.3%)	16 (26.7%)	16 (26.7%)	

radiographs only represent the lateral third of the condyle. Therefore the reliability of these radiographs or assessing condylar position is questioned. Some researchers used conventional tomography to evaluate condylar position in the glenoid fossa [20]. However because slice thickness is large ranging between 1.0 and 3.0 mm, it does not represent the margins of joint structure as clearly as CT and CBCT [22].

The recently developed CBCT represents the joint structures with high accuracy which produces submillimeter spatial resolution as high as or even superior to spiral CT [23, 24]. Kobayashi et al. reported that the measurement error in CBCT was significantly less than spiral CT [24]. The bony component can be visualized in 3 planes without any superimposition, distortion, or magnification [25, 26]. CBCT has the advantage of reduced radiation dose and shorter scanning time compared with CT [27]. Therefore, CBCT has been used in the present study.

In studies that used transcranial radiographs actually the most lateral part of the joint is evaluated. Rammelsberg et al. selected three tomograms including central, 3 mm more lateral, and 3 mm more medial and measured data in tomograms [28]. Ikeda and Kawamura evaluated joint spaces on the central cuts of joints within 3.5 mm range medially and laterally to the central cut in CBCT [29]. They found that landmark identification outside this range was default because of the glenoid fossa anatomy. They also suggested that there were not significant differences in the joint spaces in this section [29]. Therefore we only considered the central slice of sagittal section of condyles in order to simplify analyzing the data.

There is a controversy over the clinical significance of condylar position [5]. Many studies have reported nonconcentric condylar position in association with disk displacement [14, 17], osteoarthritic changes [5], remodeling of the articular eminence and the condyle [30], and predisposition to arthrosis [31]. Nonconcentric condylar positioning is seen in one-third to one-half of asymptomatic volunteers [3]. On the other hand, concentric positioning in patients with TMD has high prevalence [32]. Aggressive condylar repositioning therapies are frequently performed to reestablish the mandibular condyle in an optimal position [6, 10]. However, according to the present study, condylar eccentricity is not a sufficient evidence for diagnosis of TMD and besides the evaluation of TMJ clinical symptoms and assessment of condylar eccentricity, additional investigations are required before a therapeutic change is performed.

Some studies represented no significant association between condylar positioning and clinical findings [12, 33, 34]. However, many studies showed significant difference in

Table 2: The condylar position in the symptomatic and asymptomatic groups according to gender.

Group	Sex	Condylar position			P value
		Posterior	Concentric	Anterior	
Asymptomatic	Female	10 (27.8%)	14 (38.9%)	12 (33.3%)	0.757
	Male	5 (20.8%)	9 (37.5%)	10 (41.7%)	
Symptomatic	Female	20 (50%)	10 (25%)	10 (25%)	0.020*
	Male	3 (15%)	6 (30%)	11 (55%)	

* A P value less than 0.05 was considered statistically significant.

the condylar positions in patients with TMD and asymptomatic subjects [27, 35]. Cho and Jung found concentric condylar position was more common in the asymptomatic group and posterior condylar position was more frequent in the symptomatic group [5]. Paknahad and Shahidi reported posteriorly seated condyles in patients with severe TMD and anteriorly and concentric seated condyles in patients with mild to moderate TMD [36]. Lelis et al. evaluated the condyle-mandibular fossa relationship in young individuals with intact dentitions and compared it to that between individuals with and without symptoms of temporomandibular disorder using CBCT [37]. They concluded that the presence or absence of temporomandibular disorder was not correlated with the condyle position in the temporomandibular joint which was similar to our findings.

In some previous studies asymptomatic groups represented more posterior condylar position in women and more anterior positions in men [20, 38]. Madsen found in the transcranial radiographs of asymptomatic adults that women and men were more likely to present posterior and anterior condylar positioning, respectively [39]. However in the present study, no significant difference in condylar position was found between men and women in asymptomatic subjects. Similarly some previous studies found no significant sex difference in condylar position joint spaces in normal joints [35, 40]. Ikeda and Kawamura found no significant sex difference in joint spaces, using CBCT in symptom-free subjects [29].

On the other hand in the symptomatic group posterior condylar position in women and anterior position in men were noticed. Some authors have reported an association between posterior condylar positioning and internal derangement [14, 16]. Higher incidence of posterior condylar position in women may be the etiological factor for preponderance of TMD and disk instability in women.

In this study the subjects who had history of occlusal therapy, prosthodontics treatment, and any systemic disorders such as rheumatoid arthritis were not included because these factors could affect the condylar morphology and position.

The present study did not demonstrate any significant differences in condylar position between symptomatic and asymptomatic groups. However several different factors such as radiographic technique used, accuracy of clinical examination, sample size, and the method of condylar position measurement can influence the results. Therefore, further investigations for assessing the correlation between temporomandibular disorder and condylar position are necessary.

Conflict of Interests

The authors declare that there is no conflict of interests regarding the publication of this paper.

Acknowledgments

The authors thank the Vice-Chancellery of Shiraz University of Medical Sciences for supporting this research. The authors would like to thank Dr. Sh. Hamedani (DDS, M.S.) for his suggestions and English writing assistance in the paper. The authors also thank Dr. M. Vosoughi of the Center for Research, of the School of Dentistry, for statistical analysis.

References

[1] C.-K. Wu, J.-T. Hsu, Y.-W. Shen, J.-H. Chen, W.-C. Shen, and L.-J. Fuh, "Assessments of inclinations of the mandibular fossa by computed tomography in an Asian population," *Clinical Oral Investigations*, vol. 16, no. 2, pp. 443–450, 2012.

[2] P. M. Som and H. D. Curtin, *Head and Neck Imaging*, Elsevier Health Sciences, 5th edition, 2011.

[3] S. C. White and M. J. Pharoah, *Oral Radiology: Principles and Interpretation*, Elsevier Health Sciences, 6th edition, 2009.

[4] R. M. Ricketts, "Variations of the temporomandibular joint as revealed by cephalometric laminagraphy," *American Journal of Orthodontics*, vol. 36, no. 12, pp. 877–898, 1950.

[5] B.-H. Cho and Y.-H. Jung, "Osteoarthritic changes and condylar positioning of the temporomandibular joint in Korean children and adolescents," *Imaging Science in Dentistry*, vol. 42, no. 3, pp. 169–174, 2012.

[6] L. A. Weinberg, "An evaluation of occlusal factors in TMJ dysfunction-pain syndrome," *The Journal of Prosthetic Dentistry*, vol. 41, no. 2, pp. 198–208, 1979.

[7] L. A. Weinberg, "Correlation of temporomandibular dysfunction with radiographic findings," *The Journal of Prosthetic Dentistry*, vol. 28, no. 5, pp. 519–539, 1972.

[8] D. D. Blaschke, W. K. Solberg, and B. Sanders, "Arthorgraphy of the temporomandibular joint: review of current status," *The Journal of the American Dental Association*, vol. 100, no. 3, pp. 388–395, 1980.

[9] W. B. Farrar and W. L. McCarthy Jr., "Conventional radiography compared with arthrography in internal derangements of the temporomandibular joint," *The Journal of Prosthetic Dentistry*, vol. 50, no. 4, pp. 585–586, 1983.

[10] F. Mongini, "Combined method to determine the therapeutic position for occlusal rehabilitation," *The Journal of Prosthetic Dentistry*, vol. 47, no. 4, pp. 434–439, 1982.

[11] L. A. Weinberg, "Definitive prosthodontic therapy for TMJ patients. Part I: Anterior and posterior condylar displacement," *The Journal of Prosthetic Dentistry*, vol. 50, no. 4, pp. 544–557, 1983.

[12] E. G. Herbosa, K. S. Rotskoff, B. F. Ramos, and H. S. Ambrookian, "Condylar position in superior maxillary repositioning and its effect on the temporomandibular joint," *Journal of Oral and Maxillofacial Surgery*, vol. 48, no. 7, pp. 690–696, 1990.

[13] F. O'Ryan and B. N. Epker, "Surgical orthodontics and the temporomandibular joint. I. Superior repositioning of the maxilla," *American Journal of Orthodontics*, vol. 83, no. 5, pp. 408–417, 1983.

[14] K. Ikeda and A. Kawamura, "Disc displacement and changes in condylar position," *Dentomaxillofacial Radiology*, vol. 42, no. 3, Article ID 84227642, 2013.

[15] A. V. Menezes, S. M. de Almeida, F. N. Bóscolo, F. Haiter-Neto, G. M. B. Ambrosano, and F. R. Manzi, "Comparison of transcranial radiograph and magnetic resonance imaging in the evaluation of mandibular condyle position," *Dentomaxillofacial Radiology*, vol. 37, no. 5, pp. 293–299, 2008.

[16] L. Incesu, N. Taşkaya-Yilmaz, M. Oğütcen-Toller, and E. Uzun, "Relationship of condylar position to disc position and morphology," *European Journal of Radiology*, vol. 51, no. 3, pp. 269–273, 2004.

[17] H. Kurita, A. Ohtsuka, H. Kobayashi, and K. Kurashina, "A study of the relationship between the position of the condylar head and displacement of the temporomandibular joint disk," *Dentomaxillofacial Radiology*, vol. 30, no. 3, pp. 162–165, 2001.

[18] P. W. Major, R. D. Kinniburgh, B. Nebbe, N. G. Prasad, and K. E. Glover, "Tomographic assessment of temporomandibular joint osseous articular surface contour and spatial relationships associated with disc displacement and disc length," *American Journal of Orthodontics and Dentofacial Orthopedics*, vol. 121, no. 2, pp. 152–161, 2002.

[19] M. L. Hilgers, W. C. Scarfe, J. P. Scheetz, and A. G. Farman, "Accuracy of linear temporomandibular joint measurements with cone beam computed tomography and digital cephalometric radiography," *American Journal of Orthodontics and Dentofacial Orthopedics*, vol. 128, no. 6, pp. 803–811, 2005.

[20] A. G. Pullinger, L. Hollender, W. K. Solberg, and A. Petersson, "A tomographic study of mandibular condyle position in an asymptomatic population," *The Journal of Prosthetic Dentistry*, vol. 53, no. 5, pp. 706–713, 1985.

[21] S. Shahidi, M. Vojdani, and M. Paknahad, "Correlation between articular eminence steepness measured with cone-beam computed tomography and clinical dysfunction index in patients with temporomandibular joint dysfunction," *Oral Surgery, Oral Medicine, Oral Pathology and Oral Radiology*, vol. 116, no. 1, pp. 91–97, 2013.

[22] K. Ikeda, A. Kawamura, and R. Ikeda, "Assessment of optimal condylar position in the coronal and axial planes with limited cone-beam computed tomography," *Journal of Prosthodontics*, vol. 20, no. 6, pp. 432–438, 2011.

[23] A. Nakajima, G. T. Sameshima, Y. Arai, Y. Homme, N. Shimizu, and H. Dougherty Sr., "Two- and three-dimensional orthodontic imaging using limited cone beam-computed tomography," *Angle Orthodontist*, vol. 75, no. 6, pp. 895–903, 2005.

[24] K. Kobayashi, S. Shimoda, Y. Nakagawa, and A. Yamamoto, "Accuracy in measurement of distance using limited cone-beam computerized tomography," *International Journal of Oral & Maxillofacial Implants*, vol. 19, no. 2, pp. 228–231, 2004.

[25] M. A. Sümbüllü, F. Çağlayan, H. M. Akgü, and A. B. Yilmaz, "Radiological examination of the articular eminence morphology using cone beam CT," *Dentomaxillofacial Radiology*, vol. 41, no. 3, pp. 234–240, 2012.

[26] Z. T. Librizzi, A. S. Tadinada, J. V. Valiyaparambil, A. G. Lurie, and S. M. Mallya, "Cone-beam computed tomography to detect erosions of the temporomandibular joint: effect of field of view and voxel size on diagnostic efficacy and effective dose," *American Journal of Orthodontics and Dentofacial Orthopedics*, vol. 140, no. 1, pp. e25–e30, 2011.

[27] O. B. Honey, W. C. Scarfe, M. J. Hilgers et al., "Accuracy of cone-beam computed tomography imaging of the temporomandibular joint: comparisons with panoramic radiology and linear tomography," *American Journal of Orthodontics and Dentofacial Orthopedics*, vol. 132, no. 4, pp. 429–438, 2007.

[28] P. Rammelsberg, L. Jäger, and J.-M. Pho Duc, "Magnetic resonance imaging-based joint space measurements in temporomandibular joints with disk displacements and in controls," *Oral Surgery, Oral Medicine, Oral Pathology, Oral Radiology, and Endodontics*, vol. 90, no. 2, pp. 240–248, 2000.

[29] K. Ikeda and A. Kawamura, "Assessment of optimal condylar position with limited cone-beam computed tomography," *American Journal of Orthodontics and Dentofacial Orthopedics*, vol. 135, no. 4, pp. 495–501, 2009.

[30] R. P. Scapino, "Histopathology associated with malposition of the human temporomandibular joint disc," *Oral Surgery, Oral Medicine, Oral Pathology*, vol. 55, no. 4, pp. 382–397, 1983.

[31] P.-L. Westesson and M. Rohlin, "Internal derangement related to osteoarthrosis in temporomandibular joint autopsy specimens," *Oral Surgery, Oral Medicine, Oral Pathology*, vol. 57, no. 1, pp. 17–22, 1984.

[32] M. A. Markovic and H. M. Rosenberg, "Tomographic evaluation of 100 patients with temporomandibular joint symptoms," *Oral Surgery, Oral Medicine, Oral Pathology*, vol. 42, no. 6, pp. 838–846, 1976.

[33] J. W. Brand, J. G. Whinery Jr., Q. N. Anderson, and K. M. Keenan, "Condylar position as a predictor of temporomandibular joint internal derangement," *Oral Surgery, Oral Medicine, Oral Pathology*, vol. 67, no. 4, pp. 469–476, 1989.

[34] S. R. Alexander, R. N. Moore, and L. M. DuBois, "Mandibular condyle position: comparison of articulator mountings and magnetic resonance imaging," *American Journal of Orthodontics & Dentofacial Orthopedics*, vol. 104, no. 3, pp. 230–239, 1993.

[35] H. Bonilla-Aragon, R. H. Tallents, R. W. Katzberg, S. Kyrkanides, and M. E. Moss, "Condyle position as a predictor of temporomandibular joint internal derangement," *The Journal of Prosthetic Dentistry*, vol. 82, no. 2, pp. 205–208, 1999.

[36] M. Paknahad and S. Shahidi, "Association between mandibular condylar position and clinical dysfunction index," *Journal of Cranio-Maxillofacial Surgery*, vol. 43, no. 4, pp. 432–436, 2015.

[37] É. R. Lelis, J. C. Guimarães Henriques, M. Tavares, M. R. de Mendonça, A. J. Fernandes Neto, and G. d. Almeida, "Cone-beam tomography assessment of the condylar position in asymptomatic and symptomatic young individuals," *The Journal of Prosthetic Dentistry*, vol. 114, no. 3, pp. 420–425, 2015.

[38] C. E. Rieder and J. T. Martinoff, "Comparison of the multiphasic dysfunction profile with lateral transcranial radiographs," *The Journal of Prosthetic Dentistry*, vol. 52, no. 4, pp. 572–580, 1984.

[39] B. Madsen, "Normal variations in anatomy, condylar movements, and arthrosis frequency of the temporomandibular joints," *Acta Radiologica*, vol. 4, no. 3, pp. 273–288, 1966.

[40] E. L. Christiansen, T. T. Chan, J. R. Thompson, A. N. Hasso, D. B. Hinshaw Jr., and S. Kopp, "Computed tomography of the normal temporomandibular joint," *European Journal of Oral Sciences*, vol. 95, no. 6, pp. 499–509, 1987.